# The Involvement of Activated Microglia In The Cardiovascular Complications of Diabetes and Heart Failure

A thesis submitted in fulfilment of the requirements for

the degree of Doctor of Philosophy

Indrajeetsinh Rana

B.Sc (Biochemistry), M.Sc (Biochemistry)

School of Medical Sciences

College of Science, Engineering and Health

RMIT University

April 2012

# Short Table of Contents

# Declaration

I certify that except where due acknowledgement has been made, the work described in this thesis is that of the author alone; the work has not been submitted previously, in whole or in part, to qualify for any other academic award; the content of the thesis is the result of work which has been carried out since the official commencement date of the approved research program; and, any editorial work, paid or unpaid, carried out by a third party is acknowledged.

Signed: …… (Indrajeetsinh Rana)

Date: …….

# Acknowledgements

I wish to proceed by thanking my supervisors who have supported me over the duration of this research project. I begin by extending my gratitude to my supervisor Dr Martin Stebbing for his invaluable guidance, patience and tireless support throughout the project. I would also like to thank Prof. Emilio Badoer for his kindness, support and his understanding at times that were difficult for me during the duration of this project.

I would like to take this opportunity to thank everyone who helped me to complete this research project. My special thanks to all the member of neuropharmacology and neuroinflammatory research group supporting me during my PhD candidature.

I would like to give a special vote of thanks to Dr Joo Lee Chem and Jennifer Lawrence for their constant help with different techniques in the laboratory. I would also like to thank my friends especially Markus, Samin, Sepideh, Melissa, Eloise, James, Leo, Anjali, Rhiannon and Alex for all the laughs and their moral support during the stressful times of my study.

I heartily thank my partner Chaitali for her love and support during my good and bad times. I would like to acknowledge my family, for their love and support and numerous emails and phone calls that meant so much to me and almost made me feel at home even though I was so far away.

# Abbreviations

| | |
|---|---|
| $[Ca^{+2}]i$ | intracellular $Ca^{+2}$ concentration |
| ADP | adenosine diphosphate |
| AMPA | α-amino-3-hydroxy-5-methyl-4-isoxazolepropionic acid receptor |
| Ang II | angiotensin II |
| Arc | arcuate nucleus |
| ATP | adenosine-5'-triphosphate |
| BDNF | brain derived neurotrophic factor |
| CNS | central nervous system |
| COX-2 | cyclooxygenase-2 |
| DMEM | dulbecco's modified eagle's medium |
| eNOS | endothelian nitric oxide synthase |
| FBS | fetal bovine serum |
| GABA | γ-aminobutyric acid |
| $H_2O_2$ | hydrogen peroxide |
| HCR | high capacitant runner (rats) |
| HEPES | 4-(2-hydroxyethyl)-1-piperazineethanesulfonic acid |
| i.c.v. | intracerebroventricular |
| IL-10 | interleukin 10 |
| IL-1β | interleukin-1β |
| IR | immunoreactive |
| LCR | low capacitant runner (rats) |
| LPS | lipopolysaccharides |
| MAPK | mitogen-activated protein kinase |
| MCP | monocyte chemoattractant protein |
| MCP-1 | myeline oligodendrocytes glycoprotein-1 |
| MI | myocardial infarction |
| mM | millimolar |
| NADPH | reduced nicotinamide adenine dinucleotide phosphate |
| NF-kB | nuclear factor-kappaB |
| nm | nanometre (wavelength) |
| NMDA | N-methyl-D-aspartic acid |

| | |
|---|---|
| nNOS | neuronal nitric oxide synthase |
| NO | nitric oxide |
| NPY | neuropeptide Y |
| NTS | nuclear tractus solitarius |
| NTS | nucleus tractus solitarius |
| PBS | phosphate buffered saline |
| PKC | protein kinase C |
| POMC | pro-opiomelanocortin |
| PVN | paraventricular hypothalamic nucleus |
| ROS | reactive oxygen species |
| RVLM | rostoventral medulla |
| SD | sprague dawley |
| SOCE | store operated $Ca^{2+}$ entry |
| SON | supraoptic nucleus |
| STZ | streptozotocin |
| TNF- α | tumor necrotic factor alpha |
| UDP | uredines diphosphate |
| UTP | uredines triphosphate |
| VH | ventral hypothalamus |
| VMH | ventromedial hypothalamus |

# Thesis Summary

Microglia are the immune cells in the central nervous system. Upon activation by insult or injury they secrete a variety of pro-inflammatory cytokines, chemokines and reactive oxygen species (ROS). Recent studies of neurodegenerative disease and animal models of nerve injury suggest a pathological involvement of microglia in the development of these diseases. Elevated sympathetic nerve activity and increased paraventricular hypothalamic nucleus (PVN) neuronal activity have been reported in rats with myocardial infarction (MI) as well as in STZ-induced diabetic rats. Elevated sympathetic nerve activity is well known as a contributing factor to the pathology of heart failure following MI. Cardiovascular complications are also common in diabetes, and include cardiomyopathy, hypertension, and increased risk of sudden cardiac death. Diabetes also causes pathological changes in peripheral nerves and blood vessels. However, there is increasing evidence that inflammation within the central nervous system and dysregulation of sympathetic nerves both play a role in diabetic complications. The PVN is involved in regulation of sympathetic nerve activity and excitation of the PVN can elevate sympathetic nerve activity. We therefore investigated whether microglia are activated in cardiovascular centres in animal models of heart failure and diabetes and the time course of any such activation. Then we used *in vivo* and *in vitro* methods to gain insight into the mechanisms and consequences of microglial activation in these disorders.

Following MI, inflammatory cytokines are reportedly elevated in the PVN, as well as in plasma, indicating that inflammation occurs in the brain in addition to the periphery. In the present study, we investigated whether MI in rats induces activation of microglia in the brain. We used immunohistochemistry to detect CD11b (clone OX-42) microglial receptors. We characterised microglia on the basis of their morphology and intensity of OX-42 staining.

Microglia with longer branches, secondary branches and small somata were considered as ramified (non-activated). As in previously reported studies, microglia with shorter, stubbier processes, swollen cell bodies and expressing relatively increased OX-42 labelling were considered activated. Compared to control rats that had undergone sham surgical procedures, there was a significant increase in the percentage of microglia that were activated in the PVN following MI. The increase was observed as early as 2 weeks after the MI and occurred predominantly within the parvocellular subdivision containing neurons involved in regulation of sympathetic activity. Activated microglia were not observed in the ventral hypothalamus, adjacent to the PVN, nor in the cortex, indicating the response was not the result of a generalised inflammatory reaction in the brain. Echocardiography and haemodynamic parameters at 2 weeks after MI indicated reduced left ventricular function, but congestive heart failure had not yet developed.

As inflammation and elevated sympathetic nerve activity are also reported to occur in diabetes, we investigated whether microglial activation occurred within central cardiovascular centres in several diabetes-related rat models. In brains harvested from streptozotocin (STZ)-induced diabetic rats (at 2 weeks, 6 weeks, and 8−10 weeks after intravenous STZ administration) and from vehicle-treated normoglycaemic control rats, microglia were identified using specific antibody for CD11b receptors (OX-42 clone), while activated neurons were identified using an antibody for Fos protein. A significant increase in the percentage of microglia activated in the PVN, supraoptic nucleus (SON) and the nucleus tractus solitarius (NTS) regions was observed in STZ-induced diabetic rats at the 8−10 week time point. Individual rat data suggested variability in the time of onset of microglial activation in these regions. In the PVN, microglial activation was significantly higher in the parvocellular subdivision as well as in the oxytocin/vasopressin-producing magnocellular subdivision. Time course data in STZ-induced diabetic rats suggested that intense neuronal

activation immediately preceded microglial activation; excitotoxicity may therefore be responsible for the microglial activation observed. Neuronal and microglial activation in the SON and magnocellular subdivision of the PVN may be due to elevated plasma osmolarity in STZ-induced diabetic rats. Our results from insulin-resistant and leptin receptor deficient rats did not show significant microglial activation in the PVN, SON and NTS regions, indicating that this activation in STZ-induced diabetes is linked with overt diabetes.

To understand the role of activated microglia in MI and STZ-induced diabetic rats, we injected activated microglia into the PVN in naïve rats and observed the effect on systolic blood pressure in conscious rats using the tail cuff method. We observed that activated microglial injection, but not vehicle or conditioned medium injection, increased systolic blood pressure, suggesting that activated microglia in the PVN itself can elevate sympathetic nerve activity. Therefore, targeting these activated microglia may be one way to reduce the pathological contribution of elevated sympathetic nervous system activity in diseases such as MI and diabetes.

In order to design therapies to inhibit microglial activation, it is important to understand the cellular mechanisms involved. Previous studies of nerve injury models have reported increased expression of the ATP receptor type P2X4 and elevated phosphorylated p38 MAPK in microglia, and have suggested their involvement in microglial activation. Surprisingly, we observed neither any increase in P2X4 receptor expression nor any increased phosphorylation of p38 MAPK in activated microglia present in STZ-induced diabetic rats. Further study is required to investigate the involvement of other microglial purinergic receptors and intracellular markers that have been shown to be associated with microglial activation in other disease conditions.

Many *in vitro* studies of microglia have suggested that intracellular calcium concentration ($[Ca^{2+}]i$) is an important intracellular messenger in microglia, and that microglial activation is associated with a sustained increase in intracellular calcium. ATP and UDP are thought to be released from damaged neurons during excitotoxic neuronal death, but whether they can increase basal calcium levels in microglia has not been investigated. We therefore studied the mechanism of microglial activation under *in vitro* conditions using these purines as activators. Both ATP and UDP caused a sustained increase in $[Ca^{2+}]i$ but only ATP was able to induce motility in microglia. These results suggest that increased $[Ca^{2+}]i$ may be sufficient to induce some functions of activated microglia but not all.

In conclusion, microglia are activated in the PVN but not in the adjacent hypothalamus following myocardial infarction. Microglia were also activated in cardiovascular centres of the brain, including the PVN, in STZ-induced diabetic rats. Activated microglia may contribute to the increased local production of pro-inflammatory cytokines and ROS in the PVN, resulting in increased sympathetic drive. Activated microglia within the PVN are capable of increasing blood pressure, and inhibition of microglial activation may have beneficial effects on humans suffering from diabetes and myocardial infarction. The processes leading to microglial activation in STZ rats remain to be determined. It appears, however, that this activation is associated with overt diabetes, rather than insulin resistance or obesity. As ATP and UDP acts on different microglia receptors, our study also suggests that targeting one single receptor type may have beneficial effects, but will not completely block activated microglial function. Thus, a better understanding of the mechanism of microglial activation may lead to more targeted therapies for inhibiting microglial activation during various pathological conditions.

# Publications:

**Publications in International Journals:**

Rana I, Stebbing M, Kompa A, Kelly DJ, Krum H, Badoer E, Microglia activation in the hypothalamic PVN following myocardial infarction. *Brain Res,* 2010. 1326: 96-104.

Rana I, Badoer E, Leo CH, Woodman OL**,** Stebbing MJ, , Microglia are Activated in the Cardiovascular Centres of Brain in STZ Diabetic Rats. *Manuscript in preparation*.

**Publications in Proceedings:**

Rana I, Stebbing MJ, Kompa A, Kelly DJ, Krum H, Badoer E, Microglia are Activated in the Hypothalamus following Myocardial Infarction. *Proceedings of HBPRCA*, 2009.

Rana I, Badoer E, Stebbing MJ, Microglia are Activated in the Cardiovascular Centres of Brain in STZ Diabetic Rats**.** *Proceedings of sfn*, 2010.

# Index of Tables and Figures:

**Index of Tables:**



Index of Figures:

# Long Table of Contents

# Chapter 1: Microglia and Their Role in Neuro-inflammation and Cardiovascular Diseases

## 1. Microglia as immune cells of the central nervous system

The presence of a blood-brain barrier prevents entry of immune cells from the periphery into the central nervous system (CNS). Hence, the CNS contains specialised cells known as microglia which perform the function of immune cells. In 1927, del Rio-Hortego first suggested, based on silver carbonate staining of neural tumors, that microglia belong to a glial cell type distinct from astrocytes and oligodendrocytes (del Rio-Hortega 1927). Using this method, he observed differences in morphology between microglial cells, and suggested the existence of diverse microglial populations in the CNS. Discoveries in the early and mid-19$^{th}$ century established the role of microglia as immune cells, protecting the CNS from injury and infection (del Rio-Hortega 1927; del Rio-Hortega 1932), but studies carried out in the last three decades of the 19$^{th}$ century have demonstrated the pathological role of microglia in various neurodegenerative diseases (Graeber 2010; Liu 2006; Sawada et al. 2006). The contrasting evidence on the role of microglia has made them one of the most controversial cells of the CNS. In fact, with more than 11,000 publications on the subject in last two decades, the study of microglia has emerged as a very active branch of neuroscience. Based on the current understanding of microglial function in other pathologies, I have investigated their role in the pathology of diabetes and heart failure (which often co-exist), since neurohormonal imbalance is known to play a significant role in the pathology of these diseases. Since the number of people with either diabetes or heart failure is increasing worldwide (Lloyd-Jones et al. 2010), the outcomes of this study have significant implications for human health.

It is now known that microglia constitute approximately 20% of the total glial cell population, and that they are distributed throughout the brain and spinal cord (Kreutzberg

1995). In the CNS, microglia perform a protective function by constantly moving their processes to analyse the CNS for damaged neurons, extracellular debris, and infectious agents (Gehrmann et al. 1995; Nimmerjahn et al. 2005, Boycott and Hopkins. 1981). The presence of a blood-brain barrier stops entry of infectious agents from the blood stream into the brain, which prevents most infections from reaching the vital nervous tissue. In severe disease states, this blood-brain barrier can become weak and leaky. In such cases where infectious agents are directly introduced into the brain, microglial cells react quickly in an attempt to neutralise them before they damage the sensitive neural tissue. Under prolonged pathological conditions, microglia secrete signalling molecules that facilitate T cell entry into the brain. Because of the unavailability of antibodies from the rest of the body (due to the blood-brain barrier; Sas et al. 2008), microglia must be able to recognise foreign bodies during pathological conditions, and engulf them much like peripheral macrophages. Since brain infection is a rare but catastrophic event, microglia must act quickly to prevent potentially fatal damage. Therefore, microglia are extremely sensitive to even small pathological changes in the CNS.

Although microglia have similarities to peripheral macrophages in terms of their role as immune cells, there are important differences between them. One is that macrophages are always ready to act, while microglia need to be activated to perform their function as immune cells (Aloisi 2001). Another difference between microglia and other cells of the myeloid lineage is their turnover rate. Macrophages and dendritic cells are constantly being used up and replaced by myeloid progenitor cells, which differentiate into the required type. Due to the blood-brain barrier, it is difficult for the body to constantly replace microglia. That is why microglia remain in an inactive state under normal conditions and only proliferate rapidly to maintain their numbers when they become activated. However, in cases of extreme infection when the blood-brain barrier is damaged, microglia may be replaced with myeloid progenitor cells and macrophages (Flugel et al. 2001; Hickey & Kimura 1988; Ritter et al. 2006). Once the infection decreases, the disconnection between peripheral and central systems is

reestablished and only microglia are present for the recovery and re-growth period (Gehrmann 1996).

## 2. Microglial morphology, origin and distribution in the central nervous system

### *2.1. Microglial morphology indicates functional state*

Microglia are highly dynamic and vigilant (Nimmerjahn et al. 2005; Parkhurst & Gan 2010). They remain vigilant towards any infection or neuronal injury in the CNS by the means of various receptors present on their processes. In an adult brain, these cells have small somata with long and highly branched processes, and are called "ramified microglia." In response to stressful stimuli, brain injury or infection, microglia become "activated." This activation is associated with drastic morphological changes, where their somata become enlarged and processes become shorter, thicker and stubbier (Nakajima & Kohsaka 2001; Stence et al. 2001b; Streit et al. 1988). Prolonged activation of microglia is thought to transform them into "phagocytic microglia," which are similar in appearance and function to peripheral macrophages. Fig.1.1 shows the morphological features of (A) ramified, (B) activated and (C) phagocytic microglia present in the adult rat brain.

Recent studies have reported morphological changes in microglial cells present in the CNS of animal models of stroke, multiple sclerosis, neuropathic pain, and in humans with Alzheimer's disease, Parkinson's disease and schizophrenia (Aloisi 2001; Aloisi et al. 1997; Liu 2006; Mrak et al. 1995; Sawada et al. 2006).

### *2.2. Varying microglial morphology and distribution in the CNS*

Immunohistochemistry on cerebellum obtained from dead human infants (14 weeks old) using anti-ferritin antibody has shown that all microglia display amoeboid morphology (Maslinska et al. 1998). This study also reported more ramified microglial cells than amoeboid cells in 20-week old human infants. This increase in the proportion of ramified microglia was greater in some regions of the cerebellum than others. The authors concluded

that the morphology and localisation of microglial cells depends on the developmental stage of the brain (Maslinska et al. 1998). In addition, the results of this study clearly indicate that transformation of amoeboid cells into ramified microglial cells starts during early gestation in the human brain. A study of cerebellum in mice using specific immunological markers for microglia has reported heterogeneous distribution and morphology of microglia throughout the cerebellum, but no there was no significant difference between young (25−30 days) and adult (3−4 months) animals (Vela et al. 1995), suggesting that ramification of microglia occurred before the earliest time point for this study. Moreover, the study showed the mean number of microglia varied in different layers of the cerebellum. The cerebellar nuclei had the highest microglial density, and the molecular layer had the lowest, while the granular layer and the white matter had intermediate densities. Using both coronal and horizontal sections Vela et al. (1995) demonstrated that the length of microglial processes was different in each layer. From analysis of two previous studies (Triarhou & Ghetti 1991; Wilson & Molliver 1994), Vela et al. (1995) found a correlation between serotonergic innervation between cerebellar layers and density of microglial cells, suggesting the possibility of microglial involvement in the regulation of neurotransmission. This study did not provide any experimental evidence for this claim, and further studies are required to investigate the hypothesis.

Quantitative analysis of microglial cells from adult rat brain sections stained using three different microglial markers, lipocortin 1 (LC1) (a glycoprotein), phosphotyrosine and lectin GSA $B_4$, showed that LC1 labeled the highest numbers of cells and GSA $B_4$ labeled the least in any particular brain region (Savchenko et al. 2000). Each of the three markers demonstrated different microglial density in different brain regions, eg. 123±10, 121±1 and 98±8 cells/$mm^2$ in the frontal lobe, hypothalamus and occipital lobe respectively using LC1. Thus, the study clearly demonstrated that microglial density varies between brain regions (Savchenko et al. 2000). It also supported the idea, first proposed in 1927 by del Rio-Hortego,

that different microglial phenotypes are present in the brain. Another possible cause of the observed variation in labelling of microglia with different methods is that microglia express a variety of immunological and histological markers, and that some of these markers get up-regulated upon microglial activation. For example, ED1 antibody strongly labels amoeboid microglial cells, but does not label (Flaris et al. 1993) or only weakly labels ramified microglial cells (Milligan et al. 1991). Increased levels of microglial CD11b receptors (recognised by the OX-42 antibody), as seen in spinal microglia after nerve injury (Tsuda et al. 2003), also suggest that an increase in certain immunological markers occurs upon microglial activation.

Circumventricular organs are situated around the ventricular system of the brain. They possess a weak blood-brain barrier which allows macrophage infiltration in these areas. Perry et al. (1992) reported expression of sialoadhesin receptors in microglial cells and in macrophages present in circumventricular regions. This receptor type is normally present in macrophages, but not in ramified microglia present in brain regions with a strong blood-brain barrier. Based on this evidence, the authors claimed that the "phenotype of microglia is, in part, regulated by the presence of the blood-brain barrier." One possibility is that plasma components can modulate microglial morphology (see Perry et al. [1992] for further discussion). Similarly, another study has reported that microglia in circumventricular organs express high levels of CD4 receptors, similar to macrophages, whereas ramified microglial cells present in other area of the brain do not (Perry & Gordon 1987). This study also reported the presence of cells with microglial morphology expressing high levels of CD4 in damaged areas following injury to the CNS and damage to the blood-brain barrier.

### *2.3. Origin of microglia*

As discussed, microglia and macrophages are immune cells that perform many similar functions and share common features. However, they do show some differences as

well. One well known difference between microglia and macrophage cells is their morphology. Microglial cells are present in their resting ramified form in the CNS and undergo morphological change upon activation (Fig 1.1). The immune function of microglia is restricted to the CNS, while macrophages provide immunity mainly outside the CNS. It is now accepted that monocytes and macrophages arise from a mesodermal origin, but there is controversy over the origin of microglial cells. Based on experimental data, there are two principal views regarding microglial origin: that microglial cells are (i) of mesodermal origin, or that (ii) they originate from neuroepithelial cells. Compare reviews by Cuadros & Navascues (1998) and Kaur et al. (2001).

One of the main argument supporting a different origin for microglia from that of monocytes/macrophages is that some immunohistochemical markers present on macrophages are not expressed by ramified microglia (Oehmichen et al. 1979; Wood et al. 1979). Electrophysiological studies have reported the presence of outward K+ current in macrophages and the absence of outward K+ current in isolated unstimulated microglial cells (Kettenmann et al. 1990). These different expression levels of surface immunohistochemical markers and ion channels could be due to the difference in the microenvironments of microglia and macrophages. These data support the idea of a different functional state in microglia, but do not give any direct information about microglial origin. Stronger support for the neuroectodermal origin of microglia came from the *in vitro* findings of Hao et al. (1991) and Richardson et al. (1993), where microglia were generated from embryonic neuroepithelium in culture.

The view that microglia are of mesodermal origin is supported by the evidence that microglia and monocytes/macrophages have many common immunohistochemical markers and functions (Chugani et al. 1991; Imamura et al. 1990). There is similarity in the type of ion channels expressed by activated microglia and macrophages (Brown et al. 1998). Experimental evidence demonstrating labelled microglia in the brain following labelling of

circulating white blood cells shows monocytes as a microglial precursor. However, macrophages/microglial cells appear within the CNS before it is vascularised (Ashwell 1991; Cuadros et al. 1993) and before monocytes are produced in hemopoietic tissues (Naito et al. 1996; Sorokin et al. 1992). Therefore, not all microglial cells can originate from circulating monocytes during development. Strong support for this view of a microglial haematopoietic origin is based on results obtained by several animal studies of bone marrow chimeras (Hickey & Kimura 1988; Matsumoto & Fujiwara 1987). One bone marrow transplantation study has reported replacement of 10−20 % of microglial population by donor cells by 3−4 months after transplantation (Krall et al. 1994).

Collectively, a large proportion of authors and studies have supported the view that microglia derive either from monocytes that leave the blood stream and colonise the nervous parenchyma, or directly from hemopoietic stem cells that differentiate as microglial cells. However, it is difficult to draw a final conclusion due to variation in experimental procedures, duration of experiments, the initial time point of experiments and variation in the species used.

## 3. Microglial receptors and their involvement in microglial activation

Microglia express a variety of receptors, including purinergic receptors, toll-like receptors, calcium-sensing receptors, glutamate receptors, and receptors for cytokines and chemokines (Illes et al. 1996; Koizumi et al. 2007; Morigiwa et al. 2000; Seo et al. 2008; Takeuchi et al. 2006; Tsuda et al .2003; Wu et al. 2004a; Wu et al. 2004b; Eun et al. 2004; Noda et al. 2000). Microglial glutamate receptors include ionotropic receptors N-methyl-D-aspartic acid (NMDA), (S)-a-amino-3-hydroxy-5-methyl-4-isoxazolepropionic acid (AMPA), kainic acid (KA) receptors and metabotropic glutamate receptors (mGluRs), mGluR1, mGluR2 and mGluR4.

Of all microglial receptors, purinergic receptors have received the most attention, due their reported roles in microglial activation in various pathological conditions linked to inflammation (Abbracchio & Verderio 2006; Inoue 2008; Koles et al. 2005; Tsuda et al. 2003). Purinergic receptors can be divided into two main categories: ionotropic (P2X) and metabotropic (P2Y) receptors. Ionotropic P2X receptors are a family of cation-permeable ligand gated ion channels that open in response to the binding of extracellular purines such as ATP. ATP is thought to be released from damaged tissue/neurons. In microglial cells, activation of these receptors results in entry of $Ca^{2+}$, which can activate various $Ca^{2+}$ sensitive intracellular processes. Metabotropic P2Y receptors are G protein coupled receptors, and act via secondary intracellular messengers to induce cellular responses. There is discrepancy in the literature in terms of which of these receptors is most important for microglial activation and pathological functions. Some studies have suggested a vital role for microglial P2X receptors (Ferrari et al. 1997a; Tsuda et al. 2003), while others have linked microglial P2Y receptors (Honda et al. 2001; Inoue et al. 2009) with activation and the pathological role of ATP in neuropathic pain. Some reports have suggested a role for P2X receptors in microglial cytokine release and P2Y receptors in microglial chemotaxis (Honda & Kohsaka 2001; James & Butt 2002).

Microglial receptors may respond to microglial secretions acting in an autocrine manner to further activate microglia. For instance, neurotransmitters can induce microglial cytokine release which can then act back on microglia to induce more neurotransmitter release. Similarly, cytokines produced by neurons or glial cells can act on microglia to induce neurotransmitter release which then further increases microglial cytokine release. This type of autocrine action of microglial secretions has been reported by various *in vitro* studies on microglia (Jantaratnotai et al. 2009; Liu et al. 2006; Seo et al. 2008; Takeuchi et al. 2006). Thus, microglia express a wide range of receptors on their surfaces whose actions interact in complex ways. However, the possibility that microglia do not express all these receptors in

their resting condition and express some of them only upon their activation cannot be eliminated. Activation of those receptors may be linked with pathological or beneficial effects of microglia.

## 4. Microglial secretions: their pathological and beneficial roles

Upon activation by various mechanisms, microglia secrete various proinflammatory or anti-inflammatory cytokines, chemokines, growth factors, reactive oxygen species, glutamate and nitric oxide. Microglial can sense even small changes in their surrounding environment and can exert neuroprotective or neuroinflammatory effects on surrounding neurons via their diverse variety of secretions. Some of the major microglial secretions and their functional roles are described below.

### *4.1. Tumor necrotic factor alpha (TNF-α)*

Tumor Necrotic Factor alpha (TNF-α) is involved in the pathogenesis of many neurodegenerative diseases such as Parkinson's disease, Alzheimer's disease and multiple sclerosis (Brosnan et al. 1988; Fillit et al. 1991). It is one of the best-documented cytokines produced by microglia upon activation. The study of Hide et al. (2000) on cultured rat microglia reported an ATP-induced dose-dependent increase in microglial TNF-α secretion, suggesting that ATP secreted from dead or damaged neurons can trigger microglial TNF-α secretion. Takeuchi et al. (2006) used microglial-neuronal co-culture to demonstrate that TNF-α acts on microglia to induce glutamate secretion, which can then act on neurons to induce neurotoxicity. The possibility of a further increase in TNF-α secretion from microglia due to an autocrine action of this cytokine was also suggested. Interestingly, an *in vivo* study by Gullilam et al. (2007) demonstrated that inhibition of TNF-α protein expression in the paraventricular hypothalamus (an area responsible for cardiovascular control of blood pressure) using a pentoxifylline (PTX) had beneficial effects on the heart in animals with left coronary artery ligation. This study raised the possibility of a pathological role of brain TNF-

α in the consequences of myocardial infarction. On the other hand, mice lacking the receptor for TNF-α (p55 receptor-1) showed increased neurotoxicity under excitatory and ischemic conditions, suggesting a neuroprotective action for this cytokine (Bruce et al. 1996; Gary et al. 1998). TNF-α has also been reported to be neuroprotective by various other studies (Barger et al. 1995; Cheng et al. 1994). Thus, TNF-α can be either neuroprotective or neurodegenerative, but the factors that determine its protective or pathological role are not known.

### *4.2. Interleukin-1β (IL-1β)*

Interleukin-1β (IL-1β) is an inflammatory cytokine secreted by activated microglia and macrophages. In microglia, IL-1β is synthesised in an inactive form which undergoes proteolytic cleavage to produce the mature form which is then released. Many *in vitro* studies of microglia have suggested a role for ATP and the purinergic P2X7 receptor type in the process of maturation and secretion of IL-1β (Ferrari et al. 1997b; Sanz & Di Virgilio 2000; Solle et al. 2001), but none of them have reported ATP mediated IL-1β release from microglia that are not LPS pre-treated. An *in vitro* study has reported that LPS alone can stimulate microglial IL-1β release, but an ATP application to LPS pre-treated (for 2 hours) microglia produced IL-1β release several fold greater (Sanz & Di Virgilio 2000). The study suggested that ATP stimulates production as well as release of IL-1β.

Increased IL-1β cytokine has been reported in brains after insult or injury and in humans with Alzheimer's disease (Griffin & Mrak 2002; Rothwell 2003). IL-1β released from cultured activated microglia can directly increase acetlycholinesterase production and activity in primary neuronal cultures (Li et al. 2000). These findings suggest that the increased concentration of IL-1β in an Alzheimer's affected brain may contribute to the observed decreases in the tissue acetylcholine levels by increasing synthesis and activity of neuronal acetlycholinesterase. IL-1β is involved in hypothalamic regulation of corticotrophin-releasing hormone secretion and autonomic activation (Hsieh et al. 2010; Shi et al. 2010a). The action

of IL-1β on the hypothalamus also results in fever, anorexia and analgesia, and this may be due to an IL-1β mediated increase in norepinephrine (NE) levels in the PVN and the median eminence (ME) regions of the hypothalamus (MohanKumar & MohanKumar 2005).

### *4.3. Interleukin-10 (IL-10)*

Interleukin 10 (IL-10) is an anti-inflammatory cytokine (Levin & Godukhin 2007; Moore et al. 1993; Opal et al. 1998; Pajkrt et al. 1997; Sawada et al. 1999). Studies have reported IL-10 secretion from human, rat and mouse microglia (Chabot et al. 1999; Correa et al. 2010; Kim et al. 2002; Zhang et al.). IL-10 exerts an inhibitory effect on microglial production of proinflammatory cytokines TNF-α, IL-1β, chemokines and ROS and their secretion (Aloisi et al. 1997; Sawada et al. 1999). Every type of glial cell, as well as neurons in the CNS, express receptors for IL-10. Apart from brain cells, monocytes, macrophages, and B and T lymphocytes also synthesise IL-10. Studies have demonstrated an association between increased IL-10 levels and reduced clinical symptoms of stroke, multiple sclerosis, Alzheimer's disease, meningitis, and the behavioural changes in experimental animals that occur during bacterial infections (Frenkel et al. 2005; Levin & Godukhin 2007; Paris et al. 1997; Strle et al. 2001). Another study has reported reduced ability of immune cells to produce IL-10 in human patients suffering from type-2 diabetes (van Exel et al. 2002). The cellular mechanisms leading to the anti-inflammatory effects of IL-10 are not completely known.

### *4.4. Reactive oxygen species (ROS)*

Reactive Oxygen Species (ROS) are reactive molecules that contain the oxygen atom. Phagocytic cells such as microglia have the capability to produce ROS in large quantities, and they use the lethal effect of oxidants to kill phagocytosed pathogens. ROS are continuously being produced in all cells as a byproduct of various biochemical reactions, but are largely neutralised by cellular antioxidant defense mechanisms to prevent cellular damage.

However, excessive production of reactive oxygen species or inhibition of cellular defense enzymes can result in lipid peroxidation, protein denaturation and DNA damage which leads to oxidative stress mediated cell death (Bennett 2001; Rana & Shivanandappa 2010; Srivastava & Shivanandappa 2006). One major cellular source of ROS is mitochondria, which generate ROS during oxidative phosphorylation. In activated microglia, the NADPH oxidase enzyme is the major source of excessive superoxide production (Barger et al. 2007; Li et al. 2005). Cellular defense mechanisms against ROS include the enzymes glutathione peroxidase, glutathione reductase, superoxide dismutase (catalyze superoxide conversion to $H_2O_2$), and catalase (converts $H_2O_2$ to water and oxygen). Oxidative stress and increased levels of ROS in the brain have been suggested to be involved in the pathology of various neurodegenerative diseases such as Alzheimer's disease and Parkinson's disease and myocardial infarction (Halliwell 2001; Lindley et al. 2004).

Interestingly, activated microglia are capable of production of ROS as well as of nitric oxide. Nitric oxide has a dual role, as it can act as a signalling molecule in the brain and can also participate in reactions leading to production of toxic oxidative molecules. Nitric oxide signalling in the paraventricular nucleus plays a major part in the regulation of renal sympathetic nerve activity (Zheng et al. 2006). Nitric Oxide can also act as a chemoattractant signalling molecule, causing microglial migration to a site of injury in the CNS (Chen et al. 2000). On the other hand, nitric oxide combines with superoxide to form the much stronger and more toxic oxidant peroxynitrite ($ONOO^-$) (Beckman 1999) which could be the reason for reported apoptosis in motor neurons by application of both nitric oxide and superoxides (Estevez et al. 1995). The study of Li et al. (2005) showed that LPS (lipopolysaccharides) treatment increases protein expression of the inducible nitric oxide synthase enzyme and activates NADPH oxidase which contributes to highly toxic peroxynitrite generation from microglia (Li et al. 2005). Activation of microglia also results in production of hydrogen peroxide ($H_2O_2$), which can again act back on the cell of origin or on

nearby microglial cells to activate them. $H_2O_2$ is also suggested to act as a signalling molecule that attracts microglia to the site of injury. Apart from acting as a chemokine, $H_2O_2$ also induces microglial proliferation (Mander et al. 2006). Proinflamatory cytokines TNF-α or IL-1β caused an increase in microglial proliferation which was inhibited by catalase, indicating that the proliferative effect of these cytokines is mediated by $H_2O_2$ (Mander et al. 2006). Using an inhibitor of NADPH oxidase, this study also suggested that increased production of reactive oxygen molecules by activation of this enzyme provides more substrate for the enzyme superoxide dismutase (SOD), which increases production of $H_2O_2$ . Therefore, $H_2O_2$ might be responsible for localised increases in the number of microglia observed during various pathological conditions.

### *4.5. Glutamate*

Glutamate is required for normal synaptic functioning, but excessive release from synaptic terminals overexcites neurons and results in excitoxicity. Excessive glutamate induces a very high cellular calcium level by increasing calcium influx and triggering calcium release from intracellular stores, which results in deregulation of cellular calcium homeostasis (Arundine & Tymianski 2003). Neuronal over-excitation by glutamate can result in neuroinflammation and neurodegeneration and occurs in ischemia, epilepsy and Alzheimer's disease (Hynd et al. 2004; Sattler & Tymianski 2000; 2001).

Upon activation by LPS, microglia release glutamate (Barger et al. 2007), suggesting that microglia could be a potential source of glutamate inducing neurotoxicity in various neurodegenerative diseases. Barger et al. (2007) also demonstrated that LPS mediated microglial glutamate release can be inhibited by boosting cellular antioxidant machinery (inducing cellular level reduced glutathione) by using antioxidant vitamin E or by using inhibitors of NADPH oxidase. These results indicate that glutamate release from activated microglia requires an oxidative burst. Interestingly, several studies on microglia have reported

that glutamate induces microglial proliferation and the release of cytokines and nitric oxide (Noda et al. 2000; Tikka et al. 2001; Tikka & Koistinaho 2001).

### *4.6. Brain-derived neurotrophic factor (BDNF)*

Brain-Derived Neurotrophic Factor (BDNF) is a member of the "neurotrophin" family of proteins. It acts as a neuronal growth factor and is produced by activated microglia as well as by neurons in the adult brain. BDNF acts via binding to tyrosine kinase receptors of which TrkB is preferred receptor. BDNF is expressed by neurons under normal physiological conditions and expression increases with increased neuronal activity in the brain (Gorba et al. 1999). In contrast, microglia require activation or stimulation to produce and secrete BDNF. BDNF plays a vital role in cell survival, gene expression, neutrite outgrowth, regulating cellular morphology, neurotransmitter release, synaptic plasticity and memory functions in the CNS (Lu & Chow 1999; Lu & Figurov 1997; Lu & Martinowich 2008; Mizoguchi et al. 2003a; Mizoguchi et al. 2003b; Mizoguchi et al. 2006; Mizoguchi et al. 2009; Phillips et al. 1991; Poo 2001). BDNF is reported to be involved in microglial proliferation and survival (Elkabes et al. 1996; Zheng et al. 1995). Although, BDNF is widely distributed throughout the brain, a high level of BDNF is observed in hippocampal granule neurons. Decreased BDNF mRNA levels have been reported in these neurons by RNAase protection assay performed on samples from humans with Alzheimer's disease, leading to the suggestion of a neuroprotective role for BDNF (Phillips et al. 1991).

Microglial BDNF is reportedly elevated in the spinal cord for several days after spinal injury (Cho et al. 1998) and may be responsible for enhancing neuronal excitation and injury by attenuating the inhibitory effect of GABA (γ-aminobutyric acid) (Coull et al. 2005; Prescott et al. 2006). Another study of spinal cord slices has reported an inhibitory effect of BDNF on GABAergic neurons (Lu et al. 2009a). The pathway for BDNF release in microglia is not known, but a study of cultured neurons has demonstrated that activation of neuronal

AMPA receptors (glutamate receptors) induces neuronal BDNF secretion via phosphatidylinositol 3-kinase (PI3-K) mediated activation of a mitogen activated protein kinase (MAPK) pathway. The study also reported that the activation of this pathway confers neuroprotection against excitotoxicity (Wu et al. 2004a). An *in vitro* study has demonstrated that the phagocytic activity of macrophages depends on BDNF synthesis and TrkB expression (Asami et al. 2006). However, the involvement of BNDF in microglial phagocytic function has not been investigated.

## 5. Studies of the mechanisms of microglial activation

### *5.1. Increased intracellular calcium is associated with microglial activation and secretion*

Microglial proliferation, secretion of cytokines and reactive oxygen species, migration and morphological changes are usually associated with an increase in microglial intracellular $Ca^{+2}$ concentration ($[Ca^{+2}]_i$)(Eder 2005; Farber & Kettenmann 2006).

ATP (which is thought to be released from damaged neurons) and lipopolysaccharide (LPS, present in the bacterial cell wall) are both capable of activating microglia during *in vitro* as well as *in vivo* conditions (Buttini et al. 1996; Hide et al. 2000; Li et al. 2005; Montero-Menei et al. 1996; Zheng et al. 2008). LPS is reported to cause a sustained increase in basal $[Ca^{+2}]_i$ in microglia (Hoffmann et al. 2003). An intracellular calcium chelator prevented the LPS-stimulated increase in microglial NO, cytokines and chemokine release, suggesting a requirement of elevated intracellular calcium for microglial secretion (Hoffmann et al. 2003). On the other hand, calcium ionophore (ionomycin) mediated elevation of microglial $[Ca^{+2}]_i$ was not sufficient to induce microglial nitric oxide, cytokine and chemokine release, suggesting that another intracellular messenger may also have a vital role to play in the secretion function of microglia (Hoffmann et al. 2003).

Calcium imaging experiments on microglia have reported that ATP induces a transient increase in $[Ca^{+2}]_i$ in a dose dependent manner (Moller et al. 2000). The highest calcium level was caused by 300 µM ATP, which was not changed further at higher concentrations. The observed increase in calcium with 100 µM ATP treatment was transient and biphasic. However, cells treated with 100 µM ATP in the absence of extracellular calcium showed a monophasic increase in cellular calcium level (Fig. 1.2). Moreover, a smaller proportion of cells responded to the ATP treatment as compared to cells tested in presence of extracellular calcium. These results clearly indicate that ATP triggers calcium release from intracellular stores in microglia as well as calcium entry from the extracellular medium.

Interestingly, a 5-minute treatment with thapsigargin (a specific blocker of the endoplasmic reticulum calcium pump), increased basal calcium levels in 53 % of microglia (Fig 1.3). After this 5-minute treatment, cells with elevated basal calcium levels did not respond to ATP, while the population of cells with no increase in basal calcium level did respond, although the strength of this response was lower than that prior to the thapsigargin treatment (Moller et al. 2000). These results support the involvement of ionotropic as well as metabotropic receptors in ATP mediated calcium response, but do not explain why there are two different responses to thapsigargin treatment in microglia. Selective P2X receptor agonists 2-methylthio ATP and αβ-methylene ATP activate all P2X receptor types, but their power to do so is variable between receptor types (North & Surprenant 2000). Interestingly, 2-methylthio ATP but not αβ-methylene ATP effectively increased [Ca2+]i in microglia (Inoue 2006c). This could be because the P2X receptor agonist αβ-methylene ATP is a weak activator of P2X4 and P2X7 receptor types as compared to 2-methylthio ATP (North & Surprenant 2000; Volonte et al .2006). Treatment with suramin (100 µM, a broad antagonist of P2 receptors) was not effective enough to inhibit the ATP-evoked increase in [Ca2+]i (20 out of 20 cells) (Inoue 2006c). Suramin inhibits P2X4 and P2X7 receptor types only at higher concentration (North & Surprenant 2000). Selective P2X7 receptor agonist 2'- and 3'-O-(4-

benzoylbenzoyl) adenosine 5'-triphosphate (BzATP) evoked a long-lasting increase in [Ca2+]i even at 1 μM concentration, but at this concentration ATP does not cause any change in [Ca2+]i, suggesting that BzATP is the more potent activator of P2X7 receptors. One hour pretreatment with oxidized ATP (oATP; 100 μM), a selective antagonist of P2X7 receptors, was able to block the increase in [Ca2+]i induced by ATP (Inoue 2006c).

Mizoguchi et al. (2009) have demonstrated that BDNF induces sustained elevation of intracellular $Ca^{2+}$ through binding to the TrkB receptors on microglia (Fig 1.4). The use of either a calcium-free medium or thapsigargin (200nM) was able to prevent the BDNF-induced microglial $[Ca^{+2}]_i$ increase completely, indicating that both extracellular calcium and calcium released from internal stores are equally required for achieving the increase in $[Ca^{2+}]_i$. In contrast, this study also demonstrated that pretreatment with BDNF suppresses IFN-γ induced calcium influx. This inhibitory effect of BDNF on $[Ca^{+2}]_i$ in activated microglia is accompanied by inhibition of nitric oxide release (Mizoguchi et al 2009; Nakajima et al 1998), which may be due to BDNF mediated inhibition of iNOS expression (Mizoguchi et al. 2009). These results suggest a complex role of BDNF in regulation of the microglial inflammatory response. This study did not provide any evidence demonstrating a mechanism for the suppression of IFN- γ responses in BDNF pretreated cells. However, one hypothesis is that elevated basal intracellular $[Ca^{2+}]_i$ due to BDNF pretreatment is responsible for suppression of calcium response. *In vitro* studies of microglia have demonstrated that elevation of microglial basal calcium level leads to reduced ability to respond to other external stimuli (Hoffmann et al. 2003; Moller et al. 2000). The reason for this reduced ability to respond is not well understood.

As discussed earlier, microglia have been reported expressing glutamate receptors *in vitro* and *in vivo* (Eun et al 2004; Noda et al 2000). The *in vitro* study of Yong Eun et al. (2003) also reported that activation of microglial glutamate receptors induces microglial c-Fos gene expression. The study demonstrated involvement of both $Ca^{2+}$ ions entered from the

extracellular medium and $Ca^{2+}$ released from the intracellular stores in induction of c-Fos expression in microglia. Even treatment with ionomycin was sufficient to induce microglial c-Fos expression (Eun et al 2004) suggesting that microglial c-Fos expression is a completely calcium dependant event.

One study of cultured microglia has demonstrated ATP release from glutamate activated microglia (Liu et al. 2006). This study also reported that inhibition of this ATP release can be achieved by specific AMPA receptor antagonists (GYKI 52466), but not by NMDA or any metabotropic glutamate receptor antagonist. Moreover, the study demonstrated that glutamate induced microglial ATP release was inhibited either by inhibiting calcium release from intracellular stores or by applying the protein kinase C inhibitor chelerythrine (Liu et al. 2006). As use of $Ca^{2+}$ free buffer did not inhibit ATP release, the results suggest that calcium release from intracellular stores and activation of protein kinase C are necessary events for glutamate induced ATP release from microglia.

Thus, $Ca^{2+}$ is an important intracellular messenger for microglial function (Fig. 1.5). Detailed downstream mechanisms activated by $Ca^{2+}$ in microglia are perhaps less well characterised but may involve activation of protein kinases.

### *5.2. Protein kinase (p38 MAPK) phosphorylation associated with microglial activation*

Phosphorylation of p38 mitogen-activated protein kinase (p38 MAPK) is required for cell growth, cell differentiation and cell cycle in a variety of cell types. It can be activated by many stimuli, including inflammatory molecules, UV light, LPS and withdrawal of trophic factors. *In vivo* as well as *in vitro* studies have reported increased phosphorylation of p38 MAPK with microglial activation and cytokine production (Ji et al. 2009; Ji & Suter 2007; Wen et al. 2009). MKK3 (mitogen-activated protein kinase kinase 3) and MKK4 are possible intracellular up-stream kinases that lead to p38 MAPK activation in microglia (Brancho et al. 2003; Uesugi et al. 2006). A study of microglia has reported that protein kinase C (PKC) is

also an upstream regulator of p38 MAPK (Nakajima et al. 2004). Activation of p38 MAPK in turn regulates NF-κB, COX-2 and iNOS in microglia, all of which play important roles in cytokine as well as ROS production (Ji & Suter 2007). Studies using drugs that inhibit microglial activation further bear out the above evidence that phosphorylation of p38 MAPK is important for microglial activation and cytokine production (Fordyce et al. 2005; Tikka & Koistinaho 2001).

### *5.3. Role of protein kinase C in microglial activation*

Earlier studies of microglia have shown they express protein kinase C (PKC) in many different isoforms, e.g., α, δ and Є (Nakai et al. 2001). PKC has been reported to activate NADPH oxidase through phosphorylation of $p47^{phox}$ (McNamara et al. 1993; Turgeon et al. 1998). A study by Ryu et al. (2000) has reported that thrombin, a well known protease involved in blood coagulation and wound healing, induces nitric oxide release from microglia in a dose dependent manner. Thrombin activates protein kinase C, mitogen-activated protein kinases and NF-kB, which leads to up-regulation of iNOS expression in microglia and induces NO production (Ji & Suter 2007; Ryu et al. 2000). Interestingly, Uesugi et al. (2006) reported that NF-kB inhibitor ammonium pyrrolidinedithiocarbamate (APDC) could not inhibit LPS- induced TNF-α production in microglia. The study also provided evidence to support previous observations that MKK3/6-p38 MAPK and MKK4-JNK take part in an intracellular signalling cascade that induces TNF-α production in LPS-stimulated microglia. Another study has reported involvement of the α (alpha) isoform of protein kinase C (PKC) and p38 MAPK in TNF-α production from LPS-stimulated microglia (Nakajima et al. 2004). Moreover, this study also demonstrated, using specific pharmacological blockers, that PKC-α is necessary for p38 MAPK activation, suggesting a higher order of PKC-α in the intracellular cascade that stimulates TNF- α production (Fig 1.6).

## 6. Ion channels on microglia and their role in microglial function

### *6.1. Microglia express a variety of ion channels*

An earlier article has extensively reviewed the literature treating ion channels present on microglia (Eder 1998). There is evidence for the presence of $H^+$ channels, $Na^+$ channels, voltage-gated $Ca^{2+}$ channels, $Ca^{2+}$ release-activated $Ca^{2+}$ channels, voltage-dependent and voltage-independent $Cl-$ channels and at least six different types of $K^+$ channels on microglia (Eder 1998). The latter include inward rectifier, delayed rectifier, HERG-like, G protein-activated, as well as voltage-dependent and voltage-independent $Ca^{2+}$-activated $K^+$ channels. Some of these channels are species specific, while others are commonly expressed between species. Rat microglia express inward rectifier $K^+$ channels, HERG-like $K^+$ channels, delayed rectifier $K^+$ channels, $Na^+$ channels, $H^+$ channels, voltage activated $Ca^{2+}$ channels, $Ca^{2+}$ release-activated $Ca^{2+}$ channels and voltage-independent stretch- activated $Cl^-$ channels (Eder 1998). In addition to the types of ion channel expressed in rats, mouse microglia have been shown to express G protein-activated $K^+$ channels and voltage independent $Ca^{2+}$ activated $K^+$ channels (Eder 1998). Human microglia express similar ion channels to mice, except that voltage-dependent $Ca^{2+}$ activated $K^+$ channels and voltage-dependant $Cl^-$ channels are expressed only by human microglia (Eder 1998). Ion channels in microglia are involved in maintaining the membrane potential and may also be involved in regulation of proliferation, activation, and the respiratory burst (Khanna et al. 2001; Kotecha & Schlichter 1999). The expression level of most of these ion channels on microglia depends on their functional state.

### *6.2. Role of $K^+$ channels in microglial function*

Resting microglia express only inward rectifying K+ channels (Norenberg et al. 1992). *In vitro* studies on purine-, LPS-, gamma interferon-, or granulocyte macrophage colony-stimulating factor-stimulated microglia have demonstrated that an outward $K^+$ conductance (Fischer et al. 1995; Langosch et al. 1994; Norenberg et al. 1993; Norenberg et al. 1992) is expressed only in response to activating stimuli. Using patch clamp, Norenberg et

al. (1992) demonstrated that expression of $K^+$ channels depends on the exposure time to inflammatory stimuli. In this study there was a gradual increase in the number of cells showing outward $K^+$ conductance up to 3 hours after LPS exposure, which then gradually decreased after 1 day and become negligible after 5 days despite the continued presence of LPS (Norenberg et al 1992). The study did not investigate the reason for the decreased expression at later time points. A later report demonstrated suppression of the outward current by cyclohexamide (an inhibitor of protein synthesis), suggesting that LPS induced production of new membrane channels (Norenberg et al 1993). The presence of outward $K^+$ channels only on activated microglia suggests that they are involved in the process of microglial activation.

### 6.2.1 Kv 1.5 channels are involved in regulation of microglial proliferation and nitric oxide release but not in chemokine release function

Khanna et al. (2001) reported the presence of both Kv1.5 and Kv1.3 channels in unstimulated microglial cell lysate by isolating proteins. Surprisingly, microglia did not show a Kv1.5-like current, but did show Kv1.3 current as demonstrated by the complete blockade of the voltage-dependent current by the Kv1.3 blocker agitoxin-2 (Khanna et al. 2001). Immunohistochemical analysis using the OX-42 antibody as a marker of microglia, along with antibodies for Kv1.3 and Kv1.5 channels, demonstrated that Kv1.3 is found on the microglial cell membrane while Kv1.5 is present mainly intracellularly. Another *in vitro* study investigated the role of Kv1.5 and Kv1.3 channels in the function of microglia (Pannasch et al. 2006). This study compared the effect of LPS (100ng/ml) on microglia isolated from wild type 129SVEV mouse brains to that on microglia isolated from $Kv1.5^{-/-}$ knockout mice. Unlike in wild type microglia, LPS treatment did not trigger nitric oxide release from $Kv1.5^{-/-}$ microglia, but did cause chemokine release as in wild type microglia. The study also used microglial cells pre-treated with antisense oligonucleotide (AO) for Kv1.5 and for Kv1.3 followed by the LPS treatment as another approach to investigating the role of these channels.

This showed inhibition of NO release by AO Kv1.5 but not by AO Kv1.3, suggesting that Kv1.3 is not involved in the microglial NO release function. The study also reported that decreasing expression of either Kv1.5 or Kv1.3 channels can prevent the LPS mediated decrease in microglial proliferation. These results suggest that LPS mediated inhibition of the microglial cell cycle is via increased expression of these two channels. Moreover, Pannasch et al. (2006) also reported increased microglial proliferation in Kv1.5$^{-/-}$ mice after facial nerve injury *in vivo*. Collectively, these studies suggest that LPS treatment increases expression of microglial Kv1.5 channels, which is responsible for inhibition of microglial cell cycle and increased NO release but not LPS-induced chemokine release.

### 6.2.2 Microglia Kv1.3 channels are required for morphological changes and ROS production via a p38 MAPK independent pathway

Interestingly, an *in vitro* study has reported involvement of microglial Kv1.3 channels in their proliferation (Kotecha & Schlichter 1999) and the respiratory burst (Khanna et al. 2001). Khanna et al. (2001) demonstrated that the phorbol ester PMA (a protein kinase C activator) stimulates respiratory burst that can be inhibited up to 66±8% by a specific blocker of Kv1.3 channels, agatoxin 2. The study also used diphenylene iodonium as a blocker of NADPH oxidase to demonstrate that the PMA-induced respiratory burst was mainly mediated by the activation of NADPH oxidase. Blocking Kv1.3 channels was sufficient to inhibit PMA-mediated microglial morphological changes. The study also demonstrated that not only Kv1.3 but also a blockade of $Ca^{2+}$/calmodulin gated channels SK2, SK3 and SK4 was able to inhibit the PMA-induced microglial respiratory burst, but not the morphological changes (Khanna et al. 2001). Fordyce et al. (2005) also demonstrated inhibition of the respiratory bust by pharmacological blockers of Kv1.3 channels but not by Kv1.2, Kv1.5 and Kv1.6 channel blockade. Interestingly, blocking Kv1.3 type channels was sufficient to prevent microglial superoxide production, but did not change microglial nitric oxide release. Moreover, the study reported that microglia previously activated with LPS

could induce apoptosis of neurons when co-cultured. Neither non-activated microglial cells nor direct action of LPS alone was able to induce such neuronal apoptosis (Fordyce et al. 2005). The authors suggested that the action of peroxynitrite (a product of reaction between superoxide and nitric oxide) from activated microglia induced neuronal apoptosis via caspase-3 activation. The study also reported that Kv1.3 plays a vital role in this superoxide and ROS production in microglia. To demonstrate the cellular mechanism being affected by Kv1.3 blockade, the authors showed that minocycline inhibited neuronal killing and also inhibited activation of p38 MAPK, but that none of the Kv1.3 blockers affected p38 MAPK activation (Fordyce et al. 2005). These results suggest that the Kv1.3 blocker has neuroprotective effect which via inhibiting a pathway other than p38 MAPK activation in microglia unless that p38 MAPK is an upstream regulator of the Kv1.3 channel.

Integrins are transmembrane glycoproteins responsible for regulation of adhesion and the ability of immune cells to migrate. Microglia express several different integrins including α4, α5, α6, β1, lymphocyte function associated antigen-1 and Mac 1 β2-integrin. Interestingly, the pharmacological inhibition of Kv1.3 channels or of β-integrin also inhibits microglial migration towards various chemo attractants, although this cited study did not test the effect of ATP (Nutile-McMenemy et al. 2007). These results clearly indicate that Kv1.3 channels are also involved with microglial migration.

### 6.2.3. Microglial Kv1.1 and Kv1.2 channels are involved in cytokine, nitric oxide and ROS production

Apart from Kv1.3 and Kv1.5 channels, Kv1.1 and Kv1.2 have also been reported to be involved in the microglial activation process. Kv1.1 and Kv1.2 are shaker-like voltage gated $K^+$ channels. These channels are present in early postnatal microglia but disappear in ramified microglia present in adult rat brains. *In vitro* studies have reported induced expression (mRNA as well as protein) of Kv1.1 and Kv1.2 channels in microglia upon activation with LPS or hypoxia (Li et al. 2008; Wu et al. 2009). Li et al. (2008) also reported

that microglial activation via ATP increases microglial Kv1.2 expression. Interestingly, a recent study by Wu et al. (2009) of BV-2 cells demonstrated that neutralising microglial Kv1.1 using an antibody results in reduction of microglial cytokine (TNF-α, IL-1β) and nitric oxide production upon exposure to LPS or hypoxia. However, the authors did not suggest any mechanism for this Kv1.1 dependant cytokine and nitric oxide release. Interestingly, Kv1.1 channels are also expressed by neurons in the paraventricular hypothalamus, where they have been reported to be involved in nitric oxide signalling (Yang et al. 2007). Li et al. (2008) also showed, using microglia and BV-2 cells, that Kv1.2 channels are required for microglial secretion. An inhibitor of Kv1.2 channel successfully reduced microglial cytokine mRNA production (TNF-α and IL1-β) and completely prevented ROS production in microglia exposed to LPS or hypoxia (Li et al. 2008). Notably, none of the studies of Kv1.1 and Kv1.2 channels have reported complete inhibition of cytokine production, suggesting the involvement of other pathways or ion channels.

### *6.3. Role of $H^+$ channels in the functioning of microglia*

$H^+$ channels in neutrophils are involved in superoxide anion production demonstrated by blocking this channel with $Zn^{2+}$ or $Cd^{2+}$ (Henderson et al. 1988). This study also suggested involvement of these channels in maintaining pH in neutrophils. $H^+$ channels are present on microglia but little information is available on their functional role.

### *6.4. Role of sodium channels in microglial function*

Cultured rat microglia express sodium channels Nav1.1, Nav1.6 and Nav1.5, but do not express detectable levels of Nav1.2, Nav1.3, Nav1.7, Nav1.8, or Nav1.9 (Black et al. 2009). Sodium channel blockading with phenytoin (40 μM) and TTX (0.3 μM) significantly reduced phagocytic activity of LPS-activated microglia and migration in ATP-activated microglia, which is consistent with a role for Nav1.6 in microglial function. Inhibition of these channels using phenytoin significantly inhibited IL-1α, IL-1β, and TNF-α release from

LPS-stimulated microglia (Black et al. 2009). Microglia from mice which lacked Nav1.6 channels showed an approximately 65% reduction in phagocytic capacity compared to microglia from wild type mice (Craner et al. 2005). No study has investigated the role of sodium channels in microglial proliferation.

### *6.5. Role of calcium channels in microglial function*

As discussed earlier, rat, mice and human microglia express a variety of $Ca^{2+}$ channels, including voltage-gated $Ca^{2+}$ channels and $Ca^{2+}$ release-activated $Ca^{2+}$ channels (Eder 1998; Tokuhara et al. 2010). A recent study by Tokuhara et al. (2010) demonstrated involvement of N-type calcium channels in monocyte chemoattractant protein-1 (MCP-1) production from microglia. MCP-1 released from glial cells acts as chemokine and attracts a variety of cells including monocytes, T lymphocytes and dendritic cells (Simpson et al. 1998). Store operated $Ca^{2+}$ entry (SOCE) is one of the mechanisms that supply $Ca^{2+}$ for intracellular processes in microglia (Ohana et al. 2009). This study also demonstrated that $Ca^{2+}$ release-activated $Ca^{2+}$ channels are responsible for SOCE in cultured microglia. Entry of $Ca^{2+}$ through SOCE then triggers activation functions in microglia, although $Ca^{2+}$ entry through ligand gated channels also plays a role (as discussed earlier). Despite the rapid pace of discovery of novel $Ca^{2+}$ permeable channels on microglia, knowledge about the involvement of individual $Ca^{2+}$ channels in microglial function is limited and requires further investigation.

## 7. Minocycline as an inhibitor of microglial activation

Minocycline is an antibiotic of the tetracycline class. Recent studies of microglia and animals have demonstrated an inhibitory action of minocycline on microglial activation (Fan et al. 2005b; Fordyce et al. 2005; Krady et al. 2005; Tikka et al. 2001). A study of cultured microglia has reported minocycline mediated inhibition of microglial migration towards brain homogenate, LPS, glutamate, and ADP, but not towards ATP (Nutile-

McMenemy et al. 2007). The study also reported that the inhibitory action of minocycline on microglial activation is time- and concentration-dependent. The greatest inhibitory effect of minocycline was observed at 120 minutes and 60μM but not at 1μM concentration (Nutile-McMenemy et al. 2007). Minocycline also inhibits proliferation, release of inflammatory cytokines and nitric oxide production from LPS-activated microglia (Henry et al. 2008; Tikka et al. 2001; Tikka & Koistinaho 2001).

Details of the exact mechanism by which minocycline inhibits microglial activation are not known, but it has been reported to inhibit certain cellular machinery that is characteristic of microglial activation. For example, the *in vitro* study of Fordyce et al. (2005) has reported inhibition of LPS-induced p38 MAPK activation in microglia. Minocycline appears to be able to inhibit multiple intracellular pathways and intracellular signalling molecules causing inhibition of various functions of activated microglia. The inhibitory effect of minocyline on microglial activation can be characterised as inhibition of matrix metalloproteinases, impairment of microglial cytokine production, inhibition of microglia iNOS expression, inhibiting phorphorylation of p38 MAPK and COX-2 expression in microglia (Giuliani et al. 2005; Henry et al. 2008; Krady et al. 2005; Tikka & Koistinaho 2001). Minocycline pre-treatment can inhibit induction in microglial COX-2 expression in TNF-α treated microglia, but not in IL-1β or IL-6 treated microglia (Krady et al. 2005). These results suggest that minocycline inhibits microglial activation but not in response to all the activating stimuli. As discussed above, all the microglial activators lead to increased intracellular calcium in microglia, but the direct effect of minocycline on intracellular calcium has not been investigated.

Recently, it has been shown that minocycline inhibits phosphorylation of microglial PKC-α and PKC-βII in IFN-γ stimulated microglia (Nikodemova et al. 2007). This study also demonstrated that via inhibiting PKC α / βII, minocycline reduced microglial MHCII expression (Fig 1.5). The ability to express MHCII makes microglial cells antigen

presenting cells, which can in turn activate T cells. Therefore, reduced MHCII expression may reduce intervention of T cells at the site of brain injury. As discussed previously, the pharmacological inhibition of Kv1.3 channels or of β-integrin inhibits microglial migration. Interestingly, minocycline reduced expression of both Kv1.3 and β -integrin in microglia (Nutile-McMenemy et al. 2007).

Both *in vitro* and *in vivo* studies indicate that minocyline can exert neuroprotection via a direct action on neurons (Gonzalez et al. 2007; Pi et al. 2004). Minocyline has been shown to inhibit neuronal apoptosis by inhibiting neuronal caspase 1 and caspase 3 activation and by inhibiting cytochrome c release (Chen et al. 2000; Lee et al. 2004; Tikka et al. 2001; Tikka & Koistinaho 2001; Zhu et al. 2002). Thus, the reported neuroprotection by minocycline treatment in various animal models of neuropathic pain and neurodegenerative disease may be due to a direct action of minocycline on neurons in addition to inhibition of microglial activation.

## 8. Cardiovascular centres in the brain

Inflammation in the CNS is reported during various pathological conditions including diabetes and heart failure (Lindley et al. 2004; Tsuda et al. 2008; Yu-Ming Kang 2009), although the involvement of microglia in these conditions has not been addressed. Various animal studies on diabetic rats as well on rats with myocardial infarction have reported abnormally increased neuronal activity and inflammation in specific cardiovascular centres of the brain (Lindley et al. 2004; Zheng et al. 2002).

Blood pressure and heart rate are regulated in a narrow range by the combined function of sympathetic and parasympathetic nerve activity. Both sympathetic and parasympathetic nerves are controlled by the various brain centres also known as cardiovascular centres. A detailed description of the anatomy, location and function of some of the most important cardiovascular centres is given below.

### *8.1. Paraventricular hypothalamic nucleus (PVN)*

The paraventricular hypothalamic nucleus (PVN) is located adjacent to the third ventricle and projects to diverse brain regions, including the brain stem, other hypothalamic regions and the spinal cord. The rostroventral medulla (RVLM), caudal ventrolateral medulla (CVLM) and nucleus tractus solitarius (NTS) are major brain stem sites that receive projections from the PVN, while the acuate nucleus, ventromedial hypothalamus and median eminence are hypothalamic areas that receive substantial projections from the PVN. The PVN is also a site for biosynthesis of a variety of neuropeptides, including arginine vasopressin, oxytocin, and corticotropin releasing hormones, and endogenous opiate peptides (Kawashima et al. 2004; Millan et al. 1984; Vandesande et al. 1974; Vandesande & Dierickx 1975; Vandesande et al. 1975) as well as neurotransmitters including norepinephrine (NA), epinephrine, dopamine, acetylcholine and y-aminobutyric acid (Flak et al. 2009; Liposits & Paull 1989; Panksepp et al. 1973; Peinado & Myers 1987).

Functionally and anatomically, there are two major categories of PVN neuron: magnocellular and parvocellular. The majority of parvocellular neurons are located close to the wall of the third ventricle, while the magnocellular neurons are located in parts of the PVN that are relatively distant from ventricle edge. Parvocellular neurons are mainly involved in regulating activity of the sympathetic nervous system, while magnocellular neurons are responsible for neurohormone (arginine vasopressin and oxytocin) secretion in the posterior pituitary gland. Hyperthermia and hemorrhage, but not hypotension, increase the activity of non-RVLM projecting PVN neurons, suggesting they have a role in blood volume and temperature control (Badoer & Merolli 1998). Activation of spinally projecting PVN neurons upon heat exposure has been reported in a rat model (Cham et al. 2006). The PVN also represents a major site for nitric oxide-producing neurons in the brain. Some of these neurons project to the spinal cord and are responsive to heat exposure (Cham et al. 2006). Nitric oxide signalling in the PVN plays an important role in blood pressure regulation via its effects on

renal sympathetic nerve activity. A nitric oxide donor injected into the PVN reduced arterial blood pressure, heart rate, and renal sympathetic nerve activity via activating the GABAnergic system (Zhang & Patel 1998). Altered nitric oxide signalling in the PVN has been reported in an animal model of type-1 diabetes, suggesting its possible role in cardiovascular complications of diabetes (Zheng et al. 2006). Interestingly, resident microglia can also serve as a source of nitric oxide (Choi et al. 2003) in these cardiovascular centres. Nitric oxide modulates the secretion of AVP (Cao et al. 1996; Chiodera et al. 1994; Kadowaki et al. 1994; Ota et al. 1992). Electrical stimulation of PVN induces an analgesic effect via enhanced arginine vasopressin (AVP) release into the brain stem. This analgesic effect is at least partially mediated by AVP action on NTS neurons (Jiang et al. 1991). Collectively, these studies suggest that the PVN, by means of its diverse projections to other CNS regions and secretions of neuropeptides and neurotransmitters, plays a major role in controlling cardiovascular activity, maintaining fluid homeostasis, controlling temperature, controlling hunger and thirst as well as in modulating pain (Badoer 1998; Badoer & Merolli 1998; Badoer et al. 2002; 2003; Cham & Badoer 2008b; Cham et al. 2006; Yang et al. 2009a; Yang et al. 2009b; Zhang & Patel 1998; Zhang et al. 1998; Zheng et al. 2006).

### *8.2. Supraoptic nucleus (SON)*

The supraoptic nucleus (SON) is a region of the hypothalamus situated at the base of the brain, adjacent to the optic chiasm. The SON also plays a vital role in blood volume and blood pressure homeostasis. The nucleus contains a large population of arginine vasopressin (AVP) and oxytocin (Oxy) producing neurons (Doi et al. 1998; Moos et al. 1984). The SON has projections to the pituitary gland, where it delivers these neurohormones which are then released and enter the blood stream when required. Apart from its role as a hormone acting peripherally on the kidneys and arteries, vasopressin also acts as neurotransmitter in the brain. Central administration of AVP (intracerebroventricular injection) in pentobarbital anesthetised rats reduces blood pressure, while the same concentration in conscious rats

increases mean arterial blood pressure and heart rate (Zerbe & Feuerstein 1985). Therefore, there is clear evidence for the different effects of vasopressin in the presence and absence of anesthesia (pentobarbital). Intracerebroventricular injection of AVP is also reported to increase plasma norepinephrine and epinephrine levels in conscious rats, suggesting a contribution from elevated sympathetic nerve activity in the increased mean arterial pressure (King et al. 1985).

### *8.3. Nucleus tractus solitarius (NTS)*

The nucleus tractus solitarius (NTS) is an important area of brain stem involved in cardiovascular regulation. The NTS receives projections from and has projections to other areas involved with cardiovascular regulation, including the PVN and rostroventral medulla. This allows the NTS to mount a coordinated response to regulate blood pressure changes. The NTS also contains nitric oxide producing neurons (Yang et al. 1999). Microinjection of L-arginine (a substrate for enzymes producing nitric oxide) into the NTS reduces renal sympathetic nerve activity (Tseng et al. 1996).

The NTS receives and processes afferent signals from a variety of visceral regions and organs. The NTS receives afferent projections from the carotid chemoreceptors, arterial baroreceptors, and cardiopulmonary receptors, and as a function of this information, produces autonomic adjustments in order to maintain arterial blood pressure within a narrow range of variation (Machado et al. 1997; van Giersbergen et al. 1992). The baroreceptor reflex or baroreflex is one of the mechanisms by which the body maintains blood pressure. The baroreceptor reflex provides a negative feedback loop in which reduced blood pressure suppresses the baroreflex, causing increase in heart rate and then a rise in blood pressure. Alternatively, elevated blood pressure induces baroreflex, which then reduces heart rate and blood pressure. Direct injection of the amino acid L-glutamate and its excitatory analogues into the NTS produce dose-dependent hypotension and bradycardia, a baroreceptor reflex-like response (Talman et al. 1984). This study also demonstrated that neurotransmitters,

acetylcholine and serotonin, produce similar responses upon direct microinjection into the NTS. NTS lesion-induced hypertension is also reported by many studies on rats (Doba & Reis 1973; 1974; Sved et al. 1985). Bilateral electrolytic NTS lesion resulted in elevated plasma levels of vasopressin, norepinephrine and epinephrine, but not in plasma rennin activity (Sved 1986). Based on these results, the authors suggested that NTS lesion-induced hypertension is due to increased sympathoadrenal activity and increased vasopressin release into blood. Increased release of vasopressin is one of the major contributors to hypertension in NTS lesioned rats (Kubo & Kihara 1986; Sved 1986; Sved et al. 1985) but elevated sympathetic drive also contributes (Doba & Reis 1974). The later study demonstrated that intracisternally administered 6-hydroxydopamine (6-OH-DA) (which destroys dopaminergic and noradrenergic neurons) lowered the concentration of norepinephrine only in the spinal cord and blocked the development of hypertension following NTS lesion. Moreover, intravenous injection of the β-receptor blocker propranolol (1mg/kg) partially reversed the elevated blood pressure in these rats. The authors suggested that the fall in blood pressure was due to reduced heart rate in these rats via a direct effect on the heart. By performing adrenalectomy in 6-hydroxydopamine (6-OH-DA) treated NTS-lesioned rats, Doha et al. (1974) demonstrated a complete abolition of the hypertension. They also showed that without adrenalectomoy, 6-hydroxydopamine (6-OH-DA) was unable to fully abolish hypertension. Based on this evidence, the authors suggested that following the destruction of most peripheral sympathetic terminals by 6-OHDA, blood pressure may be partially maintained by increased secretion of catecholamines from the adrenal medulla.

### *8.4. Rostroventral medulla (RVLM)*

The rostroventral medulla (RVLM) is an important autonomic area responsible for controlling blood pressure, blood volume, breathing and many other autonomic functions (Kanbar et al. 2010). The RVLM receives a variety of inputs via its connections with the PVN, NTS and other cardiovascular centres (Accorsi-Mendonca et al. 2009; Badoer 2001;

Cham & Badoer 2008a; Suzuki et al. 1997). RVLM neurons contain nitric oxide synthase (Chan et al. 2001) and unilateral microinjection of L-arginine into the RVLM produced bradycardic effects, hypotension, and reduced renal sympathetic nerve activity (Tseng et al. 1996). Another study of conscious rats demonstrated that increased NO production caused by the over-expression of endothelial nitric oxide synthase (eNOS) bilaterally in the RVLM decreases blood pressure, heart rate, and sympathetic nerve activity in conscious rats (Kishi et al. 2001). Thus, nitric oxide signalling plays an important role in controlling RVLM activity.

The PVN, SON, NTS and RVLM play an important role in cardiovascular regulation. Direct injection of cytokines or nitric oxide in any of these regions causes increase or decrease in blood pressure, heart rate and/or sympathetic nerve activity. Therefore, activation of local microglia present in these regions could also serve as a potential source of these cytokines as well as of nitric oxide. Hence, microglial activation in these cardiovascular regions needs to be investigated in diabetes rats as well as in diseases where cardiovascular disturbances occur and brain inflammation is implicated. Another possibility is that elevated peripheral cytokines serve as a trigger for microglial activation in cardiovascular centres.

## 9. Studies reporting the role of elevated peripheral cytokines in activating cardiovascular centres in the brain

Plasma cytokines are reported to be up-regulated in humans with a failing heart. Studies have shown a correlation between the severity of heart disease and plasma cytokine levels. Interestingly, even in diabetic patients plasma cytokines are reportedly elevated. Zheng et al. (2003) showed that a single i.v. injection of TNF-α (one of the cytokines reported to be up-regulated in humans or animal models of hypertension) increased neuronal activity in the PVN and RVLM. Interestingly, i.c.v. injection of a COX-2 inhibitor reduced the effect of peripherally injected TNF-alpha on blood pressure, heart rate and sympathetic nerve activity in rats (Zhang et al. 2003) . The authors hypothesised that peripheral injection of TNF-alpha acts on perivascular macrophages present in the blood-brain barrier that release PGE2 via

increased COX-2 expression. This PGE2 then acts on PVN neurons to increase blood pressure through an increase in renal sympathetic nerve activity. In support of this, injection of PGE2 (50 ng) into the PVN increased PVN and RVLM activity and sympathetic drive (Zhang et al. 2003). Results of a recent study by Yu et al. (2010) also supported this hypothesis, as the authors reported increased COX-2 activity, particularly in the PVN, and increased PGE2 in the cerebrospinal fluid in myocardially infarcted animals, but the cellular location was not known (Yu et al. 2010). A similar role for PGE2 as a secondary messenger in the brain has also been suggested by other studies (Fabricio et al. 2006; Watanobe & Takebe 1994). However, the possibility of microglia as a central source of PGE2 has not been investigated by any of these studies.

It is evident from the study of Rivest et al. (1992) that i.c.v. injection of IL-1β increases neuronal activity in the PVN and arcuate nucleus. A recent study demonstrated that hypertension is induced by cytokines specifically acting on PVN neurons by injecting IL-1β in the PVN of naïve rats (Shi et al. 2010a). Another study has reported that IL1β administered intravenously increases mean arterial blood pressure, heart rate and plasma AVP levels (Yamamoto et al. 1994). Three doses, 1.73 (low dose, LD), 8.63 (medium dose, MD), and 43.16 pmol/100 grams body weight (high dose, HD) of human recombinant IL-1R were given intravenously (i.v) in conscious rats, and all the doses increased serum levels of AVP. The lowest dose increased mean arterial blood pressure but not heart rate, while the other two doses caused initial decreases (at 30 minutes) followed by increased blood pressure as well as heart rate, which lasted at least 120 minutes. Interestingly, the lowest dose of IL1β increased rectal temperate while the other two doses decreased rectal temperature (Yamamoto et al. 1994). This result clearly indicates that IL1β has different effects on blood pressure, heart rate, and thermoregulation at low and high doses. The authors hypothesised that these effects of IL1β are mediated via PGE2, but no convincing evidence was given for this hypothesis. The study of Veening et al. (1993) used Fos-immunohistochemisty to demonstrate that IL-1β

injected intravenously can activate neurons in the hypothalamus. They reported the highest density of Fos positive neurons in the paraventricular hypothalamus. These Fos positive neurons were mainly in the parvocellular part of the PVN. Double label immunohistochemistry revealed that they were corticotropin-releasing hormone positive, suggesting that intravenous IL-1β treatment activates the hypothalamic pituitary-adrenal axis (Veening et al. 1993). A recent study by Shi et al. (2010) demonstrated activated microglia specifically in the PVN region of the hypothalamus in the chronic (Angiotensin II) Ang II infusion rat model of hypertension. Increased levels of proinflammatory cytokines and reduced levels of anti-inflammatory cytokines in the PVNs of hypertensive rats were reported. The authors also demonstrated that increasing expression of IL-10 in the PVN by administering IL10 genes via viral vectors can attenuate Ang II-induced hypertension in rats. The study demonstrated that minocycline treatment inhibited microglial activation in the PVN and attenuated hypertension, suggesting microglia as a source of proinflammatory cytokines in the PVN at least in part responsible for Ang II-induced hypertension.

## 10. Leptin action on the hypothalamus involves microglia

Peripheral leptin may also serve as activator of microglia in the hypothalamus and other cardiovascular centres. Leptin is a hormone produced by adipocytes involved in regulation of food intake, blood pressure, and body weight (Campfield et al. 1995; Hopkins et al. 1996; Schwartz et al. 1999). Leptin performs all these functions by acting primarily in the hypothalamic region of the brain. Initially, it was thought that obese humans may have less leptin, which might be responsible for their obesity, but now it is well known that such individuals are hyperleptinemic, implying they are leptin-resistant. Halaas et al. (1997) reported that i.c.v. infusion of leptin reduced body fat mass by reducing food intake, but not by increasing energy expenditure in lean mice. The study also reported that i.c.v. infusion of the same amount of leptin was 100 times less effective in terms of reducing body fat mass and

food intake in diet-induced obese mice. Moreover, the effects of subcutaneous leptin injection at higher doses were comparable to the results of i.c.v. leptin, suggesting that obesity leads to leptin resistance and that this resistance is probably due to defective leptin responses in the hypothalamus (Halaas et al. 1997).

The hypothalamic arcuate nucleus (Arc) is a major site of leptin action (Nagamori et al. 2003). Proopiomelanocortin (POMC) neurons and neuropeptide-Y producing neurons in the arcuate nucleus express a high density of leptin receptors and serve as a principle source of neuropeptide modulators and melanocortins (Cone 1999; Cowley et al. 2001; Hakansson et al. 1998; Kalra et al. 1999). The Arc has strong connections with the PVN, and disruption of activity in either of these two nuclei can induce obesity, as demonstrated by experiments on animals (Baker & Herkenham 1995; Sawchenko & Swanson 1983). Neuropeptide Y (NPY) is synthesised by neurons in the Arc. When injected into the PVN, it stimulates food intake and causes obesity upon cerebroventricular infusion (Stanley et al. 1992).

There is mounting recent evidence that leptin action in the brain is at least partially mediated by the cytokine IL-1β. Mice lacking the gene for the endogenous IL-1R (receptor for interleukin-1) antagonist (IL-1ra) are more resistant to diet-induced obesity as compared to wild type controls (Garcia et al. 2006; Irikura et al. 2002; Matsuki et al. 2003; Somm et al. 2005). Interestingly, several studies have reported that IL-1R1 knockout mice are resistant to the appetite suppressing effect of leptin, suggesting that the anti-appetite effect of leptin may involve the cytokine IL-1β (Garcia et al. 2006; Luheshi et al. 1999). A recent *in vitro* study by Pinteaux et al. (2007) showed that microglia express receptors for leptin, and that stimulation with leptin induces IL-1β release from microglia (Pinteaux et al. 2007). The POMC neuron in the Arc express receptor for IL-1β and i.c.v. injection of IL-1 β can activate these neurons (Scarlett et al. 2007), suggesting that the action of leptin in Arc is mediated via IL-1β from microglia.

## *11. Summary and Hypothesis*

In summary, microglia perform a protective function by removing damaged neurons, extracellular debris, and infectious agents from the central nervous system. A variety of stimuli, including LPS, purines, cytokines, thrombin and leptin (Badoer 2010a; Fan et al. 2005b; Pinteaux et al. 2007; Wang et al. 2005b) can activate these microglia. Upon activation, they can serve as source of inflammatory cytokines, glutamate, nitric oxide and ROS in the CNS (Krady et al. 2005; Li et al. 2008; Mander et al. 2006; Mizoguchi et al. 2009; Sawada et al. 1999; Zheng et al. 2008). Various studies of humans and animal models of neurodegenerative diseases and neuropathic pain have demonstrated microglial activation and inflammation in the CNS (Tsuda et al.,2007; Aloisi et al.,2001; Swada et al.,2006). Recent studies have demonstrated the neuromodulatory role of activated microglia (Lu et al.,2009), and suggested this could be the cause of excitotoxicity mediated neuronal death. Various animal studies of diabetic rats as well of rats with myocardial infarction have reported abnormally increased neuronal activity and inflammation in specific cardiovascular centres of the brain (Lindley et al.,2004; Gullilam et al.,2007). Despite this, the involvement of activated microglia in this increased neuronal activity has never been investigated. Various animal studies of diabetic models and models of hypertension have reported that elevated peripheral cytokines and/or leptin may be a trigger for the central inflammation (Gullilam et al.,2007; Mayers MG Jr., 2004) but it is not clear if microglia are involved in this process. Hence, I am hypothesising that microglia are activated in cardiovascular centres in rat models of diabetes and myocardial infarction, and that these activated microglia contribute to the pathology and reported cardiovascular complication in both diseases.

## Figures:

**F**ig. 1.1

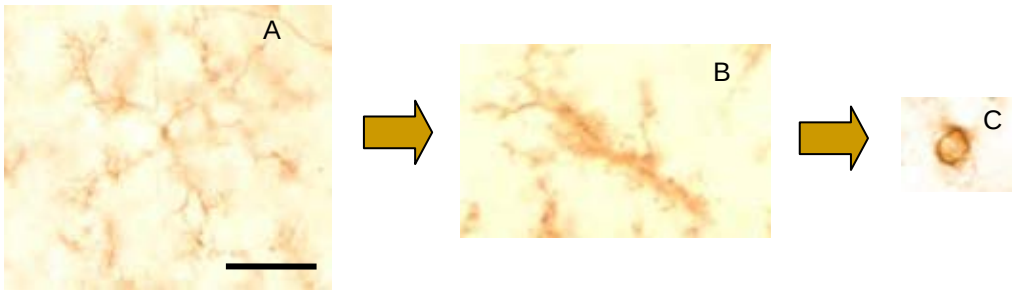


**F**ig. 1.1 : Morphological features of OX-42 stained rat microglia. Figure shows (A) ramified (B) activated and (C) phagocytic microglia in adult rat brain (Scale bar = 10µm).

Fig. 1.2

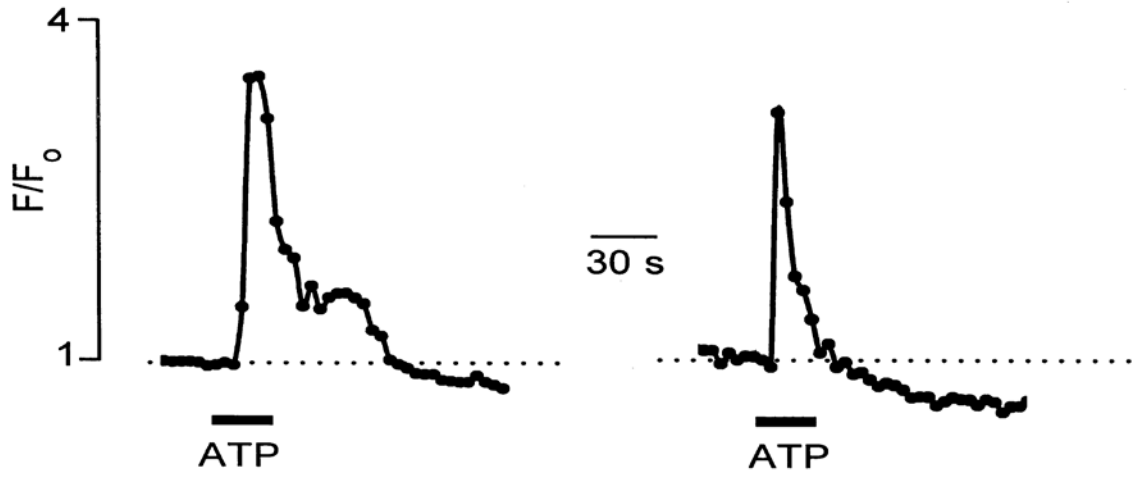


**Fig. 1.2** : ATP-triggered $[Ca^{2+}]i$ signals in microglia are modified by changes in extracellular $Ca^{2+}$. Change in fluorescence ratio ($F/F_0$) in response to ATP (100 μM) application for 30 seconds indicating change in intracellular calcium in presence [left] and in absence [right] of $Ca^{2+}$ in the extracellular medium [Source: Moller et al. (2000)].

**Fig. 1.3**

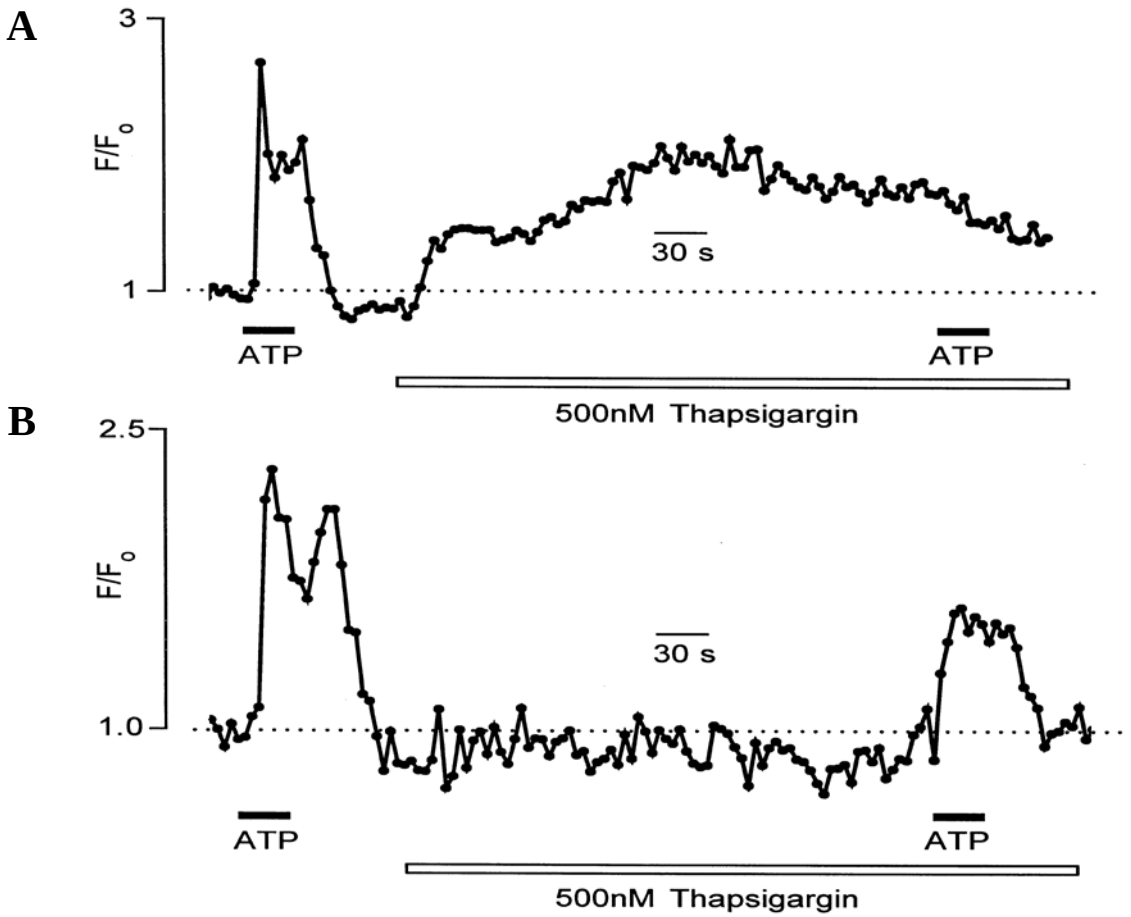


**Fig. 1.3:** ATP-triggered $[Ca^{2+}]i$ signals in microglia are modified by thapsigargin. A 5-min incubation with thapsigargin (500nM) triggered an increase in $F/F_0$ fluorescence ratio and abolished the ATP-induced change fluorescence ratio ($F/F_0$) in a cultured microglial cell (Panel A). In a second population thapsigargin (500nM) application did not increase the fluorescence signal, but ATP still was able to produce a response after 5 min of incubation with thapsigargin (Panel B) [Source: Moller et al. (2000)].

**Fig. 1.4**

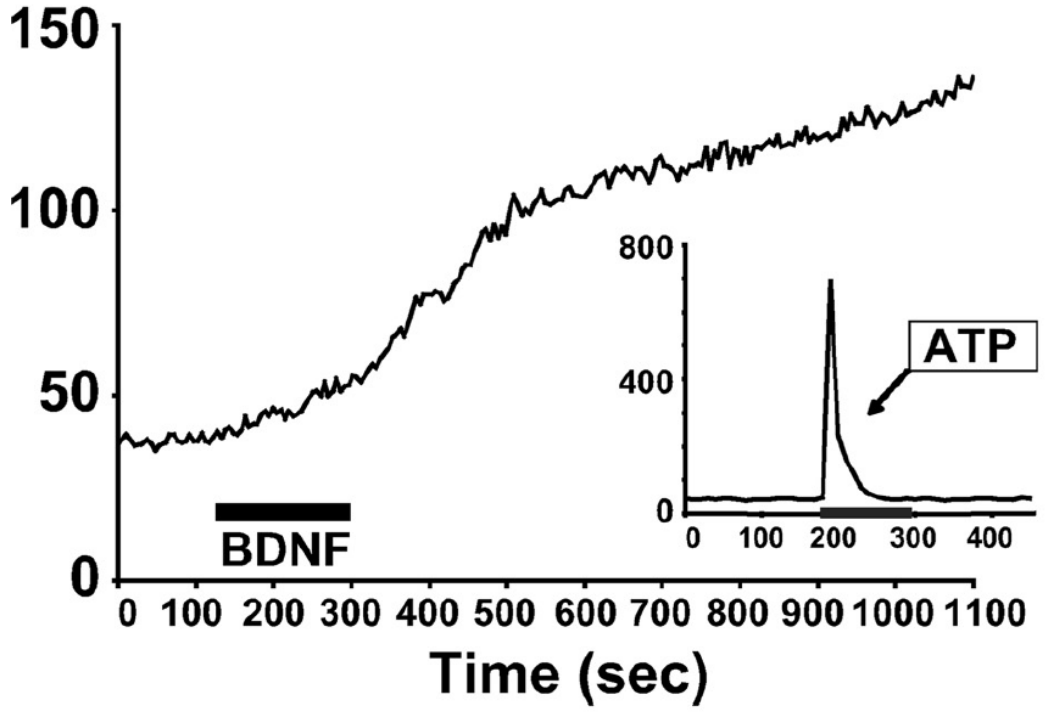


Fig. 1.4 : BDNF (20ng/ml for 3 minutes) induced a sustained increase in $[Ca^{2+}]i$ in primary rat microglia. The inset shows that ATP (100 μM for 2 minutes) induced a transient increase in $[Ca^{2+}]i$ [ Source: Mizoguchi et al.(2009)].

**Fig. 1.5**

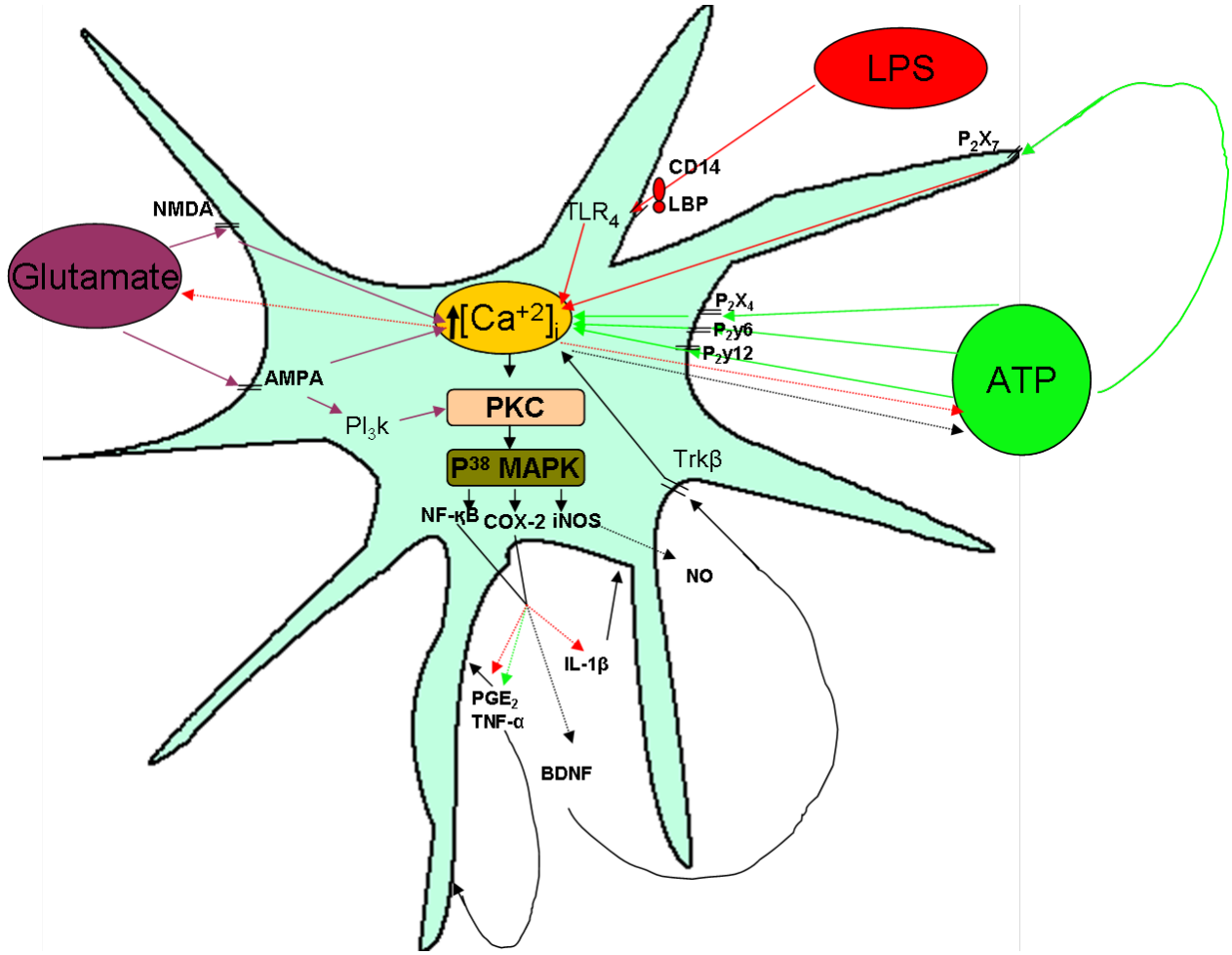


Fig. 1.5 : A schematic representation of the mechanisms of microglial activation showing the central role of $[Ca^{2+}]i$. (Red arrows indicate pathways, receptors and release due to LPS stimulation, Green arrows indicate pathways, receptors and release due to ATP stimulation. Brown arrows indicate pathways, receptors and release due to glutamate stimulation of microglia).

**Fig. 1.6**

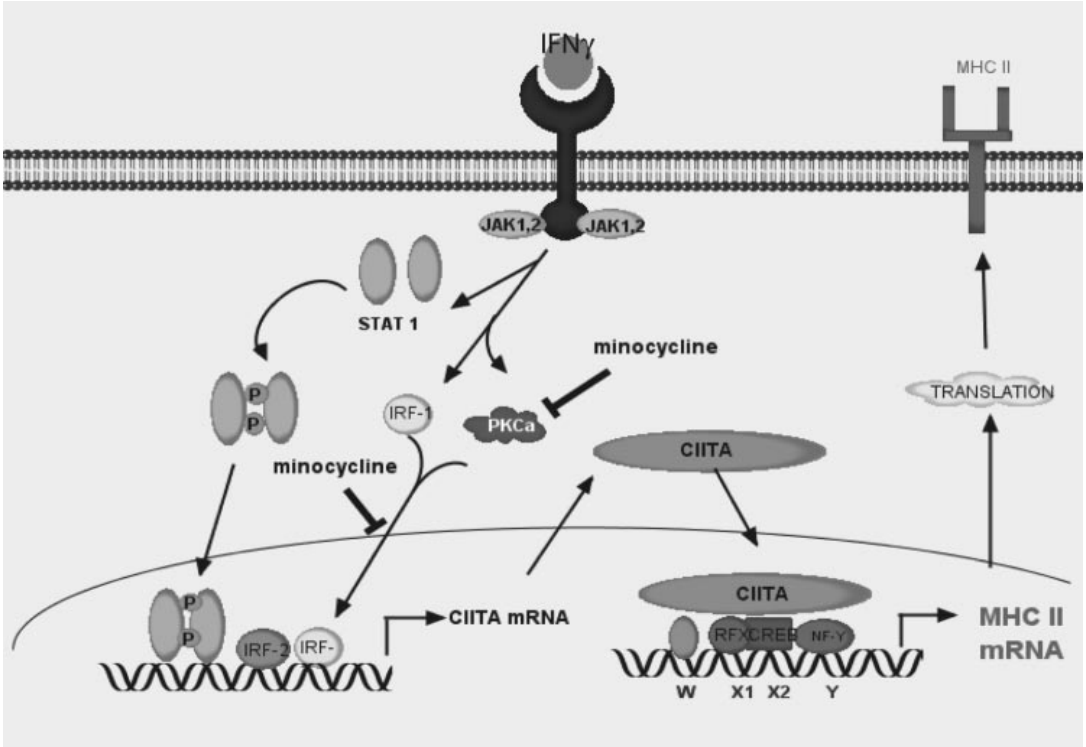


Fig. 1.6：A schematic representation of the mechanism by which minocycline inhibits MHCII expression in microglia stimulated with IFN-γ [Source: Nikodemova et al. (2007)].

# Chapter 2: Microglia are Activated in the Paraventricular Hypothalamic Nucleus Following Myocardial Infarction

## *Introduction*

Heart failure is the inability of the heart to pump sufficient blood adequately through the body and a common cause is myocardial infarction (Hunt et al 2005). In the elderly population the incidence of heart failure is increasing and is associated with a poor prognosis and a severely reduced quality of life (Hunt et al 2005; Kaye et al 1995). Heart failure is characterized by neurohumoral activation, which contributes to salt and fluid retention (via activation of the renin angiotensin system), and an elevation in sympathetic nerve activity to the heart and kidneys (Mann 1999b; Packer 1988). Although an elevated sympathetic nerve activity to the heart, as measured by noradrenaline spillover, correlates with the severity of heart failure and its prognosis in humans (Kaye et al 1995), the cause of the abnormal activation of sympathetic nerve activity in heart failure is not well understood.

Pathophysiological changes in the brain are undoubtedly critical to the elevated sympathetic nerve activity seen in heart failure (Felder et al 2003; Francis et al 2004a). A key site within the brain that contributes to sympathetic nerve regulation is the hypothalamic paraventricular nucleus (PVN) (Felder et al 2003; Francis et al 2004a; Guggilam et al 2007; Patel 2000). In animal models of heart failure there is increased neuronal activity within the PVN which contributes to the abnormally elevated sympathetic nerve activity (Lindley et al 2004; Patel et al 1993). Neurons in the PVN can influence sympathetic nerve activity by; (i) direct connections to sympathetic preganglionic motor neurons located in the intermediolateral cell column of the thoracolumbar spinal cord (Sawchenko & Swanson 1983; Shafton et al 1998), or (ii) indirect connections such as via the pressor region of the rostral ventrolateral medulla (Shafton et al 1998), which projects directly to the sympathetic

preganglionic motor neurons.

A common cause of heart failure and left ventricular dysfunction is myocardial infarction. Following a myocardial infarct there is activation of the immune system, and pro-inflammatory cytokines such as TNF-α, IL-6 and IL-1β are increased in the heart (Levine et al 1990). Circulating levels of the pro-inflammatory cytokines are increased in plasma following damage to the heart and the plasma levels have been shown to correlate with the degree of heart failure and increased mortality in this condition (Maeda et al 2000; Orus et al 2000; Rauchhaus et al 2000; Torre-Amione et al 1996a; Torre-Amione et al 1996b; Tsutamoto et al 1998). Evidence is now emerging to suggest that in addition to the elevation of pro-inflammatory cytokines in the periphery, they are also increased in the hypothalamic PVN (Felder et al 2003; Francis et al 2004a; Francis et al 2004b). The increased level of cytokines in the brain may result from peripherally produced cytokines transported across the blood brain barrier; however, local production also contributes as mRNA levels of pro-inflammatory cytokines are elevated within the hypothalamus (Francis et al 2004a; Francis et al 2004b). The mechanisms responsible for the local production of cytokines are not clarified.

Microglia are the primary immune cells in the brain and during normal physiological conditions, they constantly sample the extracellular environment (Nimmerjahn et al 2005). In response to stressful stimuli, brain injury or infection, microglia become activated and undergo a dramatic morphological change from their 'normal' ramified appearance to a morphology where the soma becomes enlarged and their processes become shorter and ultimately can retract entirely (Nakajima & Kohsaka 2001; Stence et al 2001a; Streit et al 1988; Streit & Kreutzberg 1988). Activated microglia increase their production of various neurochemicals includings CD11b, a protein that is expressed on the surface of microglia and is involved in immune processes. When microglia are activated they also secrete cytokines and thereby contribute to the local elevation of pro-inflammatory cytokines reported in conditions like Alzheimer's, Parkinson's, and chronic neuropathic pain (Liu 2006;

Mrak et al 1995; Sawada et al 2006). Whether this occurs in following a myocardial infarction is unknown. Thus, the aim of the present study was; firstly, to investigate whether microglia are activated in the PVN following a myocardial infarction in the rat, and secondly to determine whether the activation was generalized by investigating whether microglia in the ventral hypothalamus adjacent to the PVN were activated. We also examined areas of the cortex.

## *Methods*

### Animals

Adult male Sprague Dawley rats were obtained from the Animal Resource Centre (ARC, Western Australia). All experimental protocols used in this study were performed in accordance with the Prevention of Cruelty to Animals Act, Australia 1986, conformed to the guidelines set out by the National Health and Medical Research Council of Australia (2007) and were approved by the St Vincent's Hospital animal ethics committee. Under general anesthesia (3% isoflurane in oxygen), a myocardial infarction was induced by ligation of the left anterior descending coronary artery (N = 8 survived) as previously described (Kompa et al 2008). To minimise the variation in infarct size, the ligation was aimed about 2mm below the apex of the left atrium left of the pulmonary arch. The survival rate was 75%. Sham animals underwent the same procedure except the coronary artery was not tied (N = 5). All animals were monitored daily and allowed free access to food and water. At 2 weeks (N = 3) or 5 weeks (N = 5) after the myocardial infarction or the sham procedure, the rats were anaesthetized with ketamine and xylazine (80 mg/kg and 10 mg/kg respectively i.p.) and echocardiography was performed using a Vivid 7 echocardiography machine with a 10-MHz phased array probe (GE Vingmed, Horten, Norway). Echocardiographic images in the first instance were obtained from a 2 dimensional parasternal short axis view of the left ventricle at the mid-papillary muscle level. From this view one dimensional m-mode images were taken

for the determination of percentage fractional shortening (Phrommintikul et al 2008). A 2-dimensional parasternal long axis view was obtained for the determination of ejection fraction using single plain area-length method. ECG data was acquired simultaneously. All parameters were assessed using an average of 3 consecutive cycles, and calculations were made in accordance with the American Society of Echocardiography guidelines (Schiller et al 1989). All data were acquired and analysed by a single blinded observer using EchoPAC (GE Vingmed, Horten, Norway) offline processing. Immediately after the echocardiography procedure, a Millar catheter was introduced into the left ventricle via the right carotid artery to measure left ventricular end diastolic pressure and obtain dP/dtmax (a measure of left ventricular contractility). Technical difficulties prevented haemodynamic measurements in one sham animal and in one rat at 5 weeks after the myocardial infarction.

## Tissue collection

On completion of the hemodynamic measurements, the animals were decapitated. The brains were removed and immediately immersed in freshly prepared, ice cold 4% paraformaldehyde in phosphate buffered saline (PBS) (0.1M, pH 7.2) and stored for 4 hours at $4^{o}$C. The brains were then transferred to a solution containing 30% sucrose in PBS and left for approximately 48 hours at $4^{o}$C. The hearts and lungs were also removed, blotted dry and weight measured.

## Immunohistochemistry

Microglia were detected immunohistochemically by the presence of the protein CD11b (clone OX-42). This protein is expressed on the surface of microglia and forms part of complement receptor 3 and its levels increase markedly upon activation of microglia. (Kim et al 2000; Tsuda et al 2003). Serial coronal sections (20 µm thick) of the brain were cut using a cryostat (Leica, CM1900). One in five sections was collected, placed onto gelatin coated slides, dried for 2 hours at room temperature and then processed immunohistochemically. Standard immunohistochemical procedures were performed in which endogenous peroxidase

activity was blocked by 0.5% $H_2O_2$ for 30 minutes. The sections were incubated in 10% normal horse serum (NHS) for 60 minutes prior to 0.5% Triton X-100 for 10 minutes to facilitate antibody penetration. Subsequently, the sections were incubated for 72 hours with a mouse monoclonal primary antibody directed against CD11b (clone OX-42) (1:100, Chemicon, Temecula, USA) in 2% NHS and 0.2% Triton X-100 in PBS. This was followed by incubations in a biotinylated antimouse secondary antibody raised in horse (1:100, rat adsorbed), (Vector Laboratories, Burlingame, USA), and Extravidin (1:400, Sigma-Aldrich, St Louis, USA), for 2 hours each. All washes and solutions were made using phosphate buffered saline (pH=7.2). 3,3' Diaminobenzidine hydrochloride (0.05%) (Sigma-Aldrich, St Louis, USA) was used as the chromogen. Sections from the respective time point sham control rats and from rats with myocardial infarctions were processed simultaneously.

## Morphological analysis and quantification

### Heart

The atria and right ventricle of the heart were removed. The left ventricle (including the interventricular septum) was cross-sectioned into 2 halves at the mid-papillary level, and fixed in 10% neutral buffer formalin for 24 hours. The tissue was paraffin embedded and sliced into 4 µm-thick sections using a rotary microtome (Leica, Wetzlar, Germany). The sections were placed on silanated slides and dried at 37$^{o}$C overnight before staining with hematoxylin and eosin. Subsequently, the stained sections were scanned into digital format using a color scanner (Epson) at 1200dpi, and saved as a TIFF file. The circumference of the epicardial and luminal surfaces of the left ventricle were measured using Analytic Imaging Station software (AIS, Version 6, Imaging Research Inc; St Catherine's, ON, Canada). The length of the perimeter of the infarct was measured on both the epicardial and luminal surfaces and expressed as a percentage of the circumference for each surface. The resultant values in each rat were averaged to obtain a measure of the infarct size. Only

animals with a transmural infarction were used in this study.

**Microglia**

Morphological analysis and quantification of microglia was performed with a light microscope using 400 times magnification. Within the PVN, ventral hypothalamus (ventral of the PVN), and the cortex (at the same anterior-posterior level as the PVN), the number of microglia were counted in several squares, each 0.2 x 0.2 mm in size. To avoid experimenter bias the squares were placed using systematic rules. In the PVN the medial-lateral distribution of microglia was determined by counting the number of microglia in four adjacent squares that covered the region from 0.0 - 1.0 mm lateral to the edge of the third ventricle. This was performed at the level of the PVN shown in Fig. 2.1 and encompassed the dorsal aspect of the parvocellular and magnocellular regions of the PVN. Within these same regions, the number of activated microglia were also counted and expressed as a percentage of the total number of microglia (activated + non-activated). In the ventral hypothalamus and cortex the number of normal and activated microglia were counted in two squares and the average was calculated.

Immunohistochemistry for the marker CD11b (clone OX-42) detected the microglia present. Non-activated microglia were identified by their small soma from which there emanated extensive, highly branched, long, thin processes, a morphology termed ramified. Activated microglia were defined by three main criteria; (1) stronger immunohistochemical staining for the marker CD11b (clone OX-42), (McNamara et al) the presence of a clearly enlarged soma, and (Lessard et al) marked changes in the appearance of the processes which were now reduced in number, but considerably thicker and shorter giving a stubby appearance. Thus, activated microglia no longer showed the extensive ramified appearance typical of non-activated microglia but had fewer, shorter and thicker processes and an enlarged soma. Only microglia in which these changes were present were defined as activated, as described previously (Nakajima & Kohsaka 2001; Stence et al 2001a; Streit &

Kreutzberg 1988). Changes in the morphology of microglial processes were quantified by measuring the longest process of 10 randomly selected microglia in each animal in each brain region examined. These microglia were located within the areas that were used for counting microglia; in the PVN the most medial sampling square (0.2 x 0.2 mm) was used for this analysis. In the ventral hypothalamus and the cortex, ten microglia were selected from within a single square in each region. Thus, since 15-25 microglia were found in each square in each region, approximately half the microglia in a square in each region were selected for analysis of their process length.

**Statistical analysis**

In each brain region examined, the data were compared using one-way ANOVA to determine overall significant differences between groups. If a statistical difference was obtained, subsequent comparisons between individual groups were made using Student's unpaired t-test with the P-value modified using the Bonferroni correction for multiple comparisons.

## *Results*

### 1) Activation of microglia in the hypothalamic PVN

In sham rats there were few microglia with an activated morphology in any of the areas examined (Fig. 2.1), hence data from sham rats tested at different time point pooled together and presented as microglial activation in sham rats (2.2 and 2.3). In contrast, at 2 and 5 weeks following myocardial infarction, activated microglia were clearly observed in the PVN. Within the PVN, the proportion of activated microglia in the infarcted animals was greatest medially, within 0.5 mm of the third ventricle, and decreased more laterally (Fig. 2.1 and 2.2). The average proportion of activated microglia in those medial regions of the PVN was significantly greater at both time points after myocardial infarction compared to the sham group ($F(2,12) = 87.2$, $P<0.001$, Fig. 2.2). In contrast, there was no significant difference in the proportion of activated microglia in the ventral hypothalamus or in the cortex at either time point following myocardial infarction compared to shams (Fig. 2.3). In our preliminary observations, none of the brain regions other than the PVN showed marked microglial activation following MI, hence we did not quantify microglial activation from all cardiovascular centres.

### 2) Decreased length of microglial processes in PVN

When microglia are activated, their processes reduce in size and become thicker and stubby in appearance (Marco et al 1997; Nakajima & Kohsaka 2001). We therefore, measured the length of processes in microglia in the three brain regions investigated. We found that, compared to shams, the length of microglial processes were significantly reduced by over 50% in the medial region of the PVN at 2 and 5 weeks following myocardial infarction ($F(2,10)=46.89$, $P<0.001$) (Fig. 2.4). In the ventral hypothalamus and cortex of the animals that had undergone myocardial infarction, the average lengths of the microglial processes were not different from that observed in the sham group (Fig. 2.4).

### 3) Increased density of microglial cells in PVN

The number of microglia detected in the PVN after myocardial infarction was significantly greater in animals 5 weeks after the myocardial infarction ($P<0.01$ compared to sham group) (Fig. 2.5). This was observed primarily within 0.25 mm of the edge of the third ventricle (Fig. 2.5). At 2 weeks following the myocardial infarction the number of microglia detected in the PVN did not attain a statistically significant difference compared to the sham group.

### 4) Infarct size and lung weight

After ligation of the coronary artery, the myocardial infarct size averaged 29.0 $\pm$ 2.8% and 30.8 $\pm$ 4.3% of the ventricular circumference 2 weeks and 5 weeks after myocardial infarction respectively. All of the 8 MI rats had a transmural infarct, varying from 26-45%.

The average weight of the lungs in sham rats (1.41 $\pm$ 0.08g) was not significantly different to that observed in rats following myocardial infarction (1.44 $\pm$ 0.11g, 1.48 $\pm$ 0.07g; 2 and 5 weeks after myocardial infarction respectively ($F(2,10) = 0.232$).

### 5) Ventricular function

### i) Echocardiography

Compared to sham animals, percent fractional shortening was significantly reduced by over 50% at 2 and 5 weeks following myocardial infarction ($F(2,10) = 15.61$, $P<0.01$) (Fig. 2.6). Similarly, ejection fractions were significantly lower at 2 and 5 weeks following myocardial infarction compared to that observed in the sham group ($F(2,10) = 31.44$, $P<0.001$) (Fig. 2.6). Table 1 shows the left ventricular internal diameter and posterior wall thickness and also the interventricular septal thickness in systole and diastole in shams and at 2 and 5 weeks following myocardial infarction. At 5 weeks following myocardial infarction all parameters, except the increase in left ventricular posterior wall thickness in systole, were significantly different compared to shams (Fig. 2.8). At 2 weeks following myocardial

infarction all parameters except the increases in left ventricular internal diameter in diastole, and the left ventricular posterior wall thickness were significantly different compared to shams (Fig. 2.8).

### ii) Haemodynamic measures

Left ventricular end diastolic pressure was significantly elevated at 2 and 5 weeks following myocardial infarction compared to the level observed in the sham group ($F(2,8) = 5.963$, $P<0.05$) (Fig.2.7). Left ventricular contractility (dP/dt max) was significantly reduced by approximately 20% at both time points after the ligation of the coronary artery compared to shams ($F(2,8) = 8.133$, $P<0.05$) (Fig.2.7).

## *Figures*

**Fig. 2.1 :**

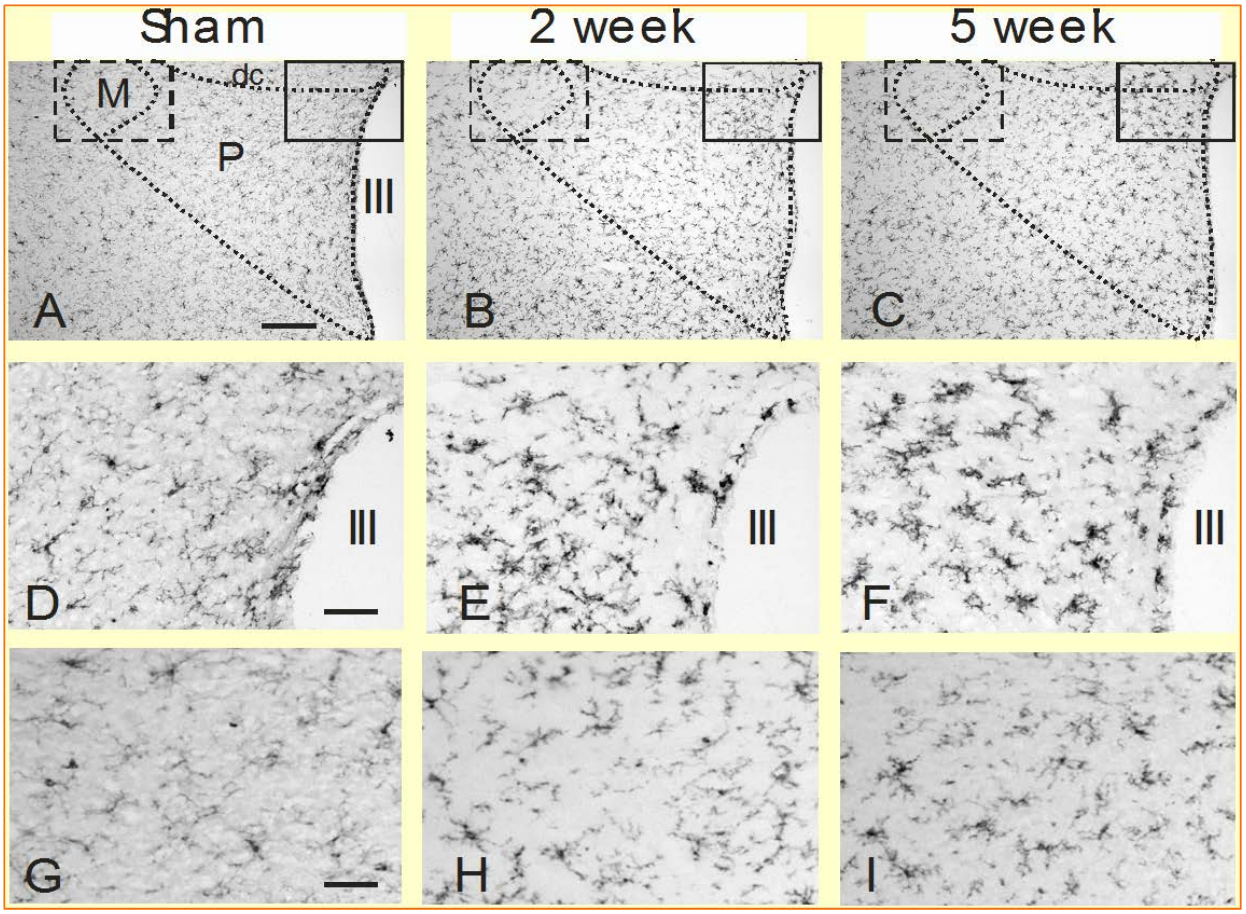

**Fig. 2.1 :** Photomicrographs of the hypothalamic area of rat brain encompassing the paraventricular hypothalamic nucleus showing microglia stained using antibody to CD11b (OX-42 clone). Parvocellular (P), magnocellular (M) and dorsal cap (dc) regions of the paraventricular nucleus are delineated. Panels A-C are low power photomicrographs. The areas in the solid line rectangles are shown in higher power in panels D-F. The areas in the dashed line rectangles are shown in higher power in panels G-I. Panels A, D and G are from a sham animal in which normal ramified microglia are observed. Note the long processes, many secondary branches, and very small soma. Panels B, E and H are from a rat 2 weeks after myocardial infarction. Panels C, F and I are from a rat 5 weeks after myocardial infarction. Note the dramatic increase in CD11b - positive staining and the morphological changes including enlarged soma and shorter, stubbier processes observed following myocardial infarction predominantly in the parvocellular region of the PVN. Abbreviations; III – third ventricle, Calibration bar = 150 µm in A - C, and 50 µm in D - I.

**Fig. 2.2 :**

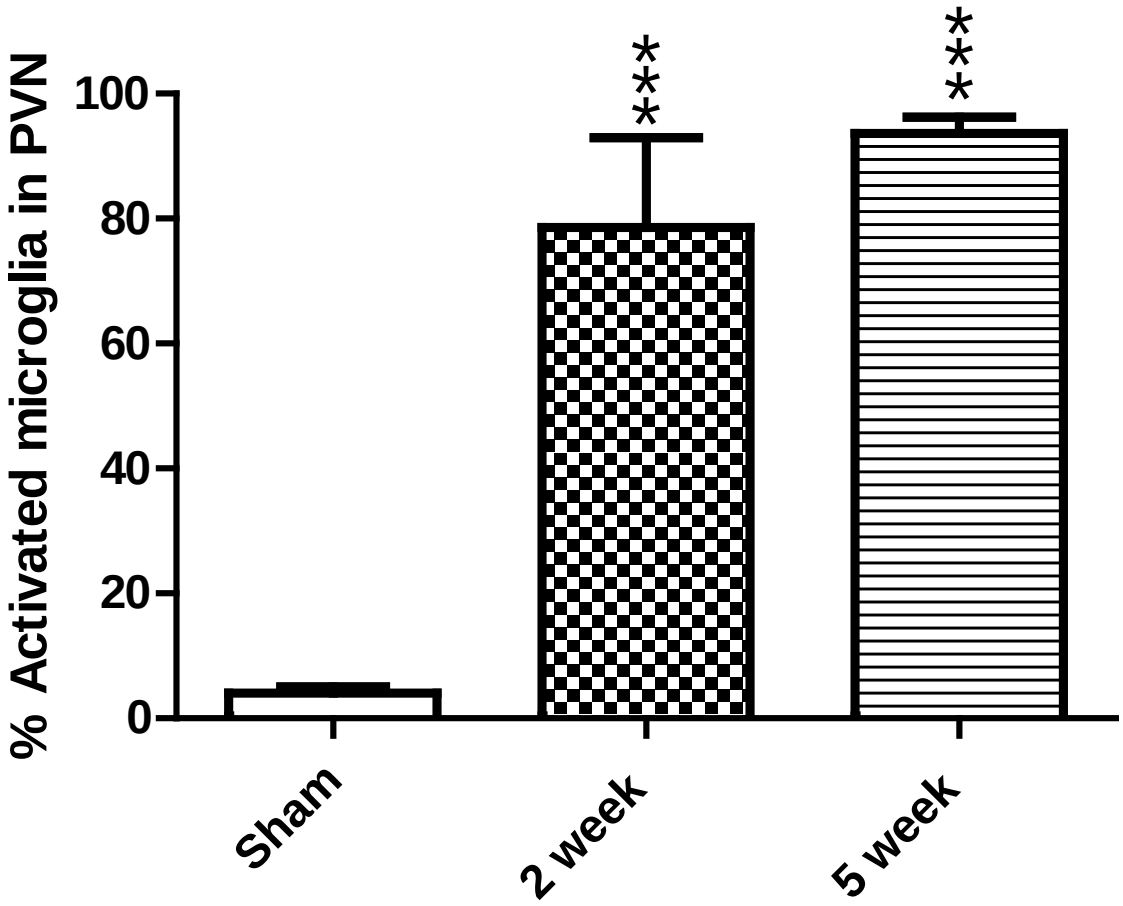

**Fig. 2.2 :** Microglial activation expressed as a percent of total microglia in the hypothalamic paraventricular nucleus in the region between the third ventricle and 1 mm lateral to it. The area encompassed the dorsal aspect of the paraventricular nucleus (both parvocellular and magnocellular) at the level shown in figure 2.1. Data were obtained from sham animals (N = 5) and in rats at 2 weeks (N = 3) and 5 weeks (N = 5) after myocardial infarction. Values are expressed as the mean ± SEM. *** $P<0.001$ compared to sham.

**Fig. 2.3 :**

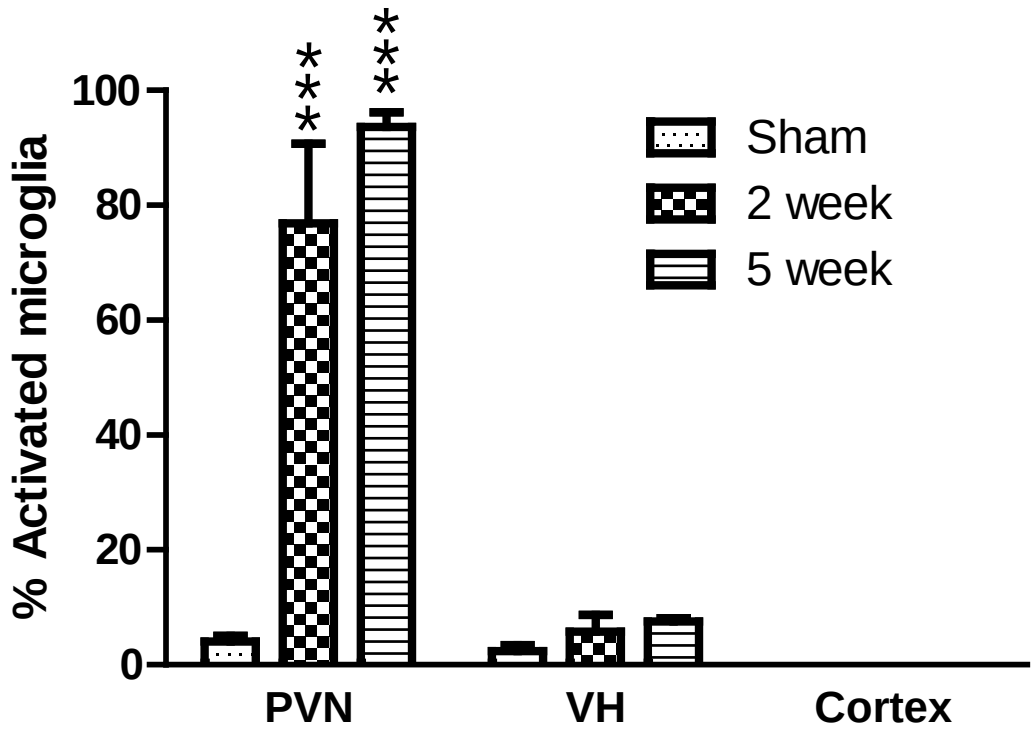
% Activated microglia
100
80
60
40
20
0
***
***
Sham
2 week
5 week
PVN
VH
Cortex

**Fig. 2.3 :** Microglia activation expressed as a percent of total microglia observed in the paraventricular hypothalamic nucleus (PVN), the ventral hypothalamus (VH) and cortex in sham rats (N=5) and in rats at 2 weeks (N = 3) and 5 weeks (N = 5) after myocardial infarction. Values are expressed as the mean ± SEM. *** P< 0.001 compared to sham.

**Fig. 2.4 :**

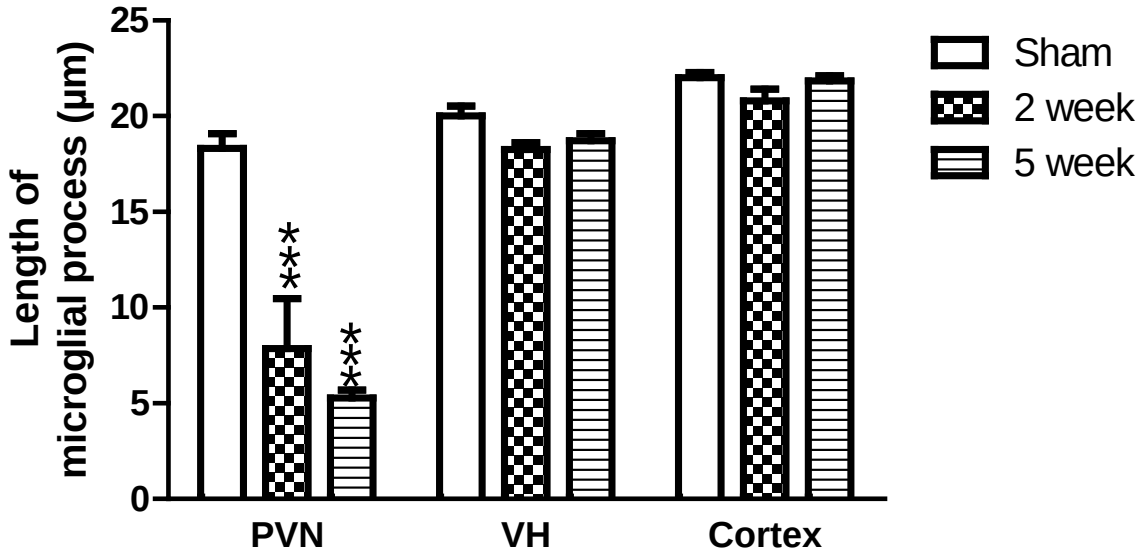
Length of microglial process (µm)
25
20
15
10
5
0
***
***
PVN
VH
Cortex
Sham
2 week
5 week

**Fig. 2.4 :** Average length of microglia processes in the hypothalamic paraventricular hypothalamic nucleus (PVN) (medially), ventral hypothalamus (VH) and cortex in sham rats (N=5) and in rats at 2 weeks (N = 3) and 5 weeks (N = 5) after myocardial infarction. Values are expressed as the mean ± SEM. *** P< 0.001 compared to sham.

**Fig. 2.5 :**

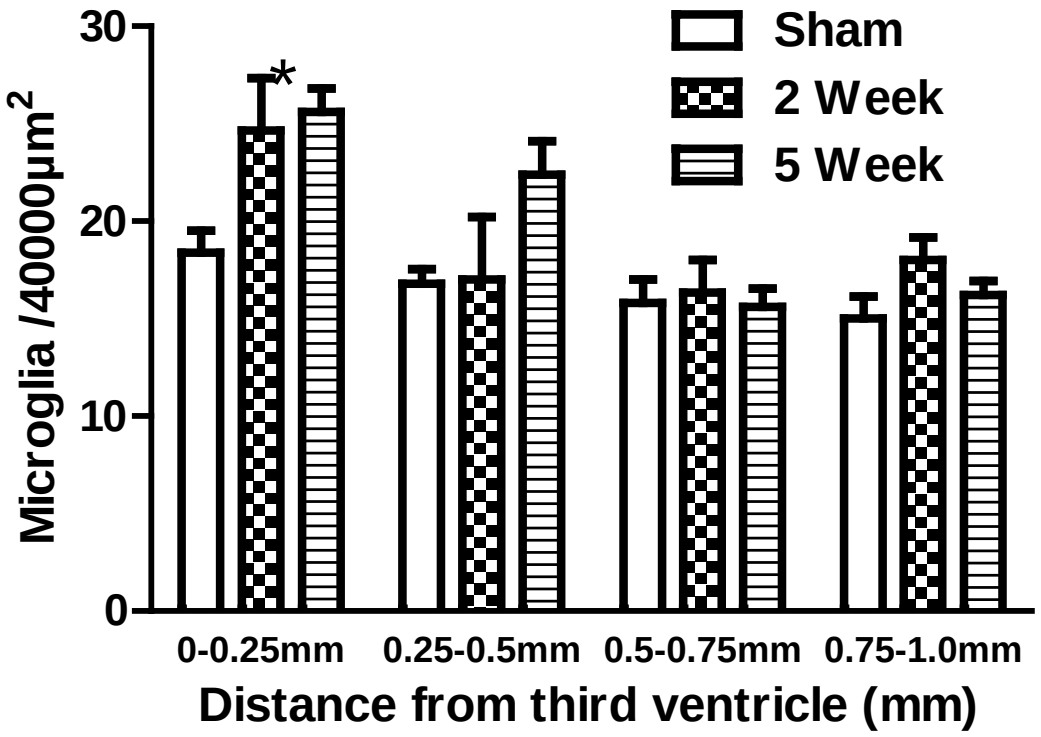
30
20
10
0
Microglia /40000µm2
*
Sham
2 Week
5 Week
0-0.25mm
0.25-0.5mm
0.5-0.75mm
0.75-1.0mm
Distance from third ventricle (mm)

**Fig. 2.5 :** Density of microglia (activated and non-activated) in the paraventricular hypothalamic nucleus in the region between the third ventricle and 1 mm lateral to it. The area encompassed the dorsal aspect of the paraventricular hypothalamic nucleus (both parvocellular and magnocellular) at the level shown in figure 1. Data were obtained from sham animals (N = 5) and in rats at 2 weeks (N = 3) and 5 weeks (N = 5) after myocardial infarction. Values are expressed as the mean ± SEM. * $P<0.05$ as compared to sham.

**Fig. 2.6 :**

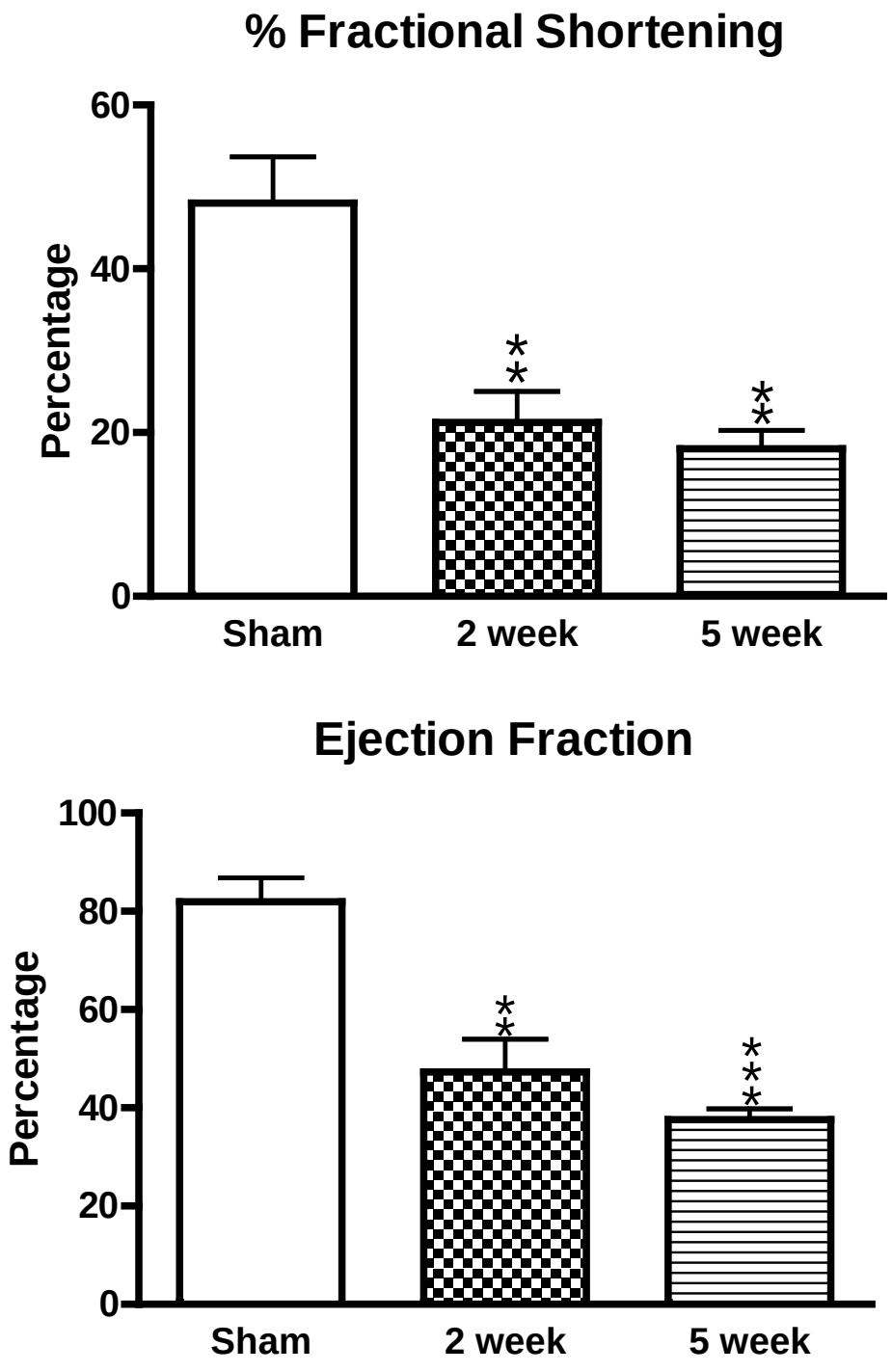
% Fractional Shortening
Percentage
60
40
20
0
**
**
Sham
2 week
5 week
Ejection Fraction
Percentage
100
80
60
40
20
0
**
***
Sham
2 week
5 week

**Fig. 2.6 :** Percent fractional shortening and ejection fraction determined from echocardiography analysis in sham rats (N=5) and in rats at 2 weeks (N = 3) and 5 weeks (N = 5) after myocardial infarction. *** P<0.001, **P<0.01 compared to sham.

(Data courtesy of Dr Andrew Kompa, Department of Epidemiology and Preventative Medicine, Monash University, Melbourne, Australia)

**Fig. 2.7:**

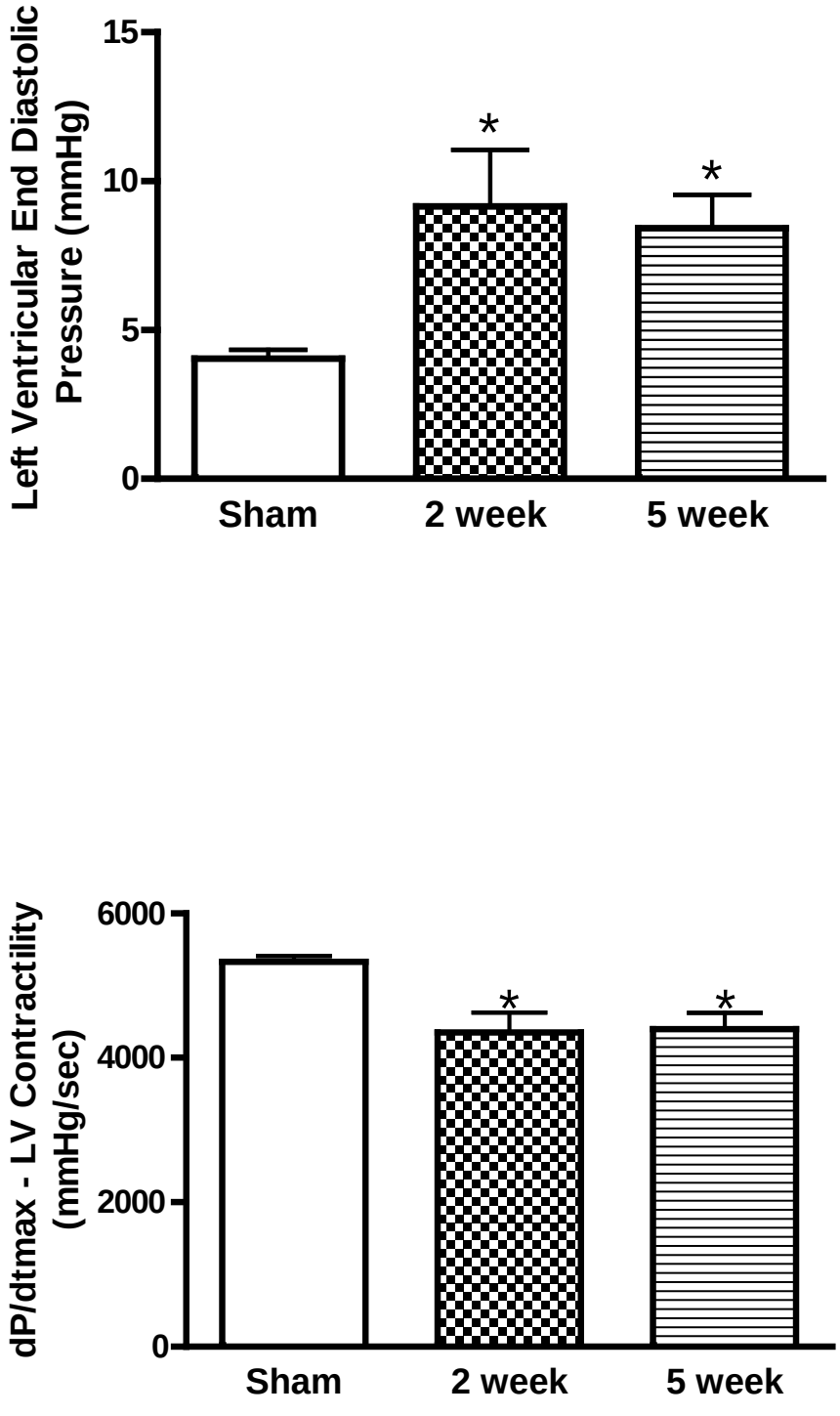
Left Ventricular End Diastolic Pressure (mmHg)
15
10
5
0
*
*
Sham
2 week
5 week
dP/dtmax - LV Contractility (mmHg/sec)
6000
4000
2000
0
*
*
Sham
2 week
5 week

**Fig. 2.7 :** Left ventricular end diastolic pressure and left ventricular contractility (dP/dt max) in sham rats (N=4) and in rats at 2 weeks (N = 3) and 5 weeks (N = 4) after myocardial infarction. * $P<0.05$ compared to sham.

(Data courtesy of Dr Andrew Kompa, Department of Epidemiology and Preventative Medicine, Monash University, Melbourne, Australia)

Fig. 2.8 :

| | Sham (N=5) | MI – 2 weeks (N=3) | MI – 5 weeks (N=5) |
|---|---|---|---|
| Left Ventricular Internal Diameter in diastole – LVIDd (mm) | 7.51 ± 0.43 | 9.89 ± 0.21 | 10.26 ± 0.67 ** |
| Left Ventricular Internal Diameter in systole – LVIDs (mm) | 4.08 ± 0.51 | 7.77 ± 0.23 ** | 8.44 ± 0.54 *** |
| Interventricular Septal Thickness in diastole – IVSd (mm) | 1.62 ± 0.11 | 1.03 ± 0.06 ** | 0.99 ± 0.09 ** |
| Interventricular Septal Thickness – in systole - IVSs (mm) | 2.89 ± 0.12 | 1.06 ± 0.09 *** | 1.00 ± 0.10 *** |
| LV Posterior Wall Thickness in diastole – LVPWd (mm)) | 2.05 ±0.15 | 2.28 ± 0.07 | 2.55 ± 0.12 * |
| LV Posterior Wall Thickness in systole – LVPWs (mm) | 2.76 ± 0.22 | 3.19 ± 0.12 | 3.27 ±0.15 |

**Fig. 2.8 :** Echocardiography parameters from sham animals and in animals 2 weeks and 5 weeks following myocardial infarction (MI), describing left ventricular internal diameter in systole and diastole, interventricular septal thickness and left ventricular posterior wall thickness in both diastole and systole. * $P<0.01$, ** $P<0.01$, *** $P<0.001$ compared to Sham. (Data courtesy of Dr Andrew Kompa, Department of Epidemiology and Preventative Medicine, Monash University, Melbourne, Australia)

## *Discussion*

The present study provides neuroanatomical evidence for an inflammatory response in the PVN following myocardial infarction. The key findings of the work show that after myocardial infarction; (i) microglia are activated in the PVN but not in adjacent hypothalamus or in the cortex, indicating there is not a generalized activation of microglia in the brain, and (ii) activation of microglia occurred without the presence of congestive heart failure. The results indicate that the activation of microglia occurs after myocardial infarction and reduced left ventricular function.

In the present study, we defined activated microglia only if they satisfied several criteria such that they showed stronger staining for CD11b (clone OX-42), an enlarged soma, fewer processes, and the processes present were shorter, thicker and had a stubby appearance. It was observed that some microglia showed stronger staining with CD11b (clone OX-42) but without the clear morphological changes. Thus, only when all the criteria were satisfied then only we defined microglia as activated. These clear morphological changes in the microglia were observed predominantly in the medial regions of the PVN. In the more lateral regions of the PVN, the proportion of activated microglia decreased, and was no longer significantly different from the control group. Our quantitative analyses of the length of the microglial processes support this mediolateral distribution. It is possible, of course, that a more widespread activation of microglia in the PVN may be observed as time increases following a myocardial infarct, but this will need investigations beyond the 5 weeks observation period that was performed in the present study.

The marked activation of microglia observed in the PVN following myocardial infarction did not occur in the ventral hypothalamus adjacent to the PVN, nor in the cortical regions examined. This suggests that activation of microglia is not generalized throughout the brain following myocardial infarction. This would indicate there was not a wholesale

breakdown of the blood brain barrier that could account for the activation of microglia, which differs from other peripheral inflammatory conditions where inflammation in the brain occurs such as inflammatory bowel disease (Natah et al 2005; Riazi et al 2008). The present findings do not exclude the possibility that activation of microglia may occur in brain regions other than the PVN, and that are involved in cardiovascular regulation.

There is always a possibility that a cell could have been cut by the cryostat blade during sectioning and hence counted as active during quantification. However, this error will not bias the interpretation of our results because sectioning will affect all the animal groups roughly equally. Moreover, the probability of cutting microglia present in a section is equal for all the regions of that section. My quantification shows microglial activation only in in the MI rats which is not possible to achieve due to sectioning. I also performed quantification from the cortex from the same sections that were used for counting activated microglia in the PVN. This quantification, presented in figure 2.3, indicates microglial activation only in the PVN which cannot be caused by sectioning.

It is well documented that over time after a myocardial infarct, cardiac remodelling in the non-infarcted myocardium occurs. This is characterized by hypertrophy initiated by neurohormonal activation and autocrine and paracrine mediators, including inflammatory cytokines. Although initially compensatory, these changes impart detrimental biological effects resulting in left ventricular chamber dilatation, eccentric hypertrophy, and reactive fibrosis contributing to systolic dysfunction (Mann 1999b; Pfeffer et al 1985; Prabhu 2005; Remme 2003; Swynghedauw 1999). In the present study, we observed activation of microglia at 2 weeks and 5 weeks after myocardial infarction. We acknowledge that with only three animals in the 2 weeks group, the sample is small; however, the results at 2 weeks following myocardial infarction were very similar to the observations made at 5 weeks following myocardial infarction. In our study, at 2 and 5 weeks after myocardial infarction, the echocardiography and hemodynamic parameters indicated reduced left ventricular

function and substantial remodeling of the heart but the rats were not technically in heart failure. Thus, our results suggest that following myocardial infarction the reduced left ventricular function is sufficient to induce activation of microglia in the PVN. In the present study, we have not investigated time points earlier than 2 weeks post myocardial infarction; however, cytokines are elevated within 24 hours following an infarct ((Francis et al 2004a)) and it would be of interest to investigate time points shorter than 2 weeks.

Activated microglia can become mobile and proliferate (Giordana et al 1994; Schiefer et al 1999), therefore microglia may have migrated to the PVN or proliferated in response to an inflammatory stimulus. This may account for the significant increase in the number of microglia observed in the PVN 5 weeks following myocardial infarction. Microglial proliferation and an increase in their mobility have been observed following peripheral nerve damage (Schiefer et al 1999). It may be possible that the increased expression of CD11b (clone OX-42) by microglia following myocardial infarction may mean that microglia are more easily detected; however, CD11b (OX-42) staining has been reported to show all resting microglia and there are no reports in the literature to suggest otherwise.

The present findings provide neuroanatomical evidence supporting an inflammatory response occurring in the PVN. Furthermore, since activated microglia secrete cytokines such as TNF-α and IL-1 β (Colton & Gilbert 1987; Frucht et al 2001; Mizuno et al 2003; Mizuno et al 1994; Sawada et al 1989; Suzumura et al 1996), our results support the possibility that activation of microglia in the PVN may contribute to local production of cytokines in this brain nucleus following myocardial infarction (Francis et al 2004a; Guggilam et al 2007; Helwig et al 2007),

The mechanisms that initiate the inflammatory process in the PVN following myocardial infarction are unknown; some authors have suggested a critical role of the pro-inflammatory cytokines which are released into the bloodstream by the damaged heart and

induce PGE2 production in endothelial cells in the cerebral blood vessels (Felder et al 2003; Francis et al 2004a; Francis et al 2004b; Kang et al 2008). PGE2 is known to increase cytokine production. Other mechanisms may include the activation of the renin-angiotensin-aldosterone system, which occurs following myocardial infarction, and increased production of reactive oxygen species (Guggilam et al 2007; Lindley et al 2004; Yu et al 2008). Finally, changes in the neurochemical and ionic milieu elicited by the increase in the neuronal activity in the PVN that occurs following a myocardial infarction (Lindley et al 2004; Patel et al 2000; Patel et al 1993), could stimulate microglia, possibly via glutamatergic or purinergic receptor activation (Bianco et al 2005; Davalos et al 2005; Hagino et al 2004; Hide et al 2000; Taylor et al 2002; Taylor et al 2005). The activated microglia can increase neuronal activity by releasing neurochemicals such as cytokines and growth factors (eg BDNF) (Lu et al 2009b), thus contributing to a detrimental feed-forward cycle.

## *Conclusion*

We have found that microglia are activated in the PVN but not in the adjacent hypothalamus following myocardial infarction. The activated microglia may contribute to the increased local production of pro-inflammatory cytokines observed in the PVN after myocardial infarction and resulting reduced left ventricular function.

## Acknowledgment

All the surgical procedure for coronary artery ligation and homodynamic measurements were performed by Dr. Andrew Kompa in Dr. Henry Krum's laboratory at Department of Epidemiology and Preventative Medicine, Monash University, Melbourne, Australia. We sincerely thank them for their valuable contribution in this project.

# Chapter 3: Microglial Activation in Cardiovascular Centres of STZ-Induced Diabetic Rat Brain

## *Introduction*

Diabetes mellitus is a major risk factor for developing cardiovascular disease in humans (Baliga & Weinberger 2006; Grundy et al 1999). Major cardiovascular complications associated with diabetes in humans include hypertension, cardiomyopathy, atherosclerosis, increased vascular resistance and sudden cardiac death (Wajchenberg et al 2008). Adult patients with diabetes mellitus show ultra-structural and functional deterioration of the myocardium (Di Bello et al 1995; Fraser et al 1995). These cardiovascular complications are considered as the cause of death in approximately 65% of persons with diabetes (Geiss LS 1995). Diabetes not only increases the chance of developing cardiovascular disease but also increases the probability of poor cardiovascular disease outcome and mortality (Luchsinger et al 2001; Stevens et al 2004; Tuomilehto et al 1996). STZ (Streptozotocin) is a chemical commonly used to induce hyperglycemia and then some symptoms of human type-1 diabetes in rodents (Leo et al 2010; Zheng et al 2006). Cardiomyopathy and increased vascular resistance have been reported in this animal model of diabetes (Akula et al 2003; Mihm et al 2001). Many studies investigating diabetic cardiovascular complications have suggested endothelial dysfunction as a mechanism but growing evidence also suggests a role for dysregulation of autonomic control and sympathetic nerve activity (Ross 1993; Vita et al 1990; Zheng et al 2006). There are conflicting reports on blood pressure changes in the STZ-induced diabetic rats; some have reported increased or decreased or no change in blood pressure. In one study, despite reduced resting systolic blood pressure, the ganglionic blocker pentolinium produced significantly greater reduction in heart rate in STZ-induced diabetic rats as compared to saline treated controls (Hebden et al 1987). Moreover, a recently published study has demonstrated significantly elevated basal renal sympathetic nerve activity in STZ-

induced diabetic rats (Patel et al 2011). Thus, sympathetic nerve activity to the heart and kidney appears to be enhanced in STZ-induced rats.

Regulation of the sympathetic nervous system is achieved by changing neuronal activity in various brain centres eg. the paraventricular hypothalamus (PVN), rostoventral medulla (RVLM), vental hypothalamus (VH) and nucleus tractus solitarius (NTS). Interestingly, markers of neuronal activity are reportedly up-regulated in cardiovascular centres of the brain involved in sympathetic regulation in STZ-induced diabetic animals (Krukoff & Patel 1990; Lincoln et al 1989; Zheng et al 2002).

It is now well known that increased sympathetic drive contributes to the pathology of heart failure following myocardial infarction. Studies on animals have also reported activation of neurons in cardiovascular centres of the brain involved in sympathetic regulation following myocardial infarction (Lindley et al 2004; Patel et al 2000). We have recently reported activation of microglia in the PVN of rats with myocardial infarction (chapter 2). Microglia are the immune cells of the central nervous system and recently published studies on microglia demonstrated their potential to exaggerate pathological processes (Tsuda et al 2003). A recent study by Lu et al. (2009) demonstrated that secretions from microglia can modulate neuronal activity. Moreover, a study has reported microglial activation in STZ-induced diabetic rat spinal cord and suggested involvement of these activated in causing hyperalgesia and neuropathic pain via excitatory effects of their secretions on spinal neurons (Tsuda et al 2008). Hence, we hypothesize that there is neuronal and microglial activation in STZ-induced diabetic rats in brain nuclei involved with cardiovascular regulation.

Therefore, we investigated: (i) if microglial are activated in CNS cardiovascular centres of STZ-induced diabetic rats (ii) time course of microglial activation and its correlation with neuronal activation observed in these STZ-induced diabetic rats (iii) correlation of neuronal and microglial activation with other physiological changes seen in these STZ-induced diabetic rats.

## *Methods*

### Animals

Male Sprague Dawley rats obtained from ARC (Animal Resource Centre, Perth) were given streptozotocin (STZ 48mg/kg body weight) in citrate buffer via the tail vein to induce diabetes. Rats were tested for elevated blood glucose one week after the injection using a one touch glucometer (Accu-Check Performa) and used at 2-4, 6 and 8-10 weeks after the injection. Control rats received citrate buffer injection and underwent all other procedures as for STZ treated rats.

### Tissue collection

All the rats used for this study were euthanized by an overdose of pentobarbital sodium (180mg/kg body weight), after which they were decapitated and had their brains removed. The brains were cut into 3 pieces to separate forebrain and brain stem area from the hypothalamus, then immediately immersed in freshly prepared, ice cold 4% paraformaldehyde in phosphate buffered saline (PBS) (0.1 M, pH 7.2) for 4 hours at 4°C. The brains were then transferred to a solution containing 30% sucrose in PBS and left for approximately 48 h at 4°C before they were used for histological analysis.

### Osmolarity measurements

Blood samples were collected from STZ-induced diabetic and control rats immediately after euthanasia. The samples were immediately mixed with heparin (anticoagulant) and centrifuged at 1500 rpm for 10 minutes. Cell free plasma samples were stored at $-80^0$ until used. Plasma osmolarity was measured by using an osmometer.

## Immunohistochemistry

As described previously (chapter 2) serial coronal sections (20µM thick) of the brain were cut using a cryostat (Leica, CM 1900). One in five sections were collected starting from the rostral PVN to the caudal PVN identified by referring to a rat atlas (Paxinos 2008) and using the morphology of the optic chiasm / optic tract and location of the fornix as land marks. All selected sections were placed onto gelatine coated slides and dried for 2 hours at room temperature. Standard Immunohistochemical procedures were performed in which endogenous peroxidase activity was blocked by 15 minutes incubation with 0.5% $H_2O_2$ in PBS. This was followed incubation in 10% normal horse serum (NHS) for 60 minutes prior to 0.5 % Triton X-100 for 10 min to facilitate antibody penetration. Subsequently, the sections were incubated for 72 hours with a mouse monoclonal primary antibody directed against CD11b (clone OX-42) (1: 100, Chemicon, Temecula, USA) in 2% NHS and 0.2% Triton X-100 in PBS. This was followed by incubation in horse biotinylated antimouse secondary antibody raised (1: 100, rat adsorbed, Vector Laboratories, Burlingame, USA), and Extravidin-HRP (1:400, Sigma-Aldrich, St Louis, USA), DAB (2,4-Diaminobutyric acid, Sigma-Aldrich, St Louis, USA) was used as the chromogen. Sections from the respective time point sham rats and sections from STZ-induced diabetic rats were processed simultaneously. Similar procedures using rabbit polyclonal anti-c-Fos (1:400, SantaCruz Biotechnology) and goat anti-rabbit secondary antibody (1:400, Sigma-Aldrich, St Louis, USA) were performed to detect Fos and Fos related antigens, except that the primary antibody was incubated overnight instead of 72 hour.

## Quantification and morphological analysis of microglia

Morphological analysis and quantification of microglia was performed with a light microscope using 400 times magnification. Within the PVN, NTS, ventral hypothalamus (ventral of the PVN), and the cortex (at the same anterior-posterior level as the PVN), the number of microglia were counted in several squares, each 0.2 x 0.2 mm in size. To avoid experimenter bias the squares were placed by systematic rules. In the PVN, the medial-lateral distribution of microglia was determined by counting the number of microglia in four adjacent squares that covered the region from 0.0 - 1.0 mm lateral to the edge of the third ventricle. This was performed at the level of the PVN encompassing the parvocellular and magnocellular regions. The percentage of activated microglia was determined by counting activated microglia and total microglia present in the same field. In the ventral hypothalamus, NTS and cortex the number of normal and activated microglia were counted in two squares and the average was calculated. The region of the NTS analysis is shown in Fig. 3.7

## Statistical analysis

Statistical analysis was performed using Graph Pad Prism version 5 software. In each brain region examined, the data were compared using one-way ANOVA to determine if there were overall significant effects between groups. If a statistical difference was obtained, subsequent comparisons at each time point were made using student's unpaired t-test with the α-value modified using the Bonferroni correction for multiple comparisons.

## *Results*

### 1) Body weight and blood glucose measurements

When rats were tested 1 week after STZ or vehicle injection, average blood glucose levels were 11.1 ± 0.7 mg/dL in control rats (N=25). Blood glucose levels in STZ-induced diabetic rats (N=25) were greater than 25 mg/dL indicating extreme hyperglycaemia within a week of STZ injection. Ten weeks after treatment with STZ or vehicle, both groups of rats gained weight; however, the weight gained in normal rats was significantly greater than in diabetic rats (Fig. 3.9).

### 2) Microglial activation in PVN in STZ-induced diabetic rats

We observed microglia with long branched processes, secondary processes, and small cell bodies throughout the PVN region in control rats as shown in Fig.1.1 of chapter 1. This was the case in all the control rats tested at different time points after vehicle injection hence data obtained from different time point control rats combined as presented as activation in sham rats. Many microglia in the PVN region in STZ-induced diabetic rats at the 8-10 weeks time point had swollen cell bodies with relatively thicker, shorter, and stubbier processes. Based on morphology, the vast majority of microglia visualized using the OX42 immunohistochemistry were parenchymal. I have attached a 3D reconstruction of a PVN section showing OX-42 stained microglia in an appendix (fig.1) which shows no staining present within any blood vessels confirming the parenchymal location of microglia. This microglia activation was observed throughout the PVN region (Fig. 3.1).

It appeared that the intensity of OX-42 immunolabelling was increased in the PVN of STZ rats, but this was difficult to quantify due to the inherent variability in the immunohistochemical technique. However, higher intensity of immunolabelling is expected to cause fine microglial processes to appear more clearly visible while I observed reduced microglial process length in STZ rats.

Quantitative analysis showed no significant difference in the percentage of microglia that were activated at 2-4 and 6 weeks time points when controls and STZ-induced diabetic rats were compared. We observed a significant increase in the percentage of activated microglia at 8-10 weeks following STZ injections when compared to control ($P<0.001$) (Fig. 3.2 (A)). Interestingly, individual rat data showed that some rats had a much higher percentage of microglial activation as compared to the highest level of activation seen in controls even at earlier time points (Fig. 3.2 (B)). No significant microglial activation was observed in areas of the ventral hypothalamus and cortex region (Fig. 3.3).

### 3) Microglial activation in SON

Quantitative analysis of microglia activation in the SON region of STZ-induced diabetic rats did not show a significant difference as compared to the control rats until 8-10 weeks ($P<0.05$ at 8-10 weeks) as shown in Fig. 3.6 (A). However, when the graph of percentage activated microglia in PVN from individual rats was plotted some STZ-induced diabetic rats had higher percentage of activated microglia even at earlier time points (Fig. 3.6 (B)). Therefore, it appears that the onset of microglial activation was different in each rat.

### 4) Microglial activation in NTS

We observed that microglia in the NTS of control rats had relatively higher OX-42 labeling, shorter processes and smaller cell bodies as compared to the surrounding areas (Fig. 3.7). These results suggest that microglia express different levels of surface receptors in different regions of the brain. Despite this, in STZ-induced diabetic rats, NTS microglia showed a relatively activated morphology with shorter, thicker, stubbier processes as compared to microglial morphology in NTS region of control rats at later time points (Fig. 3.7). Also the levels of OX-42 immunolabeling were further up regulated in STZ-induced diabetic rats compared to controls.

Quantification clearly showed a significantly higher percentage of activated microglia at the 8-10 weeks time point after STZ injection as compared to control rats ( $P<0.05$ at 8-10 weeks) (Fig. 3.8 (A)). However, like the PVN and SON data on NTS microglia from some individual rat data showed a higher % activation of microglia as compared to the controls even at earlier time points (Fig. 3.8 (B)).

## 5) Fos positive cells in PVN, SON and NTS of STZ-induced diabetic rats

In this study, we used an antibody that recognises Fos-related antigens which have been shown to have a higher long half life and are useful in recognising neurons activated chronically (Davern & Head 2007). We observed a small number of labelled neurons in the PVN of control rats at all the time points tested as shown in Fig. 3.9. There was a marked increase in the number of Fos-immunoreactive (Fos-IR) nuclei in the PVN of STZ-induced diabetic rats as compared to controls (Fig. 3.9 & 3.10) at later time points. Counts of Fos positive nuclei in the PVN showed a significant increase at 6 weeks after STZ injection as compared to control rats. This increase in Fos immunoreactive nuclei was also evident at 8-10 weeks post STZ injection (Fig. 3.10 (A)). However, when data from individual rats was examined, a small number of STZ-induced diabetic rats showed an increased number of Fos-IR neuclei at earlier time points as compared to the highest number of Fos-IR nuclei observed in control rats (Fig. 3.10 (B)). The majority of Fos-IR nuclei in the PVN on the basis their location showed that majority of Fos-IR nuclei were located within approximately 0.5-1.0 mm from the edge of the third ventricle consistent with the location of PVN magnocellular neurons. Despite this there were still significantly more Fos labeled nuclei observed in the parvocellular PVN in STZ-induced diabetic rats at 6 weeks compared to control rats (Fig. 3.11 (A)). Interestingly, this significant increase in number of Fos-IR nuclei was present in the

parvocellular as well as the magnocellular part of the PVN at 6 weeks but it was restricted to only the magnocellular region at later time points.

In the SON, there was significantly increased Fos-IR nuclei seen at 6 weeks post STZ injection (Fig. 3.12 (A); $P<0.05$ as compared to control). Again a plot showing data from individual rats indicates that some rats had high numbers of Fos-IR nuclei even at the earlier time points (2-4 weeks) (Fig. 3.12 (B)). In contrast to PVN and SON, there was significant change in the number of Fos-IR nuclei in the NTS region of STZ-induced diabetic rats compared to control rats.

## 6) Correlation between neuronal and microglial activation in PVN and SON

When the time course of microglial activation and Fos-IR were compared, it appeared that increased neuronal activation (as determined by presence of Fos-IR) preceded microglial activation. Therefore, to investigate whether there was a relationship between neuronal activation and microglial activation, we plotted graphs of microglial activation vs neuronal activation. We found that there was no significant correlation between neuronal activation and microglial activation in SON (Fig. 3.14 (B); $P=0.3206$, $N=15$ all time points together) but a trend towards a positive correlation observed in PVN (Fig. 3.14 (A); $P=0.0605$, $N=14$ all time points together).

One possible cause for the neuronal activation in STZ-induced diabetic rats is increased plasma osmolarity. Therefore, we measured plasma osmolarity at various time points after STZ treatment. We observed increased plasma osmolarity in STZ-induced diabetic rats as compared to control rats (Fig. 3.16).

## *Figures*

**Fig. 3.1 :**

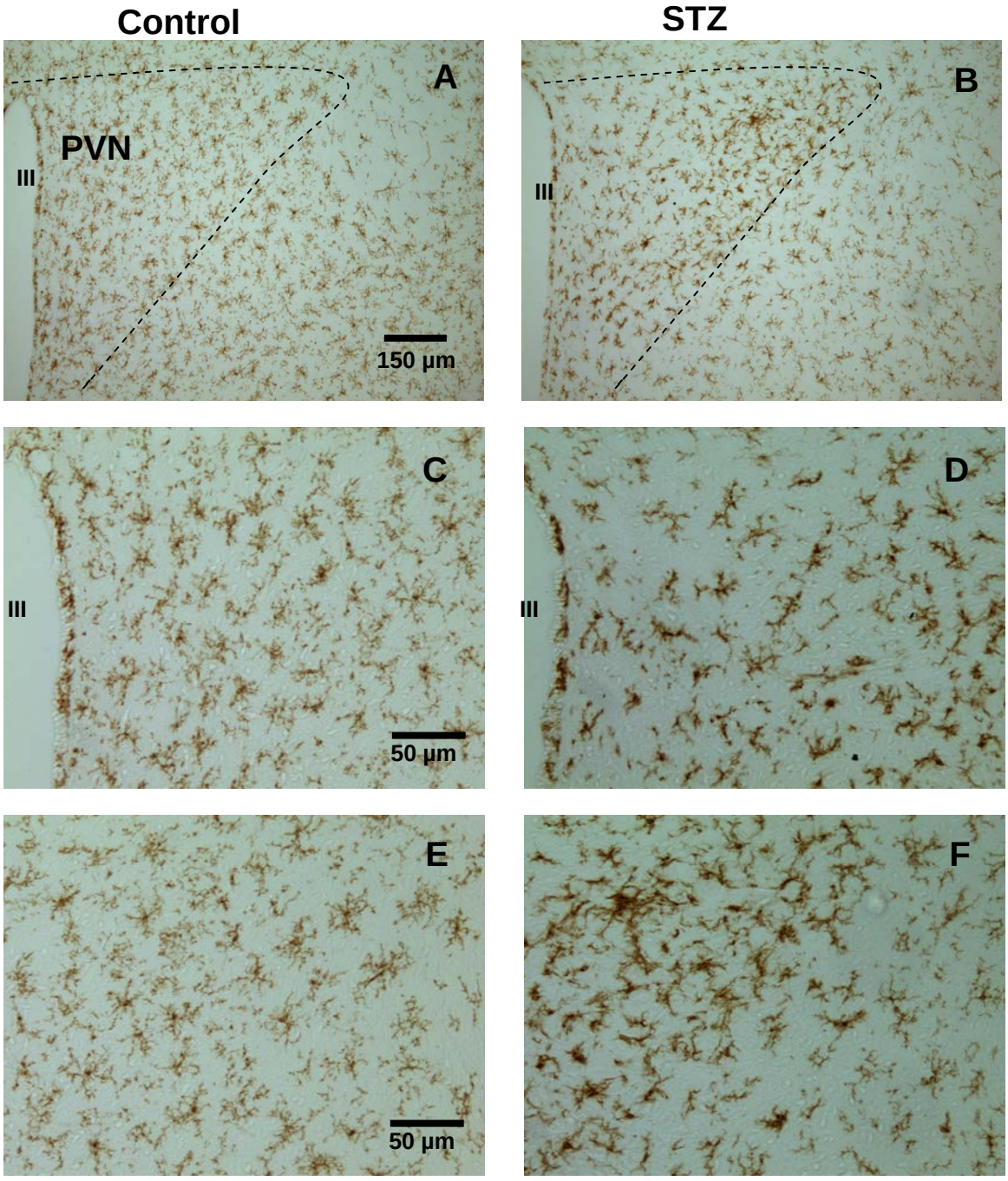

**Fig. 3.1 :** Photomicrographs of the hypothalamic area of rat brain encompassing the paraventricular hypothalamic nucleus (PVN) showing microglia stained using antibody to CD11b (OX-42 clone). Dotted line in low power images A & B outlines the PVN and III indicates third ventricle. High power images C & D show morphology of microglia in the parvocellular region and images E & F show the magnocellular part of the PVN. Note the normal ramified microglia showing long processes, many secondary branches, and very small somata in control and activated microglia showing higher immunolabelling, enlarged somata and shorter, stubbier processes in STZ- induced diabetic rat at 8-10 weeks time point.

**Fig. 3.2 :**

**A**

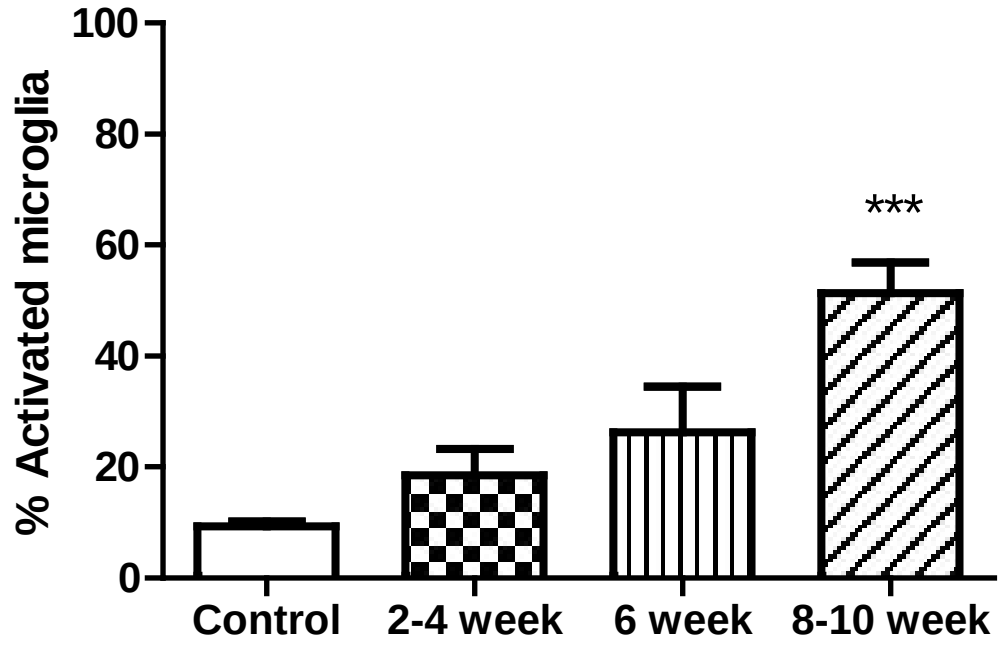
100
80
60
40
20
0
% Activated microglia
***
Control
2-4 week
6 week
8-10 week

**B**

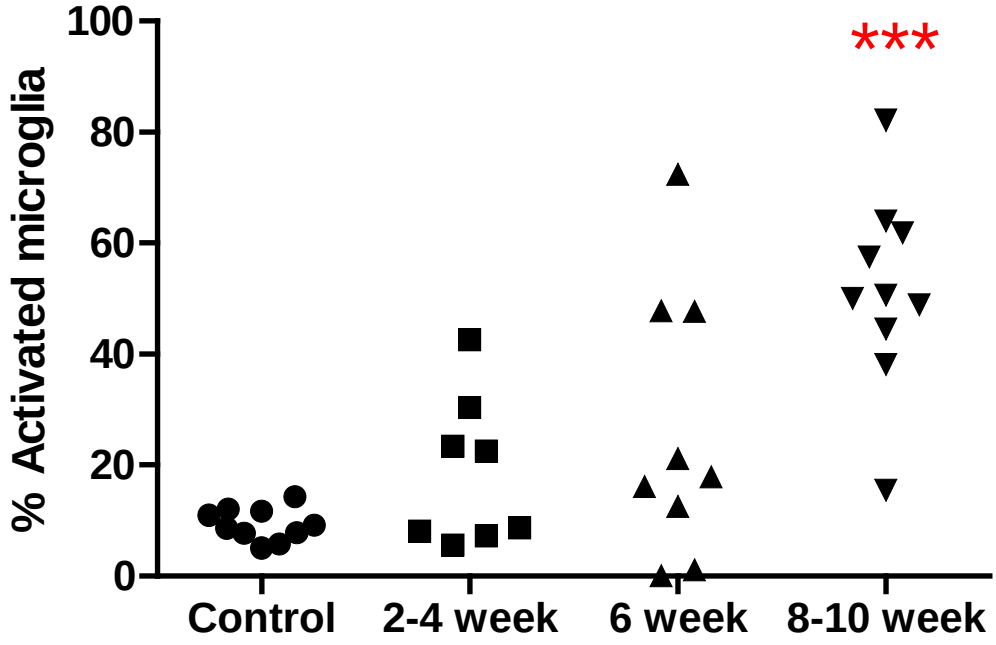
100
80
60
40
20
0
% Activated microglia
***
Control
2-4 week
6 week
8-10 week

**Fig. 3.2 :** Activated microglia expressed as a percentage of total microglia in the paraventricular hypothalamic nucleus in the region between the third ventricle and 1.0 mm lateral to it. The area encompassed both parvocellular and magnocellular regions at the level shown in Fig 3.1. Data were obtained from control (N = 10) and STZ-induced diabetic rats at 2 weeks (N = 8), 6 weeks (N = 9) and 8-10 weeks (N=10) after STZ injection. Panel A shows the average percentage of activated microglia (mean ± SEM) at the different time point. Panel B shows data from individual rats. ***P < 0.001 compared to control.

**Fig. 3.3 :**

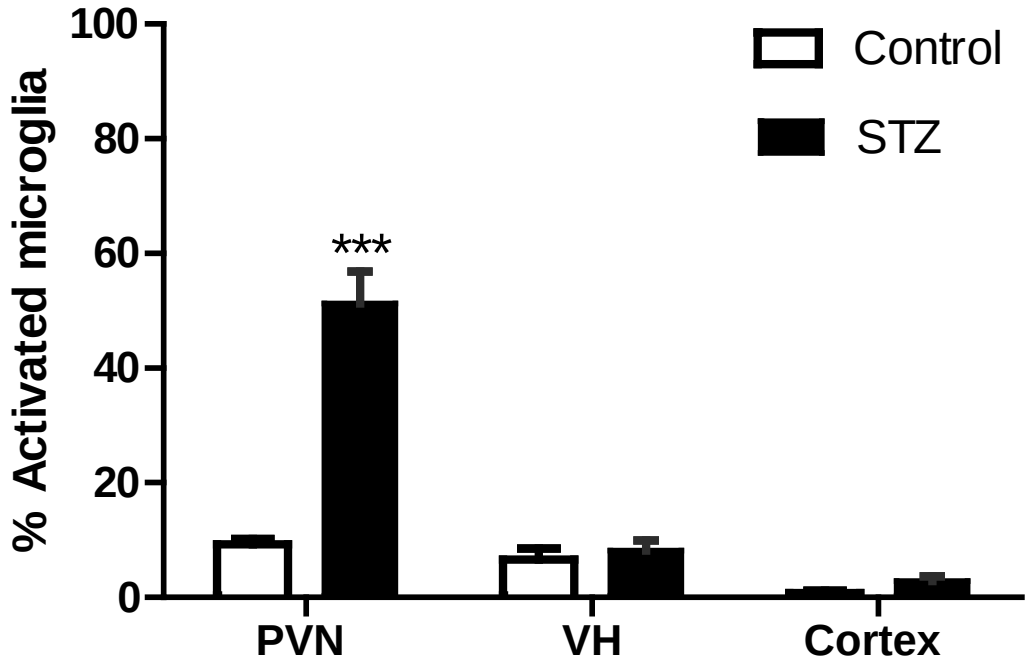
% Activated microglia
100
80
60
40
20
0
***
Control
STZ
PVN
VH
Cortex

**Fig. 3.3 :** Activated microglia expressed as a percentage of total microglia observed in the paraventricular hypothalamic nucleus (PVN), ventral hypothalamus (VH) and the cortex in control rats (N = 5) and in STZ-induced diabetic rats (N = 7) (8-10 weeks after STZ injection). Values are expressed as the mean ± SEM. ***$P < 0.001$ compared to controls.

**Fig. 3.4 :**

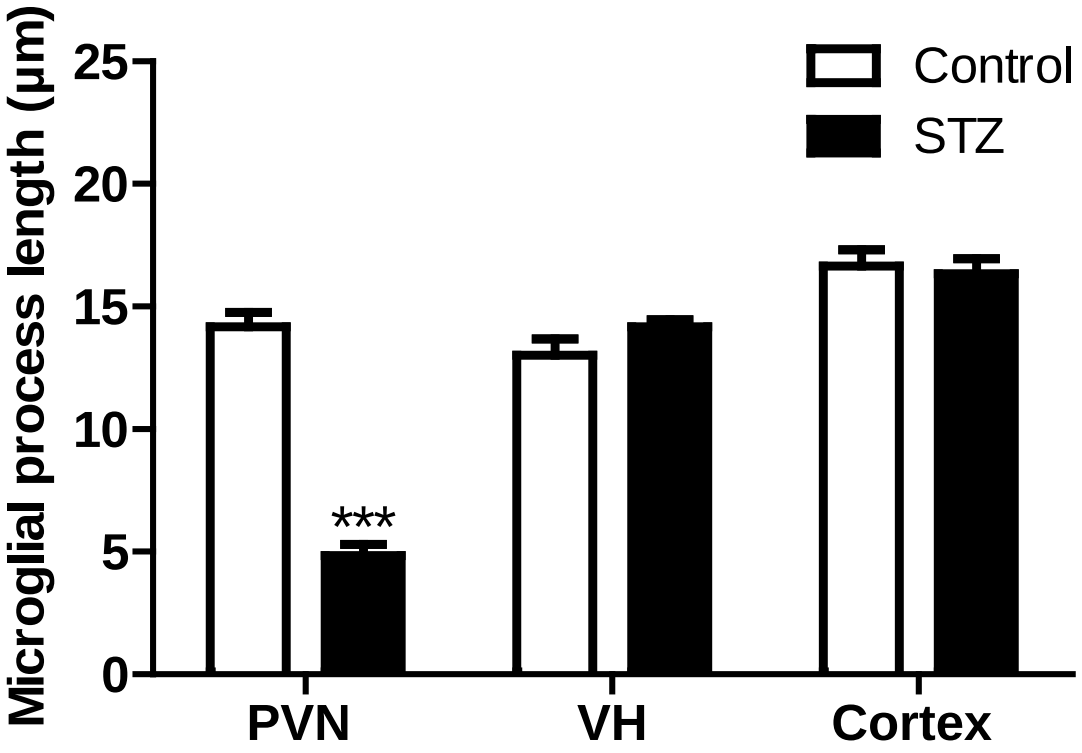
Microglial process length (µm)
25
20
15
10
5
0
***
Control
STZ
PVN
VH
Cortex

**Fig. 3.4 :** Average length of microglial processes in the paraventricular hypothalamic nucleus (PVN), ventral hypothalamus (VH) and cortex in control rats (N = 6) and in STZ-induced diabetic rats at 8-10 weeks after STZ injection (N = 6). Values are expressed as the mean ± SEM. ***$P < 0.001$ compared to controls.

**Fig. 3.5 :**

**A**

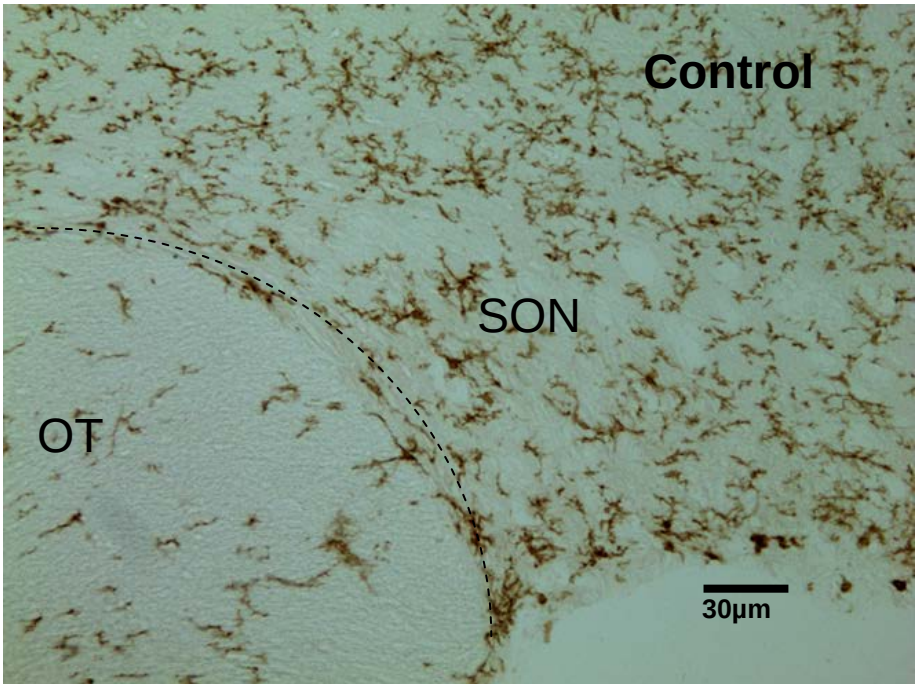


**B**

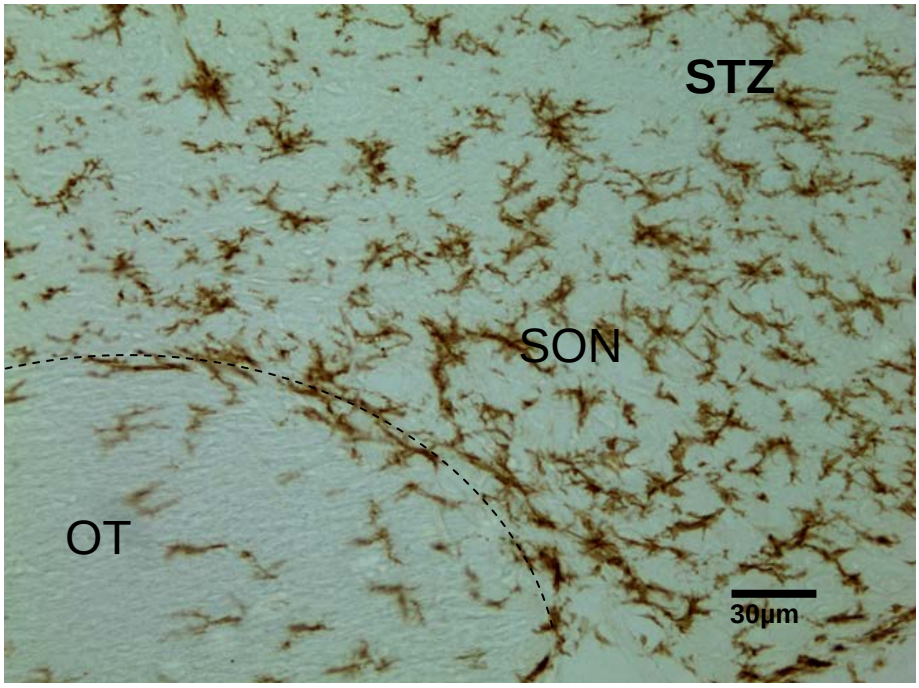

**Fig. 3.5** : Photomicrographs of the hypothalamic area of rat brain encompassing the supraoptic nucleus (SON) showing microglia stained using antibody to CD11b (OX-42 clone). Note the normal ramified microglia showing long processes, many secondary branches and small somata in control and activated microglia showing higher immunolabelling, enlarged somata, shorter and stubbier processes in STZ-induced diabetic rat at 8-10 weeks time point. OT indicates optic tract .

**Fig. 3.6:**

**A**

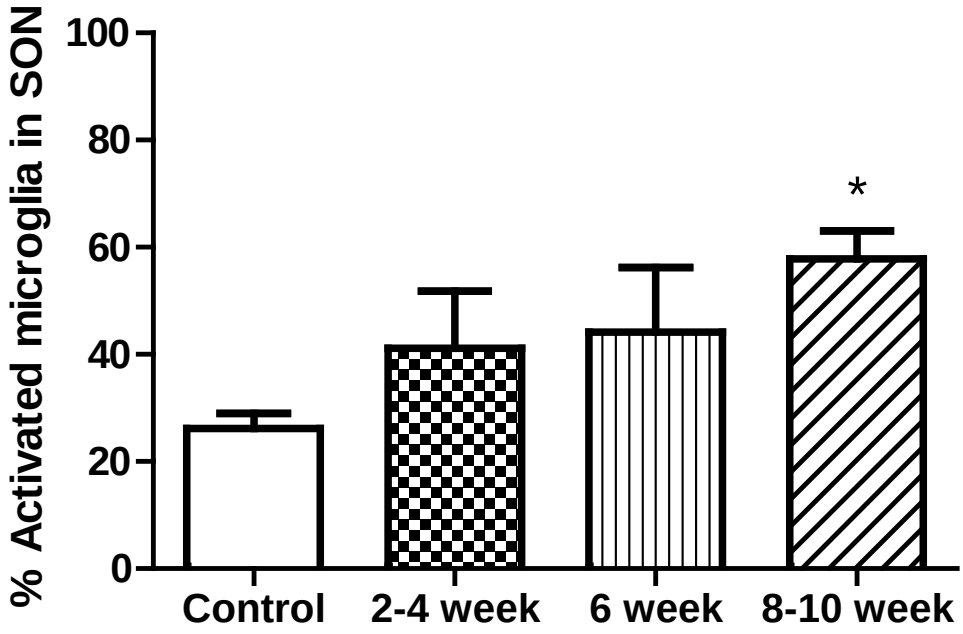
% Activated microglia in SON
100
80
60
40
20
0
*
Control
2-4 week
6 week
8-10 week

**B**

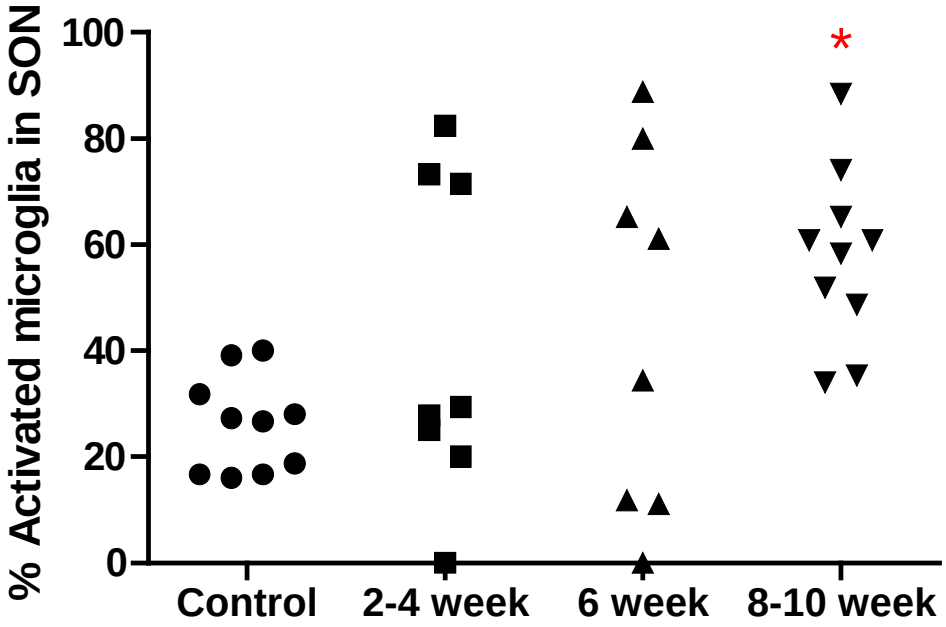
% Activated microglia in SON
100
80
60
40
20
0
*
Control
2-4 week
6 week
8-10 week

**Fig. 3.6 :** Activated microglia expressed as a percentage of total microglia in the supraoptic nucleus. Data were obtained from control animals (N = 10) and STZ-induced diabetic rats at 2 weeks (N = 8), 6 weeks (N = 8) and 8-10 weeks (N=10) after STZ injection. Panel A shows the average percentage of activated microglia (mean ± SEM). Panel B shows data from individual rats. * $P < 0.05$ compared to control.

**Fig. 3.7:**

**A**

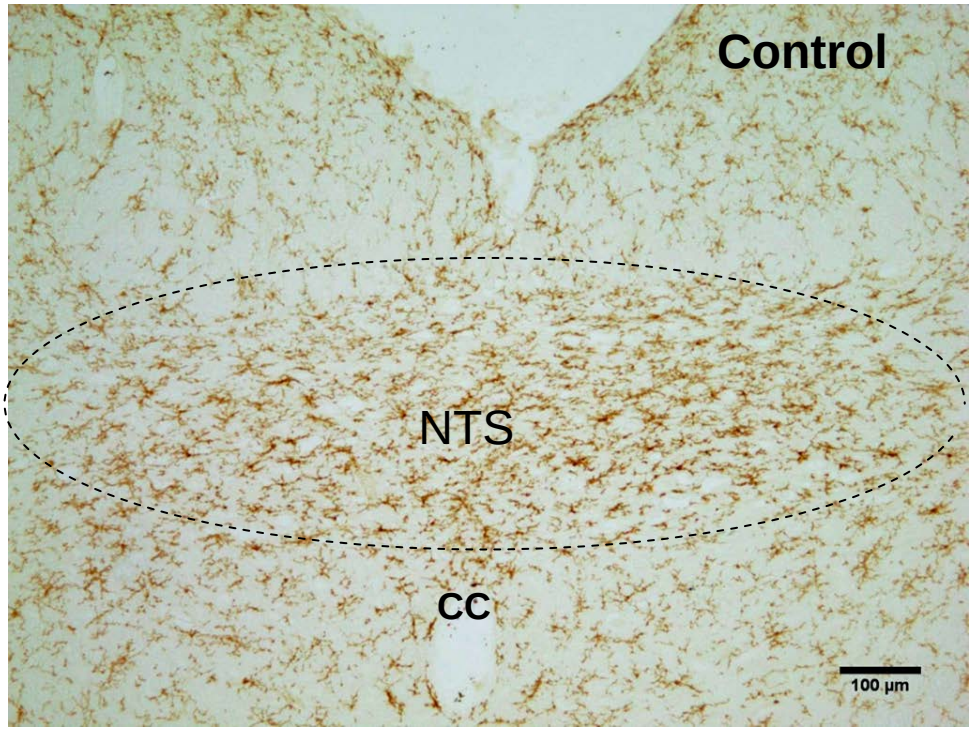


**B**

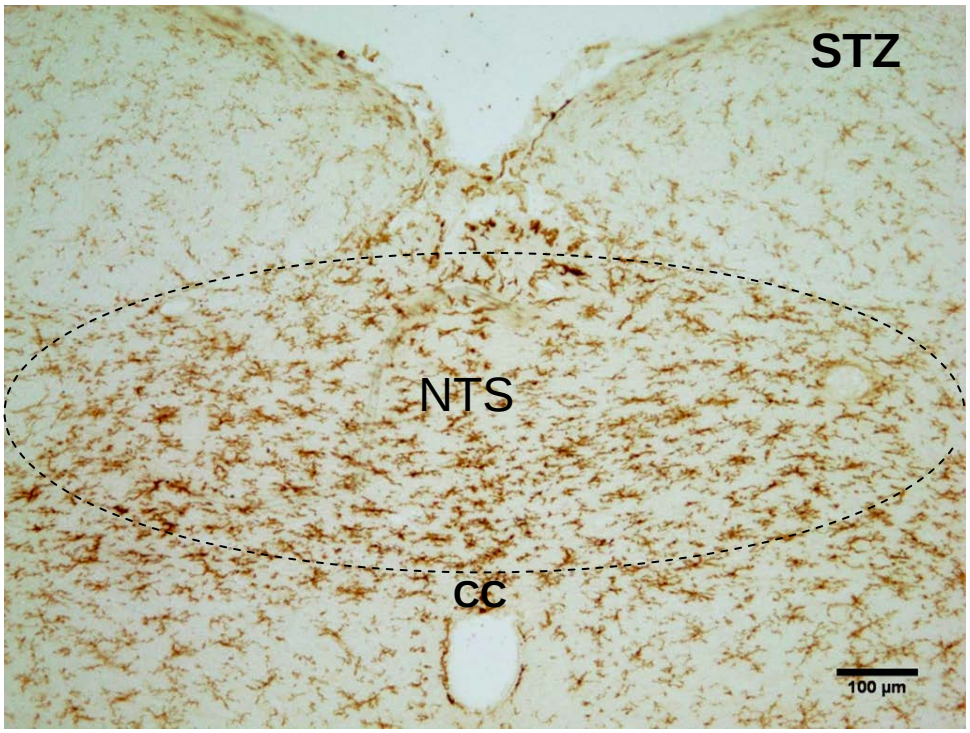

**Fig. 3.7** : Photomicrographs show microglia stained using antibody to CD11b (OX-42 clone) in the nuclear tractus solitarius (NTS) region. Note the normal ramified microglia showing long processes, many secondary branches and very small somata in control and activated microglial showing comparatively higher immunolabelling, enlarged somata and shorter, stubbier processes in STZ treated diabetic rat at 8-10 weeks time point. CC indicates central canal. NTS is adjacent to the central canal, roughly outlined by dotted lines.

**Fig. 3.8 :**

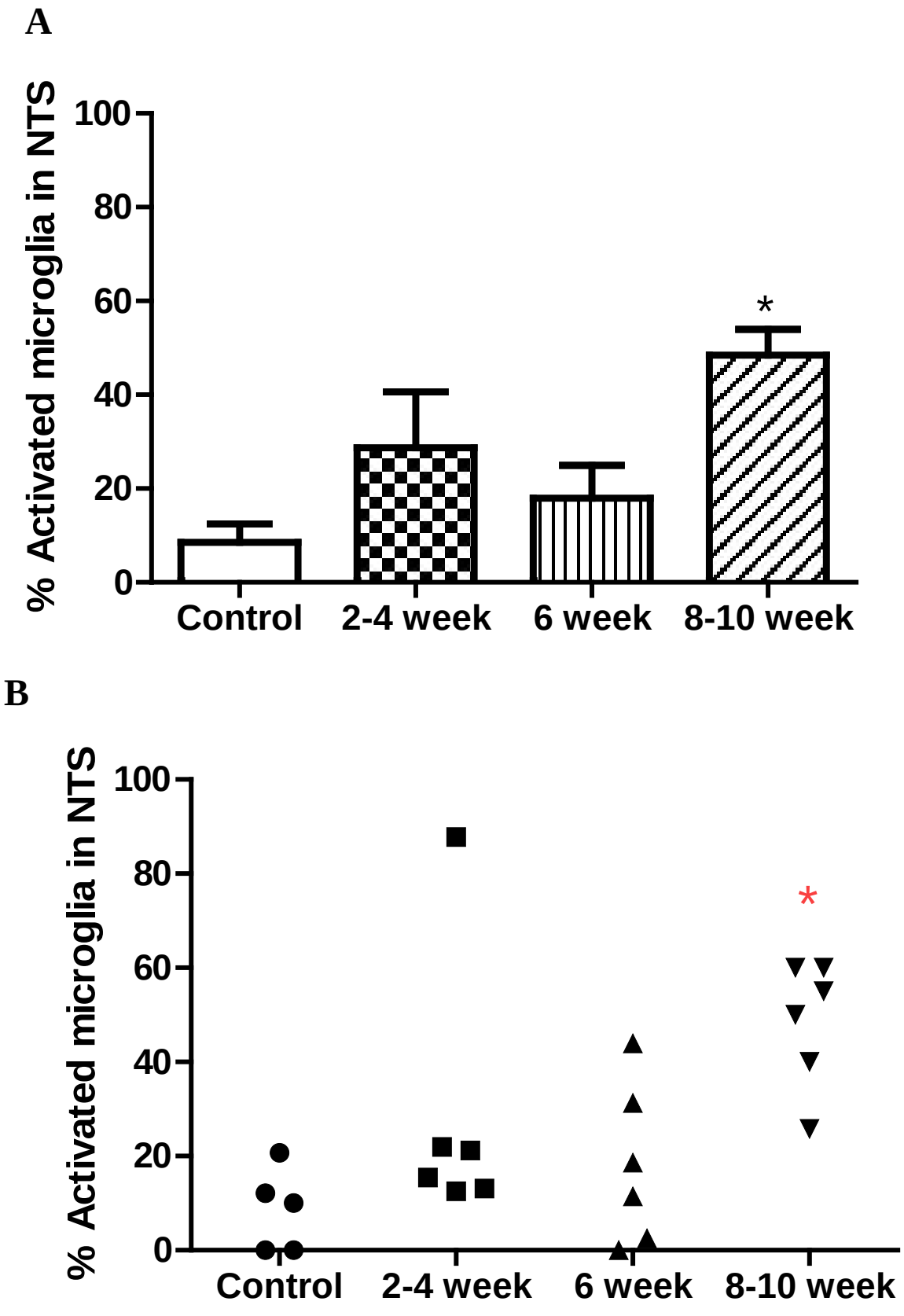
A
% Activated microglia in NTS
100
80
60
40
20
0
*
Control
2-4 week
6 week
8-10 week
B
% Activated microglia in NTS
100
80
60
40
20
0
*
Control
2-4 week
6 week
8-10 week

**Fig. 3.8 :** Activated microglia expressed as a percentage of total microglia in the nuclear tractus solitarius (NTS). Data were obtained from control animals (N = 5) and rats at 2 weeks (N = 6), 6 weeks (N = 6) and 8-10 weeks (N=6) after STZ injection. Panel A shows the average percentage of activated microglia (mean ± SEM). Panel B shows data from individual rats. * $P < 0.05$ compared to control.

**Fig. 3.9 :**

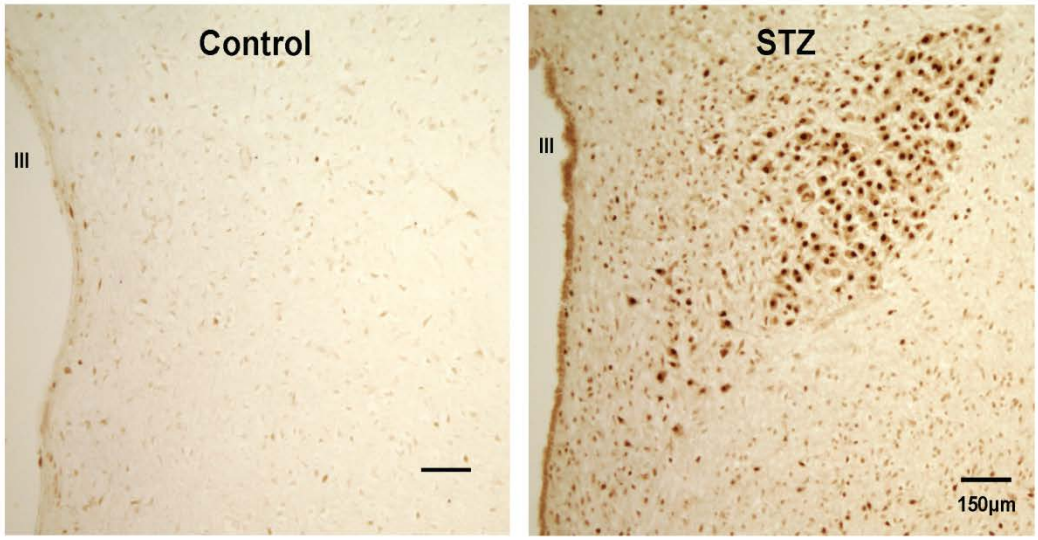

**Fig. 3.9** : Photomicrographs of the hypothalamic area of rat brain encompassing the paraventricular hypothalamic nucleus showing neuronal nuclei stained with anti-Fos antibody in control (Panel A) and in STZ-induced diabetic rat at 8-10 weeks time point (Panel B). III indicates third ventricle.

**Fig. 3.10 :**

**A**

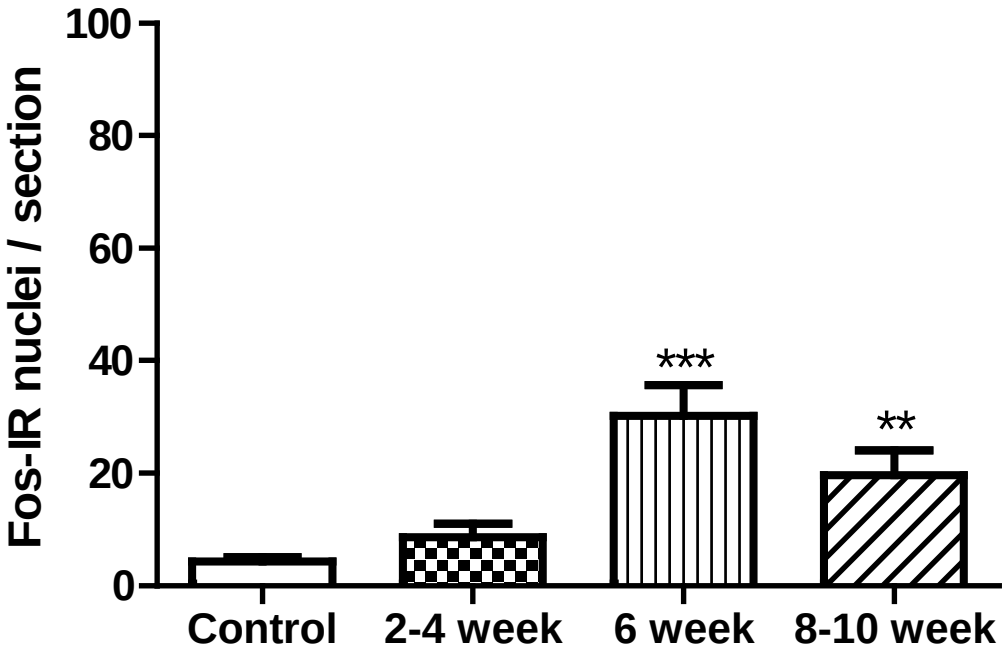
Fos-IR nuclei / section
100
80
60
40
20
0
***
**
Control
2-4 week
6 week
8-10 week

**B**

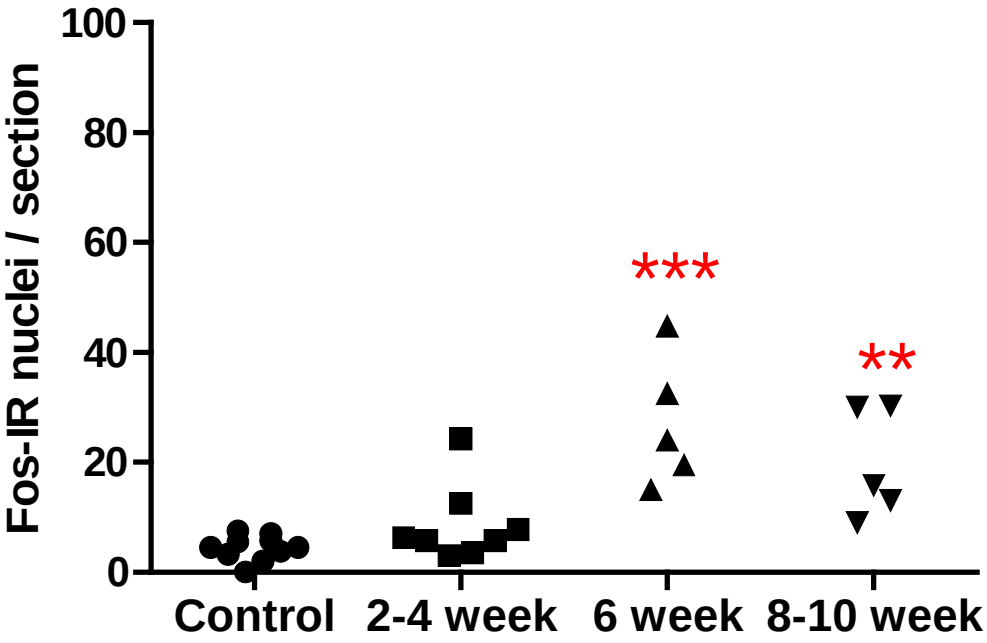
Fos-IR nuclei / section
100
80
60
40
20
0
***
**
Control
2-4 week
6 week
8-10 week

**Fig. 3.10 :** Quantification of number of Fos-IR nuclei within the paraventricular hypothalamic nucleus. Data obtained from control (N = 10) and STZ-induced diabetic rats at 2 weeks (N = 8), 6 weeks (N = 5) and 8-10 weeks (N=5) after STZ injection. Panel A shows the average number of Fos-IR nuclei per section (mean ± SEM). Panel B shows data from individual rats. ** $P < 0.01$ & *** $P < 0.001$ compared to control.

**Fig. 3.11 :**

**A**

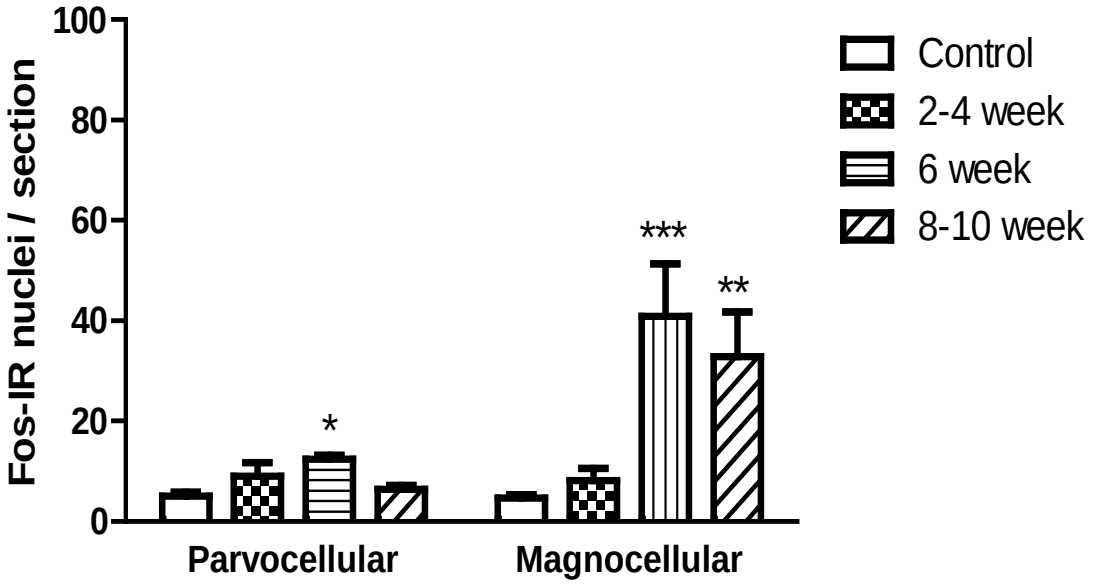
Fos-IR nuclei / section
100
80
60
40
20
0
*
***
**
Parvocellular
Magnocellular
Control
2-4 week
6 week
8-10 week

**B**

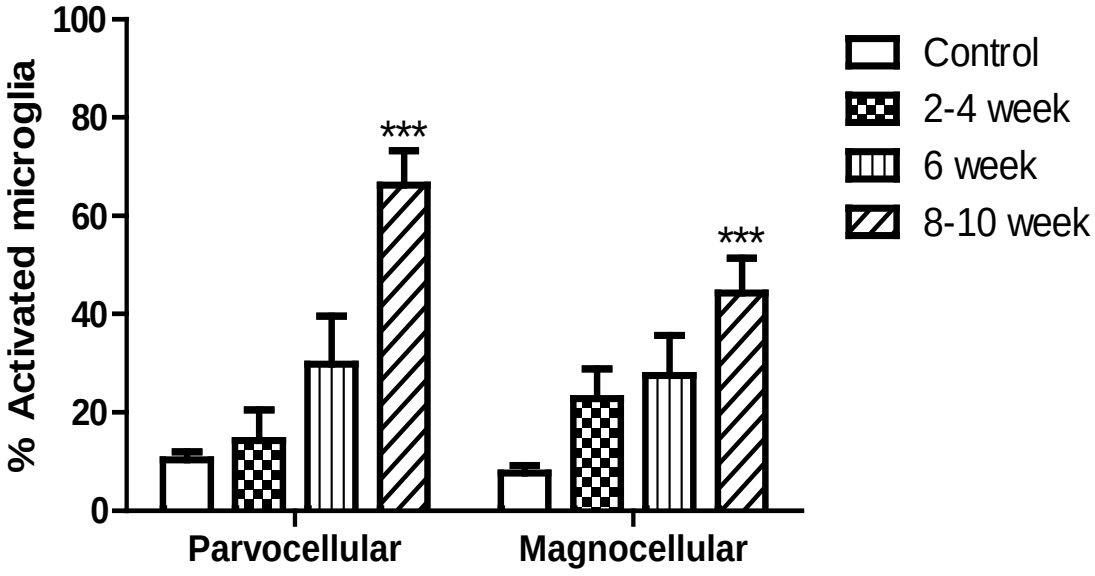
% Activated microglia
100
80
60
40
20
0
***
***
Parvocellular
Magnocellular
Control
2-4 week
6 week
8-10 week

**Fig. 3.11 :** Neuronal and microglial activation in the parvocellular subdivision and magnocellular subdivision of the paraventricular hypothalamic nucleus. Panel A shows quantification of number of Fos-IR nuclei per section. Data were obtained from control (N = 9) and STZ-induced diabetic rats at 2 weeks (N = 8), 6 weeks (N = 5) and 8-10 weeks (N=5) after STZ injection. Panel B shows the average percentage of activated microglia (mean ± SEM). Data were obtained from control (N = 10) and STZ-induced diabetic rats at 2 weeks (N = 8), 6 weeks (N = 9) and 8-10 weeks (N=10) after STZ injection. Values are expressed as the mean ± SEM. ** $P < 0.01$ & *** $P < 0.001$ compared to control.

**Fig. 3.12 :**

**A**

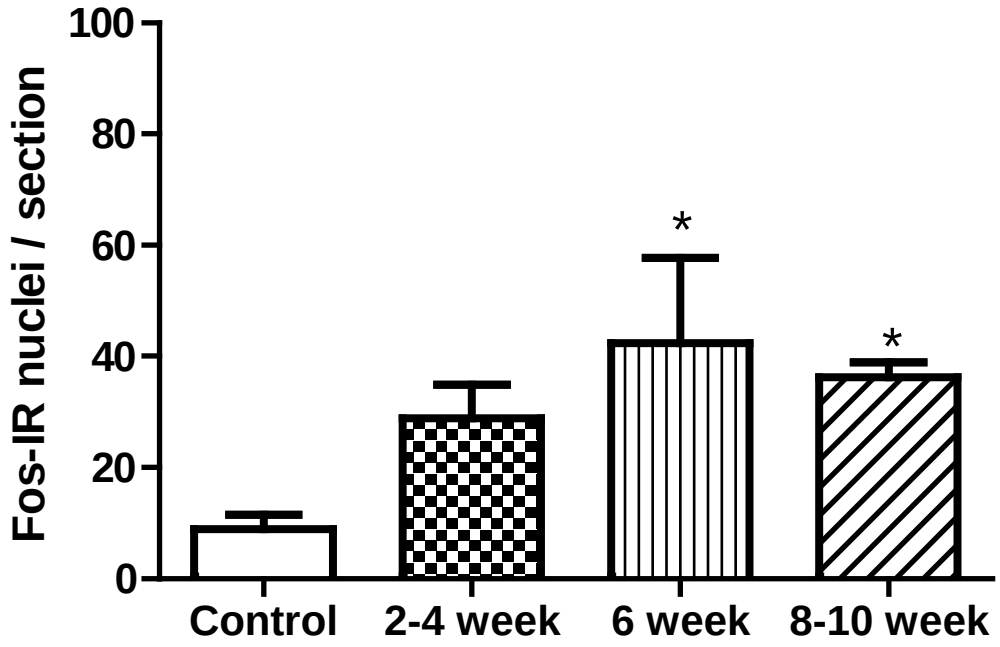
Fos-IR nuclei / section
100
80
60
40
20
0
*
*
Control
2-4 week
6 week
8-10 week

**B**

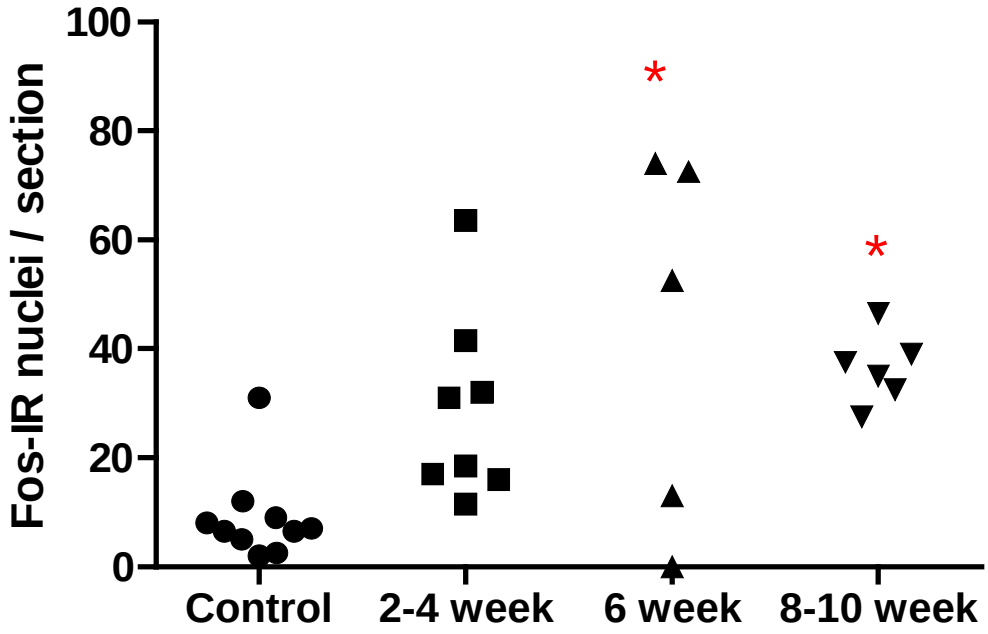
Fos-IR nuclei / section
100
80
60
40
20
0
*
*
Control
2-4 week
6 week
8-10 week

**Fig. 3.12 :** Quantification of the number of Fos-IR nuclei in the supraoptic nucleus. Data were obtained from controls (N = 10) and STZ-induced diabetic rats at 2 weeks (N = 8), 6 weeks (N = 5) and 8-10 weeks (N=6) after STZ injection. Panel A shows average Fos-IR nuclei per section in the supraoptic nucleus (mean ± SEM). Panel B shows data from individual rats.* $P < 0.05$ compared to control.

**Fig. 3.13 :**

**A**

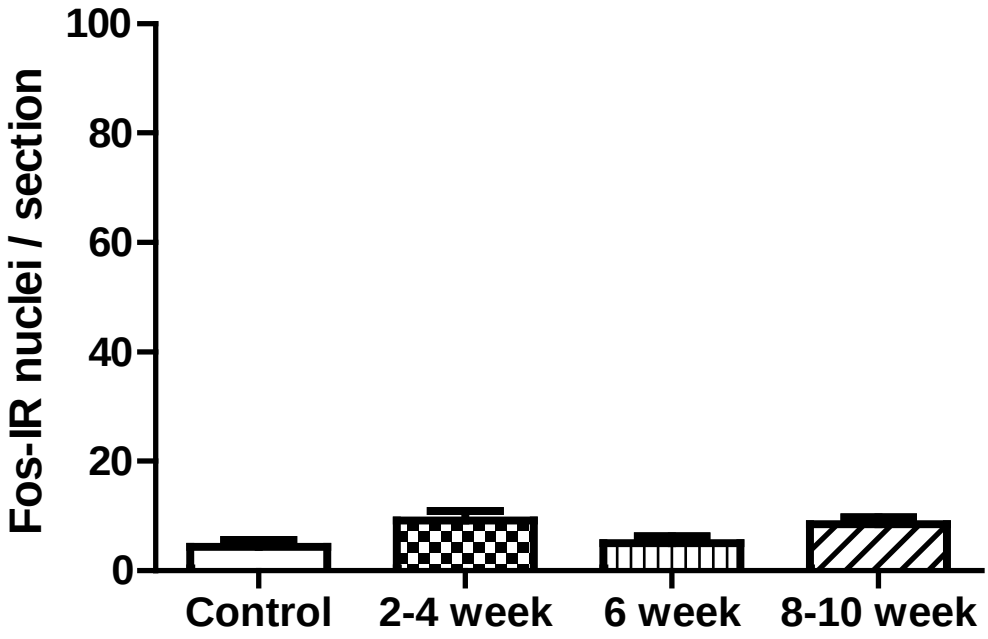
Fos-IR nuclei / section
100
80
60
40
20
0
Control
2-4 week
6 week
8-10 week

**B**

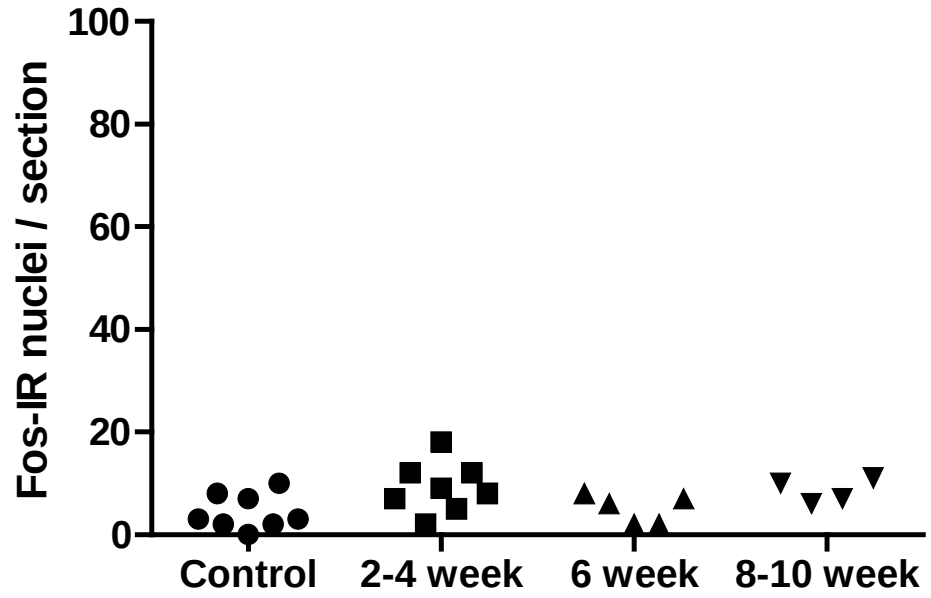
Fos-IR nuclei / section
100
80
60
40
20
0
Control
2-4 week
6 week
8-10 week

**Fig. 3.13 :** Quantification of the number of Fos-IR nuclei per section in the nuclear tractus solitarius. Data were obtained from control (N = 8) and STZ-induced diabetic rats at 2 weeks (N = 8), 6 weeks (N = 5) and 8-10 weeks (N=4) after STZ injection. Panel A shows the average number of Fos-IR nuclei (mean ± SEM). Panel B shows data from individual rats.

**Fig. 3.14 :**

**A**

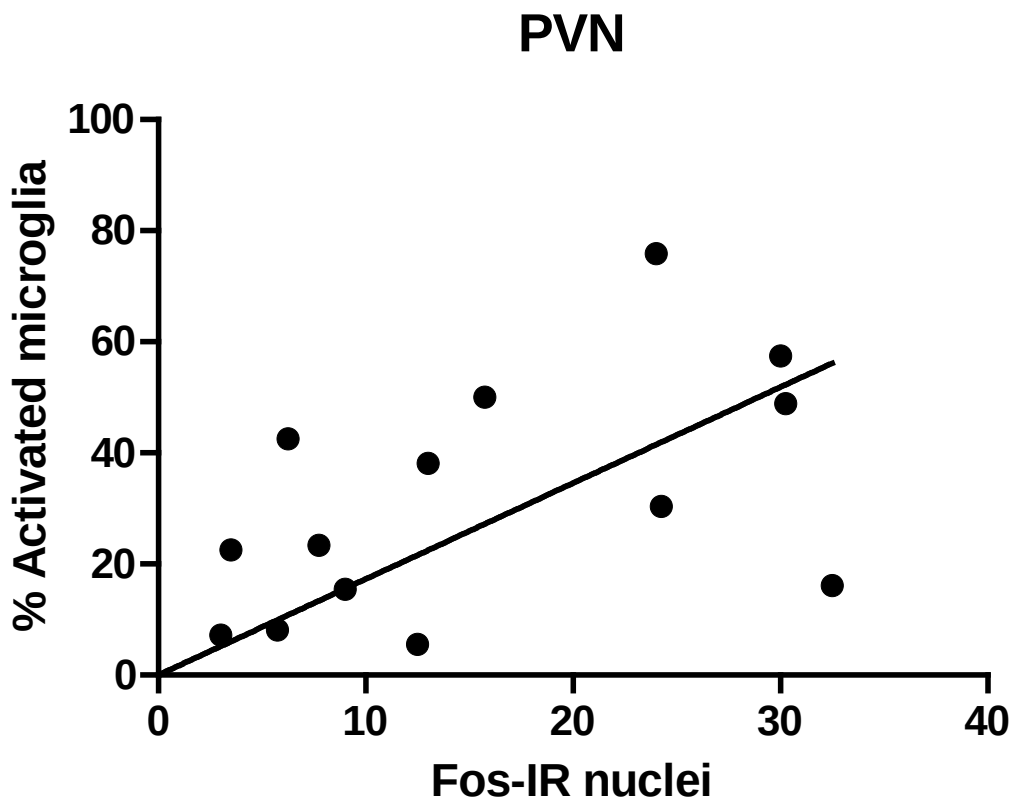
PVN
% Activated microglia
100
80
60
40
20
0
0
10
20
30
40
Fos-IR nuclei

**B**

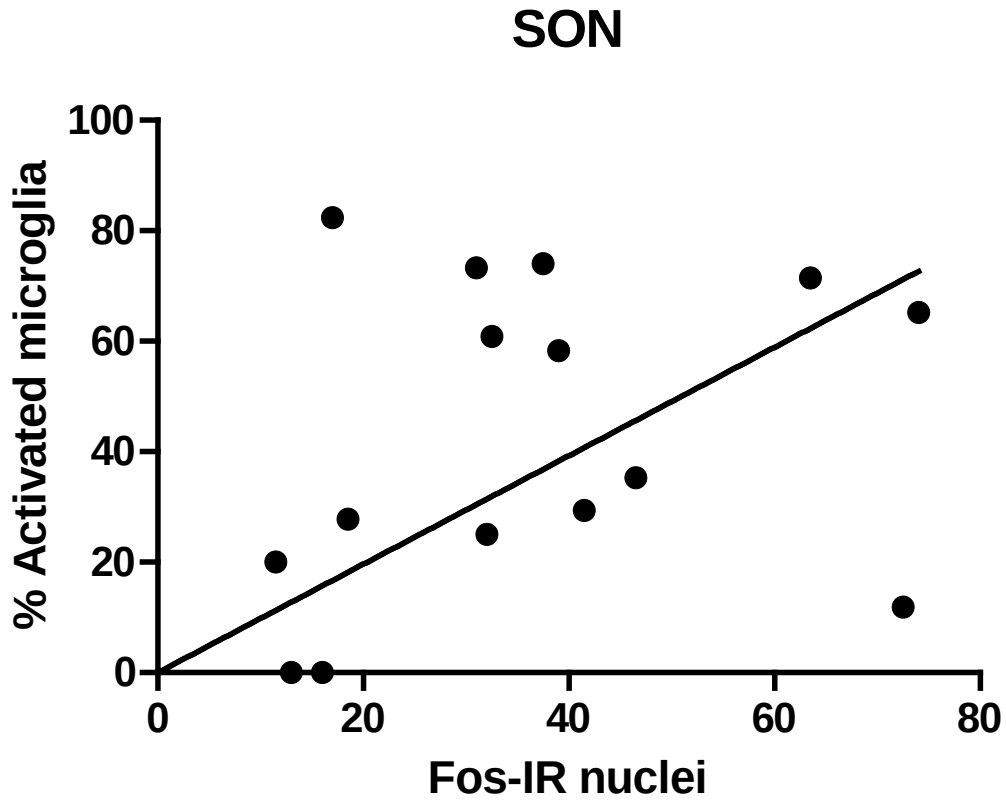
SON
% Activated microglia
100
80
60
40
20
0
0
20
40
60
80
Fos-IR nuclei

**Fig. 3.14 :** Graphs showing the relationship between the Fos-IR nuclei and percentage activated microglia present in (A) PVN (P=0605; r=0.51) and (B) SON (P=0.3276; r=0.27), in STZ-induced diabetic rats. Two tailed pearson's correlation test was performed using Graph Pad Prism Version 5.

**Fig. 3.15 :**

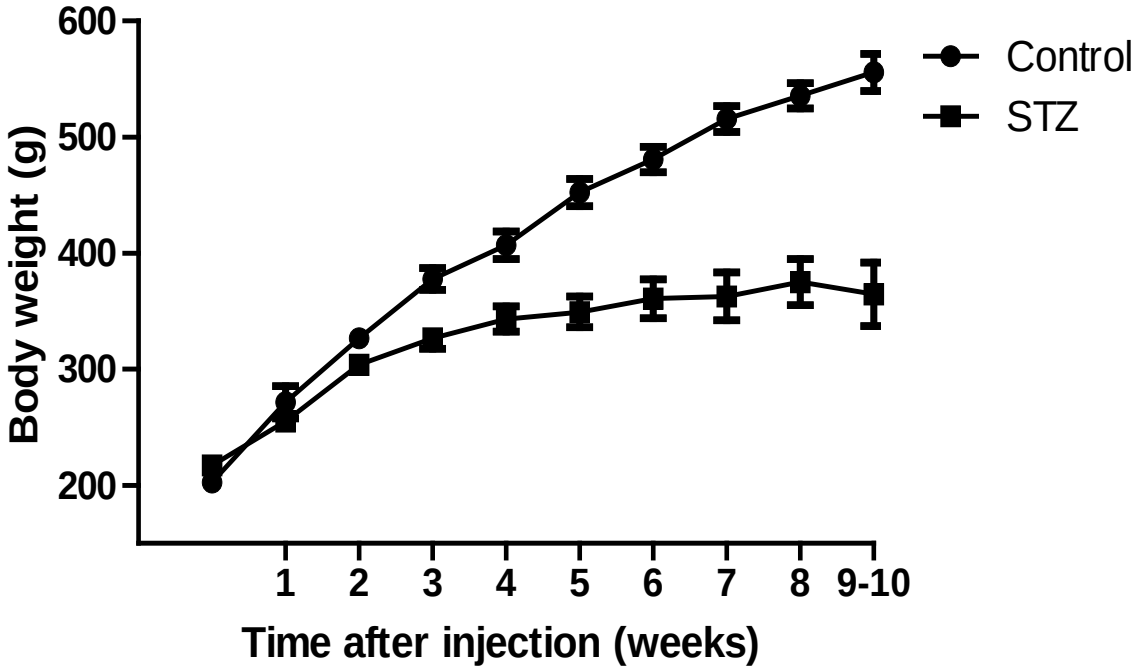
600
500
400
300
200
Body weight (g)
1
2
3
4
5
6
7
8
9-10
Time after injection (weeks)
Control
STZ

**Fig. 3.15 :** Body weight of control and STZ-induced diabetic rats measured at weekly intervals. Values are expressed as the mean ± SEM

**Fig. 3.16 :**

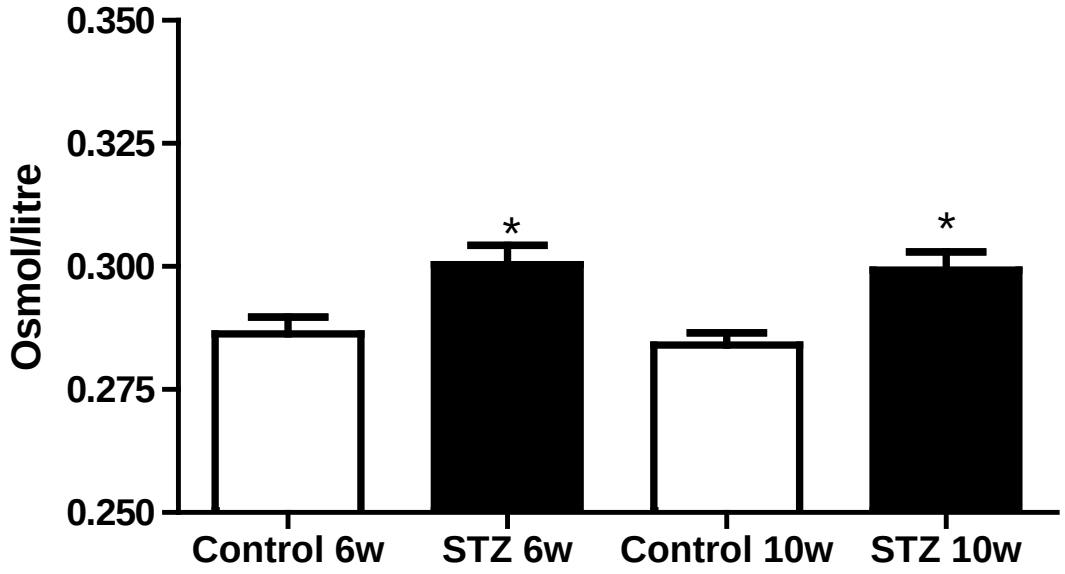
0.350
0.325
0.300
0.275
0.250
Osmol/litre
*
*
Control 6w
STZ 6w
Control 10w
STZ 10w

**Fig. 3.16 :** Plasma osmolarity in control and STZ-induced diabetic rats. Values are expressed as the mean ± SEM. * indicates significantly different than control $P<0.05$.

## *Discussion*

In this study, we observed microglial activation in STZ-induced diabetic rats in specific brain regions associated with the cardiovascular system. We have previously reported microglial activation in the PVN of rats with myocardial infarction, a condition associated with elevated sympathetic nerve activity to the heart and kidney (chapter 2). The novel findings of the present study are that (i) microglial activation occurs in the PVN, SON and NTS regions of STZ-induced diabetic rats but this activation is not seen until 6-8 weeks after STZ injection, (ii) although the time of onset of neuronal and microglial activation in PVN was variable in individual rats, neuronal activation appeared to proceed microglial activation, and (iii) neuronal and microglial activation in the PVN were present in parvocellular as well as magnocellular subdivisions.

Our results suggest that in STZ-induced diabetic rats there may be substantial changes in the function of the PVN, SON and NTS, all of which have well known cardiovascular functions. Increased serum levels of both adrenaline and noradrenaline along with increased cardiac peak ejection and cardiac peak filling rate, suggests elevated sympathetic nerve activity in humans with developed type 1 diabetes (Ferraro et al 1990). Studies on diabetic human patients and STZ-induced diabetic rats have reported abnormal autonomic control of sympathetic and parasympathetic nervous systems (Makimattila et al 2000; Reynolds et al 1996; Zheng et al 2006) which may be linked to the cardiovascular complications of diabetes. Abnormal autonomic control has been suggested to be responsible for other complications of diabetes in humans eg. diabetic nephropathy (Spallone et al 1994).

Our results showing increased Fos-IR neurons in the PVN and SON regions of STZ -induced diabetic rats (Fig. 3.9, 3.10 (A) & 3.12 (A)) are consistent with a previous study by Zheng et al. (2002), although they did not investigate the time course of neuronal activation.

We also observed that increased fos labeling was present in the parvocellular as well as in the magnocellular part of the PVN, although there were more Fos-IR neurons in the magnocellular subdivision (Fig. 3.11 (A)). The parvocellular neurons of the PVN are involved in controlling autonomic functions including blood pressure, heart rate and the cardiovascular responses contributing to homeostatic functions like temperature regulation (Badoer 2001; van den Pol 1982; Wotjak et al 2001). Thus, increased activation of these the PVN autonomic neurons could be a possible reason for the reported increased sympathetic nerve activity in STZ -induced diabetic rats.

The magnocellular part of the PVN contains oxytocin and vasopressin hormone producing neurons as does the SON. The role of these neurohormones in blood volume and blood pressure regulation have been demonstrated by many previous animal studies (Badoer & Merolli 1998; Zheng et al 2002). Vasopressin acts peripherally on arteries causing vasoconstriction and on the kidney to decrease urine formation by increasing water reabsorption. These peripheral actions of vasopressin lead to increases in blood volume to maintain cardiac output and arterial pressure. Studies on STZ-induced diabetic rats have reported elevated levels of plasma vasopressin (Brooks et al 1989; Charlton et al 1988) and demonstrated a possible role of cardiovascular changes and hyperosmolarity in triggering neuronal activity and vasopressin production from magnocellular neurosecretory cells (Brooks et al 1989; Charlton et al 1988). Thus, the abnormally increased neuronal activity that we see in PVN and SON (Fig. 3.9, 3.10 (A) & 3.11 (A)) may be due to the increased plasma osmolarity observed in these rats (Fig. 3.16).

Interestingly, we observed marked variation in number of Fos-IR neurons between individual rats at any time point (Fig. 3.9 (B), 3.10 (A) & 3.8 (B)) suggesting variability in onset. Even in humans, some develop cardiovascular complications earlier than others who

have suffered from the diabetes for the same period of time, suggesting a role of the genetic background of individuals. However, the detailed mechanism responsible for this variability is not clear. Interestingly, we also observed that the time point of the onset of neuronal activation was delayed (up to 6-8 weeks after STZ treatment) despite the fact that the blood glucose levels were raised several fold within the first week. The reason for this delayed activation is not known and requires further investigation, but is consistent with delayed onset of cardiovascular complications in humans.

Our study is the first to investigate the time course of microglial activation in the PVN and SON in STZ-induced diabetic rats. As mentioned earlier in the result section, the intensity of the OX-42 staining appeared increased in microglia present in these regions in STZ-induced diabetic rats but this was difficult to quantify due to the inherent variability in the immunohistochemical technique. However, the variability in staining intensity cannot explain the differences seen in microglial morphology, since the increased intensity of staining would be expected to cause fine microglial processes to appear more prominent. Interestingly, while the time of onset of both microglial activation and neuronal activation was delayed in the PVN as well as in the SON (Fig. 3.6 (A), 3.2 (A) & 3.10 (A), 3.12 (A)), it appears that neuronal activation preceded microglial activation. Under certain circumstances neuronal activation is sufficient to directly cause microglial activation (Hathway et al 2009). In addition, a study on STZ-induced diabetic rats has shown apoptotic cell death in SON neurons and suggested chronic over activation of SON neurons as a mechanism responsible for neuronal death (Klein et al 2004). The study also reported activation of microglia in SON by showing reduced microglial process length. The authors hypothesised that neuronal over activation and apoptotic cell death is responsible for the microglial activation. Our results showing significant neuronal activation earlier than microglia activation in PVN and SON (compare Fig. 3.6 (A) with Fig. 3.12 (A) and Fig.3.10 (A) with Fig. 3.2 (A)) supports this

hypothesis. Interestingly, we did not see a correlation between microglial and neuronal activation (Fig. 3.14 (A) & 3.14 (B)), although there was a trend towards correlation in the PVN. There are however, several possible reasons why the relationship between neuronal and microglial activation may be complex. Firstly, neuronal death due to over- excitation may lead to a decreased number of Fos-IR cells at later time points (Fig. 3.11 (A)) but would be expected to cause more activation of microglia. Secondly, neuronal activation may be responsible for the initiating but not for maintaining microglial activation. Our results do not eliminate the possibility of involvement of mechanisms other than neuronal over-excitation responsible for microglial activation (Refer to Chapter 1).

Our study is the first to show activation of microglia in the NTS region of STZ-induced diabetic rats. The NTS contains terminals from peripheral autonomic sensory neuronal axons. The NTS also receives projections from the PVN that play an important role in regulation of blood pressure (Krukoff et al 1997). Their study also demonstrated increased Fos-IR in NTS neurons upon change in blood pressure and blood volume suggesting that at least some NTS neurons that are involved in cardiovascular regulation can express Fos protein. We observed significant activation of microglial cells but did not observe any change in the number of Fos labeled neurons in this region at 8-10 weeks after STZ injection (Fig. 3.13 (A) and Fig. 3.8 (A)). A study on STZ-induced diabetic rats has also reported no change in baseline NTS expression of fos at 8 weeks and 16 weeks after STZ injection (Gouty et al 2001) which agrees with our results. Therefore, it is possible that microglial activation in the NTS may be via different mechanism to that in PVN and SON.

A recent study on NTS neurons using multi electrode electrophysiology has demonstrated barosensitive NTS impairment in the baseline condition for STZ-induced diabetic rats (Chen et al 2008b). Compared to controls, diabetic rats showed similar pressor

responses to PE but the number of Fos-IR neurons in the NTS of diabetic rats were significantly lower (Gouty et al 2001). The authors claimed that this reduced afferent baroreceptor input to the NTS in STZ-induced diabetic rats may be the result of diabetes-induced damage to baroreceptive afferent nerves. These studies collectively suggest an impaired cardiovascular regulation function of the NTS. A recent study on STZ-induced diabetic rats has shown increased microglial activation dorsal horn of spinal cord (Tsuda et al 2008). The study suggested that damage to peripheral sensory neurons that terminate in the dorsal horn are responsible for the microglial activation. It is therefore possible that degeneration of axon terminals of autonomic sensory neurons terminating in NTS are responsible for the microglial activation there. In contrast to the study of Tsuda et al. (2008), which has reported microglial activation in spinal cord within two weeks after STZ injection, we saw consistent microglial activation in NTS at the 8-10 weeks time point. This is consistent with the delayed nature of diabetic autonomic neuropathy as compared to sensory neuropathy (Verrotti et al 2009).

If excitotoxicity mediated neuronal death is responsible for the microglial activation in cardiovascular centres, then activated microglia can then further damage or modulate neuronal activity by releasing toxic substances. Previous *in vitro* and *in vivo* studies on microglia have demonstrated that microglial activation results in a change in their morphology, proliferation, migration to the site of injury and secretion of variety of cytokines, chemokines, nitric oxide, superoxides, and growth factors (Hide et al 2000; Ifuku et al 2007; Li et al 2005; Lu et al 2009a; Perregaux & Gabel 1994; Tsuda et al 2003). Interestingly, a recent study on angiotensin II (Ang II) induced hypertension in rats has reported activation of microglia in the PVN (Shi et al 2010b). Based on their results showing increased sympathetic nerve activity and the PVN neuronal activity upon direct injection of IL-1β into the the PVN, they suggested that secretion of IL-1β from activated microglia activates the PVN neurons to

increase sympathetic nerve activity. Thus, activated microglia in cardiovascular centres of the brain in STZ-induced diabetic rats may contribute to further neuronal over-excitation in the PVN and SON. Neuronal over-excitation in the PVN may leads to elevated sympathetic drive. In the NTS, microglial activation may be responsible for the impaired cardiovascular neuronal function.

## *Conclusion*

We have found increased neuronal and microglial activation in the cardiovascular centres of the brain in STZ-induced diabetic rats. Over-excitation of neurons due to increased plasma osmolarity in STZ-induced diabetic rats may be responsible for the microglial activation in PVN and SON. Microglial activation in NTS may be due to the damage to autonomic sensory neurons. These activated microglia may contribute to the increased local production of pro-inflammatory cytokines to modulate neuronal activity in those cardiovascular centres which may contributes to the elevated sympathetic nerve activity and reduced baroreceptor sensitivity in STZ-induced diabetic rats.

# Chapter 4: Microglia are not Activated in Hypothalamic Cardiovascular Centres of Fat Fed and Zucker Obese Rats

## *Introduction*

Elevated sympathetic nerve activity contributes to the pathology of heart failure (Refer Chapter 2). Sympathetic nerve activity is also elevated in diabetic humans and may contribute to the cardiovascular complications of diabetes. Indeed, the rate of sudden cardiac death in diabetic patients (Jouven et al 2005) may be in part due to this elevated sympathetic nerve activity, therefore it is important to determine the cause and mechanism responsible for elevated sympathetic nerve activity.

Sympathetic nerve activity is controlled by neuronal activity in various autonomic nuclei in the brain. We have reported microglial activation in the paraventricular hypothalamic nucleus (PVN) and suparaoptic nucleus (SON) in STZ-induced diabetic rats (Refer Chapter 3). As described before (in chapter 3), the PVN is one of the cardiovascular centers in the brain while the SON outputs are solely directed to the posterior pituitary gland and have an impact on hemodynamic outcomes via the kidney and vasopressin release. Activated microglia can secrete a variety of cytokines, chemokines, reactive oxygen species, neurotramitters, neurotrophins and nitric oxide (Refer Literature review). There are growing numbers of studies indicating that secretions from activated microglia can modulate neuronal activity (Biggs et al 2010; Lu et al 2009a; Shi et al 2010b; Tsuda et al 2003). Collectively these data suggest that activated microglia in STZ-induced diabetic rats contributes to the reported increase in the neuronal activity in cardiovascular centres (Zheng et al 2002). However, the mechanisms responsible for the microglial activation seen in STZ-induced diabetic rats are not clear. It is also not known whether microglial are activated in other forms of diabetes. Hence, to understand the mechanism, we investigated microglial activation in

cardiovascular centres other models of diabetes eg. High Fat Fed, Zucker Obese and Low Capacitant Runner (LCR) rats.

The STZ-induced diabetic rat model resembles to human type 1 diabetes. In this model rats develops extreme hyperglycemia. The most common form of diabetes in humans is type 2 diabetes where they exhibits some similar and some dissimilar symptoms to type 1 diabetes. It is generally agreed that individual genetic background, diet and lifestyle contribute to the pathogenesis of diabetes type 2. One of the major contributing factors is high fat western diet. Chronic feeding of a high fat diet is known to cause hyperglycemia in rodents primarily by inducing insulin resistance and obesity (Oakes et al 1997; Pedersen et al 1991; Srinivasan et al 2004). Various studies have linked obesity and insulin resistance with the pathology of cardiovascular diseases and hypertension (Aronne et al 2007; Chapman & Sposito 2008; Hintz et al 2003; Lamounier-Zepter et al 2006; Sowers 2003). Therefore we investigated whether microglia were activated in cardiovascular centres in rats fed a high fat diet for 8 weeks and in leptin receptor deficient Zucker Obese rats (24-26 weeks old). Zucker Obese rats are widely used animal model of obesity and hypertension

We also used Low (LCR) - capacity runners as an model of insulin resistance against their control High (HCR)- capacity runner rats. This rodent model of metabolic syndrome was developed via selective breeding for intrinsic running capacity. This selection strategy resulted in animals with high or low intrinsic running capacity, referred to as high capacity runners (HCR) and low capacity runners (LCR), respectively (Koch & Britton 2001). Previous study on these rats have reported that Insulin-stimulated glucose transport, insulin signal transduction, and rates of palmitate oxidation are lower in LCR vs. HCR (Lessard et al 2011).

Therefore, we investigated microglial activation in hypothalamic cardiovascular centre in high fat fed rats, Zucker Obese and LCR rats in this study. These diabetic models share some common complications with STZ-induced diabetic rats as well as they have some

unique symptoms that is not present in STZ-induced diabetic rats. Therefore, we compared the results obtained in this study with those in STZ-induced diabetic rats to understand mechanism of microglial activation.

## *Methods*

### Animals

Sprague Dawley (SD) 8 weeks high fat fed rats (Animal Resource Centre, Perth, Western Australia) were obtained from Prof. John Hawley's laboratory at RMIT University. The rats were fat fed high fat diet (SF03-002) or normal chow diet. Composition of the diet by mass was as follows:

**Table 4.1:**

| | SF03-002 (Fat Containing Diet) | Normal Chow Diet |
|---|---|---|
| Protein | 19.5 % | 19.6% |
| Fat | 36% | 4.6% |
| Carbohydrates | 35.7% | 56.8% |

Zucker Obese and Zucker Lean rats were obtain from Prof. Julianne Reid's research laboratory at RMIT University. All the Zucker rats used for experiments were between 24 weeks to 26 weeks old. LCR and HCR rats were obtained from Britton, S.L laboratory, University of Michigon, USA. These rats were obtained following 22 generations of artificial selection. They were phenotyped for intrinsic running capacity at 11 wk of age using an incremental treadmill running test, and their average running capacity (in meters) was recorded as described previously (Koch & Britton 2001). All these rats were housed two per cage in a temperature controlled animal room ($21^0$C) maintained on a 12 : 12 hrs reverse light-dark cycle and provided with standard chow diets and water ad libitum.

For STZ experiments, as described previously (chapter 3), Sprague Dawley rats obtained from ARC (Animal Resource Centre) were given streptozotocin (STZ) in citrate buffer 48mg/kg body weight via tail vein to induce diabetes. Rats were tested for diabetes after one week of injection and used after 2-4, 6 and 8-10 weeks of injection. Control rats had received only vehicle injection and underwent all the other procedure in a same way as STZ treated rats.

## Tissue processing

All the rats used for this study were euthanized by an over dose of pentobarb (180mg/kg body weight). After which they were decapitated and the brains were removed. Forebrain and bran stem area was separated from hypothalamus by cutting brain into three pieces, then immediately immersed in freshly prepared, ice cold 4% paraformaldehyde in phosphate buffered saline (PBS) (0.1 M, pH 7.2) and stored for 4 h at 4 °C. The brains were then transferred to a solution containing 30% sucrose in PBS and left for approximately 48 h at 4 °C before they were used for immunohistochemistry.

## Immunohistochemistry

Sectioning and Immunohistochemistry was performed as described previously (chapter 2). In brief, transverse 20 µm-thick cryostat sections were cut from a region of hypothalamus encompassing the PVN and arcuate nuclei. These sections were processed immunohistochemically to detect microglial cells using an antibody to Cd11b (clone OX-42). Sections were incubated with this OX-42 (Anti-mouse primary antibody) for 72 hrs at $4^0$ C. Then sections were washed, incubated 2 hrs with secondary biotinaylated- antimouse antibody followed by 2 hrs incubation with peroxidate labeled Extravidin-HRP. At the end DAB chromogen was used to visualise microglia.

## Morphological analysis and quantification

As described previously (chapter 2 and chapter 3) the number of microglia and their morphological characteristics were examined within multiple square areas (0.2 X 0.2 mm) with a light microscope using 400x magnification. To find the % Activated microglia, the total and activated microglia were manually counted from the approximately same region of interest in all rats.

## *Results*

### 1) Fasting blood glucose and body weights in fat fed vs chow fed rats and LCR vs HCR

Rats fed a high fat diet for 8 weeks did not gain significantly high body weight (N=6; 437 ± 9 g) as compared to chow fed rats (429 ± 16 g; N=6) (P=0.6810). However, they had significantly higher fasting blood glucose levels as compared to the chow fed rats (5.650 ± 0.1254 μM (N=8) vs 6.613 ± 0.3159 μM (N=8); P= 0.0133). Overt obesity, hypercholesterolemia, hyperlipidemia, and hyperglycemia are characteristic features of Zucker Obese rat model reported in literature. We observed significantly higher body weight and fasting blood glucose levels in Obese Zucker rats (N=23) as compared to control Lean Zucker rats (N=21) (P<0.001).

The LCR rats used for this study had initial running capacity of 282 ± 12 meters while HCR rats had running capacity of 1927 ± 57 meter. These LRC rats had significantly high body weight (497 ± 19 g vs 331 ± 8 g; N=10; P<0.05) and fasting blood glucose as compared to HCR rats (6.2 ± 0.1 μM vs 5.3 ± 0.1μM; N=10; P<0.05).

### 2) Microglial morphological observations and quantification of microglial activation in PVN and SON

In normal adult rat brain, microglia have small soma, long and highly branched processes and are called “ramified microglia”. Microglial cells in the PVN of both high fat fed rats (N=5) and chow fed rats (N=5) showed long, thin and branched processes and small nuclei, similar to symptoms of ramified microglia (Fig. 4.1 (C)). Moreover, there was no difference in intensity of OX-42 staining between high fat fed and Chow fed rats. Quantification of % activated microglia from the PVN of chow fed Vs high fat fed rats showed no significant difference ( 8.2±1.3 vs 11.1±1.12; P= 0.1019) (Fig. 4.2 (C)).. Similarly, we did not observe difference in microglial morphology in the SON region of fat fed rats as compared to chow fed control rats (Data not shown).

As seen in high fat fed and chow fed rats, we observed no difference in microglia morphology and OX-42 intensity in Obese Zucker vs Lean Zucker rats and HCR Vs LCR rats (Fig. 4.1 (A) & 4.1 (B)). Quantification of % microglial activation in the PVN of Obese Zucker vs Lean Zucker as well as HCR vs LCR rats showed no significant difference (P=0.1169 and P=0.4670 respectively) suggesting there was no activation of microglia in the PVN in those rats (Fig. 4.2 (A) & 4.2 (B)). Similar to the PVN microglia in the SON region also exhibited ramified morphology in HCR, LCR, Obese Zucker and Lean Zucker rats (Data not shown).

## 3) Activation of microglia in VMH/Arcuate region in Fat fed rats

Microglia in some high fat fed rats showed markedly shortened, thicker, and stubbier processes and stronger staining for OX-42 in VMH/Arcuate region as compared to the microglia in same region of chow fed rats (Fig. 4.3). When % activated microglia in these two sets of animals was compared using a t test, no significant difference was observed (Fig. 4.4 (A); P=0.0551) despite the fact that average of % activated microglia was markedly high in high in some fat fed rats.

Interestingly, the number of % activated microglia in PVN and VMH/Arcuate area in chow fed rats was never higher than 15% activation. Therefore, all the rats showing less than 20% activated microglia were defined as showing no activation while all the rats showing more than 20% activation were defined as showing activation. 3 out of 5 high fat fed rats but none of the control rats fell into the categories of activation (Fig. 4.4 (B). Chi-Square test comparing the proportion of rats with and without activation performed on chow fed and high fat fed rats did show a significant difference between two groups (P=0.0384).

## 4) Microglia were not activated in VMH/Arcuate region of Zucker Obese rats and LCR rats

In contrast to fat fed rats, none of the Zucker obese rats and LCR rats used for this study showed microglial activation in VMH/Arcuate region as demonstrated in Fig. 4.5 (A), 4.5 (B) & 4.5 (C).

## *Figures*

**Fig. 4.1 :**

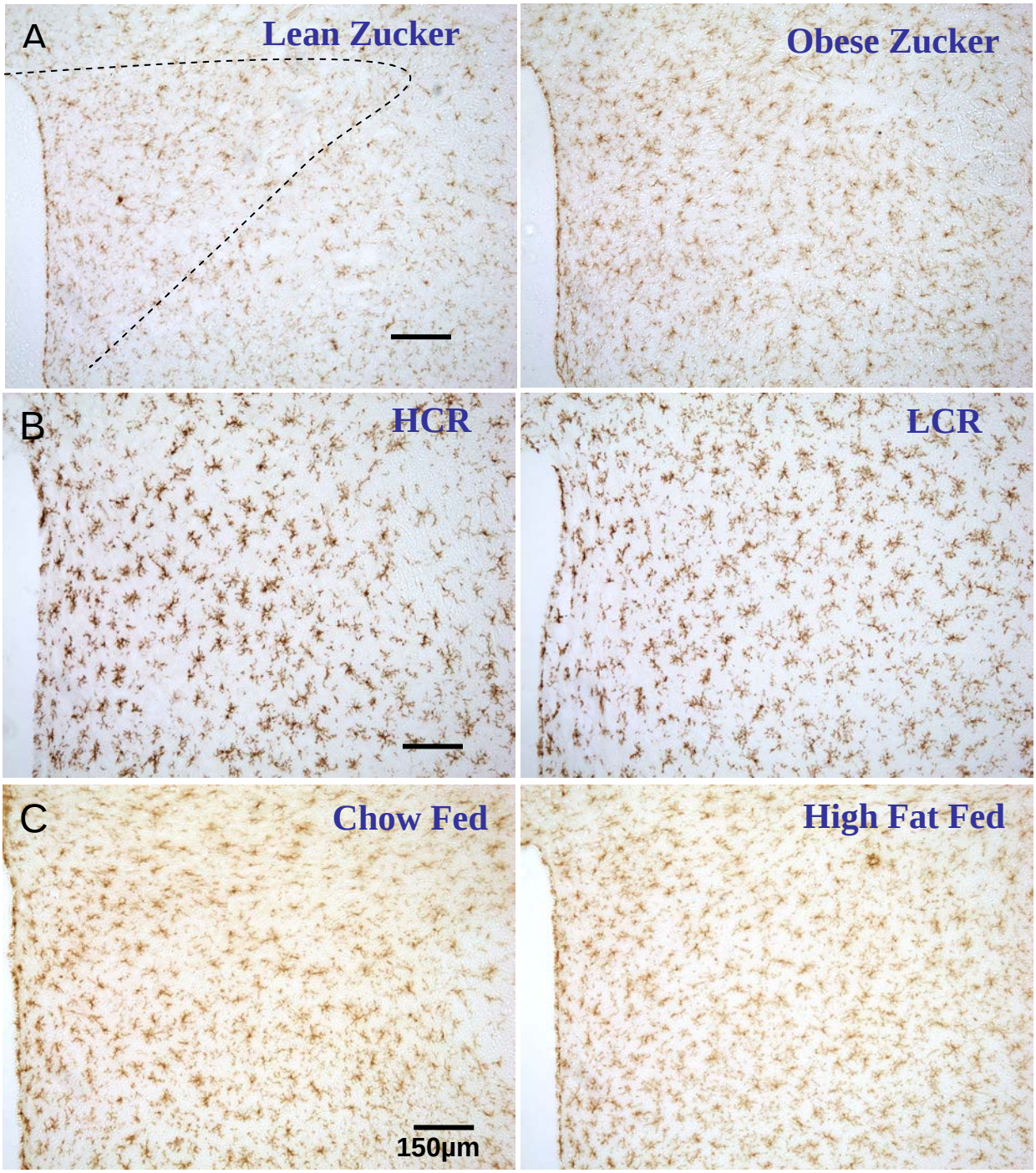

**Fig. 4.1 :** Photomicrographs of the hypothalamic area encompassing the paraventricular hypothalamic nucleus showing OX-42 immunolabeled microglia in (A) Zucker Lean and Zucker Obese rats (B) HCR and LCR rats (C) chow fed and high fat fed rats.

**Fig. 4.2 :**

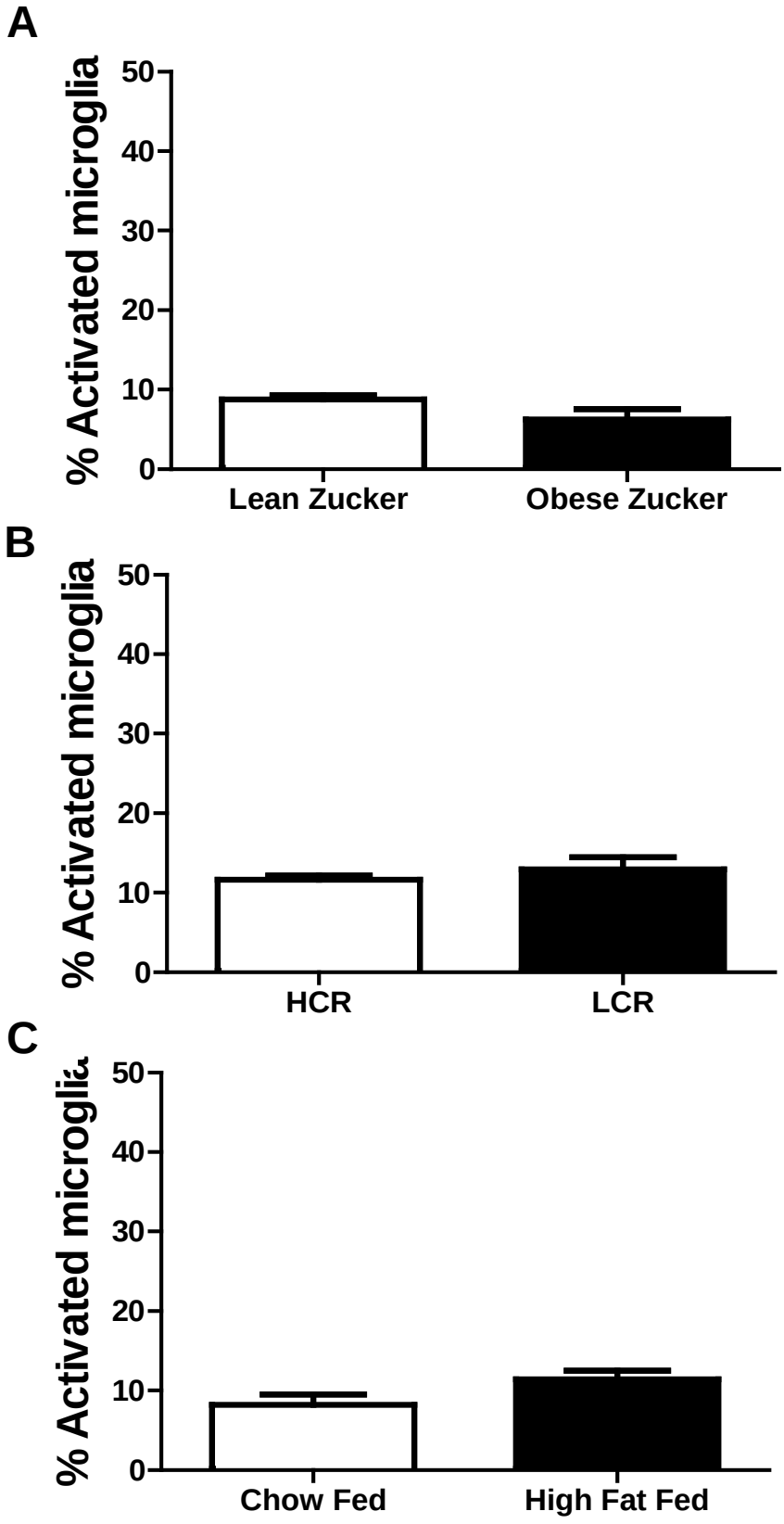
A
% Activated microglia
50
40
30
20
10
0
Lean Zucker
Obese Zucker
B
% Activated microglia
50
40
30
20
10
0
HCR
LCR
C
% Activated microglia
50
40
30
20
10
0
Chow Fed
High Fat Fed

**Fig. 4.2 :** Activated microglia expressed as a percentage of total microglia in the hypothalamic paraventricular nucleus. Figure shows data from the PVN of (A) Zucker Lean (N=4) and Zucker Obese rats (N=4). (B) HCR (N=4) and LCR (N=4) rats (C) chow fed (N=5) and high fat fed rats (N=5).

**Fig. 4.3 :**

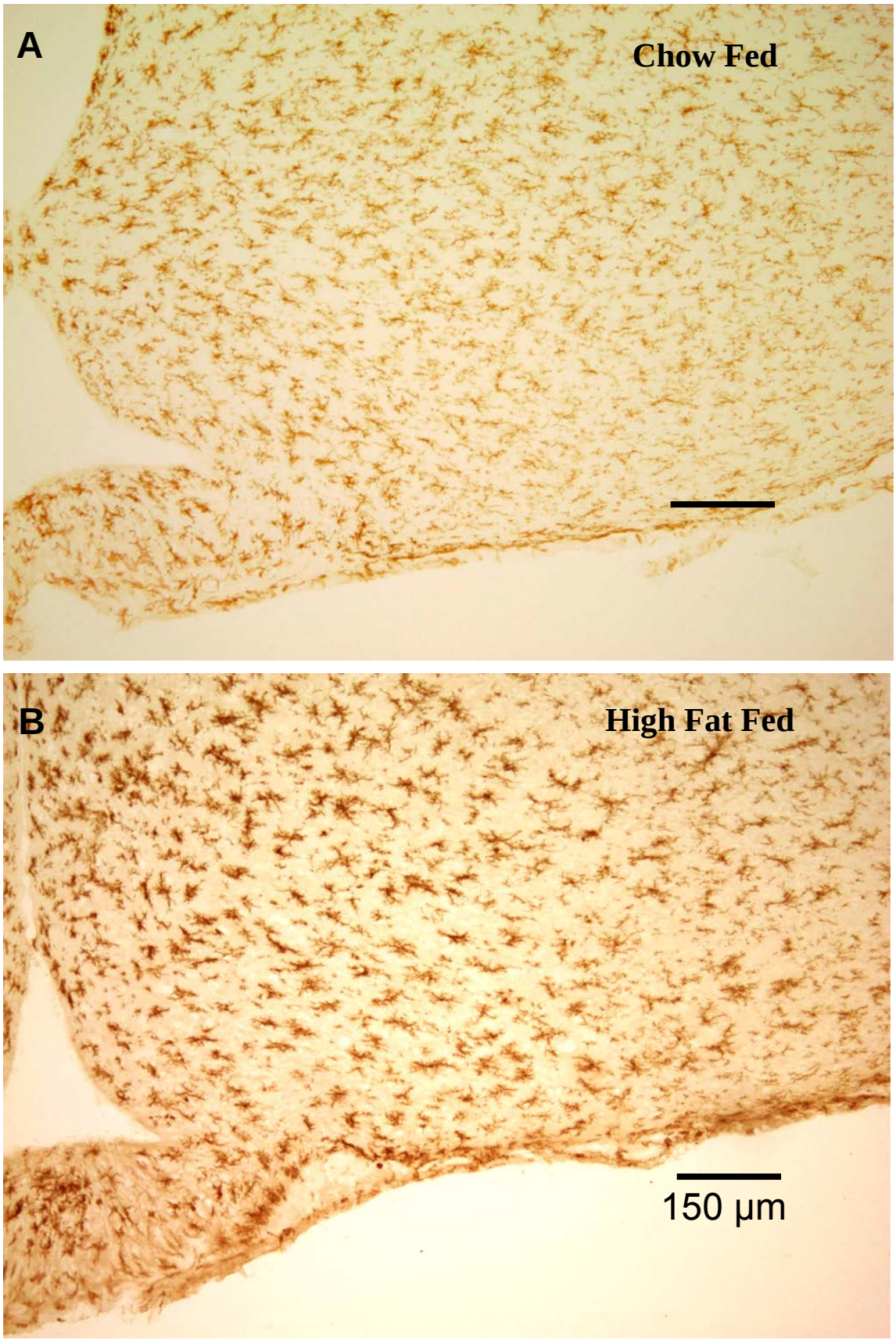

**Fig. 4.3 :** Photograph of the hypothalamic region encompassing the ventromedial hypothalamus / arcuate nucleus area (VMH/Arcuate) showing OX-42 immunolabeled microglia. In chow fed rats normal ramified microglia were observed in VMH/Arcuate region. (Panel A) Note the long processes, many secondary branches and very small somata. Activated microglia were present specifically in VMH/Arcuate region of high fat fed rats. (Panel B) Note the drastic increase in OX-42 staining and the morphological changes including enlarged somata and shorter, stubbier processes.

**Fig. 4.4 :**

**A)**

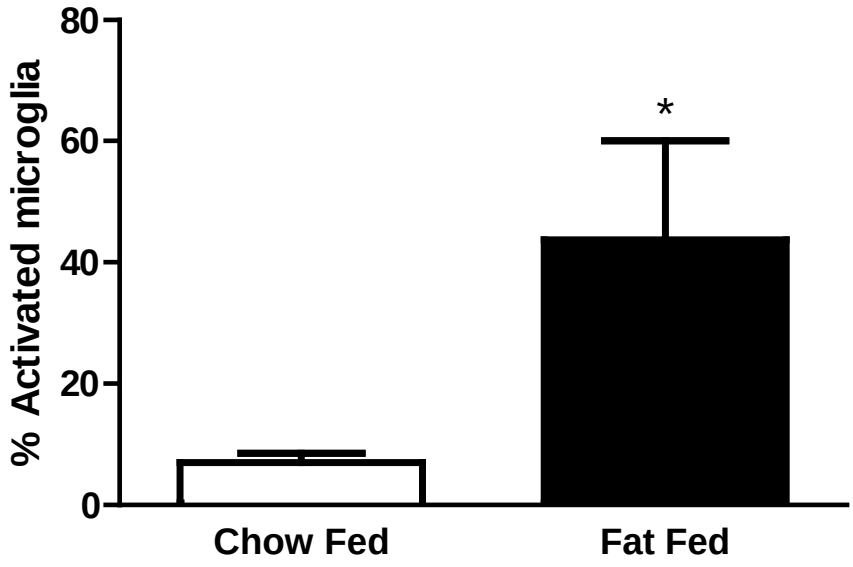
80
60
40
20
0
% Activated microglia
*
Chow Fed
Fat Fed

**B)**

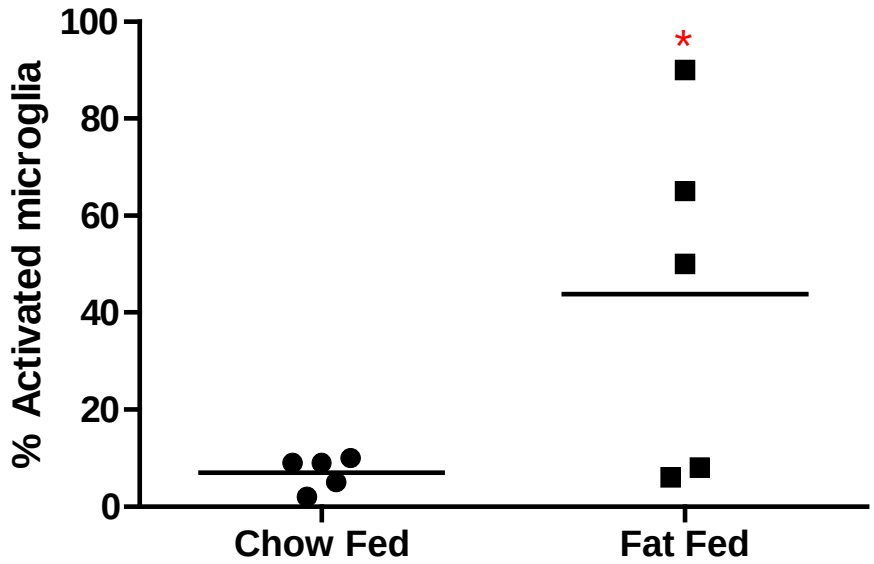
100
80
60
40
20
0
% Activated microglia
*
Chow Fed
Fat Fed

**Fig. 4.4 :** Activated microglia expressed as a percentage of total microglia in the hypothalamic arcuate nucleus and ventromedial hypothalamus. Panel A shows the average percentage of activated microglia (mean ± SEM). Panel B shows data from individual rats where horizontal line indicates mean percent activated microglia. Student t-test showed no significant difference (P=0.055) but Chi-Square test comparing the proportion of rats with and without activation in chow fed and high fat fed rats did show a significant difference between the two groups (P=0.038).

**Fig. 4.5 :**

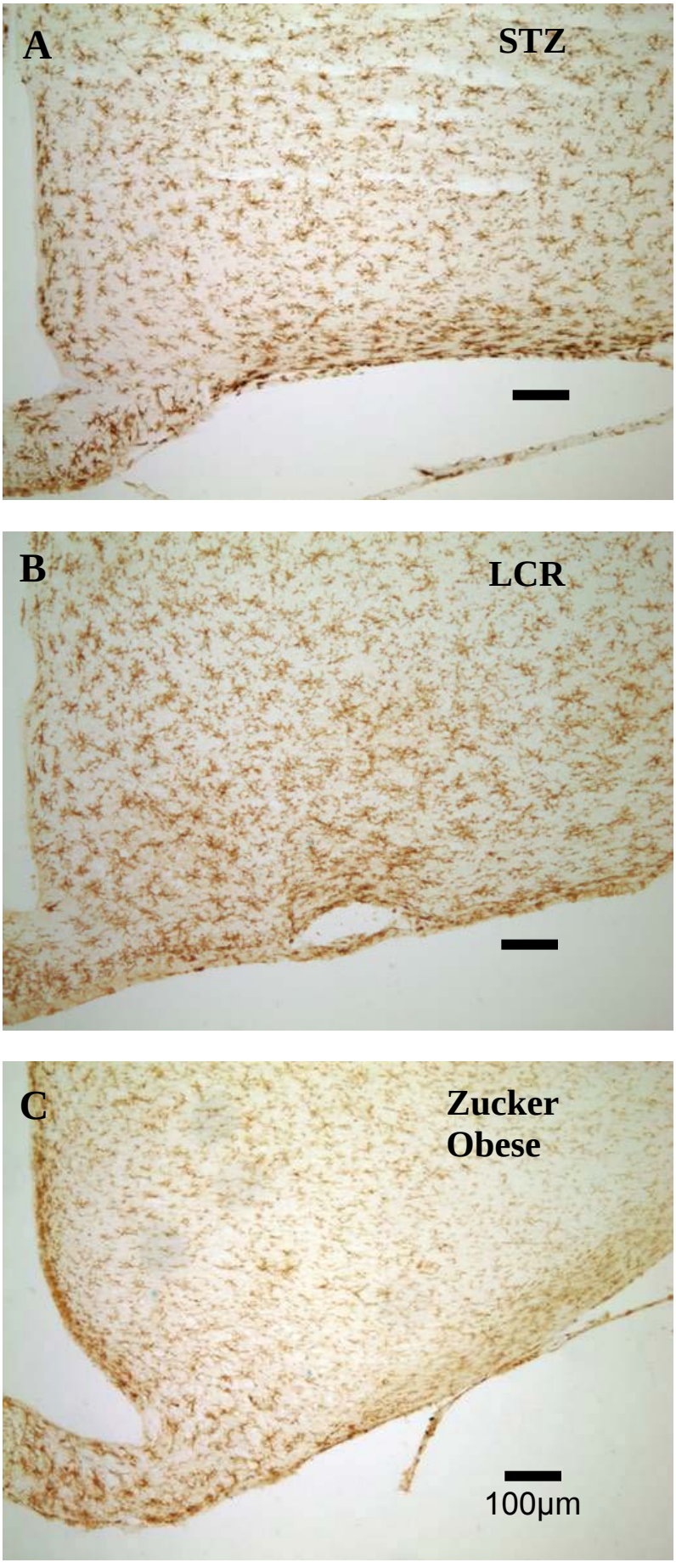

**Fig. 4.5** : Phtomicrographs showing OX-42 immunolabeled microglia in the ventromedial hypothalamus/ arcuate nucleus region showing ramified microglia in (A) STZ (B) LCR (C) Zucker Obese rats. Microglial in these animals showed long and thin processes and small somata indicating their ramified morphology.

## *Discussion*

We have previously reported microglial activation in the PVN and SON regions of the hypothalamus in STZ-induced diabetic rats (chapter 3). The key findings of the present work show that (i) microglia are not activated in hypothalamic cardiovascular centres in rats fed a high fat diet for 8 weeks. Even leptin receptor deficient Zucker Obese rats and a genetic model of insulin resistance (LCR) rats did not show microglial activation in the PVN or SON (ii) microglia are activated in VMH/Arcuate nucleus in high fat fed rats but not in obese Zucker rats suggesting involvement of leptin signalling in this activation.

The microglial activation observed in the VMH/Arcuate region was present in only 3 out of 5 high fat fed rats tested but all the rats that showed activation had more than 50% activated cells (Fig. 4.4 (B)). This is a level of activation never observed in any of the control rats in any of our studies so far. A Chi-Square test showed a significantly higher proportion of rats with activated microglia in high fat fed rats (P=0.0384). Although the mechanism of microglia activation is not clear, a high fat diet will cause increase in physiological levels of plasma leptin (Ahren & Scheurink 1998; Friedman & Halaas 1998) that is a prime candidate for causing microglial activation. Leptin is an anti-obesity hormone produced by adipose tissue. Halaas et al. (1997) reported that i.c.v. infusion of leptin reduces body fat mass by reducing food intake but not by increasing energy expenditure in lean mice (Halaas et al 1997). The study also demonstrated that chronic i.c.v. infusions of a very low dose of leptin replicate the weight–reducing effects of leptin administered peripherally at much higher doses. These results suggest those leptin receptors located in brain are more important than peripheral receptors in controlling body weight and food intake. Indeed, the selective deletion of neuronal leptin receptors causes obesity (Cohen et al 2001) and amelioration of obesity occurs upon selective expression of leptin receptors on neurons in leptin receptor deficient mice (Kowalski et al 2001). Various animal studies have reported that the hypothalamus is

the main site of leptin action in central nervous system (Lee et al 1996; Maffei et al 1995; Vaisse et al 1996). (Kurtz et al 1989). Decreased immune function was observed in leptin deficient mice. It appears from the literature that leptin increases immune responsiveness by direct effects upon the immune system and regulates feeding and neuroendocrine function by activating the long (LRb) (Mayers MG Jr. 2004), most notably in the hypothalamus but the cellular location of the immune stimulating effect of leptin is not clear. Interestingly , direct microinjection of leptin into the arcuate nucleus and ventromedial hypothalamus decreases food intake, reduces body weight gain and modulates sympathetic nerve activity suggesting that central action of leptin is mainly mediated via these two hypothalamic nuclei (Elmquist & Flier 2004; Satoh et al 1997; Satoh et al 1999).

Studies on diet induced obese rodents have demonstrated reduced central leptin signalling which our results suggest may be at least in part due to activated microglia. A study on mice had reported that i.c.v. infusion of the same amount of leptin was less effective in terms of reducing body fat mass and food intake in diet induced obese mice as compared to normal chow fed rats (Halaas et al 1997). Moreover, reduced central leptin sensitivity was also demonstrated by a study on rats showing reduced suppressive effect of i.c.v. infused leptin on NPY expression in arcuate neurons in diet induced obese rats (Levin & Dunn-Meynell 2002). These i.c.v. infusion studies suggest that obesity causes defective leptin signaling in hypothalamus. A recently published animal study by moraes et al. (2009) has demonstrated that high fat diet induces apoptosis of neurons in the arcuate region. The study also demonstrated elevated inflammatory cytokines in the hypothalamus and suggested a role for inflammatory cytokines in neuronal apoptosis. However, the study homogenised hypothalamic tissue which would have included cells outside the blood brain barrier as well, hence the cellular source of the elevated cytokines is unclear. Our results on fat feed rats showing microglia activation suggests that these activated microglia could be a source of inflammatory cytokines in hypothalamus which may then contribute to neuronal apoptosis.

Thus, by performing immunohistochemistry, instead of homogenizing tissue (like some of the previous other studies) we could interpret our results in greater detail than others.

Leptin is a likely candidate responsible for microglia activation. It appears from the literature that leptin sensitivity is reduced for the metabolic actions but not for the effects on sympathetic nerve activity. The action of leptin on microglia could be direct or indirect via neuronal activation. Apart from neurons, microglia also expresses receptors for leptin and the direct action of leptin on cultured microglia has been shown to induce IL-1β release (Pinteaux et al 2007). However, this *in vitro* study does not provide the reason for selective activation of microglia in VMH/Arcuate region. In the absence of *in vivo* evidence showing a direct leptin action on microglial activation in selective brain nuclei, it appears that leptin mediated over-excitation and damage to VMH / Arcuate neurons are responsible for reported microglia activation. It seems more likely that leptin mediated neuronal over activation precedes microglial activation but other causes must be considered. However, once activated these microglia secrete variety of inflammatory cytokines and superoxides that can exaggerate the neuronal damage in VMH/ Arcuate region and then may contributes to the reduced leptin sensing in these regions.

Microglial activation may also be involved in disruption of glucose homeostasis in high fat fed rats. Apart from leptin receptors, VMH / Arcuate region also contains glucose sensing POMC neurons. These POMC neurons have recently been shown to be excited directly by glucose (Ibrahim et al 2003). Interestingly, glucose sensing by POMC neurons becomes defective in high-fat diet mice (Parton et al 2007). A recent animal study has demonstrated that restoration of leptin signalling in the arcuate nucleus in leptin receptor deficient obese mice was sufficient to normalise blood glucose levels and markedly improved hypoinsulinaemia (Coppari et al 2005). It is possible that activated microglia may also have role to play in causing damage to glucose sensing machinery in VMH / Arcuate region by interrupting leptin sensing. Hence, microglial activation in high fat fed rats may be caused by

high leptin levels and these activated microglia may be involved in generating leptin insensitivity and insulin resistance in those rats.

Interestingly, we did not observe microglial activation in VMH/Arcuate nucleus either of Zucker Obeser rats or in STZ-induced diabetic rats (Fig. 4.5 (A), 4.5 (B) & 4.5 (C)). Zucker Obese rats are deficient in leptin receptors and unlike high fat fed rats used in this study, had significantly higher body weights as compared to their respective control rats. On the other hand, similar to fat fed rats, Zucker Obese rats had slightly but significantly elevated fasting blood glucose levels suggesting that both were developing diabetes. Moreover, STZ - diabetic rats that showing extreme hyperglycemia have been reported to have reduced levels of plasma leptin (Havel et al 1998). Thus, the lack of VMH/Arcuate microglial activation in Zucker Obese rats and STZ-induced diabetic rats support the hypothesis that leptin signaling and not hyperglycemia is responsible for activation of microglia in VMH/ Arcuate in high fat fed rats.

We did not observe microglial activation in VMH/ Arcuate region in LCR rats despite their high fasting blood glucose levels and higher body weights as compared to HCR rats. LCR rats provide a genetic model to study the effect of insulin resistance. The molecular defect(s) that result in aberrant fuel metabolism in LCR is not known. However, recent studies on this model reported that LCR rats have impaired skeletal muscle glucose and lipid metabolism (Lessard et al 2009; Lessard et al 2011). A study on 13$^{th}$ generation LCR and HCR rats has shown approx. 50% higher levels of leptin in LCR rats as compared to HCR (463± 49.9 vs 312.6± 34.1) (Noland et al 2007). The study also demonstrated that high fat fed HCR rats showed approx. 80% higher plasma leptin levels compared tho chow fed HCR's but no significant difference was found between chow fed and high fat fed LCR rats. Although, their study used a lower percentage fat than the one used here, it provides clear evidence that high fat feeding causes a higher increase in plasma leptin levels than seen in LCR rats. Interestingly, our rats fed high fat diet did not become obese which is consistent with a

previous study by Chen et al. (2010) that used a similar dietary regime (Chen et al 2010). But their study also demonstrated that even though high fat fed rats were not obese, they had 80% higher epididymal fat mass compared to controls suggesting they had high leptin levels before developing obesity (Chen et al 2010). This was confirmed by a later unpublished study from our lab on rats fed high fat diet for 12 weeks showing significantly higher plasma leptin levels as compared to controls, in the absence of obesity. We also observed that in those high fat fed rats, leptin levels were variable where some rats had leptin levels just above highest value obtained in controls while others had more than double (Unpublished data from our lab). Thus, these results suggest that only some rats had a high leptin level which is consistent with our microglial results on microglial activation. However, this hypothesis requires further investigation where plasma levels of leptin and microglial activation needs to be correlated.

In contrast to our previous findings that activation of microglia occurs in the PVN of STZ-induced diabetic rats (chapter 3), we did not observe microglial activation in this brain nucleus in the other three models used in this study. A major difference between all these models is that STZ-induced diabetic rats are a model of type 1 diabetes in humans and develop extreme hyperglycemia while all the other models develop mild hyperglycemia, and may more closely resemble a pre-diabetic stage in development of type 2 diabetes. Apart from that, STZ-induced diabetic rats do not show weight gain (chapter 3) while Zucker Obese rats and LCR rats gained significantly more weight as compared to their respective controls. Our results on body weight gain in Zucker Obese rats are consistent with previous reports on this rat model (Campfield et al 1995; Friedman & Halaas 1998; Halaas et al 1995; Pelleymounter et al 1995; Zhang et al 1994). Similarly, LCR rats gained more body weight as compared to control rats which is consistent with previous reports with this model (Lessard et al 2011; Noland et al 2007). Collectively, the data from both Zucker Obese and LCR rats suggests obesity is not directly responsible for microglial activation in the PVN in STZ-induced

diabetic rats. Thus, extreme hyperglycaemia but not obesity may be responsible for microglial activation in the PVN in STZ-induced diabetic rats.

Interestingly, all of these models do share some common pathological complications. Blood pressure measurement from unrestrained Zucker rats shows hypertension in Obese rats but not in pair fed control Zucker lean rats (Kurtz et al 1989). Zucker diabetic fatty rats or Zucker Obese rats also develops cardiomyopathy and cardiovascular dysfunction (Marsh et al 2007; Oltman et al 2006; van den Brom et al 2010). As discussed before large numbers of studies on obese humans and animal models of obesity have demonstrated elevated sympathetic nerve activity to kidney, heart, and skeletal muscle and its pathological role in development of obesity associated cardiovascular complications (Alvarez et al 2002; Barnes et al 2003; Esler et al 2006; Huggett et al 2004; Vaz et al 1997). Elevated levels of renal sympathetic nerve activity are seen in Zucker Obese rats (Morgan et al 1995) and may be a contributing factor to reported cardiovascular complications in this model. Elevated sympathetic nerve activity and blood pressure is also been reported in rats fed high fat diet for 12 weeks (Barnes et al 2003). Just like high fat fed rats and Zucker Obese rats, cardiovascular complications and elevated sympathetic drive is also been reported in STZ-induced diabetic rats (chapter 3). Unfortunately, Sympathetic nerve activity is not well studied in LCR rats. Collectively, all these results indicate the following two possibilities: (i) Elevated sympathetic drive in Obese Zucker and high fat fed rats may contribute to the pathology of reported cardiovascular complications but the mechanism responsible for sympathetic activation might be different from STZ-induced diabetic rats. (ii) Microglia are not responsible for reported cardiovascular complications in STZ-induced diabetic rats. However, further investigation is required to test both possibilities.

High fat fed rats, Low Capacitance Runner (LCR) and Zucker Obese rats can develop obesity, hypoinsulinaemia, mild hyperglycaemia, hyperleptinemia and insulin resistance (Lessard et al 2009; Lessard et al 2011; Luo et al 1998; Srinivasan et al 2004;

Srinivasan et al 2005; Storlien et al 1986; van den Brom et al 2010) but not extreme hyperglycaemia / overt diabetes as seen in STZ-induced diabetic rats (model of type 1 diabetes) (chapter 3). Despite having similar cardiovascular complication and elevated sympathetic drive as STZ-induced diabetic rats, animal models used in this study did not showed activation of microglia in PVN and SON suggesting extreme hyperglycaemia is responsible for microglial activation in PVN and SON of STZ-induced diabetic rats. Collectively, results obtained from STZ-induced diabetic rats, Zucker Obese rats, high fat fed rats and LCR rats suggest that extreme hyperleptinemia in high fat fed rats may be responsible for microglial activation in VMH/ Arcuate region. Targeting those activated microglia in VMH/ Arcuate region in high fat fed rats could reduce neuronal damage and leptin resistance in this region. Our results suggest that high intake of high fat containing western diet can cause inflammation in hypothalamus in humans. Inhibition of this inflammation could be the key to prevent growing cases of type-2 diabetes in humans.

# Chapter 5: Effect of Activated Microglial Injection in the Paraventricular Hypothalamic Nucleus on Blood Pressure

## *Introduction*

Until the last decade, it was believed that, just like other immune cells in periphery microglia perform protective immunological functions in the CNS. Recently, however, there is increasing evidence suggesting a pathological role of microglia in various neurological diseases (Badoer 2010a; Inoue & Tsuda 2009; Tozaki-Saitoh et al 2008) indicating there are two facets of microglial function. It appears that microglia can be "protective" or "injurious" to neurons depending on the prevailing conditions but the molecular switch that transforms them from their protective to their harmful state is not known. Microglia provide neuro-protection by secreting various neurotrophic factors and anti-inflammatory cytokines while their injurious role is attributed to their ability to release inflammatory cytokines, chemokines, reactivity oxygen species, and superoxide (chapter 1). These discoveries on their conflicting roles made microglia perhaps the most controversial cells of the central nervous system.

We have reported microglial activation in the paraventricular hypothalamic nucleus (PVN) in rats with heart failure as well as in STZ-induced diabetic rats (chapter 3 and chapter 4). However, it is still not clear if this microglial activation is a consequence of these diseases or whether microglial activation plays a role in the pathological consequences these conditions. The PVN plays important role in cardiovascular regulation (Badoer 2001; Coote 2005; Dampney et al 2005). Chemical stimulation of the PVN by unilateral microinjections of N-methyl-D-aspartic acid (NMDA) or L-glutamate elicits an increase in mean arterial pressure (MAP) in rats (Kannan et al 1989; Kawabe et al 2008). Activation of PVN neurons causes increased sympathetic outflow which mediates this pressor response (Kannan et al 1989; Martin & Haywood 1992). Previous studies on STZ-induced diabetic rats and rats with myocardial infarction have reported elevated sympathetic drive (Mann 1999a; Packer 1988;

Patel et al 2010; Zheng et al 2002; Zheng et al 2006) and this elevated sympathetic activity is a well known contributing factor to the pathology of heart failure (Brunner-La Rocca et al 2001; Hasking et al 1986). STZ-induced diabetic rats show increased PVN neuronal activity (Lindley et al 2004; Zheng et al 2002). Previous studies on rats with myocardial infarction also show this activation and in addition they have shown elevated cytokines levels in the PVN and suggested their involvement in pathology of heart failure (Guggilam et al 2007; Shi et al 2010a). Based on these data, we hypothesised that the secretion of a variety of cytokines, chemokines, neurotrophins and reactive oxygen species from activated microglia may cause neuronal excitation in the PVN which in turn activates sympathetic drive and contributes to cardiovascular complications.

Studies on various neurodegenerative models have suggested a role of microglia in causing neuronal damage (Badoer 2010a; Graeber 2010). Interestingly, recent studies on animal models of neuropathic pain have reported microglial activation following nerve injury and suggested they have a neuromodulatory role (Tozaki-Saitoh et al 2008; Tsuda et al 2003) since inhibition of microglial activation with the drug minocycline is able to prevents development of pain behaviors (Fan et al 2005a; Raghavendra et al 2003b). Tsuda et al. (2003) also demonstrated a decrease in paw withdrawal threshold in naïve rats injected with ATP activated microglia into the spinal cord indicating sensitization of pain pathways similar to that seen following nerve injuries. Hence, this study provides a useful tool to study the effects of activated microglia on neurons *in vivo*. Therefore, to test our hypotheses, we performed the following experiments: (i) Activated microglia were injected into the PVN of naïve rats and effect on blood pressure compared to that in rats that had received either phosphate buffer saline (PBS) or microglial conditioned medium injections (ii) We investigated the effects of inhibiting microglial activation with minocycline on blood pressure in STZ-induced diabetic rats.

## *Methods*

### Animals

Male Sprague-Dawley rats were obtained from Animal Resource Centre (ARC), Perth, Western Australia and housed in the local animal facility (RMIT University, Melbourne, Australia). Rats weighing 150 ± 10 g were used for minocycline injections experiments while 3-4 weeks old, age and weight matched rats were used for stereotaxic injections of activated microglia and control solutions.

### Induction of diabetes and minocycline treatment

As described previously (chapter 3) diabetes was induced by streptozotocin (STZ) (48mg/kg body weight) injection into the tail vein (N=9) using citrate buffer (pH 4.5, 0.1M) as a vehicle. Control rats received only vehicle injection and underwent all other procedure in a same way as STZ rats (N=6). One week after injections fasting blood glucose levels were measured using a one touch glucose meter (Accu-Check Performa). Rats showing fasting blood glucose levels higher than 18mmol/litre were considered diabetic. All the rats receiving minocycline injections were given minocycline (45mg/Kg in 0.1M PBS ,pH 7.2) via i.p. injection every second day for 5 consecutive weeks. Out of the 9 rats injected with STZ that showed hyperglycaemia, 3 were subjected to minocycline injections. The rest (N=6) STZ-induced diabetic rats did not receive any drug treatment. Out of 9 vehicle treated confirmed non diabetic rats, one rat was given minocycline injections.

### Blood pressure measurement via tail cuff

Systolic blood pressure was measured via the tail cuff method from all STZ-induced diabetic and vehicle treated rats. Prior to blood pressure recordings, all rats were first allowed to acclimatise to the new animal house for two to three days then subjected to handling for 3-4 days. After the one week of acclimatisation and handling period, they were

placed in restrainers for 15-20 minutes and systolic blood pressure measured using a tail cuff blood pressure measurement system (ML125 NIBP Controller and MLT125/R Pulse Transducer / Pressure Cuff for NIBP - Rat) but not recorded. This protocol was followed every day for at least 3 days to reduce stress levels in the rats during subsequent blood pressure measurements. Blood pressure was then measured from the rats in all treatment groups at approximately the same time of the day. Thus, approximately 10 days after receiving the animals, the blood pressure was recorded from each rat for 3 consecutive days or longer until three concordant measurements were obtained. At this time surgery was performed and blood pressure recorded again for 3 days after surgery.

Blood pressure measurements were also taken from STZ-induced diabetic and control rats used for minocycline treatment experiments in similar manner as described above. In this case, the blood pressure was measured before STZ/vehicle injection and then 2 weeks and 5-6 weeks after the injection.

## Culturing, isolation and activation of microglia for PVN injection

Microglia were isolated as described previously (Nakajima 1989; Pooler et al 2004) with some modifications. Three day old rats were decapitated and the brains removed, then minced by passage through a stainless steel mesh (40 mesh) and incubated with 0.25% trypsin and 0.01 % DNase in phosphate buffered saline (PBS) for 10 min at $37^0$ C. Horse serum was then added to terminate the digestion and the cells were passed through a second stainless steel mesh (100 mesh). Cells were centrifuged at 1500rpm for 5 minutes and the pellet washed twice by dissolving into the DMEM medium (containing 4.5g/l glucose). The final cell suspension was plated in poly D-lysine coated flasks (75 $cm^2$) at a density of approximately one brain per flask. Cultures were maintained in DMEM (4.5g/l glucose) supplemented with 10% FBS, 1% penicillin streptomycin mixture, in a 5% $CO_2$ atmosphere at $37^0$C. Half of the medium was changed twice a week. After 10-14 days flasks with cells

containing phase bright microglial cells on top of the layer of glial cells were kept on shaker at 120 rpm for 45 minutes ($37^0$ C). The supernatant was collected and centrifuged at 1500 rpm for 5 minutes. Microglial cells present in pellet were counted using a heamocytometer (Invitrogen, Australia) and then cells were resuspended (1 $X10^6$ cells/ ml) in PBS with ATP (50μM) to activate microglia and incubated for 1 hour before used for injections (Tsuda et al., 2003).

To obtain conditioned medium microglia activated with ATP (50μM) were passed through a 0.2 μm filter to remove the cells and the resulting medium containing microglia secretions used for injection.

The purity of isolated microglia was tested using fluorescent immunolabeling with OX-42 antibody and Hoechst dye. In brief, isolated microglial were replated on square glass bottom dish for 2 hours in medium before being fixed with cold 4% paraformaldehyde. After fixation, cells were washed 3 times with PBS and incubated with primary antibody (OX-42 (1: 500); Chemicon, Temecula, USA) in PBS (pH 7.2) containing 0.3% triton X-100 for one hour. Then cells were washed and incubated with biotinylated horse anti-mouse secondary antibody (1: 500; Vector laboratories, Burlingame, USA) in PBS containing 0.3% triton X-100 for one hour. After that, cells were washed with PBS and incubated with R-Phycoerythrin labeled Extravidin (1:400, Sigma-Aldrich, St Louis, USA) for one hour. Cells were again washed with PBS and then incubated with Hoechst dye for 5 minutes (1μg/ml) followed by two washes with PBS. Then cells were covered with florescent mounting medium (Dako Laboratories) and cover-slipped.

## Microinjection into the hypothalamic PVN

Stereotaxic injection experiment were carried out in groups of four rats, of which two received microglial injections and the other two control injections. Microinjections into the PVN were made as described previously (Chen et al 2008a) with some modifications. Rats

were anaesthetised using isofurane gas (2-3% in oxygen) using a small animal anesthetic machine (Vetquip, Australia). During the entire surgical procedure, reflexes were checked at least at every 10 minutes to ensure adequate anesthesia. The animals were placed prone, and the head mounted in a Kopf stereotaxic frame such that both bregma and lambda were positioned on the same horizontal plane. A midline reference point was marked 2mm rostral to bregma. This was necessary because the bregma landmark was removed during the subsequent bone-drilling procedure. To expose the dorsal surface of the brain, a hole, approximately 4 mm in diameter, was drilled into the skull centered 3.5 mm caudal from the reference point.

Microinjections were made bilaterally using a fine glass micropipette (tip diameter 50-70 µM) into the PVN (stereotaxic coordinates: 1.5mm caudal to the bregma, 0.5 mm lateral to the midline and 7.5 mm ventral to the surface of the brain). Injections (volume 500 nl, PBS only or PBS containing approximately 500 microglial cells) were made bilaterally in the PVN. To mark the injection site, a small amount of rhodamine-tagged fluorescent microspheres was included in the microinjected solution (LumaFluor, Durham, NC). After bilateral microinjections the micropipette was removed and the skin closed using sutures. Following surgery, all rats were given buprinorphine HC1 (15 µg intramuscularly, Temgesic, Reckitt and Colman Pharmaceuticals, NSW, Australia) to alleviate postoperative pain.

## Tissue collection and localization of injection sites

At the completion of the experiment, rats were euthanized by overdose with pentobarbital sodium (180mg/kg, Virbac, NSW, Australia). The brains were then carefully removed, fixed in 4% paraformaldehyde solution for 4-5 hours and then placed into PBS containing 30% sucrose for 48 hours. The hypothalamus was sectioned on a cryostat at 20-µM thickness and mounted on gelatine coated slides. For microinjection experiments, the sections were then viewed wet under fluorescent microscopy to identify the rhodamine beads

at the site of injection. Injection sites were mapped in relation to the surrounding anatomical structures.

## Immunohistochemistry

From brains with PVN microinjections, only the sections showing the injection site were used for OX-42 immunohistochemistry. One in five sections containing the hypothalamus was collected from the animals used for minocycline experiments. The sections were, dried for 2 hours at room temperature and then standard immunohistochemical procedures were performed in which endogenous peroxidise activity was blocked by 0.5% $H_2O_2$ in PBS. This was followed by 1 hour incubation in 10% normal horse serum (NHS) for 60 minutes prior to 0.5 % Triton X-100 for 10 minutes facilitate antibody penetration. Subsequently, the sections were incubated for 72 hours with a mouse monoclonal primary antibody directed against CD11b (clone OX-42 (1: 100), Chemicon, Temecula, USA) in PBS containing 2% NHS and 0.2% Triton X-100. This was followed by incubation in biotinylated horse anti-mouse secondary antibody (1: 100, rat adsorbed, Vector Laboratories, Burlingame, USA), and Extravidin-HRP linked with HRP (1:400, Sigma-Aldrich, St Louis, USA). 3,3′-Diaminobenzidine tetrahydrochloride (Sigma-Aldrich, St Louis, USA) was used as the chromogen to visualise immunolabeling as discussed in previous chapters (chapter 1 and chapter 2). Sections from the sham control rats and from rats with STZ-induced diabetes were processed simultaneously to allow comparison of the strength of immunoreactivity.

## *Results*

When the purity of isolated microglial culture was tested, fluorescently labeled cell nuclei (Hoechst Dye) and the specific microglial marker OX-42 showed almost complete overlap indicating the presence of microglia and absence of other cell types (Fig. 5.2 (A), 5.2 (B) and 5.2 (C)). Quantification from five different fields from each dish showed 100% overlap between Hoechst stained nuclei and OX-42 labeled microglia (Data not shown) indicating the isolation procedure had produced a pure culture of microglia.

### 1) Location of injection sites

The presence of green fluorescent microspheres within the PVN in experimental rats (As shown in Fig. 5.3) indicated accurate localization of microinjections. Out of 7 rats, 5 had microglial injections within the PVN on both sides while the other 2 had one injection inside the PVN and the other one in an adjacent hypothalamic area. The success rates for PBS injections and activated microglial conditioned medium injection were similar. Out of 7 PBS injected rats, 4 had both injections inside the PVN, 1 had both injection outside the PVN and 2 rats had one injection inside the PVN and the other one in the adjacent area. In the case of activated microglial conditioning medium injected rats, 3 rats had both injections inside the PVN, while the other 2 rat had one inside and the other out side the PVN (Table 5.1).

**Table 5.1.**

| Injection Type | Total Animals | Both injections inside PVN | Both injections Outside PVN | One inside PVN one Outside PVN |
|---|---|---|---|---|
| Activated Microglia | 7 | 5 | - | 2 |
| PBS | 7 | 4 | 1 | 2 |
| Activated Microglial Conditioned Medium | 5 | 3 | - | 2 |

## 2) Activated microglia but not PBS or conditioned medium caused a significant increase in blood pressure

We did not observe any major difference in results between rats that had only one injection inside the PVN as compared to those who had both inside. Therefore, recordings from rats with one injection within the PVN were analysed along with the ones that had both injections inside. As shown in Fig. 5.4, vehicle injected rats showed no significant increase in blood pressure over the period of three days after the surgery. This was also true for the rats that received activated microglial conditioning medium injections. Interestingly, rats that received activated microglial injections showed a significant increase in systolic blood pressure as compared to the blood pressure before surgery. The systolic blood pressure remained high for at least 3 days post surgery (Fig. 5.4) in these rats.

A comparison of the percentage increase in systolic blood pressure at day one post surgery in each group of rats is shown in Fig. 5.5. This figure also indicates that rats received active microglia injected rats showed a significantly higher blood pressure (Fig. 5.5).

A micrograph showing OX-42 staining of microglia around the injection site has been attached in the appendix (Fig 2). The figure shows microglial activation near the injection site but it is not possible to distinguish between injected and resident microglia.

## 3) Effect of minocycline treatment on STZ-induced diabetic rats

STZ-induced diabetic rats showed less weight gain as compared to vehicle treated control rats. Minocycline treatment had no marked effect on this reduced body weight gain in STZ-induced diabetic rats (N=3; Fig. 5.7). We have previously reported that approximately 50% of STZ-induced diabetic rats show marked microglial activation in the PVN at 6 weeks time point (chapter 3). Our results suggest that minocycline treatment (45mg/kg body weight)

every alternate day for 5 weeks starting at one week after STZ injection was not sufficient to inhibit this activation of microglia. We observed more than 50% activated microglia in 2 out of 3 STZ minocycline treated rats which was higher than the highest value of 14% activation and average 9.299 ± 0.9215 % activation in vehicle treated control rats. Microglial activation in the minocycline treated control rat (N=1) was similar to other controls allowing us to speculate that minocycline itself was not activating microglia.

Control rats (N=5) showed a gradual increase in blood pressure which attain significance at 6 weeks time point as compared to their initial blood pressure, suggesting blood pressure increases with age. In contrast to control rats, STZ-induced diabetic rats (N=6) showed significantly increased blood pressure (measured by tail cuff) within 2 weeks of STZ injection. The blood pressure was also significantly higher at 6 weeks in the STZ-induced diabetic rats. Although the numbers of rats tested were too small to perform statistical analysis, blood pressure measured from minocycline treated STZ-induced diabetic rats showed increases in blood pressure similar to those seen in STZ-induced diabetic rats at each time point (Fig. 5.6).

In summary, there was no obvious beneficial effect of the minocycline treatment regime on pathological symptoms of diabetes observed. Minocycline treatment was neither able to prevent the STZ mediated microglial activation in PVN or reduction in body weight gain (Fig. 5.7 and Fig. 5.8). As we did not observe any inhibitory effect of minocycline on microglial activation the experiment was discontinued.

## *Figures*

**Fig. 5.1.**

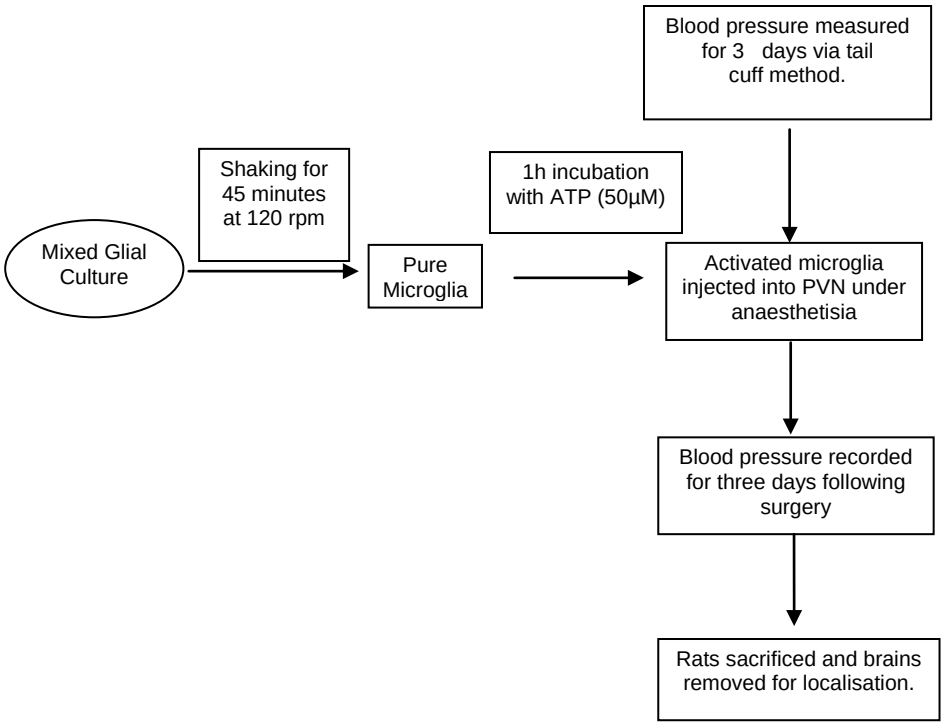

**Fig. 5.1:** Diagrammatic representation of experimental procedure for the microinjection experiments.

**Fig. 5.2 :**

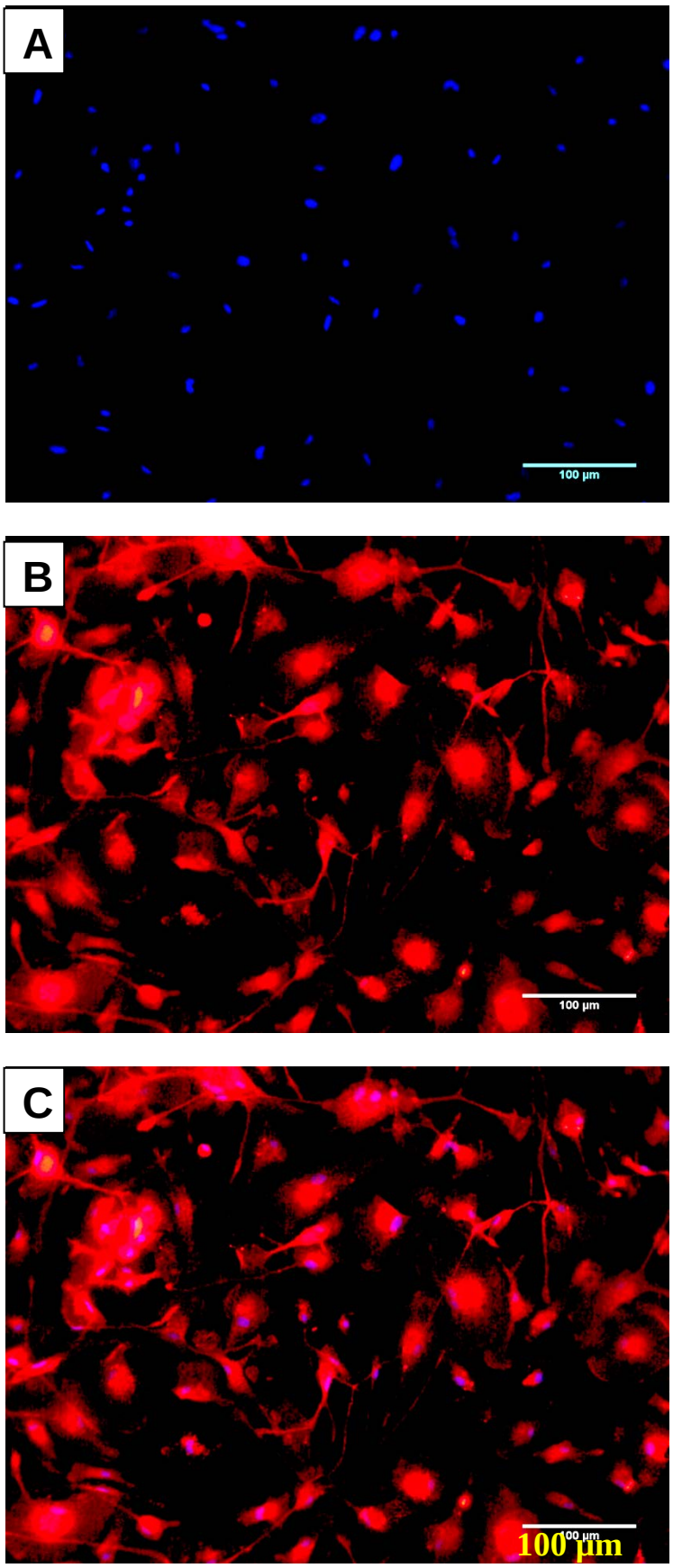

**Fig.5.2 :** Fluorescence micrographs of (A) Hoechst dye stained nuclei (B) OX-42 immunolabeled microglia in cells isolated from mixed glial culture (C) Double labelling illustrating that Hoechst dye stained nuclei show OX-42 immunolabeling (Scale bar=100 μm).

**Fig. 5.3 :**

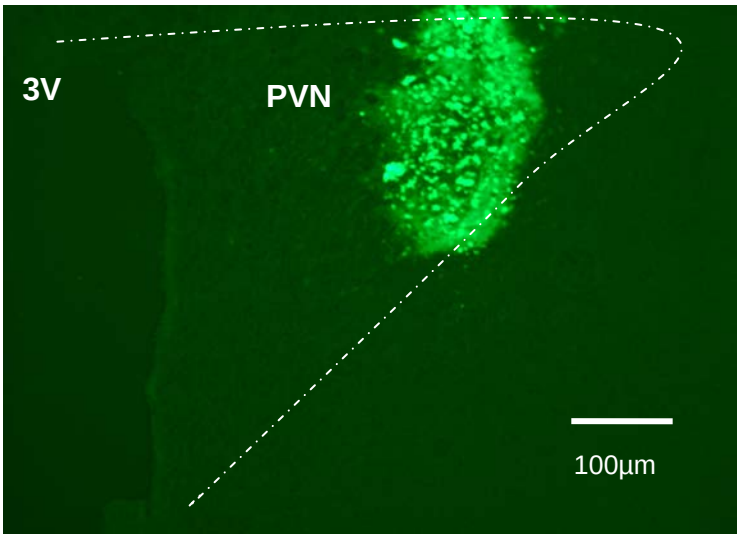

**Fig. 5.3 :** Fluorescein-tagged microspheres in the paraventricular hypothalamic neucleus (PVN) denoting an injection site. Dotted line roughly outlines the PVN area. 3V indicates 3rd Ventricle.

**Fig. 5.4 :**

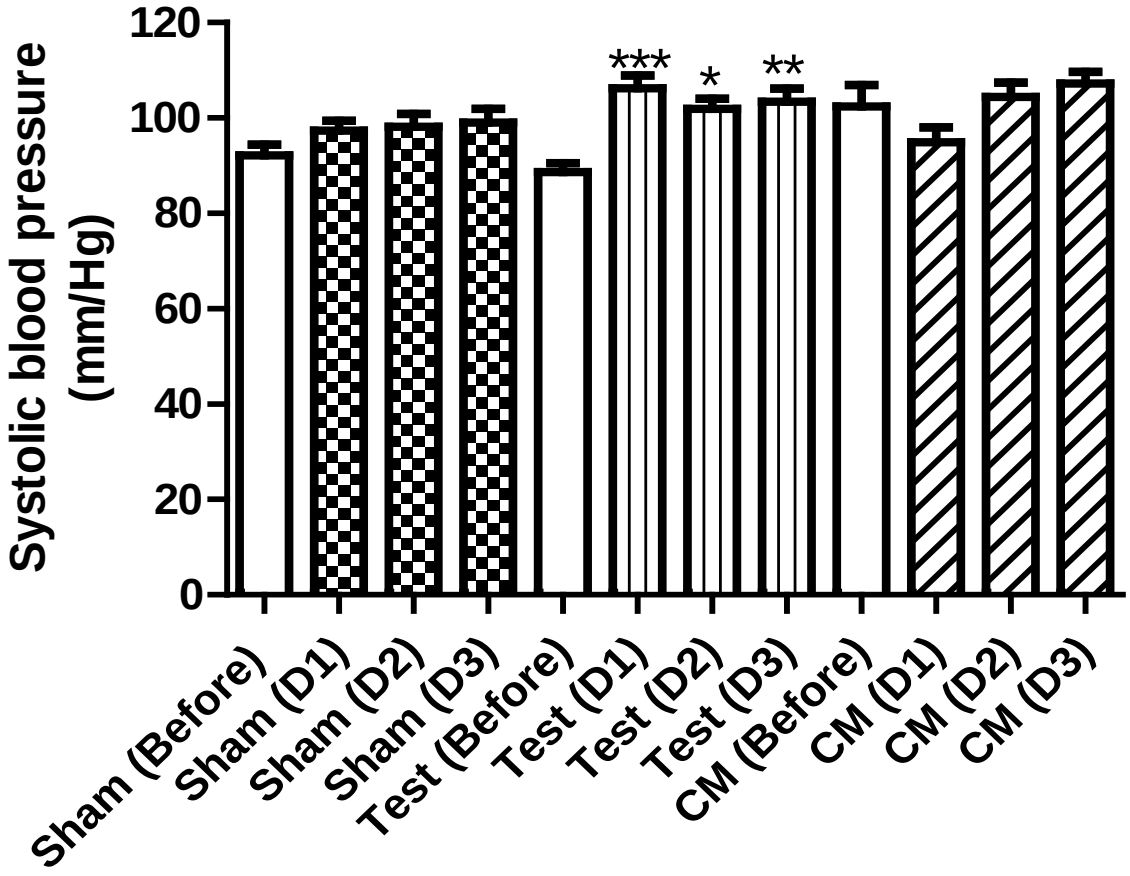
Systolic blood pressure (mm/Hg)
120
100
80
60
40
20
0
***
*
**
Sham (Before)
Sham (D1)
Sham (D2)
Sham (D3)
Test (Before)
Test (D1)
Test (D2)
Test (D3)
CM (Before)
CM (D1)
CM (D2)
CM (D3)

**Fig. 5.4 :** Average blood pressure (mm/Hg) recorded before and on the first three days after stereotaxic injections into the paraventricular hypothalamic nucleus (* indicates significantly different from PBS injection (* indicates $P<0.05$ , ** indicates $P<0.01$ and *** indicates $P<0.001$ ) Two way ANOVA followed by Boneferroni post hoc test comparing recording of D1,D2 and D3 to the respected pre-injection values.

**Fig. 5.5 :**

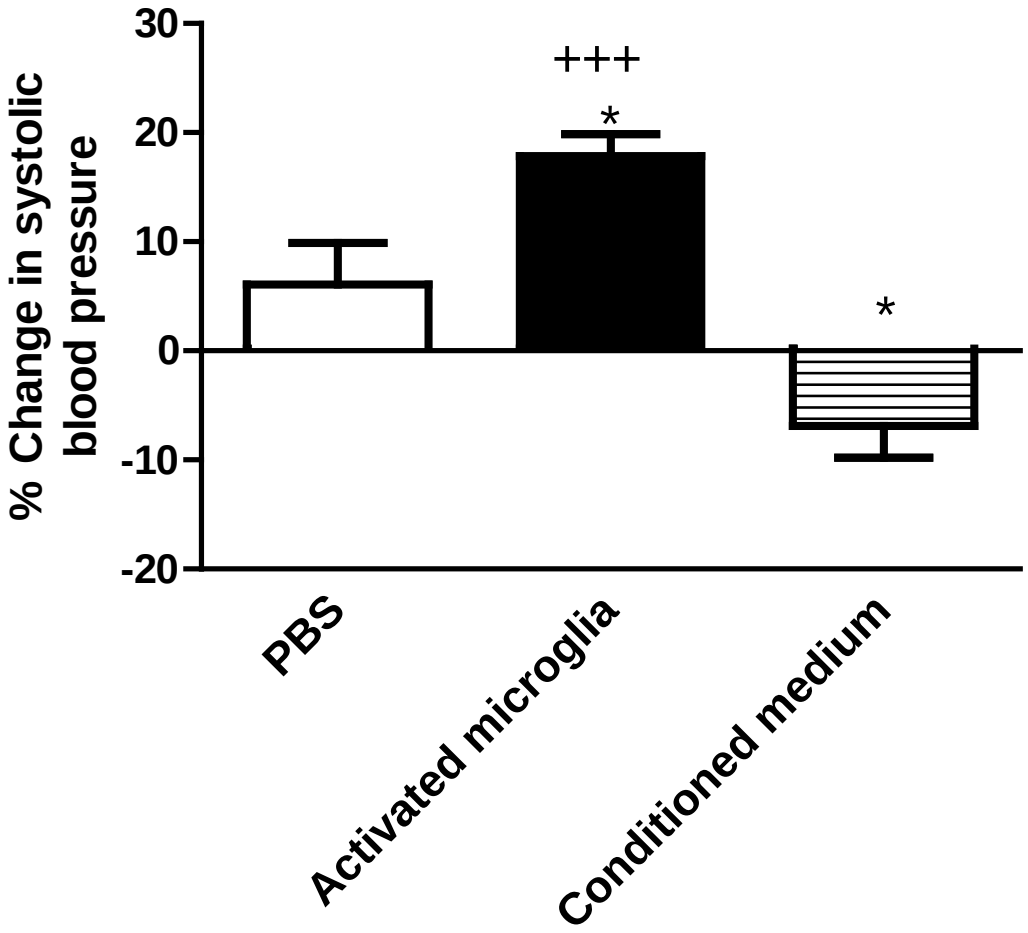
30
20
10
0
-10
-20
% Change in systolic blood pressure
+++
*
*
PBS
Activated microglia
Conditioned medium

**Fig. 5.5 :** Percentage increase in systolic blood pressure after microinjection of PBS (N=7), activated microglia (N=7) and activated microglial conditioned medium (N=5) into the PVN. ($*$ indicates significantly different from PBS injection ($P<0.05$); ++ indicates significantly different from conditioning medium injection ($P<0.01$)).

**Fig. 5.6 :**

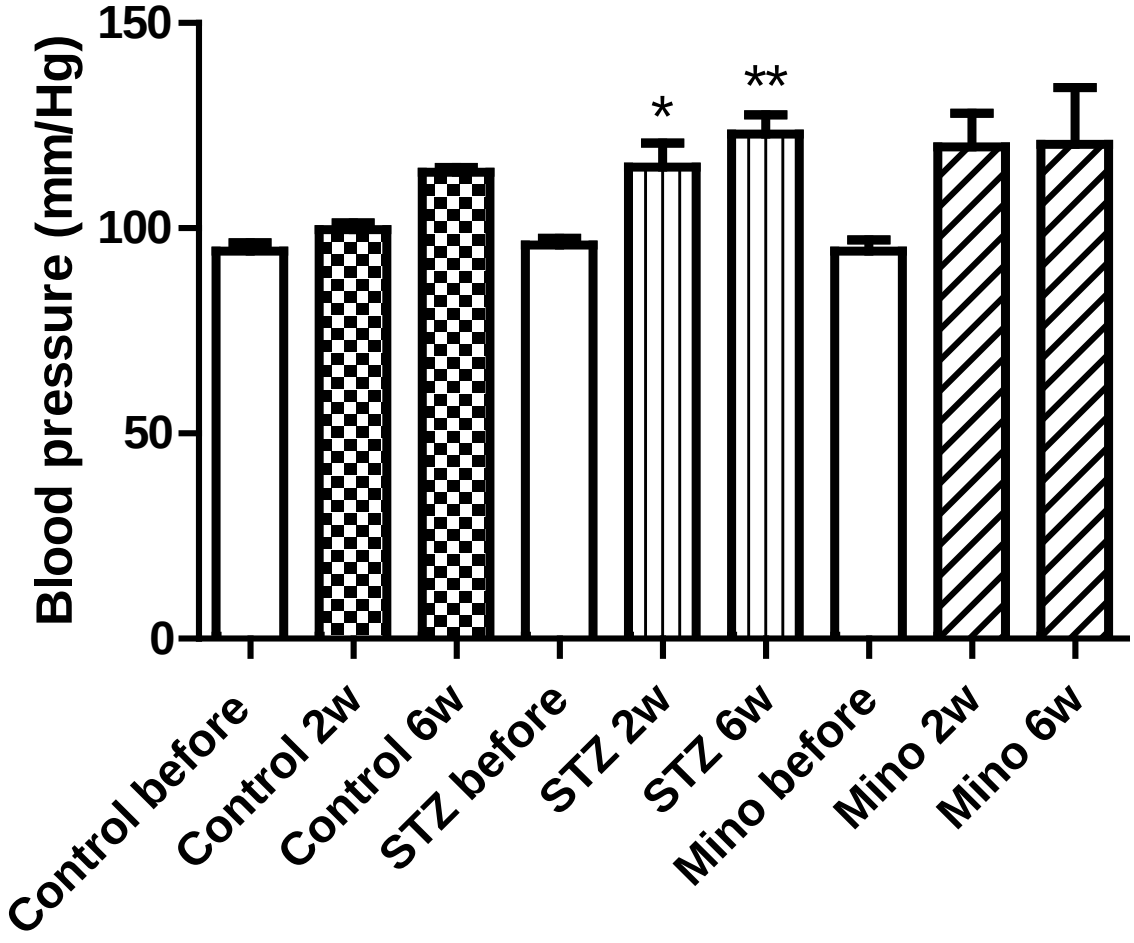
Blood pressure (mm/Hg)
150
100
50
0
*
**
Control before
Control 2w
Control 6w
STZ before
STZ 2w
STZ 6w
Mino before
Mino 2w
Mino 6w

**Fig. 5.6 :** Figure shows blood pressure recordings from control (minocycline untreated and minocycline treated, N=5), STZ-induced diabetic (minocycline untreated, N=6), and minocycline treated STZ–induced diabetic rats (N=3). Recordings were taken from all rats before STZ / vehicle injection and at 2 weeks and 6 weeks after STZ / vehicle injection. Two way ANOVA followed by Boneferroni post hoc test comparing all columns to respective before column was performed. ($*$ indicates significantly different from pre-STZ or pre-saline injection recordings ($*$ indicates $P<0.05$ , $**$ indicates $P<0.01$ )

**Fig. 5.7 :**

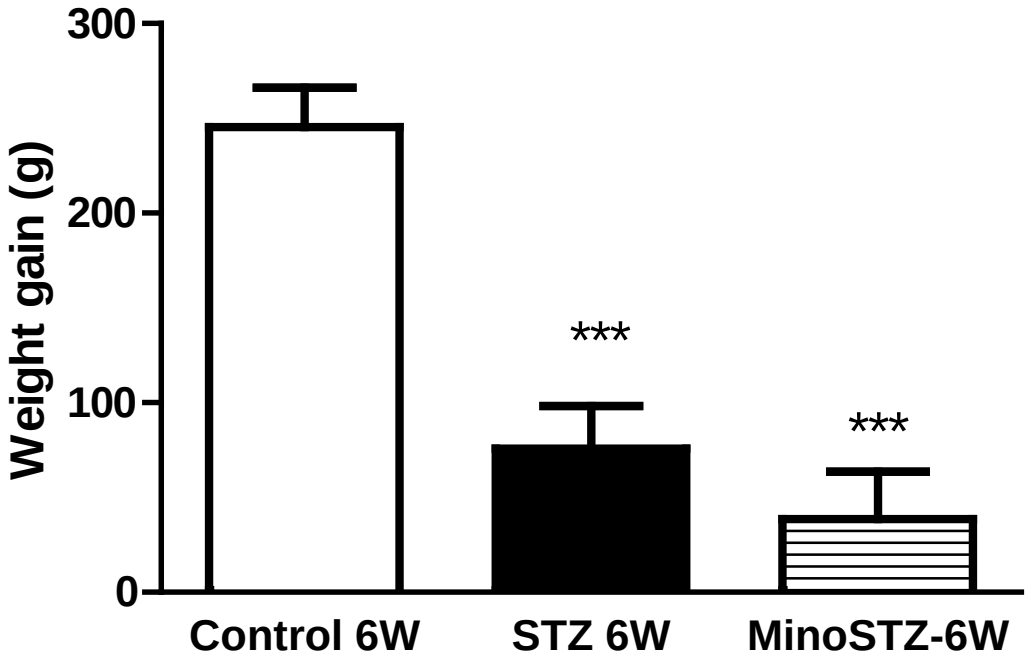

**Fig. 5.7 :** Weight gain over the six weeks period following injections on control rats (minocycline treated and untreated, N=5), STZ (minocycline untreated, N=6) and STZ (minocycline treated, N=3) rats. Note similar reduction in weight gain in minocycline treated and untreated STZ rats as compared to vehicle treated control rats. ($*$ indicates significantly different from control; $***$ indicates $P<0.001$)

**Fig. 5.8 :**

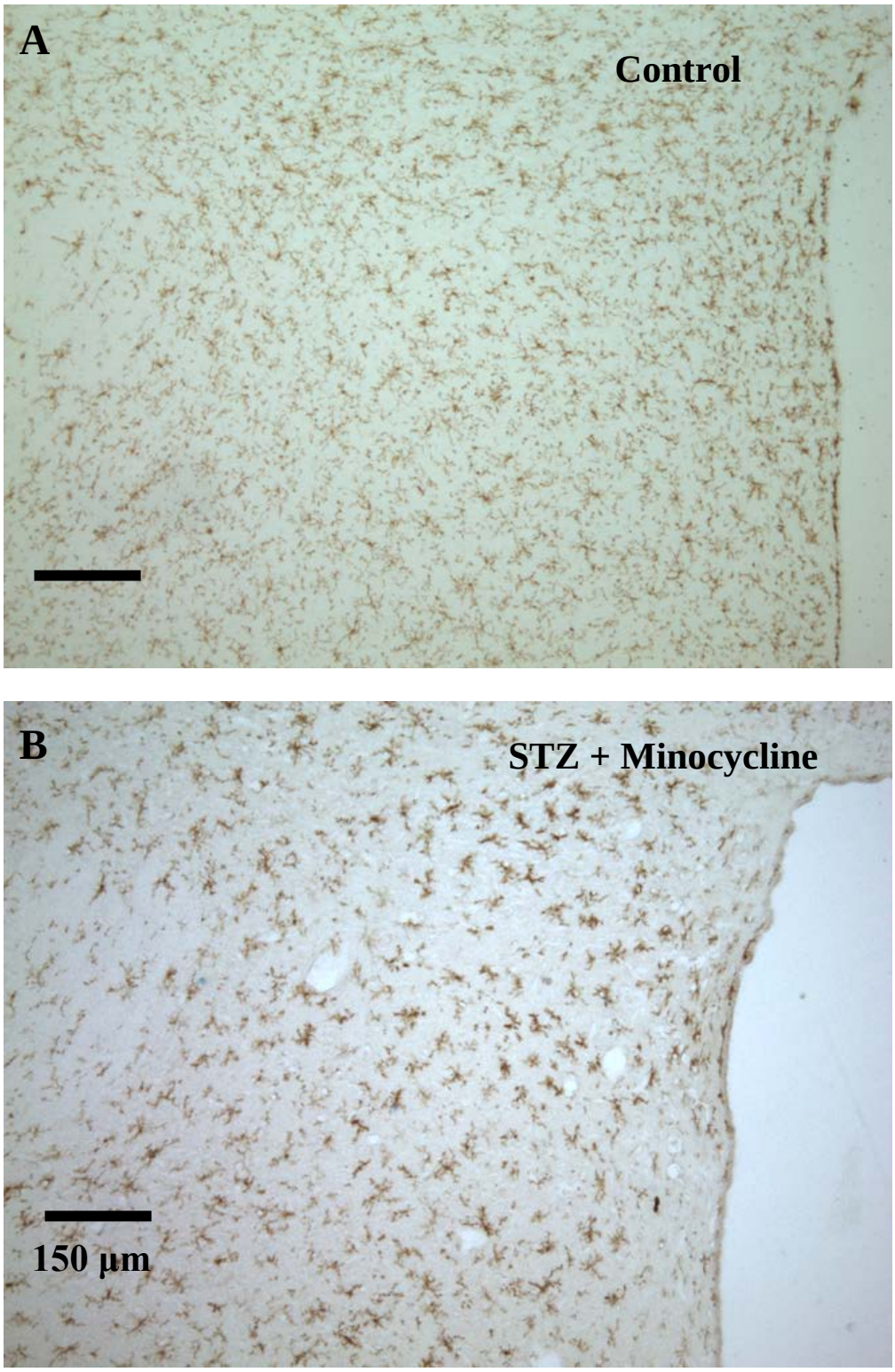

**Fig 5.8 :** Phtomicrograph showing OX-42 immunolabeled microglia in the paraventricular hypothalamic nucleus region. In control rats normal ramified microglia were observed. Note the long processes, many secondary branches and very small somata. Activated microglia were present specifically in the paraventricular hypothalamic nucleus in minocycline treated STZ rats. Note the dramatic increase in CD11b-positive staining and the morphological changes including enlarged somata and shorter, stubbier processes.

## *Discussion*

We have previously shown activation of microglia in the PVN in rats with myocardial infarction (chapter 2) as well as in STZ-induced diabetic rats (chapter 3), but the consequences of this activation is still not clear. The results presented here shows that activated microglia can influence PVN control of the cardiovascular system. The key findings of the current study are: (i) activated microglia injected into the PVN caused a significant increase in blood pressure, but neither PBS nor activated microglial conditioned medium injections were able to do so (ii) at the given dose and treatment regime used here, minocycline was not able to inhibit microglial activation or the reduction in body weight gain seen in STZ injected rats. Although the number of animals used was small, there was no indication of reduction in blood pressure in STZ-induced diabetic rats.

We have provided evidence that ATP-activated microglia when injected into the PVN cause a significant increase in blood pressure (Fig. 5.4 & Fig. 5.5). PBS injections did not cause any significant increase in blood pressure indicating that the surgical procedure and vehicle itself were not responsible for this effect. Injections of activated microglia may also contain secretions from microglia due to the 1 hour treatment with ATP (50 μM). However, injection of activated microglia conditioned medium into the PVN did not cause a significant increase in blood pressure suggesting that the microglial secretions produced during a one hour ATP treatment are not sufficient to cause a long term increase in blood pressure (Fig. 5.4 & Fig. 5.5). This indicates that the injected activated microglia serve as a long term and continuous source of various secretions (eg. cytokines and ROS) in the PVN, leading to the significant increase in blood pressure seen here.

The ATP concentration of 50 μM used here has been shown previously to activate microglia and microglia activated with this concentration when directly injected into rat spinal cord caused hyperalgesia (Tsuda et al 2003). ATP is known to activate these cells via P2

receptors (Haynes et al 2006; Kobayashi et al 2008; Tsuda et al 2003; Tsuda et al 2010). Activation of P2 receptors is also associated with microglial chemotaxis, movement and morphological changes (De Simone et al 2010; Ohsawa et al 2007; Orr et al 2009). It has also been linked with microglial secretion of inflammatory cytokines, chemokines, reactive oxygen species, and superoxides (Hide 2003; Hide et al 2000; Inoue 2006a; b; Kim et al 2007; Trang et al 2009). These secretions from activated microglia can modulate neuronal activity (Lu et al 2009a). A recently published study on rats has shown that an acute single injection of the proinflammatory cytokine IL-1β (one of the cytokines secreted by activated microglia) into the PVN resulted in significant increase in mean arterial pressure (Shi et al 2010b). The study reported blood pressure up to one hour after injection and it was higher through out that period. Hence, the longer term increase in blood pressure observed here may be due to modulation of PVN neurons by secretions from the activated microglia injected. Neurons in PVN can increase blood pressure via activation of renal and cardiac sympathetic nerves (Badoer 2010b; Badoer et al 2003).

We did not test the effect of injecting non-activated microglia into the PVN because the results would be difficult to interpret for several reasons. Firstly, the isolation procedure itself might at least partially activate microglia without ATP treatment. Secondly, injected microglia may become activated after injection. Under these conditions, if injection of non- activated microglia produced an increase in blood pressure it would not change the conclusion of this study. Thus, due to these technical issues, the outcome of such an experiment would not provide additional information.

Treatment with minocycline under the regime used here was not able to inhibit microglial activation and body weight reduction in STZ-induced diabetic rats (Fig. 5.7 and Fig. 5.8). This is despite the fact that inhibitory effects of minocycline on microglia activation have been reported by many *in vitro* as well as *in vivo* studies (Raghavendra et al 2003a; Suk 2004; Wang et al 2005a; Yrjanheikki et al 1998). Minocycline is a second generation

antibiotic commonly used for the treatment of acne in humans (Ozolins et al 2005) and can readily cross the blood brain barrier (Aronson 1980). Hence the ability of peripherally administered minocycline to act on brain cells is not in doubt. Although, the detail mechanism by which minocycline inhibits microglial activation is not known, it have been shown to inhibit various markers of microglial activation eg. $p^{38}$ MAPK activation, PKC (Protein Kinase C) activation, increased COX-2 activity, and increased expression of a variety of surface receptors (Nikodemova et al 2007; Tikka & Koistinaho 2001). An *in vitro* study on microglia has shown minocycline-mediated inhibition of proinflammatory cytokine expression and release from LPS activated retinal microglia (Wang et al 2005b) while many *in vivo* studies have shown inhibition of proinflammatory cytokine release by minocycline treatment (Krady et al 2005; Shi et al 2010b). However, these *in vivo* studies do not rule out the possibility of an anti-inflammatory or anti-apoptotic action of minocycline on neurons and inhibition of neuronal activation causing indirect inhibition of microglia activation. Despite all these promising studies suggesting minocycline as a potent inhibitor of microglia, the minocycline treatment used in this study could not inhibit microglial activation in PVN in STZ-induced diabetic rats (Fig. 5.8). There are several possible reasons for this. Animal studies have reported that minocycline pre-treatment but not post treatment prevents development of neuropathic pain and activation of spinal microglia following nerve lesions (Padi & Kulkarni 2008; Raghavendra et al 2003b). We began injecting minocycline one week after induction of diabetes which is before microglial activation becomes detectable based on our previous studies (chapter 3). However, it is possible that minocycline could not reverse some ongoing process of microglial activation that had already begun. Secondly, studies showing inhibition of microglia by minocycline treatment have given minocycline (30-45 mg/kg body weight) either once or twice a day (Guasti et al 2009; Yrjanheikki et al 1999) while we chose to give one injection of (45mg/kg body weight) every second day because of the long term nature of our experiment and because this treatment regime has been shown to

inhibit breast cancer growth in mice (Niu et al 2008). A study showing pharmacokinetics of minocycline in rats have demonstrated that minocycline (in PBS) reaches peak concentration around 2.5 hours after intra peritoneal injection then it starts declining suggesting that minocycline has plasma clearance time of few hours (Fagan et al 2004). This suggests that the dose of minocycline under the regime we used may have been inadequate. The study also reported accumulations of yellow-coloured deposits on the surface of the liver and small intestine after intraperitoneal injection of minocycline. The authors suggested that the minocycline is only incompletely and erratically absorbed. Because of this, the deposits in the peritoneal cavity may lead to unintended morbidity after repeated injections. Thus, alternative routes of minocycline treatment which allow continuous infusion of minocycline in small doses may hold the key to more promising results.

## *Conclusion*

We report that activated microglia injected into the PVN increase blood pressure in rats suggesting that microglial activation following myocardial infarction and in STZ-induced diabetic rats may be responsible for the reported elevated sympathetic drive in both cases. However, further study is required to demonstrate the effect of activated microglial injections on sympathetic nerve activity and to determine whether microglial inhibition can decrease diabetic cardiovascular complications.

# Chapter 6: Immunohistochemical Investigation of the Mechanism of Microglial Activation in the Hypothalamus of STZ-Induced Diabetic Rats

## *Introduction*

Microglia are the major cellular elements with immune functions inside the CNS and play important roles in protecting the brain against infection and injury (chapter 1). There is growing evidence suggesting that, in addition to this protective role (Badoer 2010a; Graeber 2010; Nakajima & Kohsaka 1993), microglia can also contribute to the development of many brain pathologies (Badoer 2010a; Graeber 2010; Tsuda et al. 2004; Tsuda et al. 2003), depending on the prevailing conditions. Our results suggest that diabetes and heart failure should be added to this list (chapter 2 and chapter 3). Although the mechanism by which microglia change into their pathological form is not fully understood, up-regulation of various surface receptors and activation of intracellular pathways have been linked with the undesirable effects of microglia, particularly in the case of neuropathic pain (Tsuda et al. 2004; Tsuda et al. 2003). Microglia respond to a variety of signals via receptors for cytokines, chemokines and glutamate. These receptors allow microglia to monitor activity in their surrounding tissue and are involved with microglial activation. Recently, purinergic receptors have emerged as important candidates for mediating the microglial activation process. Results from many animal studies suggest that targeting purinergic receptors to modulate microglial function can provide therapeutic benefits in neurodegenerative diseases and neuropathic pain (Bianco et al. 2005; Ji 2010; Takenouchi et al. 2010; Ulmann et al. 2008).

Microglia express ligand gated (P2X) and metabotropic (P2Y) purinergic receptors. Both can be activated by nucleotides and affect intracellular $Ca^{2+}$ in microglia. The former are responsible for nucleotide-induced depolarisation and $Ca^{2+}$ influx, and the latter for IP3-dependent $Ca^{2+}$ release from intracellular stores through a mechanism involving G protein

activation (Moller et al. 2000; Norenberg et al. 1994; Visentin et al. 1999). P2X4 and P2X7 receptors on microglia may also be associated with plasma membrane pore formation (Bernier L. 2010; Chessell et al. 1997; Takenouchi et al. 2005). Although there is controversy in the literature over the sub-type of P2 purinergic receptor involved in microglial activation, a recent study has demonstrated increased expression of P2X4 receptors on dorsal horn microglia in the spinal cords of rats after activation by nerve injury (Tsuda et al. 2003). To demonstrate the increase in P2X4 receptors in microglial cells only and not in other cell types, this study used immunohistochemistry as a tool instead of homogenizing tissue. The study also demonstrated that pharmacological inhibition of microglial P2X4 receptors reduces nerve injury-induced pain behaviours. Another study has demonstrated that P2X4-deficient mice lack mechanical hyperalgesia induced by peripheral nerve injury, suggesting the absence of a microglial neuromodulatory action in those mice (Ulmann et al. 2008). These results suggest that P2X4 receptors are necessary for microglial activation and/or action.

Activation of microglial purinergic receptors causes a large increase in $[Ca^{2+}]i$, which then activates various intracellular pathways, including phosphorylation of p38 MAPK (Ji 2010; Ji & Suter 2007; Trang et al. 2009). p38 MAPK is a member of the mitogen-activated protein kinase (MAPKs) family that plays a critical role in cell signalling and gene expression. The MAPK family includes three major members: extracellular signal-regulated kinase, p38, and c-Jun N-terminal kinase (JNK). Activation of these MAPKs by phosphorylation transduces a broad range of extracellular stimuli into diverse intracellular responses, including both transcriptional and non-transcriptional regulation. Studies of microglia *in vitro* have demonstrated inhibition of their release function upon pharmacological inhibition of p38 MAPK (Trang et al. 2009). A study of rats has also demonstrated the beneficial effect of inhibition of p38 MAPK as regards neuropathic pain (Ji & Suter 2007).

Interestingly, we have reported activation of microglia in CNS cardiovascular centres, including the PVN, SON and NTS in STZ-induced rats (chapter 3), but the cause of this microglial activation is not yet known. Based on literature demonstrating the involvement of microglial P2X4 receptors in neuropathic pain models, we investigated whether expression of microglial P2X4 receptors was up-regulated in these regions in STZ-induced diabetic rats. We also investigated if there was activation of microglial p38 MAPK by performing double labelling with OX-42 antibody, which labels microglial CD11b receptors, and an antibody for p38 MAPK, which labels the phosphorylated form of the enzyme.

## *Methods*

### Animals and induction of diabetes

As described previously (chapter 3), male Sprague Dawley rats obtained from ARC (Animal Resource Centre, Perth, Australia) were given streptozotocin (STZ) in citrate buffer (pH 4.5, 0.1M) 48 mg/kg body weight via the tail vein to induce diabetes. Rats were tested for elevated blood glucose one week after the injection using a one touch glucometer (Accu-Check Performa) and used for experiments at 2-4 weeks (n=2), 6 weeks (n=2) and 8-10 weeks (n=2) after the STZ injection. Control rats (n=6) received only vehicle injections and underwent all other procedures in the same way as STZ injected rats.

### Tissue collection

At the end of the experimental period, all the rats were euthanized by overdose with pentobarbital sodium (180 mg/kg body weight) and perfused with freshly prepared 4% paraformaldehyde in PBS (0.1M, pH 7.2). After perfusion, the brains were removed and immediately immersed in the same fixative solution for 2-3 hours at $4^0$ C. The brains were then transferred to a solution containing 30% sucrose in PBS and left for approximately 48 hours at $4^0$ C before they were used for immunohistochemistry.

## Immunohistochemistry

OX-42 and P2X4 immunohistochemistry was performed on all the STZ-induced diabetic and control rats while OX-42 and p38 MAPK immunohistochemistry was performed only on tissue from 6 weeks post STZ injection (n=2), 10 weeks post STZ injection (n=1) rats and from 3 control rats at each of these time points. As described previously (chapter 3) serial coronal sections (20µM thick) were cut using a cryostat (Leica, CM 1900). One in five sections encompassing the PVN and NTS was collected, placed onto gelatine coated slides, dried for 2 hours at room temperature and then processed immunohistochemically. Sections were first incubated with 10% normal horse serum (NHS) for 60 minutes then washed and incubated with 0.5 % triton X-100 for 10 min to facilitate antibody penetration. After incubation sections were again washed with PBS and then incubated for 72 hours at $4^0$C with a mouse monoclonal primary antibody directed against CD11b (clone OX-42) (1:100, Chemicon, Temecula, USA) and rabbit anti- P2X4 antibody (1:250, Alomone Lab) or anti-phospho p38 MAPK (1:250, Cell Signalling) in 2% NHS and 0.2% Triton X-100 in PBS. After 72 hours of incubation, all sections were washed with PBS 3 times for 5 minutes each. This was followed by incubation with biotinylated anti-mouse secondary antibody raised in horse (1: 100, rat adsorbed, Vector Laboratories, Burlingame, USA) and Alexa-488 conjugated donkey anti-rabbit secondary antibody (1:400, Invitrogen). After 2 hours of incubation with these secondary antibodies, sections were washed and incubated with R-phycoerythrin conjugated extravidin (1:400, Sigma-Aldrich, St Louis, USA) for 2 hours. After incubation sections were washed and mounted with fluorescent mounting medium followed by cover slipping. Images were taken using a confocal microscope (Nikon A1 laser scanning confocal attached to Nikon Eclipse Ti inverted microscope and equipped with 488nm and 561 nm lasers). The same laser power, gain and pinhole settings were used when imaging sections from control and STZ-induced diabetic rats.

## *Results*

### 1) OX-42 and P2X4 immunoreactivity in PVN and SON microglia

Immunohistochemistry for CD11b receptors using OX-42 clone showed small cells with long, thin processes consistent with specific microglial labeling in the PVN in control rats at all different time points (Fig. 6.1 (A)) as described previously (chapter 3). OX-42 immunohistochemistry on tissue from 2-4 weeks old STZ-induced diabetic rats showed cells with similar morphology to those in as control (Data not shown) which is also consistent with our previous observation (chapter 3). Labeled cells in the PVN of all the STZ-induced diabetic rats at later time points (6 weeks and 8-10 weeks) showed shorter, thicker and stubbier processes. There was also an apparent increase in the intensity of OX-42 immunolabeling (Compare Fig. 6.1 (A) and Fig. 6.1 (B)) as reported previously (chapter 3).

Immunohistochemistry performed with the antibody for P2X4 receptors clearly labeled two different population of cells within the PVN region of control rats (Fig. 6.2 (A)). Some cells had large round cell bodies with relatively large unstained nucleus while others had small cell bodies with clearly stained processes. High power images showing the morphology of these large cells suggested they were neurons (Fig. 6.2 (C)). Previous studies have reported the presence of P2X4 receptors on the PVN neurons in rats (Cham et al 2006; Guo et al 2009). The smaller cells labeled with the antibody for P2X4 receptors shared structural similarity with glial cells and also showed labeling with OX-42 clone suggesting they were microglia. Labeling for both large and small cells was present in tissue from the control as well as in STZ-induced diabetic rats at all the different time points tested. We observed cells double labeled with OX-42 clone and anti- P2X4 receptors antibody in the PVN of all the control and STZ-induced diabetic rats tested at the different time points. As compared to control, STZ-induced diabetic rats did not show any obvious increase in either

the intensity of labeling in microglia or the number of double labeled cells (Fig. 6.1 (A) and Fig. 6.1(B)). It appears however, that the neuronal labeling was stronger in STZ-induced diabetic rats than in controls (Fig. 6.2 (A) and Fig. 6.2 (B)), although this was not quantified.

Immunohistochemistry in tissue obtained from control rats using the antibody for P2X4 receptors did not show any marked labeling in the arcuate nucleus and median eminence, both located adjacent to PVN in hypothalamus (Fig. 6.3 (B)). However, when from STZ-induced diabetic rats observed, labeling of thread like cell structures radiating out from third ventricle was observed. The morphological characteristics and location of these thread like cells suggests that they are tanycytes (also known as tanocytes) (Miskowiak 1976; Zetterstrom et al 1994). We also observed marked labeling of ependymal lining of the third ventricular wall in this region in STZ-induced diabetic rats but not in controls (Fig. 6.3 (C)). The increased labeling for P2X4 receptors around the ventricle was presents in all the STZ-induced diabetic rats at all the time points but it was markedly higher in some rats than others. We did not however, observe any consistent relationship between the increase staining and time after STZ injection.

## 2) OX-42 and P2X4 immunoreactivity in NTS

In the NTS region of control rats the intensity of OX-42 immunolabeling was greater than in surrounding areas in the brain stem and this differential OX-42 immunolabeling was also observed in STZ-induced diabetic rats as seen in Fig. 6.4 (B). This is consistent with our previous observations (chapter 3). We also observed that the morphology of microglia at 10 weeks post STZ injections showed relatively shorter, thicker and stubbier processes as compared to their respective time point controls as seen previously (chapter 3). This was not seen at earlier time points tested.

Immunohistochemistry using the antibody for P2X4 receptors in control rats showed some cells with small nuclei and long processes in the NTS as well as other brain stem regions at all the different time points tested. Cells with similar small nuclei and long processes showing P2X4-IR were also present in the NTS region of STZ-induced diabetic rats at all the time points tested. High magnification images of nuclear tractus solitari (NTS) region of control as well as STZ-induced diabetic rats showed double labeling indicating P2X4 receptor IR in microglia (Fig. 6.4 (A) & Fig.6.4 (B). However, in controls as well as in STZ-induced diabetic rats, not all the microglia were labeled and some showed markedly higher labeling than others. P2X4-IR was seen in cells lining the central canal in STZ-induced diabetic rats (Fig. 6.3 (A)) but not in control rats (data not shown). On the other hand microglia outside the NTS region showed weak labeling for P2X4 receptors as compared to those in NTS in both controls and STZ-induced diabetic rats (compare Fig. 6.4 (A) and Fig. 6.4 (B) with Fig. 6.4 (C)) suggesting that NTS microglia expresses P2X4 receptors at a relatively higher level.

### 3) OX-42 and p38 MAPK immunoreactivity in PVN, SON and NTS

Immunohistochemistry for phosphorylated p38 MAPK showed some labeled cells in the PVN region of control rats (Fig. 6.5 (A)). In STZ-induced diabetic rats there was a clear increase in labeling in PVN (Fig. 6.5 (B)) but there was no obvious overlap between cells stained for phospho p38 MAPK and OX-42 clone in PVN, SON or NTS regions of the brain (data not shown). Cells showing phospho-p38 MAPK-IR were relatively smaller in size as compared to P2X4 stained neurons suggest that they were neuronal nuclei or glial cell type other than microglia.

## *Figures*

**Fig. 6.1 :**

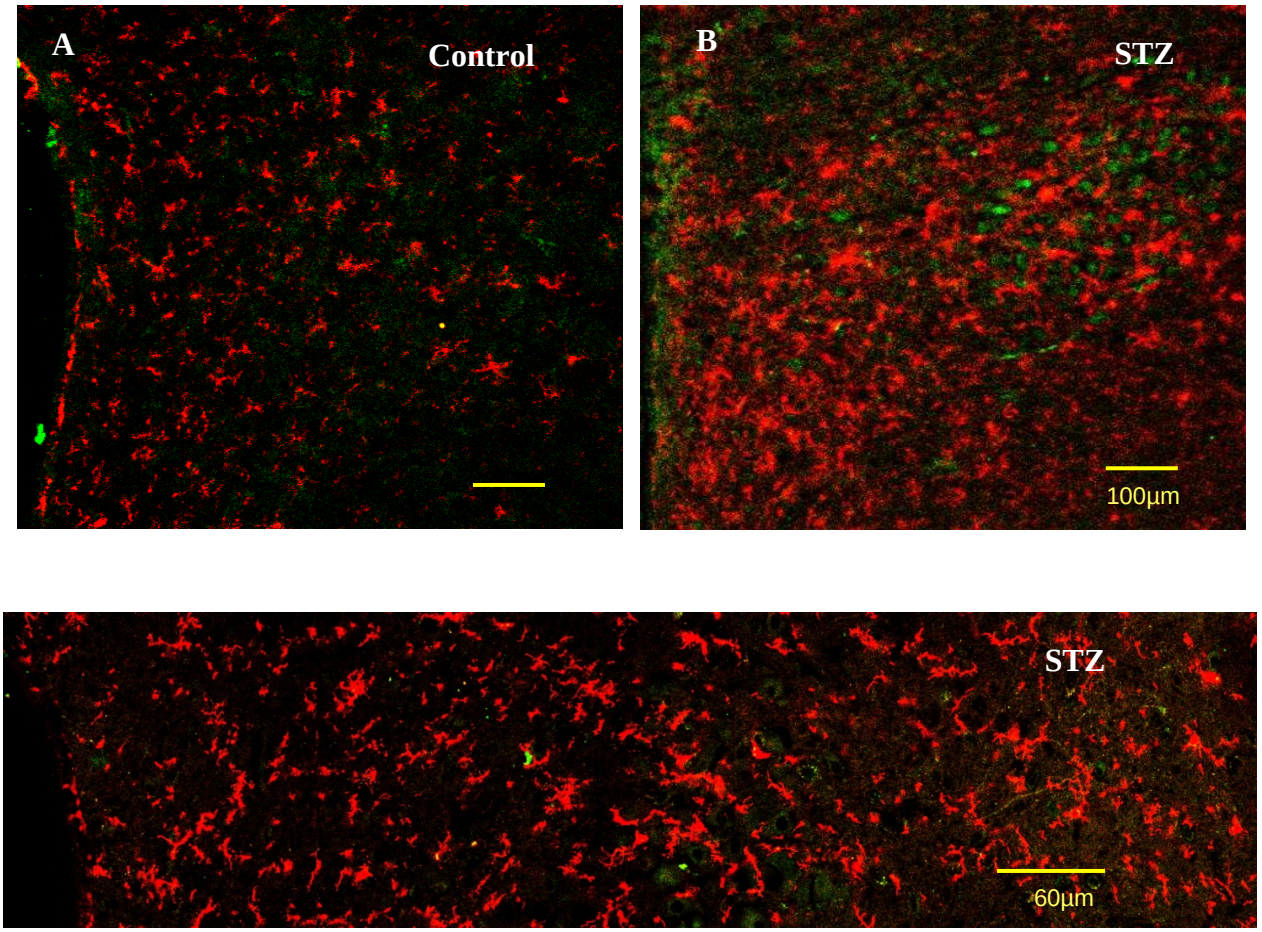

**Fig.6.1** : OX-42 (red) and P2X4 receptor (green) fluorescent immunolabelling in the paraventricular hypothalamic nucleus in (A) control rat and (B) STZ –induced diabetic rat (10 weeks after injection). Panel C shows mediolateral distribution of microglia and P2X4 receptor labelling in the paraventricular hypothalamic nucleus at higher magnification in a diabetic rat 6 weeks after STZ injection.

**Fig. 6.2 :**

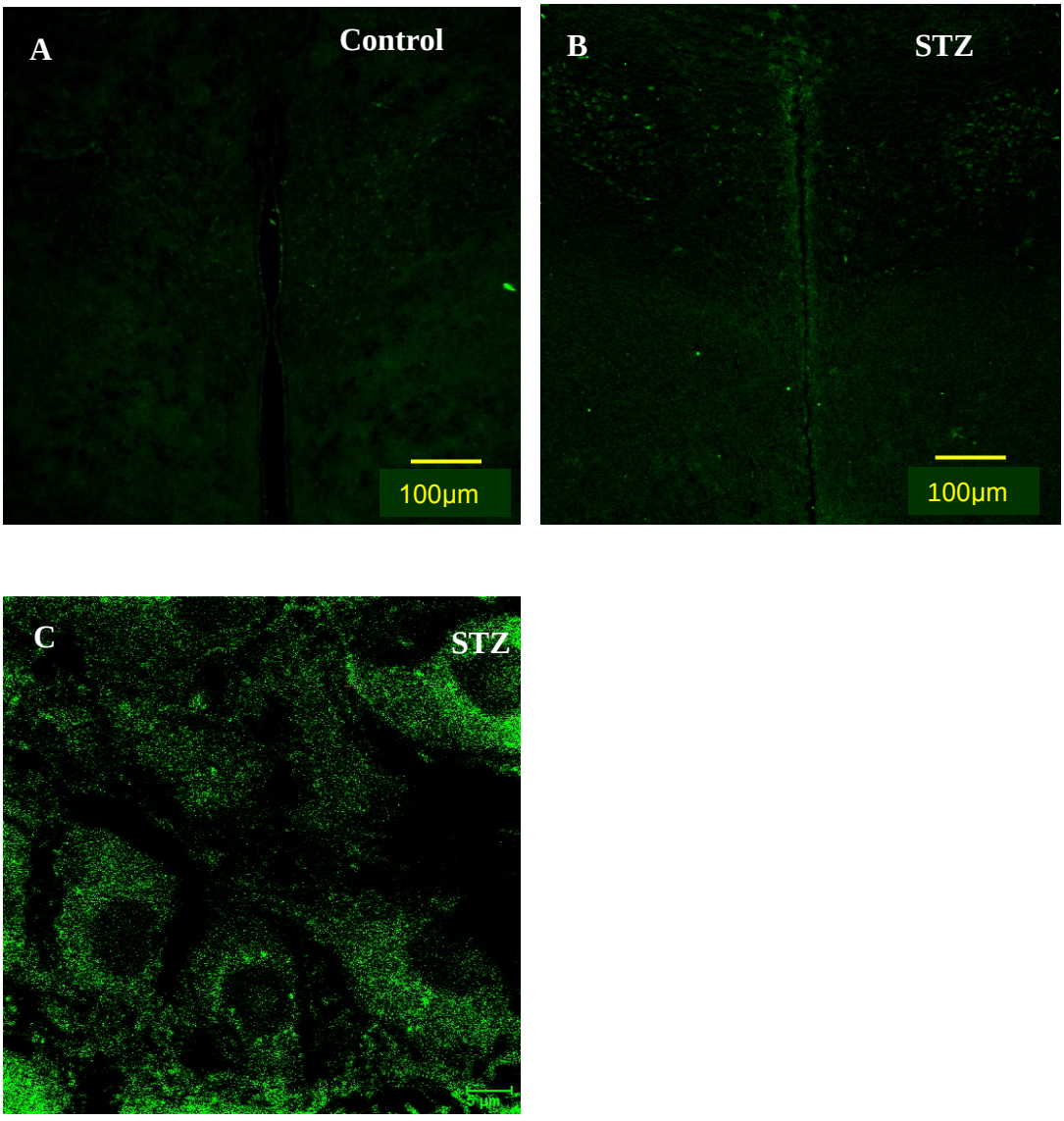

**Fig.6.2** : Fluorescence micrographs showing P2X4 immunolabelling in the paraventricular hypothalamic nucleus. Low magnification image show P2X4 receptor labelling in (A) a control rat and (B) a STZ-induced diabetic rat (8-10weeks time point ; Scale Bar= 100µm). Panel C shows a high magnification image of P2X4 receptor labelling in neurons in the paraventricular hypothalamic nucleus of an STZ rat (Scale Bar= 5µm).

**Fig. 6.3 :**

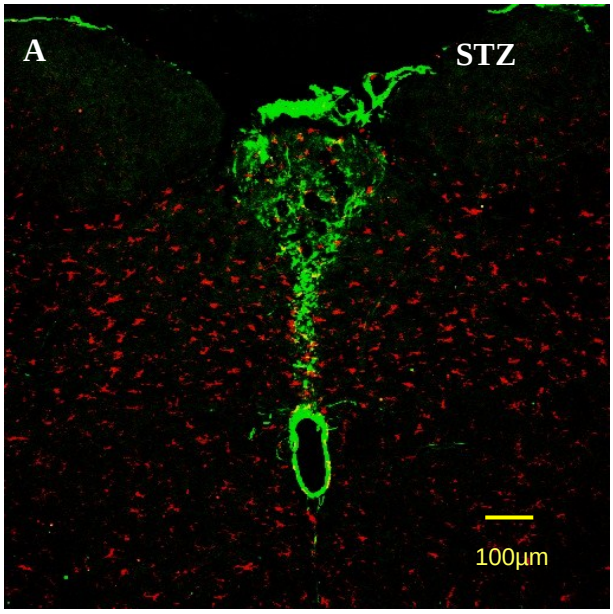


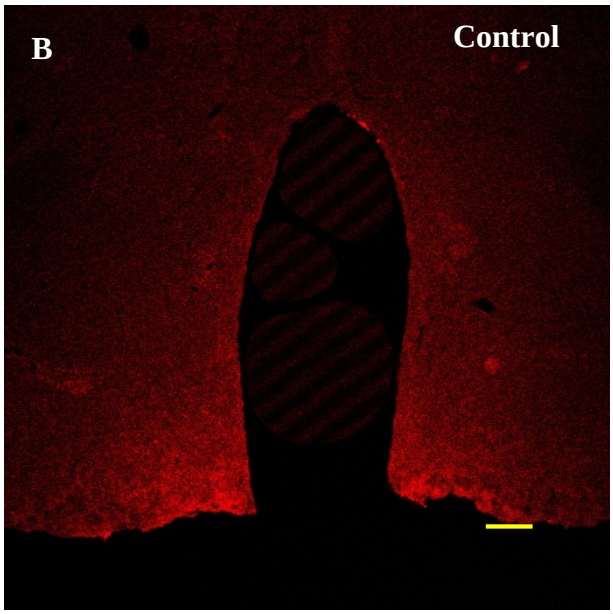


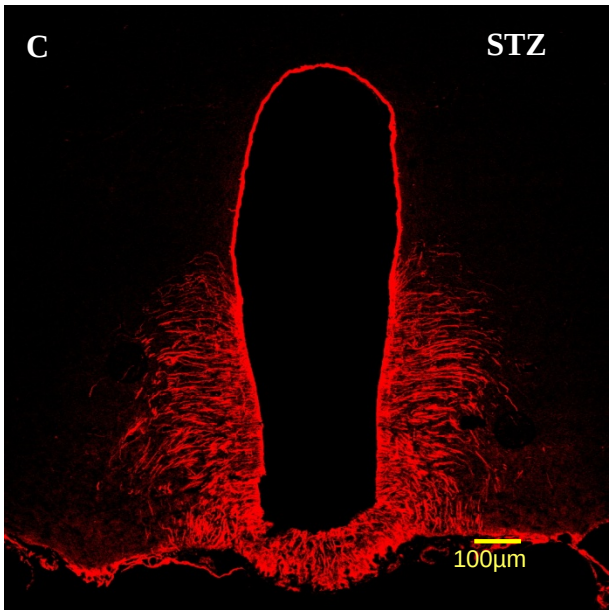

**Fig. 6.3:** (A) Fluorescence photomicrographs showing OX-42 (red) and P2X4 receptors (green) immunolabelling in the NTS region in STZ-induced diabetic rat (6 weeks after STZ injection), (B) P2X4 receptor (red) labelling in the arcuate region of control rat and (C) P2X4 receptor (red) labelling in STZ- induced diabetic rat (6 weeks after STZ injection) showed tanycyte like cells.

**Fig. 6.4 :**

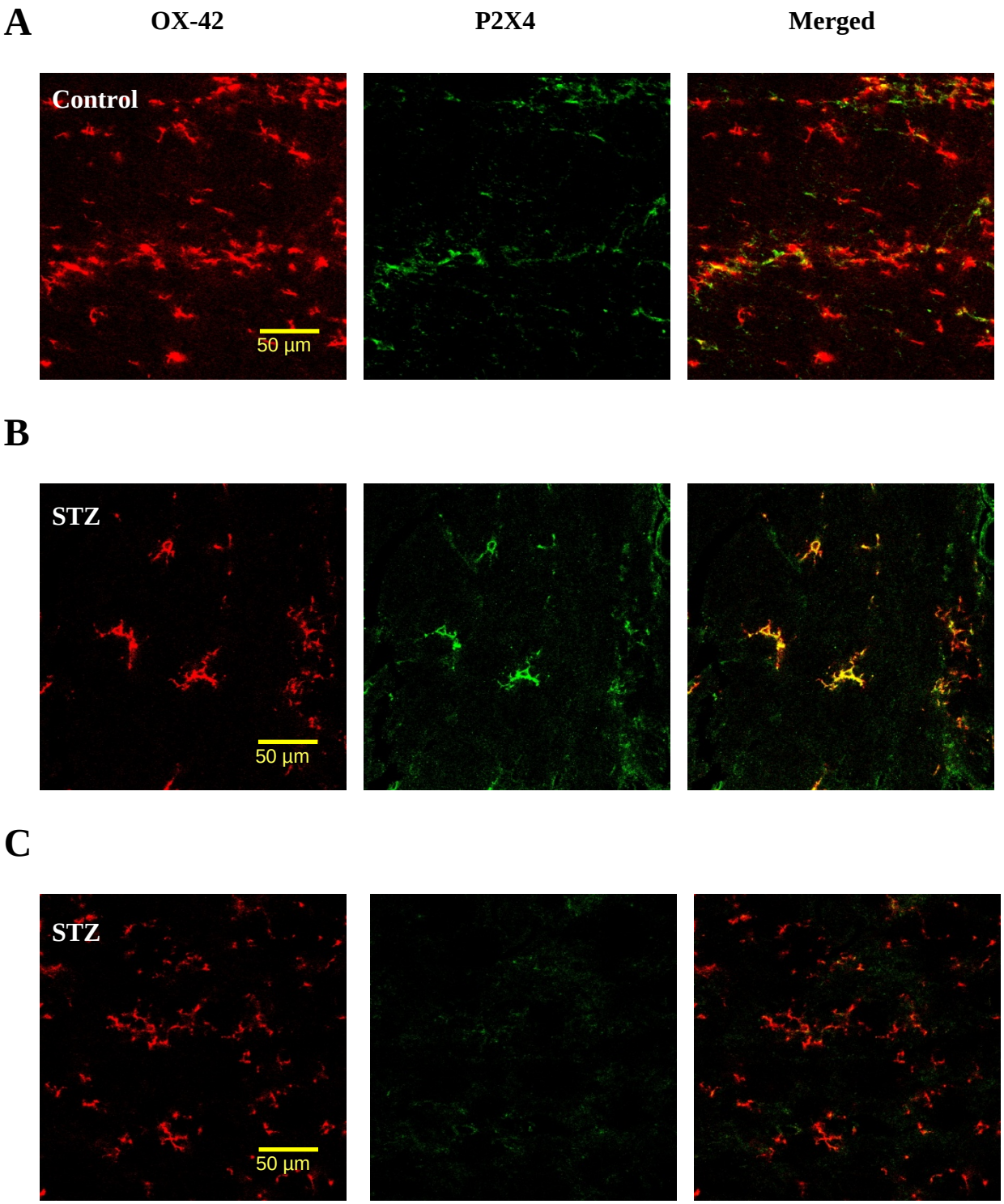

**Fig.6.4 :** High power images demonstrating P2X4 receptor immunolabeling on OX-42 immunolabeled microglia at 10 weeks after vehicle/STZ injection in (A) control nuclear tractus solitarius, (B) STZ-induced diabetic rat nuclear tractus solitarius and (C) area adjacent to the nuclear tractus solitarius in STZ-induced diabetic rat.

**Fig. 6.5 :**

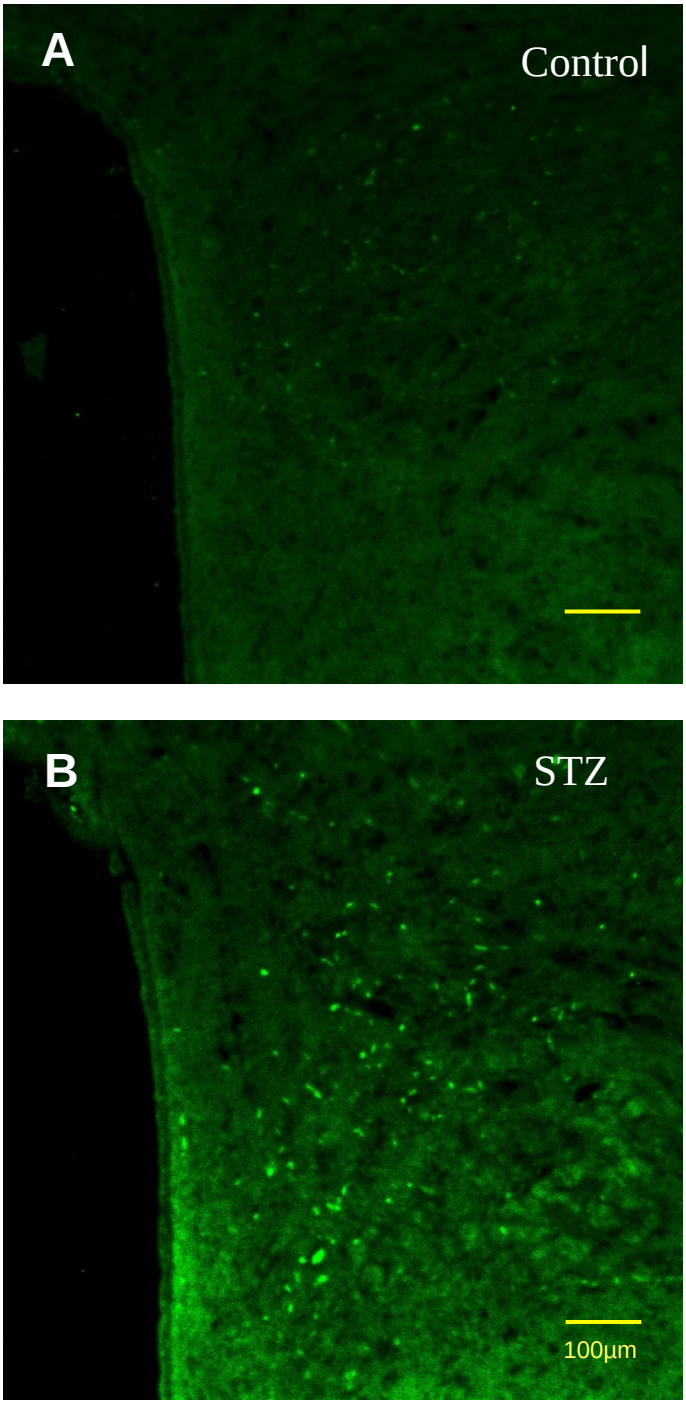

**Fig. 6.5 :** Fluorescence photomicrographs showing phosphorylated p38 MAPK immunolabelling in the paraventricular hypothalamic nucleus of (A) control and (B) STZ-induced diabetic (at 6 weeks after STZ injection) rat.

## *Discussion*

The present study has investigated the levels of two important candidates in the microglial activation process, namely P2X4 receptors and phospho-p38 MAPK, in microglia in the cardiovascular centres of STZ-induced diabetic rats. The key findings are as follows. (i) Microglial P2X4 receptor expression is not markedly up-regulated in any of the brain regions previously demonstrated to have activated microglia in STZ-induced diabetic rats (chapter 3). (ii) OX-42 labelling in the PVN, SON and NTS did not show marked overlap with P2X4-IR. (iii) P2X4-IR appeared to be up-regulated in neurons in the PVN and SON, but not in the NTS. (iv) We observed increased phosphorylated p38 MAPK labelling in the PVN, but no marked increase in microglial cells.

Activated microglia in cardiovascular centres of STZ-induced diabetic rats did not show a marked increase in expression of P2X4 receptors (Fig. 6.1, 6.3(A) and 6.4). This is not consistent with previous reports showing increased P2X4 receptor-IR in activated microglia in spinal dorsal horn after nerve injury (Tsuda et al. 2003; Ulmann et al. 2008). These studies also reported a reduction in nerve injury-induced pain upon pharmacological inhibition of P2X4 receptors or in P2X4-deficient mice, suggesting their role in microglial activation. It is important to note here that neuropathic pain models show microglial activation within hours/days of nerve injury. We have reported marked activation of PVN microglia between 6−10 weeks after the induction of diabetes (chapter 3). Thus, STZ-induced diabetes appears to be a relatively weak stimulator of microglial activation. Hence, it is possible that the mechanism of microglial activation is different in the two cases. Since they are present in control, up-regulating of these receptors may not be required for them to have a functional role in activating microglia or in activated microglial cells. We did not observe up-regulation of microglial P2X4 receptors in any brain region tested in STZ-induced diabetic rats at any time points used in this study. Despite this, it is possible that microglia in STZ-induced

diabetic rats transiently express P2X4 receptors at high levels at a time not included in this study. It is also possible that individual microglia express these receptors asynchronously. The latter possibility may have limited our ability to see a marginal increase in the number of microglial cells showing higher P2X4 immunolabelling.

Another possibility is that other purinergic receptors are important for microglial activation in the cardiovascular centres of STZ-induced diabetic rats, e.g., P2Y12 and P2X7 receptors (Chessell et al. 2005; Kobayashi et al. 2008). A recently published study has demonstrated increased P2Y12 mRNA and protein expression exclusively in spinal dorsal horn microglia after nerve injury (Kobayashi et al. 2008). This study also reported elevation of pain behaviour via intrathecal administration of the P2Y12 agonist 2-(methythio) adenosine 5´-diphosphate and suppression of pain behaviour using an antagonist, suggesting that microglial P2Y12 receptors are involved in nerve injury-induced pain. Surprisingly, P2X7 deletion or antagonism also produces significant inhibition of neuropathic pain behaviours (Chessell et al. 2005; McGaraughty et al. 2007). Thus, it is possible that either P2X7 and/or P2Y12 receptors are responsible for microglial activation in STZ-induced diabetic rats.

We did not find increased phosphorylation of p38 MAPK in microglia in any area examined at any time point studied. This is in contrast to previous studies which have reported a link between increased phosphorylation of p38 MAPK in microglia of the spinal dorsal horn and pain behaviour after nerve injury (Ji & Suter 2007; Tsuda et al. 2004). These studies have demonstrated very high levels of labelling for the phosphorylated form of p38 MAPK in microglia that are easily visualised via immunohistochemistry. Although we did not observe such marked phosphorylation of p38 MAPK in microglia, our results do not rule out the possibility of a low level increase. Moreover, as noted above in relation to P2X4 receptors, p38 MAPK phosphorylation in microglia may be present transiently and/or asynchronously. Therefore, it is possible that only a small proportion of cells exhibit high levels of the phosphorylated form at a particular time. Under these circumstances, a marked,

easily distinguishable change is less likely to be seen, and this may affect the interpretation of our results. In addition to p38 activation in spinal microglia, extracellular signal-regulated kinase (ERK), another MAPK family member, is also reportedly activated in spinal microglia in the early stages (first several days) of neuropathic pain development, and suggested to be required for neuropathic pain sensitisation (Zhuang et al. 2005). A study of STZ-induced diabetic rats showed increased phospho-ERK-IR in microglia of dorsal horn and reduced pain behaviour in these rats upon pharmacological inhibition of ERK (Tsuda et al. 2008). This result suggests that a pathway involving ERK may be responsible for the microglial activation in cardiovascular centres in STZ-induced diabetic rats.

We did observe increased labelling with the antibody for P2X4 receptors (compare Fig. 6.2 (A) and Fig. 6.2 (B)) in the PVN of STZ-induced diabetic rats, which appeared to be present in neurons. We have previously reported increased Fos labelling in PVN neurons in STZ-induced diabetic rats (chapter 3). This up-regulation of neuronal P2X4 receptors may be the cause or a consequence of reported neuronal activation in the PVN. Hence, further investigation is required to understand functional significance. We also observed increased phosphorylation of p38 MAPK (Fig. 6.5) in non-microglial cells in the PVN of STZ-induced diabetic rats. One possibility is that these non-microglial cells are neurons. A recently published study has reported increased phosphorylation of neuronal p38 MAPK in the PVN in rats with heart failure (Wei et al. 2008). These rats have increased PVN neuronal activity and elevated sympathetic drive, as do STZ-induced diabetic rats (chapter 2 and chapter 3). Another possibility is increased phosphorylation of p38 MAPK in astrocytes. Apart from microglia, astrocytes are other glial cells that are reported to be activated after nerve injury (Zhang & De Koninck 2006). It has been suggested that microglial activation is required only for the induction and initial stages of pain following nerve injury, while astrocytes are important for the long-term maintenance of the pain (Ji & Suter 2007).

## *Conclusion*

Our results provide no evidence for increased expression of P2X4 receptors in activated microglia in the cardiovascular centres of STZ-induced diabetic rats. Further study is required to investigate the involvement of P2Y12 and P2X7 receptors in these cells. We did not find any evidence for the involvement of phopho-p38 MAPK in microglial activation in STZ-induced diabetic rats in the examined areas of brain. Based on other recent studies, further study is required to investigate the involvement of phospho-ERK in the microglial activation process.

# Chapter 7: Investigation of the Role of Calcium Signalling in Microglial Activation

## *Introduction*

Inflammation in the central nervous system (CNS) is believed to play a pivotal role in various neurodegenerative diseases, including Alzheimer's disease, Parkinson's disease, prion disease and multiple sclerosis. The inflammatory response in the CNS is mainly mediated by activated microglia, which normally respond to neuronal damage and remove damaged cells by phagocytosis. Activated microglia exhibit shorter and thicker processes with swollen cell bodies when compared to resting microglia, while microglia performing phagocytosis display morphology very similar to that of monocytes and macrophages. Thus, microglia have multiple morphological states depending on their function (chapter 1). We have reported the presence of activated but not phagocytic microglia in the cardiovascular centres of rats with heart failure and STZ-induced diabetes (chapter 2 and 3). Hence, it is important to understand how this activation comes about.

*In vitro* studies of cultured microglia provide a useful tool for understanding the mechanisms of microglial activation. Such studies have measured changes in microglial morphology, secretions, in the activity of various intracellular pathways and enzymes and in phagocytic ability and motility (Hide et al. 2000; Honda et al. 2001; Koizumi et al. 2007; Lu et al. 2009a). These studies have used lipopolysaccharide (LPS), ATP and UDP as activators of microglia. LPS mimics the condition of infection, while nucleotides (ATP and UDP) are thought to mimic the conditions present when there is neuronal damage in the CNS. Each of these microglial activators have been shown to cause a transient increase in intracellular calcium in microglia (Hoffmann et al. 2003; Koizumi et al. 2007; Tsuda et al. 2003).

Receptors that mediate responses to ATP and UDP are P2 purinergic receptors. Microglia express both ionotropic (P2X) and metabotropic (P2Y) purinergic receptors. Both

can be activated by nucleotides released from damaged neurons and both affect intracellular $Ca^{2+}$ in microglia. Seven ionotropic (P2X1–7) and eight metabotropic P2 receptors (P2Y1, 2, 4, 6, 11–14) have been discovered to date. Of these receptors, microglia express P2Y1, 2, 6, 12–14 (Fischer & Krugel 2007; Kim et al. 2011; Koizumi et al. 2007; Ogata et al. 2003; Ohsawa et al. 2010) and P2X3, 4, 7 (Light et al. 2006). Different nucleotides have different affinities for these receptors. For instance, ATP has a relatively high affinity for P2Y1, 2, 4, 12, and 13 but not P2Y6, while UDP has high affinity for only the P2Y6 receptor type (Fischer & Krugel 2007; Koizumi et al. 2007). Previous studies of microglia have suggested that ATP at 50μM mainly acts on microglial P2X4 receptors (Trang et al. 2009; Tsuda et al. 2003), while UDP does not bind to this receptor (North & Surprenant 2000). Thus, it appears that ATP can activate ionotropic receptors as well as metabotropic receptors on microglia while UDP activates only the metabotropic receptor P2Y6.

Ionotropic receptors are responsible for nucleotide-induced depolarisation and $Ca^{2+}$ influx, while activation of metabotropic receptors leads to IP3-dependent $Ca^{2+}$ release from intracellular stores through a mechanism involving G protein activation and PLC stimulation (Moller et al. 2000; Norenberg et al. 1994; Visentin et al. 1999). Receptors on microglia allow them to scan and respond to damage in surrounding tissue. Thus, nucleotides released from damaged neurons in the brain are thought to activate purinergic receptors on microglial membranes which may lead to elevated intracellular calcium. It is not known whether changes in intracellular $Ca^{2+}$ levels in microglia can influence/modulate their responsiveness to ATP and UDP. However, previous *in vitro* and *in vivo* studies have reported increased expression of purinergic receptors upon microglial activation (Bianco et al. 2005; Tsuda et al. 2003) .

It is clear that elevated intracellular $Ca^{2+}$ plays a vital role in modulating microglial functions (Hoffmann et al. 2003). $Ca^{2+}$ may serve as an integrator of various cytosolic pathways that control microglial behaviour under resting and activated conditions. A sustained

increase in microglial intracellular $Ca^{2+}$ has been suggested as a prerequisite for the release of nitric oxide and cytokines (Farber & Kettenmann 2006). An *in vitro* study has demonstrated a correlation between ATP-mediated dose-dependent TNF-α release and the magnitude of the transient increase in intracellular $Ca^{2+}$ due to ATP (Hide et al. 2000). LPS, a stronger activator of microglia, causes a sustained increase in basal $Ca^{2+}$ level in microglia (Hoffmann et al. 2003). This study also demonstrated that the $Ca^{2+}$ chelator BAPTA (1,2-bis(o-aminophenoxy) ethane-N,N,N',N'-tetraacetic acid) strongly attenuates the LPS-induced release of nitric oxide (NO), and cytokines and chemokines from microglia. A transient increase in $[Ca^{2+}]i$ and increased phagocytic activity in microglia treated with UDP has also been reported (Koizumi et al. 2007). It appears from this evidence that microglial intracellular $Ca^{2+}$ levels define their activation and functional state. All these studies have demonstrated an initial transient increase in intracellular $[Ca^{2+}]i$ upon short application (30 s) of ATP or UDP, but the effects of longer-term exposure on basal $[Ca^{2+}]i$ and its involvement in the function of microglia have never been investigated.

Another molecule which has been shown to modulate microglial $[Ca^{2+}]i$ is BDNF. ATP activates microglial P2X4 receptors and induces BDNF releases from microglia (Trang et al. 2009). The BDNF released from microglia has been shown to modulate neuronal activity in spinal cord slices (Biggs et al. 2010; Lu et al. 2009a). Another *in vitro* study of microglia has shown a gradual increase in the basal $[Ca^{2+}]i$ upon BDNF exposure (Mizoguchi et al. 2009). This result suggests that BDNF released from microglia may have an autocrine effect and a role in regulating microglial activation, but the effect of BDNF exposure on microglial responsiveness to ATP has never been addressed.

Our preliminary observations showed that the initial basal $[Ca^{2+}]i$ varied between microglia. Therefore, we investigated whether transient changes in intracellular calcium in response to ATP and UDP in microglia varied with different basal $Ca^{2+}$ levels. We also studied the effect of long-term exposure to ATP and UDP on basal $[Ca^{2+}]i$ levels and on

microglial motility as a measure of microglial function. To investigate whether changes in basal $[Ca^{2+}]i$ with BDNF can influence microglial responsiveness to ATP, we incubated microglia with BDNF and measured changes in their $[Ca^{2+}]i$ as well as their responsiveness to ATP.

## *Methods*

### Microglial isolation and culture

Microglia were isolated as described in chapter 5. In brief, 3 day old rats were sacrificed and their brain minced by passage through a stainless steel mesh (40 mesh) and incubated with 0.25% trypsin and 0.01 % DNase in phosphate buffered saline (PBS) for 10 min at $37^0$ C. Horse serum was then added to terminate the digestion and the cells were passed through a second stainless steel mesh (100 mesh) and then washed twice with medium. The final cell suspension was plated in poly-D-lysine-coated flasks (75 $cm^2$) at a density of approximately one brain per bottle. Cultures were maintained in Dulbecco's modified eagle's medium (DMEM, 4.5g/l glucose) supplemented with 10% FBS, 1% penicillin and streptomycin mixture and in a 5% $CO_2$ atmosphere at $37^0$C. Half of the medium was changed twice a week. After 10-14 days, flasks were placed on shaker at 120 rpm for 45 minutes ($37^0$ C). The supernatant was collected and centrifuged at 1500 rpm for 5 minutes. The pellet was resuspended and incubated overnight in DMEM-high glucose (4.5g/l) containing 1% penicillin and streptomycin and 10% FBS at 37°C with 5% $CO_2$ on sterile, poly-D-lysine coated glass bottom chambers (World Precision Instruments Inc. Sarasota, Fl.).

### $Ca^{2+}$ imaging

On the day of experiments, cultured microglia were washed with Krebs-HEPES Buffer (NaCl 14.8 mM, KCl 2.8 mM, $MgCl_2$ 2 mM, HEPES 10mM, Glucose 10 mM, $CaCl_2$ 2 mM, pH 7.4) and incubated in 2.5 ml Krebs-HEPES buffer containing Fura- 2-AM (2μM, Invitrogen) and bovine serum albumin (5mg/ml) for 30 minutes at 37 ºC with 5% $CO_2$, to

allow the intracellular removal of the ester group from the dye. The fura-2-AM solution was removed and replaced with 2 ml Krebs-HEPES and cells left in the dark for 30 min at room temperature. Calcium Imaging was performed using an Olympus IX70 inverted microscope, a polychrome IV tunable light source (TILL Photonics) and images captured using a cooled CCD camera (Sensicam, PCO Computer Optics) and Axon Imaging Workbench™ software. The fura-2 was excited at alternating wavelengths of 340 and 380nm for periods of 100ms. The fluorescence was measured at 510 nm and the ratio of fluorescence intensity at the two excitation wavelengths (340 nm/380nm) considered as an indicator of intracellular $Ca^{2+}$ concentration. Microglia were continuously superfused with Kreb's-HEPES buffer, and drug solutions applied via the inflow lines. Freshly prepared ATP or UDP solutions in Krebs-HEPES buffer were applied for 30 s and/or one hour through inflow lines and the changes in intracellular $Ca^{2+}$ recorded. For the BDNF treatment experiment, cells were continuously superfused with BDNF in Krebs-HEPES buffer via the inflow lines.

## Microglial motility

Microglial cells were isolated and plated in glass bottom culture dishes overnight before being incubated with Cell tracker$^{TM}$ dye (1 μg/ml, Invitrogen) or DAF-FM dye (0.5ug/ml, Invitrogen) and nuclear stain (1ug/ml,Hoechst Dye, Invitrogen) in Kreb's-HEPES buffer for 45 min at $37^0$ C. Then cells were washed with Kreb's-HEPES buffer and visualised using a confocal microscope (Nikon A1) either in the presence of ATP (50μM) or UDP (100 μM) or buffer alone. Images was taken at the start of experiment and then one hour later and the movement of nucleus measured using NIS-Element Software (Nikon, version 3.0) by drawing a straight line between the centre of nucleus at t=0 and t=60.

## *Results*

### 1) Effect of brief ATP/UDP application on microglial $Ca^{2+}$

We observed that the initial fura-2 fluorescence ratio varied greatly between microglia present in culture, suggesting that their initial basal $Ca^{2+}$ levels were different and microglia in our cultures were present in different activation states. Irrespective of the initial fluorescence ratio, microglia showed a transient increase in intracellular $Ca^{2+}$ upon 30 s application of either ATP (50μM, Fig. 7.1 (A)) or UDP (100μM, Fig. 7.1 (B)). Interestingly, we also observed that the initial ratio had a marked impact on amplitude of microglial responses. Cells with a lower initial ratio showed a greater transient change as compared to the cells that had higher initial ratio irrespective of whether ATP or UDP was used as a stimulus (Fig. 7.1 (A) and Fig. 7.1 (B)). To quantify this effect, we plotted the amplitude of the response (defined as the peak fluorescence ratio minus the baseline immediately prior) against initial baseline ratio, and saw a significant inverse correlation for both ATP responses (Fig. 7.2 (A) ; $P < 0.00001$) and UDP responses (Fig. 7.2 (B); $P<0.05$). To test whether this was due to responses reaching a ceiling, we plotted the absolute value of the fluorescence ratio at the peak of the response against the initial baseline ratio. We observe that in the case of ATP, in cells with higher initial basal ratios, the absolute peak response was higher indicating that a ceiling was not reached in those cells (Fig. 7.3 (A)). However, this was not the case for UDP responses as there was no correlation, indicating that the absolute peak value reached during the response was not changing as the initial baseline increased (Fig. 7.3 (A)).

### 2) Effect of 1 hour ATP/UDP treatment application on microglial $Ca^{2+}$

ATP at 50 μM for 1 hour activates microglia (Trang et al 2009; Tsuda et al 2003) and UDP at 100μM stimulates phagocytosis in microglia (Koizumi et al 2007). We therefore investigated the effect of 1 hour treatment with ATP 50 μM and with UDP 100 μM on

microglial [$Ca^{2+}$]i. Microglia perfused with buffer for one hour showed a small change in fluorescence ratio as shown in Fig. 7.4 (A). Quantification showed that the average rise in florescence ratio from its initial level after superfused for 1 hour with buffer and in absence of any stimulus was 0.0550 ± 0.01133 (N=14; Fig. 7.5 (B)). Compared to control, a one hour treatment with UDP (100 μM) (N=16; Fig. 7.4 (B)) or with ATP (N=7; 50 μM) (Fig. 7.5 (A)) caused a markedly greater increase in fluorescence ratio, suggesting a greater increase in intracellular $Ca^{2+}$. When we generated a concentration effect curve, we observed that ATP did not cause a significant change in fluorescence ratio at concentrations of 5 μM and below (N=9). We observed the highest increase in intracellular calcium at 50 μM (N=7; $P<0.05$) and a further increase in ATP concentration did not cause a higher increase in intracellular Ca2+ after 1 hour treatment (Fig. 7.5 (A)).

In the presence of UDP (100μM) for 1 hour, the basal fluorescence ratio also increased significantly by about 0.1569 ± 0.02798 (N=16, $P<0.001$, Fig. 7.5 (B)) as compared to control.

## 3) Effect of ATP and UDP on microglial motility

Microglia are motile in both *vitro* and *vivo* conditions and migrate upon activation. The displacement of microglial cells present in control conditions in one hour was minimal (Images not shown). Fig. 7.6 (A) and Fig.7.6 (B) shows images of microglial cells at time t=0 and t=60 indicative of cell displacement in one hour in presence of ATP (50μM). Quantification showed that in these experiments, ATP (50μM) treatment caused a significant increase in microglial displacement (N=42) in one hour as compared to untreated control (N=72) cells ($P<0.001$; Fig. 7.7). Interestingly, at the end of a one hour treatment period, UDP (100μM) did not show a significantly greater displacement (N=21) as compared to cells in controls (N= 42; t=0.3957).

## 4) Response to ATP in BDNF pre-treated cells

Unlike ATP and UDP, BDNF 2ng, 5ng and 10ng/ml treatment by itself did not cause an initial transient change in fur-2 florescence ratio in microglia which is consistent with the previous observations of Mizoguchi et al., (2009). However, in contrast to their study we did not observe any significant change in $[Ca^{2+}]i$ over the 15 min period after BDNF treatment (Fig. 7.8 (A)). Moreover, pre-treatment of cells with BDNF 10ng/ml for 15 minutes did not modulate the microglial response to ATP (Fig. 7.8 (B)).

## *Figures*

**Fig. 7.1 :**

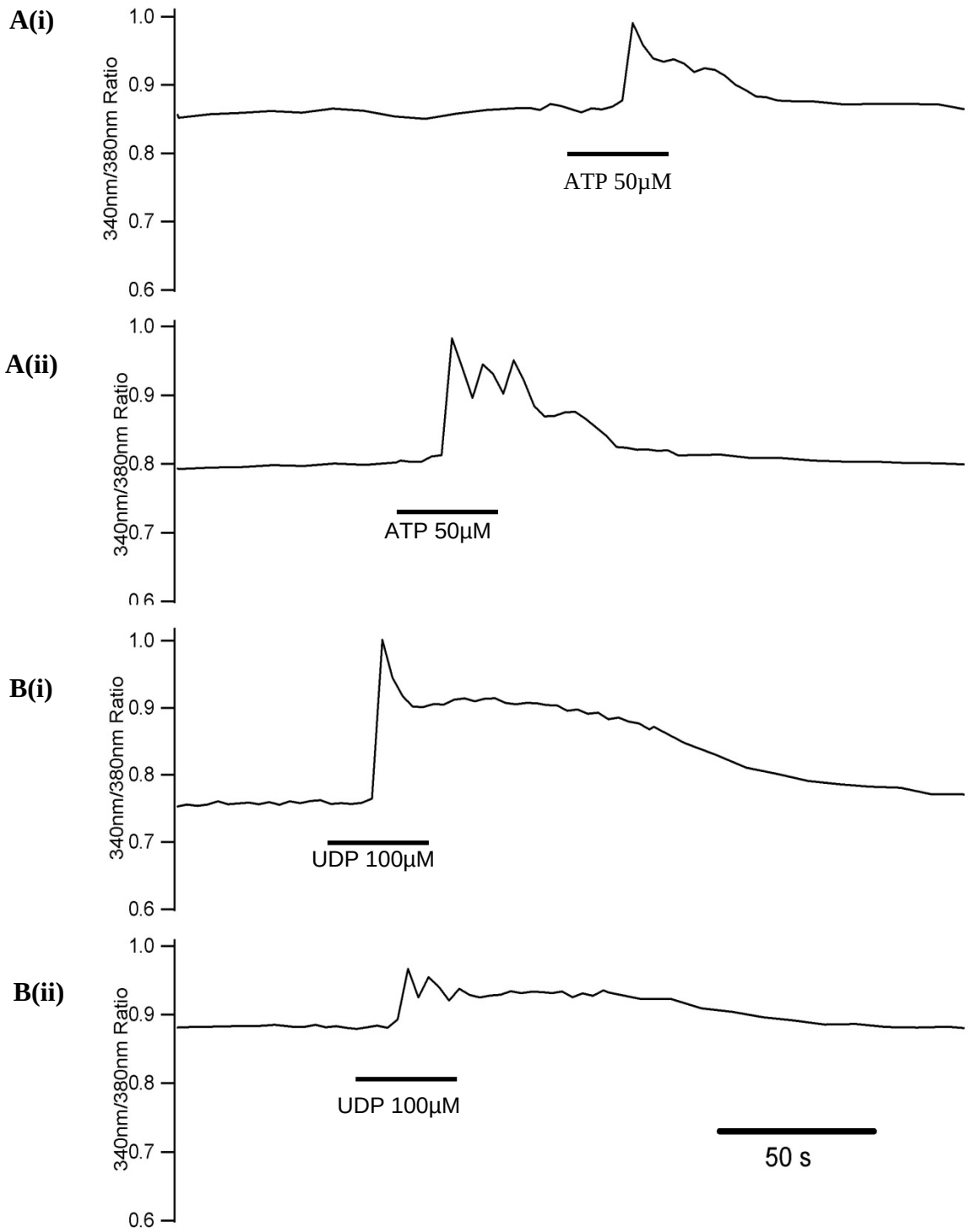

**Fig. 7.1 :** Changes in fluorescence ratio over time in response to (A) ATP 50μM application for 30 seconds in cells with (i) initial base line ratio 0.78 and (ii) initial baseline ratio 0.86 and (B) UDP 100μM application for 30 seconds in cells with (i) initial baseline ratio 0.74 and (ii) initial baseline ratio 0.89. Thin horizontal bars indicate the period of the applications.

**Fig. 7.2** :

**A**

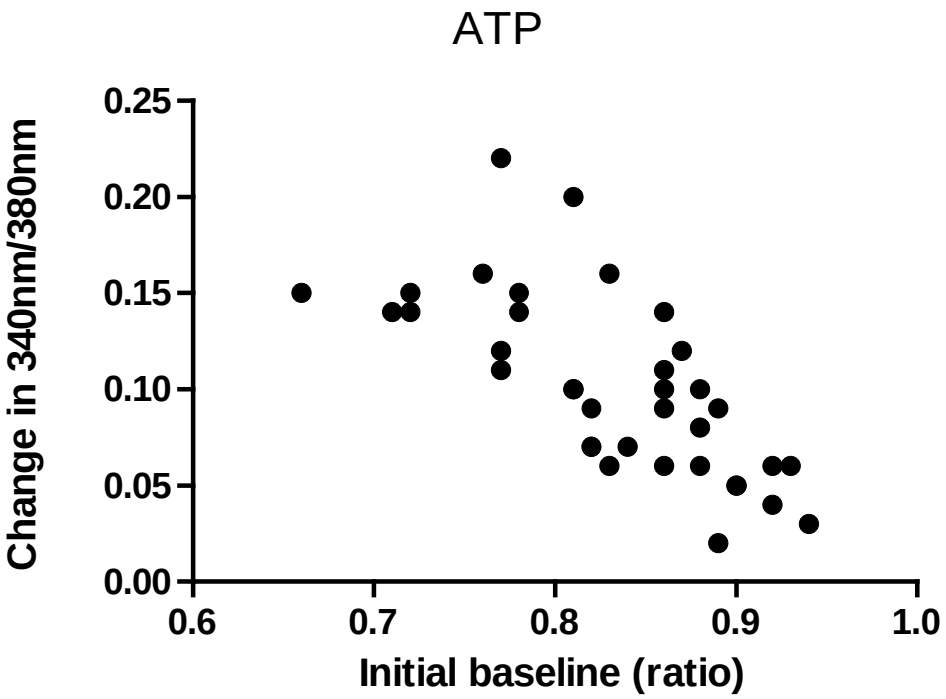
ATP
Change in 340nm/380nm
0.25
0.20
0.15
0.10
0.05
0.00
0.6
0.7
0.8
0.9
1.0
Initial baseline (ratio)

**B**

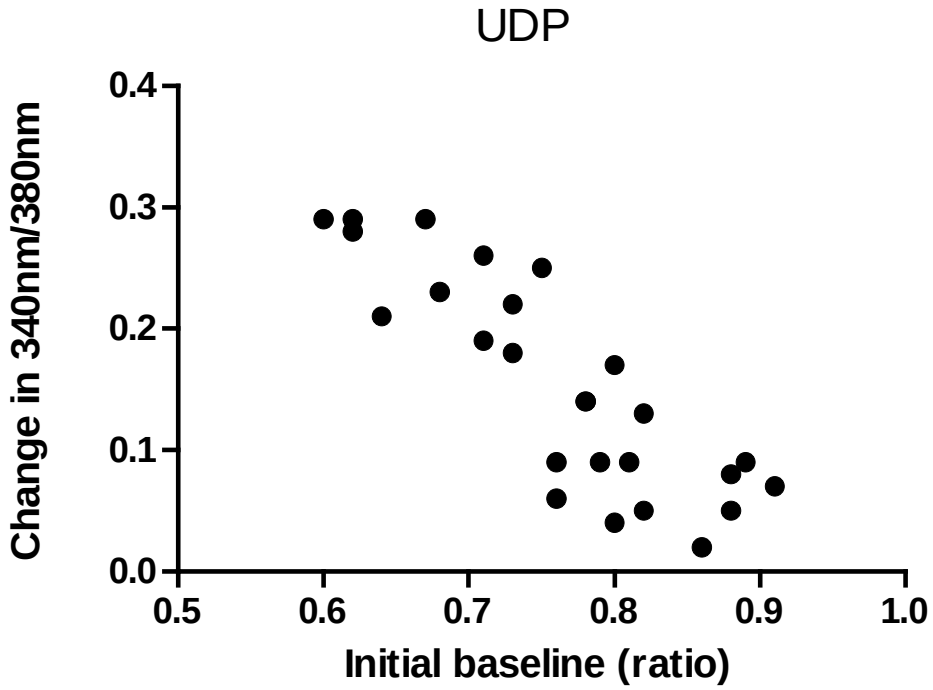
UDP
Change in 340nm/380nm
0.4
0.3
0.2
0.1
0.0
0.5
0.6
0.7
0.8
0.9
1.0
Initial baseline (ratio)

**Fig.7.2 :** Change in fluorescence ratio vs initial baseline ratio following 30s ATP (50µM) treatment. Each dot represents a single cell response. There was a significant correlation between microglial responsiveness to (A) ATP (50µM) and the initial baseline (Pearson Correlation test P value<0.00001, R squared=0.4750). There was a significant correlation between microglial responsiveness to (B) UDP (100µM) and the initial baseline (Pearson Correlation test P value<0.05, R squared=0.5389).

**Fig. 7.3 :**

**A**

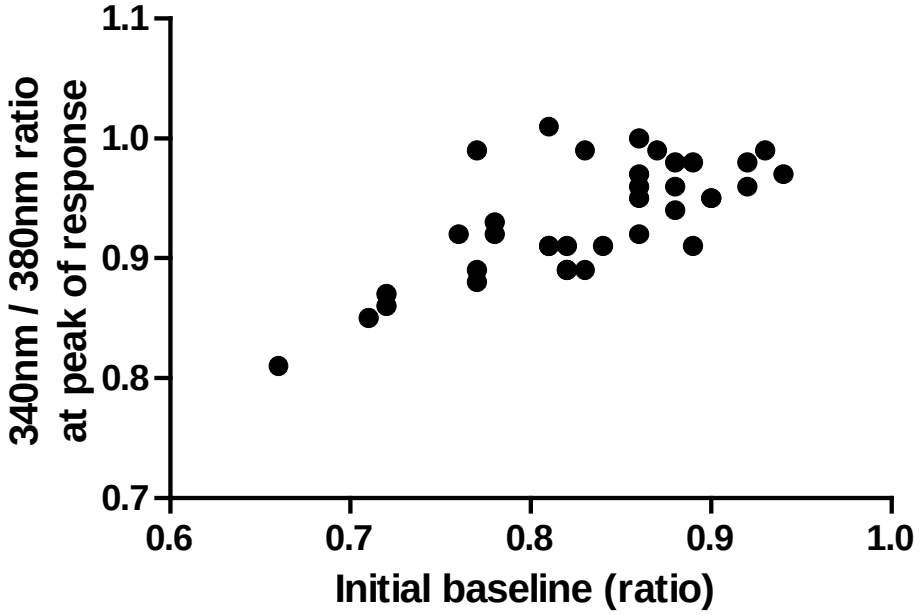
340nm / 380nm ratio
at peak of response
1.1
1.0
0.9
0.8
0.7
0.6
0.7
0.8
0.9
1.0
Initial baseline (ratio)

**B**

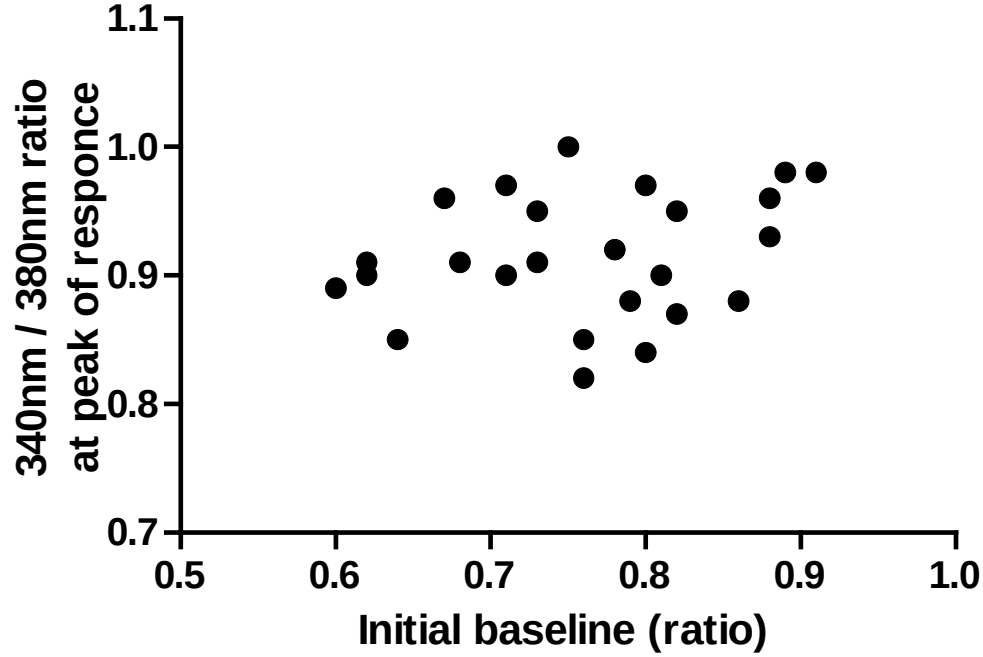
340nm / 380nm ratio
at peak of responce
1.1
1.0
0.9
0.8
0.7
0.5
0.6
0.7
0.8
0.9
1.0
Initial baseline (ratio)

**Fig. 7.3** : Absolute peak 340/380nm ratio achieved in response to ATP and UDP in cells with different baseline. Individual dots represents a single cell response. Panel A shows the absolute peak 340/380nm ratio response to ATP (50µM) treatment. There was a significant correlation; $P<0.0001$, $N=38$. Panel B shows the absolute 340/380nm ratio in response to UDP (100µM) treatment. There was no significant correlation; $P=0.2228$, $N=26$.

**Fig. 7.4 :**

**A**

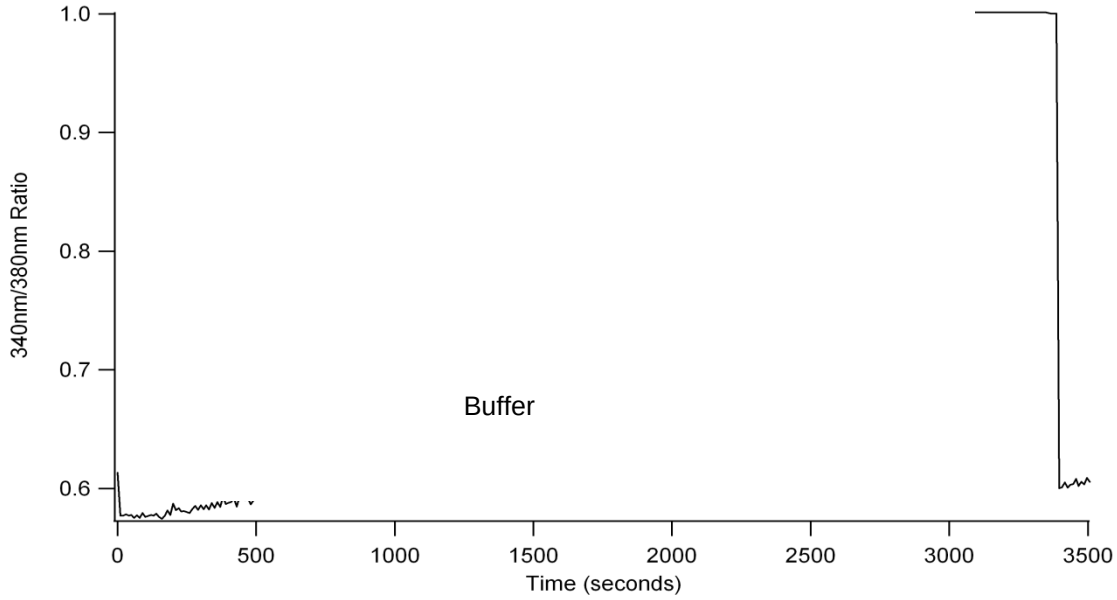
1.0
0.9
0.8
0.7
0.6
340nm/380nm Ratio
Buffer
0
500
1000
1500
2000
2500
3000
3500
Time (seconds)

**B**

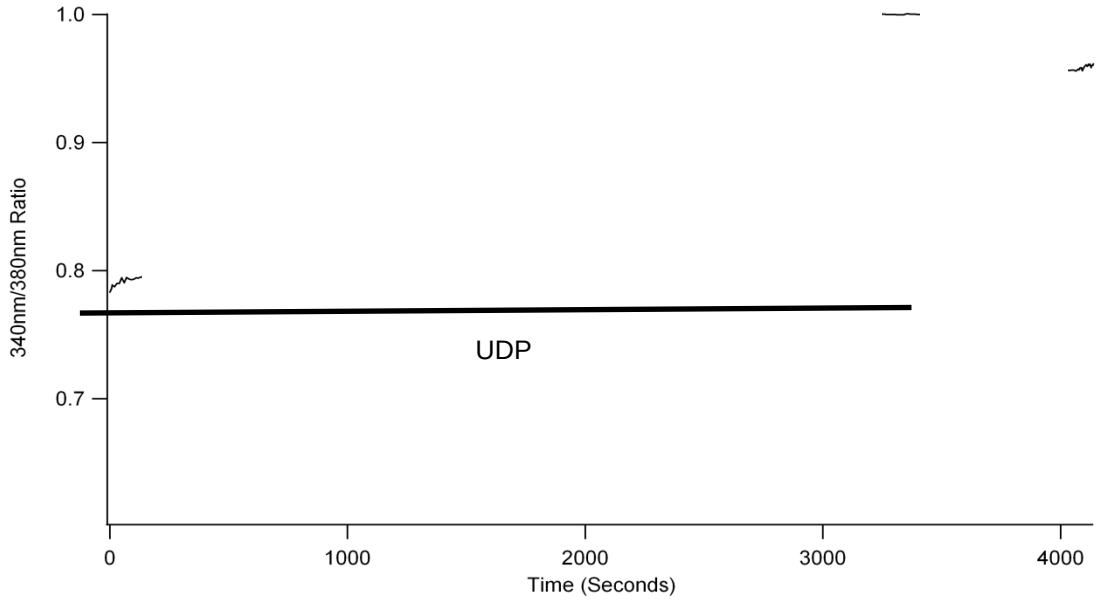
1.0
0.9
0.8
0.7
340nm/380nm Ratio
UDP
0
1000
2000
3000
4000
Time (Seconds)

**Fig. 7.4 :** Change in 340/380 flueroscence ratio over time during (A) buffer application for 1 hour and (B) UDP (100μM) application for 1 hour. Note the large change in baseline baseline between the start and end of experiment when UDP applied.

**Fig. 7.5 :**

**A**

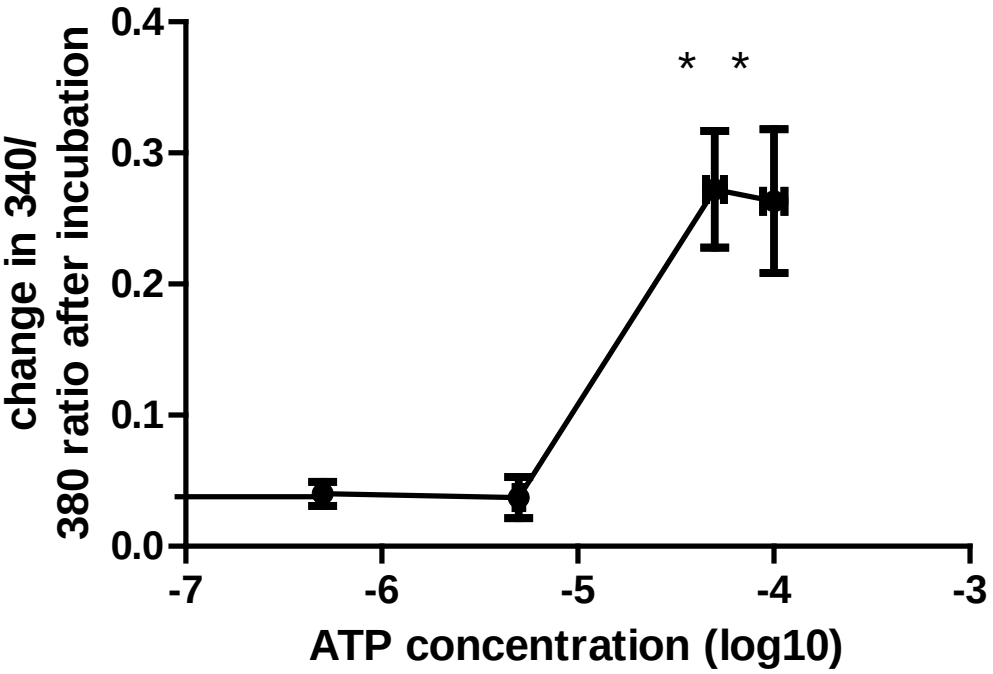
change in 340/
380 ratio after incubation
0.4
0.3
0.2
0.1
0.0
* *
-7
-6
-5
-4
-3
ATP concentration (log10)

**B**

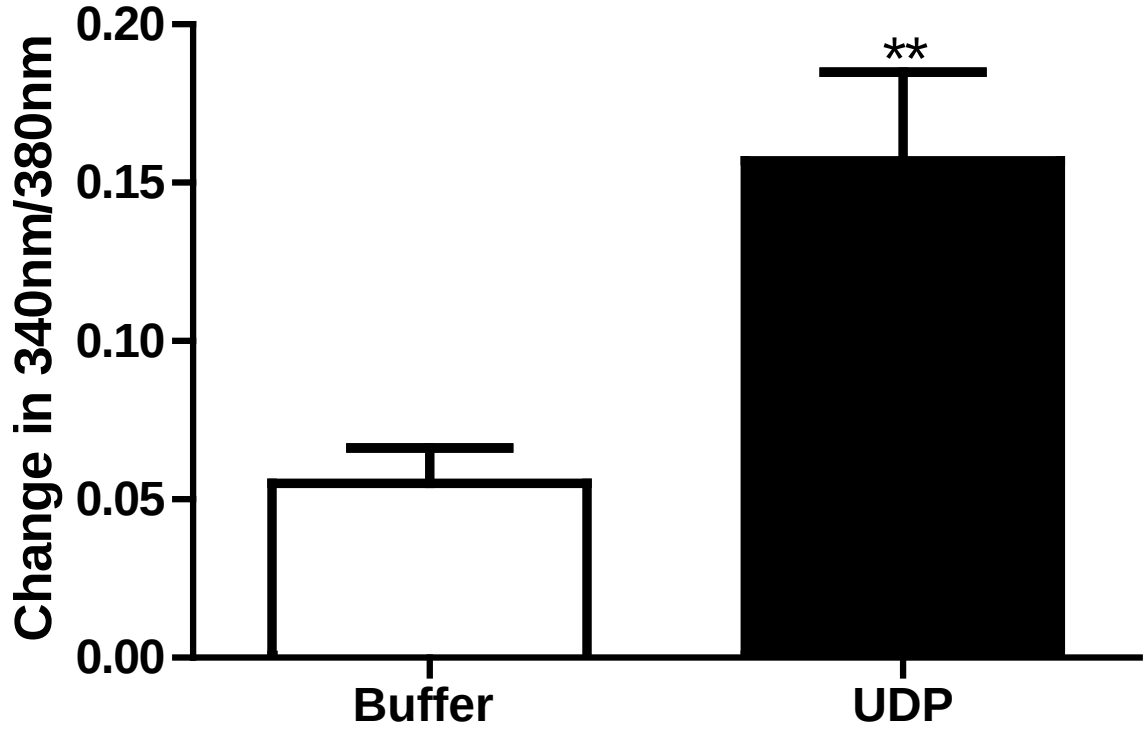
Change in 340nm/380nm
0.20
0.15
0.10
0.05
0.00
**
Buffer
UDP

**Fig. 7.5** : Increase in baseline flueroscence ratio in cells treated with buffer, ATP and UDP (100µM) for 1 hour. In Panel A the ATP dose-response curve shows the sustained calcium increase induced by various concentrations of ATP. ATP at 50µM (0.272 0.045, n=7) and 100 µM (0.263 ± 0.055, n=5) but not at 0.5µM ( 0.04 ± 0.009, n=5) and 5µM (0.037 ± 0.016, n=4), induced sustained increases in calcium after one hour incubation. One-way ANOVA with Dunn's multiple comparison post hoc test indicates significant difference (* indicates $P<0.05$, one way ANOVA with Dunns multiple comparison post-hoc test) as compared to control cells. Panel B shows increased baseline fluorescence ratio (basal calcium level) at 1 hour after cells were treated with buffer or UDP (100 µM) (** indicates $P<0.001$, t-test)

**Fig. 7.6 :**

A

(i) t=0 min

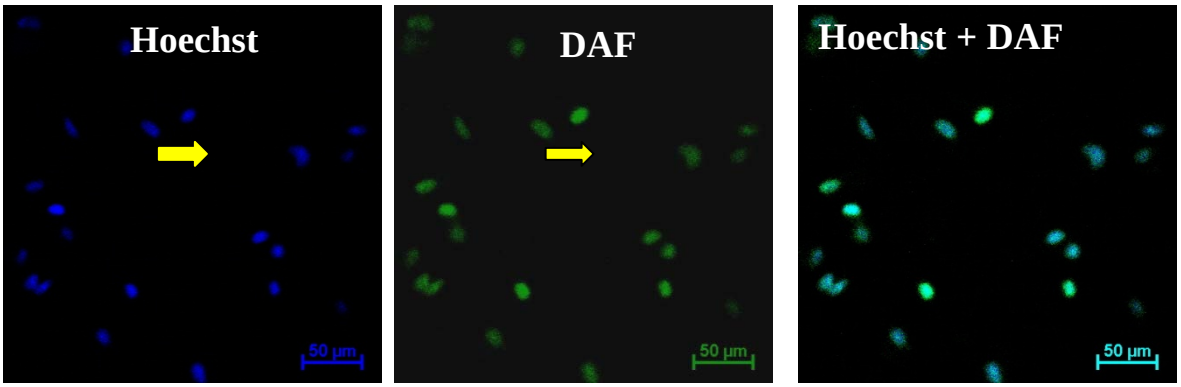


(ii) t=60 min

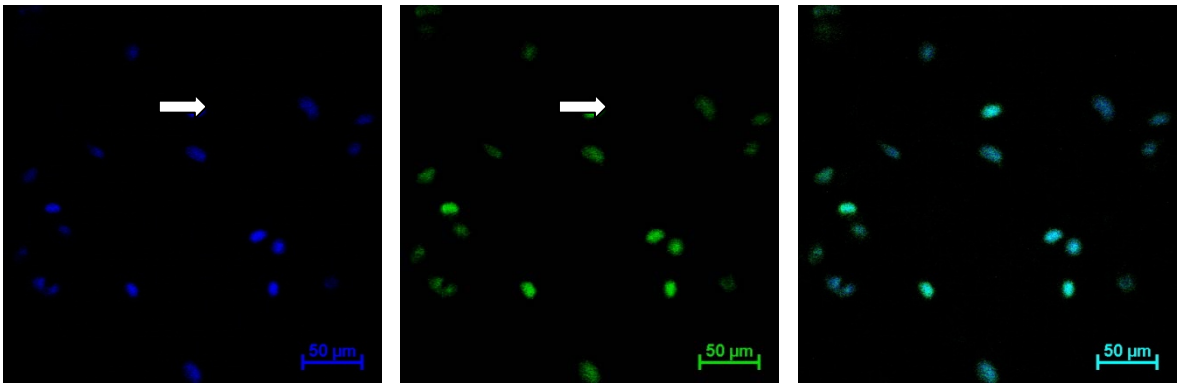


B Merged Image of Hoechst dye time t=60 min and DAF dye t=0 min.

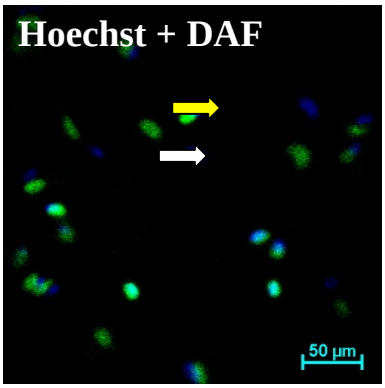

**Fig. 7.6 :** Measurement of microglial motility upon ATP-50μM treatment. Panel A shows Hoechst dye stained microglial nuclei and entire cell marked with DAF dye at (i) time 0 min and (ii) time 60 min. Panel B shows a merged image of Hoechst dye stained microglial nuclei at time 60 min and the whole cell marked with DAF dye at time 0 min. Note the displacement of the cell over one hour. Scale bar = 50μm.

**Fig. 7.7 :**

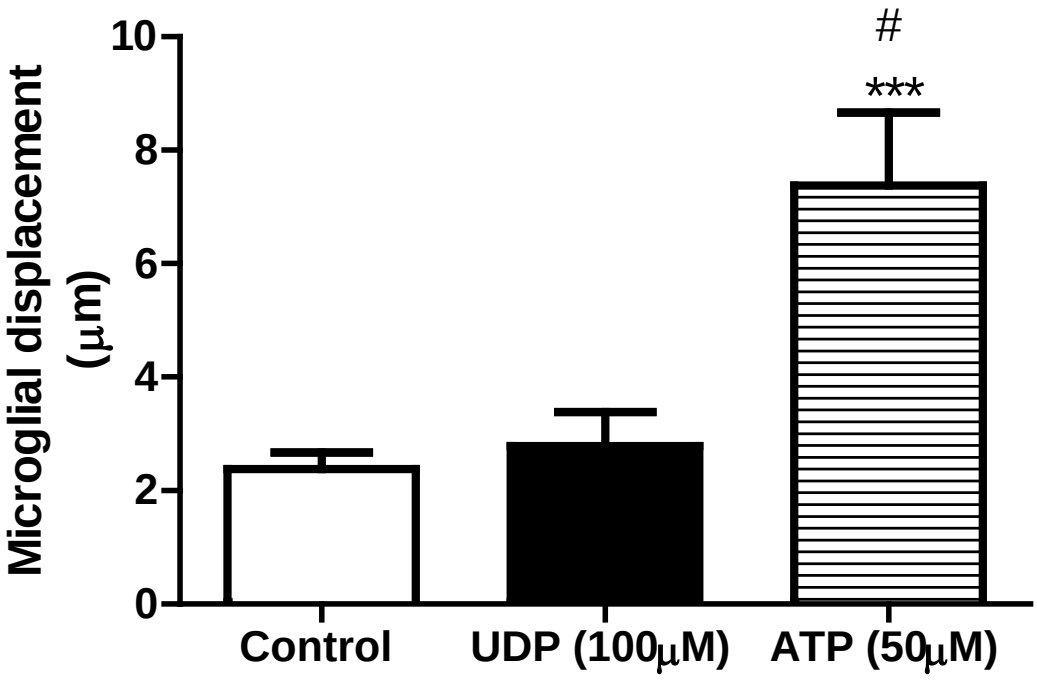
Microglial displacement (μm)
10
8
6
4
2
0
#
***
Control
UDP (100μM)
ATP (50μM)

**Fig. 7.7 :** Effect of ATP (50µM) and UDP (100µM) treatment on microglial displacement in 1 hour *in vitro*. One way ANOVA and Bonferroni post hoc tests comparing all the columns was performed; *** indicates P<0.001 compared to control and # indicates P< 0.05 compared to UDP.

**Fig. 7.8 :**

**A**

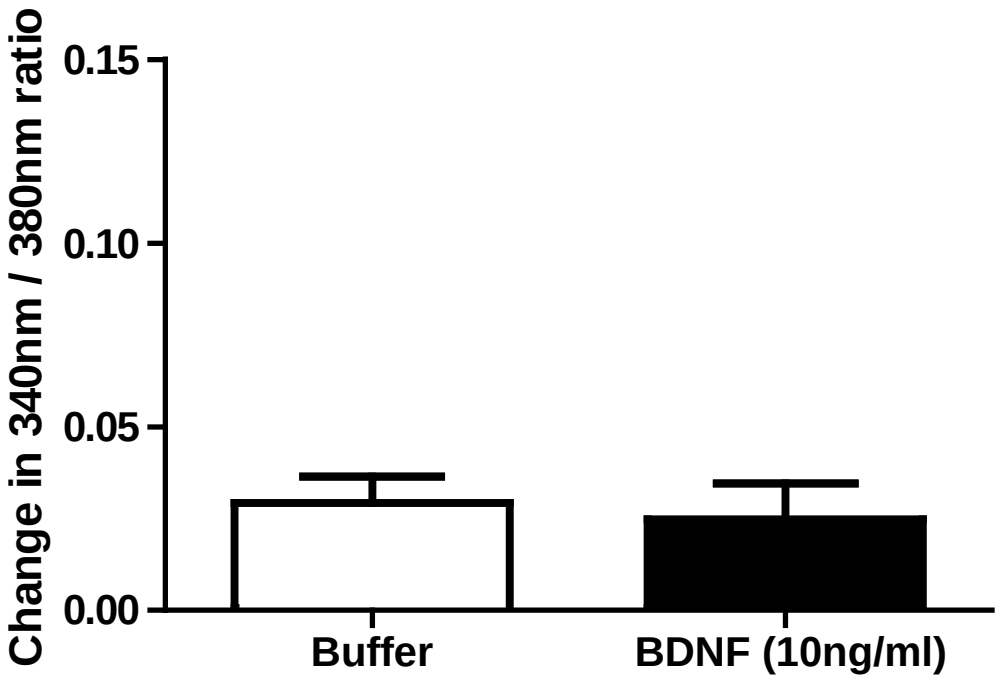
Change in 340nm / 380nm ratio
0.15
0.10
0.05
0.00
Buffer
BDNF (10ng/ml)

**B**

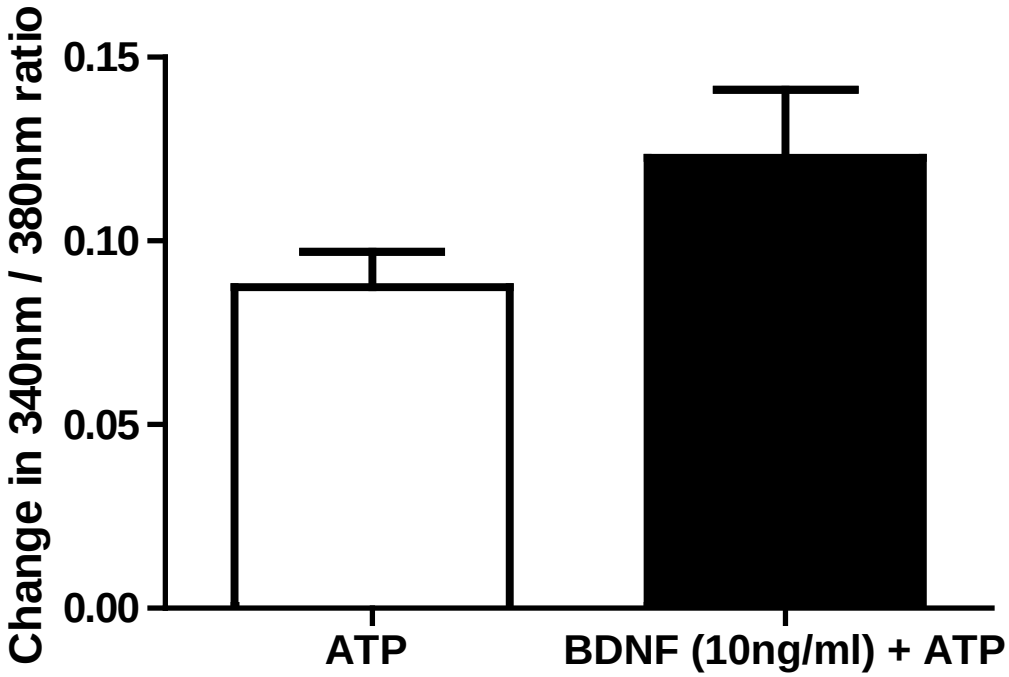
Change in 340nm / 380nm ratio
0.15
0.10
0.05
0.00
ATP
BDNF (10ng/ml) + ATP

**Fig. 7.8 :** Effect of BDNF on microglial responsiveness to ATP 50 µM (30 s application). Panel A shows the change in basal intracellular $Ca^{2+}$ after a 15 min treatement with BDNF (10ng/ml, N=17) or buffer only (N=12) (unpaired t test showed no significant difference, P=0.7389). Panel B shows the transient change in baseline in response to ATP 50 µM (N=12, 30 min) and ATP 50 µM in BDNF (10ng/ml,N=12, 30 min) pre-treated cells (t-test showed no significant difference P=0.0758). The data are derived from 3 independent experiments performed for each treatment group**.**

## *Discussion*

Changes in $Ca^{2+}$ concentration are the most immediate response to activation of both metabotropic and ionotropic receptors in microglia. A major finding of this study is that, while increased intracellular $Ca^{2+}$ may precipitate in some but not in all the effects of purines on microglial function. The specific findings of this study are as follows. (i) Microglia respond to brief exposure to ATP and UDP by showing a transient increase in $[Ca^{2+}]i$. The amplitude of this transient calcium response depends on the initial basal intracellular $Ca^{2+}$ level. (ii) Longer-term (one hour) treatment with ATP and UDP causes a significant increase in basal $[Ca^{2+}]i$. (iii) ATP causes a significant increase in microglial motility in culture as compared to buffer-treated control cells, but UDP does not. (iv) BDNF did not cause either an increase in $[Ca^{2+}]i$ or modulate microglial responsiveness to ATP in our experiments.

Our results suggests microglia with different initial baseline $[Ca^{2+}]i$ respond differently to ATP (50μM) and UDP (100μM) applications. They clearly show that cells with lower baseline produce larger responses to both ATP and UDP, while cells with relatively higher initial baselines respond less. The correlation between the absolute peak $[Ca^{2+}]i$ response and the initial $[Ca^{2+}]i$ in ATP-treated cells but not in the UDP-treated cells is probably explained by these nucleotides acting on different purinergic receptors. As discussed above, ATP 50 μM activates mainly ionotropic receptors P2X4 and metabotropic receptors P2Y12 on microglia, while UDP activates only the metabotropic P2Y6 receptor. Thus, ATP can induce $Ca^{2+}$ entry from the extracellular medium as well as release of $Ca^{2+}$ from intracellular stores. UDP can induce only release of calcium from intracellular stores, although store-operated entry may also occur (Targos et al. 2005). This may be a factor limiting the ability of UDP to raise intracellular $[Ca^{2+}]i$ above a certain level within a short time.

We found that the one-hour treatment with both ATP and UDP caused a significantly higher increase in intracellular calcium (Fig. 7.4 (A), 7.4 (B), 7.5 (A) & 7.5 (B)) as compared to buffer alone. These results indicate that activation of ionotropic receptors may not be necessary to cause long-term increases in basal intracellular $[Ca^{2+}]i$ levels in microglia. They also suggest that $Ca^{2+}$ release from intracellular stores may be sufficient to activate microglia. Interestingly, various studies have reported up-regulation of purinergic receptors upon microglial activation (Bianco et al. 2005; Kobayashi et al. 2008; Tsuda et al. 2003). Surprisingly, our results showing less rise in intracellular $[Ca^{2+}]i$ in microglia with higher initial basal $[Ca^{2+}]i$ suggest that either there is no correlation between up-regulation of receptors and microglial responsiveness, or we could not observe any effect due to already high initial basal calcium levels. Clearly, the role of these up-regulated receptors in the functioning of activated microglia is still not clear and requires further investigation.

Although both ATP and UDP had similar effects on intracellular $[Ca^{2+}]i$, ATP (50μM) but not UDP (100μM) induced motility in isolated microglia as compared to control cells treated with buffer only (Fig. 7.6 (A), 7.6 (B) & 7.7). This suggests that intracellular $[Ca^{2+}]i$ may be required but not sufficient to induce motility of microglia. Our results are in agreement with previous *in vitro* and *in vivo* studies (Davalos et al. 2005; Honda et al. 2001; Miller & Stella 2009; Nimmerjahn et al. 2005; Wu et al. 2007) reporting ATP-induced motility of microglia and suggesting that ATP is a potent chemoattractant in the CNS. A study of microglia has reported involvement of P2X4 and P2Y12 receptors in ATP-induced chemotaxis (Ohsawa et al. 2007) while UDP does not activate P2X4 and P2Y12 receptor types. These studies measured microglial movement towards the source of ATP, while we are reporting increased random movement in culture, but our conclusions are similar. Our results are consistent with the previous report of Koizumi et al. (2007), which suggested that UDP acts as a phagocytosis signal and does not induce chemotaxic movement in microglia. This study also suggested that dying neurons release ATP as a “find me” signal and that UDP acts

as a signal to induce phagocytosis in microglia. Since both ATP and UDP increased [Ca2+]i, a sustained global $Ca^{2+}$ increase is clearly not sufficient to activate the microglial phagocytosis function.

BDNF is a member of the neurotrophin family and increases survival and growth of neurons under normal conditions. In our experiments, BDNF did not increase intracellular $Ca^{2+}$ in microglia (Fig. 7.8 (A)). This is contradictory to the previous report of Mizoguchi et al. (2009), wherein the authors demonstrated an increased $Ca^{2+}$ level in BDNF-treated microglia that was dose-dependent. However, this study did not show the effect of the vehicle itself on microglial $Ca^{2+}$ levels (Mizoguchi et al. 2009). The reason for these disparate results is not known, but the cells used in our study had relatively higher initial baselines which may have made them less responsive to BDNF. Our study also shows that BDNF pretreatment does not have any modulatory effect on microglial responsiveness to ATP (Fig. 7.8.1 (B)). This suggests that the intracellular pathways activated by the BDNF may be different from those activated by ATP.

In summary, our observations suggest that microglia exist in different activation states in culture as defined by their different basal calcium levels. We also found a clear correlation between microglial responsiveness and initial intracellular $[Ca^{2+}]i$, suggesting the activation state of microglia affects their responsiveness to nucleotides. Surprisingly, we are first to report that long-term treatment with ATP and UDP causes an increase in basal $Ca^{2+}$ levels in microglia. Our results suggest that activation of ionotropic receptors is not necessary to cause long-term increase in microglial intracellular basal $[Ca^{2+}]i$ levels. Our results also suggest that microglial $[Ca^{2+}]i$ is increased by many stimuli, but is not the sole determinant of the functional state of microglia.

# Chapter 8: Thesis Conclusion and Future Directions

In this thesis, I have investigated the activation of microglia in several metabolic and cardiovascular diseases. After determining the brain regions showing microglial activation, I also attempted to investigate the role that microglial activation may play in these disease conditions. The novel findings of this thesis are as follows. (i) Microglia were activated in the PVN of rats with myocardial infarction. The activation was specific to the PVN and no activation was observed in other hypothalamic cardiovascular centres in these rats. (ii) Microglia were also activated in the PVN of STZ-induced diabetic rats. Within the PVN, microglia were activated in the parvocellular as well as in the magnocellular subdivisions. (iii) In STZ-induced diabetic rats, microglia were also activated in the SON and NTS regions. (iv) Activated microglia injected into the PVN caused a marked increase in systolic blood pressure in normal rats. (v) In high fat fed rats, microglia were activated in the VHM/Arculate region, but not in the PVN, SON or NTS. (vi) In Zucker Obese and LCR rats, microglia were not activated in the PVN, NTS, SON or VHM/Arculate hypothalamus. (vii) Both ATP and UDP caused sustained increase in microglial intracellular basal $Ca^{2+}$. ATP but not UDP induced motility in microglia.

Elevated sympathetic nerve activity contributes to the pathology of heart failure following myocardial infarction. Many studies of rats with myocardial infarction have reported increased activity of PVN neurons. My results show activation of microglia predominantly in the PVN, which is involved in regulation of sympathetic nerve activity (chapter 2). These results suggest that activated microglia in the PVN contribute to the increased activity of PVN parvocellular neurons. Microglia may modulate activity of these PVN neurons via secretion of a variety of pro-inflammatory cytokines, reactive oxygen species, neurotrophin and superoxide, which then leads to increased sympathetic drive. A

recently published study has demonstrated increased mean arterial pressure in rats with IL-1β injected into the PVN (Shi et al. 2010a). Many other studies have also suggested that cytokine action on the PVN itself is sufficient to elevate sympathetic nerve activity. Recent animal studies have shown increased levels of proinflammatory cytokines and ROS in the PVN after myocardial infarction (Guggilam et al. 2007; Infanger et al. 2010; Lindley et al. 2004). These studies have suggested the damaged heart or neurons as a source of cytokines and ROS. My report is the first to demonstrate microglial activation in the PVN in rats with heart failure. Hence, I hypothesise that cytokines and ROS produced locally by activated microglia in the PVN are responsible for elevated sympathetic drive and contribute to the pathology of heart failure following myocardial infarction. A recent study has provided supporting evidence for this hypothesis by demonstrating that increased redox signalling in the PVN of rats with myocardial infarction actually causes cardiac damage (Infanger et al. 2010) rather than vice versa.

It is now well known that elevated sympathetic drive occurs in diabetes and may contribute to the development of diabetic cardiovascular complications. My results, showing microglial activation in the PVN of STZ-induced diabetic rats (chapter 3), suggest activated microglia contribute to the reported elevated sympathetic drive in this rat model (Patel et al. 2011). I observed significant microglial activation in the parvocellular as well as in the magnocellular subdivision in STZ-induced diabetic rats. Interestingly, I also observed a significant increase in neuronal activity in the PVN. The neuronal activation was also present in both the parvocellular and magnocellular subdivisions in STZ-induced diabetic rats. Activation in the magnocellular subdivision could be due to the increased plasma osmolarity in STZ-induced diabetic rats, which is also suggested by the neuronal activation observed in the SON region that contains a similar neuronal population. Neuronal activation appeared to precede microglial activation, suggesting that excitotoxic neuronal death is the cause of microglial activation in magnocellular subdivision of the PVN. Microglial activation in the

parvocellular subdivision of the PVN may be a common cause of the elevated sympathetic drive reported in both STZ-induced diabetic rats and rats with myocardial infarction. Therefore, I speculate that microglial activation in the PVN could be a reason for the increased risk of developing cardiovascular complications in diabetic humans.

It is not clear from these studies (chapters 2 and 3) whether microglial activation is involved in the pathology of the cardiovascular complications in STZ-induced diabetic rats or in rats with myocardial infarction, or whether it is a consequence of these pathologies. My study showing increased systolic blood pressure in naïve rats with activated microglia injected in the PVN (chapter 5) suggests a pathological role for microglial activation. The PVN controls the level of sympathetic nerve activity, and activation of the PVN can increase sympathetic tone. Enhanced sympathetic tone can cause an increase in blood pressure. My results showing increased blood pressure in normal rats upon activated microglial injection into the PVN suggest that microglial activation in the PVN can enhance sympathetic tone. However, further study is required to demonstrate inhibition of elevated sympathetic drive in STZ-induced diabetic rats and in rats with myocardial infarction upon inhibition of activated microglia in the PVN.

The cause of microglial activation in rats with myocardial infarction is not clear and requires further investigation, but my results regarding STZ-induced diabetic rats suggest that intense and prolonged neuronal activation or excitotoxicity may cause microglial activation in the PVN. Previous studies of MI rats have also reported neuronal activation in the PVN. Hence, even in the case of MI rats, excitotoxicity may be the cause of microglial activation. I did not observe microglial activation in the PVN in models of type 2 diabetes showing mild hyperglycaemia (chapter 4). Hence, overt diabetes may be necessary for the reported neuronal and microglial activation in the PVN.

Interestingly, I have reported activation of microglia in the arcuate and ventromedial hypothalamus regions of rats fed a high fat diet (chapter 4). Fat feeding is known to increase plasma leptin levels in humans as well as in rodents. I did not observe microglial activation in those brain regions in leptin receptor-deficient Zucker Obese rats, suggesting a role for leptin in microglial activation. Microglia express receptors for leptin, and the activation of leptin receptors on cultured microglia stimulates IL-1β release. Thus, microglial activation may result from a direct action of leptin on microglia. Alternatively, over-excitation of arcuate and ventromedial hypothalamic neurons may lead to activation of microglia. Further studies are needed to differentiate between these two mechanisms. The arcuate and ventromedial hypothalamus are major sites for leptin action in the brain and many studies of high fat fed animals have reported reduced neuronal sensitivity for leptin. My results showing microglial activation in the arcuate and ventromedial hypothalamus suggest that microglial activation could be the cause of reduced neuronal leptin sensitivity. However, further studies are required to investigate the role of activated microglia in the arcuate and ventromedial hypothalamus nucleus of fat fed rats.

The fact that the pattern of microglial activation is different in each disease condition examined suggests that the initiating cause of microglial activation must be different. My results argue against the idea that increased circulating cytokine levels are responsible for the activation, since elevated plasma cytokines are seen in rats with heart failure and in STZ-induced diabetic rats. This does not preclude a general strategy to inhibit microglia being useful in these conditions.

Excitotoxic neuronal death is expected to release various nucleotides. Microglia express a variety of purinergic receptors. To understand the molecular mechanism of microglial activation, I looked at the regulation of the microglial purinergic P2X4 receptors and the intracellular activation marker, phosphorylated p38 MAPK in microglia in STZ-

induced diabetic rats. Studies of neuropathic pain models have reported marked up-regulation of P2X4 receptors and phosphorylated p38 MAPK in microglia and inhibition of either of these has been shown to reduce pain behaviour. In STZ-induced diabetic rats, I did not observe any marked change in the expression of P2X4 receptors or the levels of phosphorylated p38 MAPK in activated microglia, which were present in brain nuclei important for the regulation of the cardiovascular system. Hence, it appears that the mechanism of microglial activation in STZ-induced diabetic rats may differ from that occurring in the spinal cord after peripheral nerve injury. Involvement of P2X7 and/or P2Y12 receptors has also been reported in nerve injury models and investigation is required to determine whether these receptors are involved in microglial activation in STZ-induced diabetic rats.

*In vitro* studies provide a useful tool for investigating the cellular mechanism of microglial activation. Various studies of microglia have demonstrated an important role for intracellular calcium signalling in microglial activation (chapter 1), but the involvement of intracellular calcium in microglial migration has not been investigated. My present results show that two different nucleotides, ATP and UDP, were capable of causing transient as well as sustained increases in microglial intracellular $Ca^{2+}$. Interestingly, only ATP was able to induce motility in microglia, suggesting that intracellular calcium is an indicator of microglial activation but does not fully define the functional state. ATP is known to act via ionotropic and metabotropic receptors, while UDP has been shown to activate P2Y6, a metabotropic receptor type. This study suggests that activation of receptors other than P2Y6 may be necessary for certain functions of microglia, e.g., motility. Other studies of microglial activation have suggested a role for the P2Y6 receptor in microglial phagocytosis. Therefore, targeting one particular receptor type may have beneficial effects, but may not completely block all the functions of activated microglia. The present study also suggests that

intracellular calcium is required, but is not sufficient to trigger all the functions of activated microglia.

In conclusion, the results presented in this thesis show microglial activation occurs in STZ-induced diabetic rats, high fat fed rats and in rats with myocardial infarction. This microglial activation may be responsible for the cardiovascular and/or metabolic disturbances seen in these diseases. My results suggest that targeting activated microglia may be beneficial to human patients suffering from either diabetes or myocardial infarction. However, further studies are needed to investigate molecular targets for inhibiting microglial activation in these diseases. Therapeutic strategies for inhibiting microglial activation may also be beneficial in treating humans suffering from neurodegenerative diseases and/or from neuropathic pain where microglial activation and its involvement in pathology is already established.

# References


Abbracchio MP, Verderio C. 2006. Pathophysiological roles of P2 receptors in glial cells. *Novartis Found Symp* 276:91-103; discussion -12, 275-81

Accorsi-Mendonca D, Bonagamba LG, Leao RM, Machado BH. 2009. Are L-glutamate and ATP cotransmitters of the peripheral chemoreflex in the rat nucleus tractus solitarius? *Exp Physiol* 94:38-45

Ahren B, Scheurink AJ. 1998. Marked hyperleptinemia after high-fat diet associated with severe glucose intolerance in mice. *Eur J Endocrinol* 139:461-7

Akula A, Kota MK, Gopisetty SG, Chitrapu RV, Kalagara M, et al. 2003. Biochemical, histological and echocardiographic changes during experimental cardiomyopathy in STZ-induced diabetic rats. *Pharmacol Res* 48:429-35

Aloisi F. 2001. Immune function of microglia. *Glia* 36:165-79

Aloisi F, Penna G, Cerase J, Menendez Iglesias B, Adorini L. 1997. IL-12 production by central nervous system microglia is inhibited by astrocytes. *J Immunol* 159:1604-12

Alvarez GE, Beske SD, Ballard TP, Davy KP. 2002. Sympathetic neural activation in visceral obesity. *Circulation* 106:2533-6

Aronne LJ, Brown WV, Isoldi KK. 2007. Cardiovascular disease in obesity: A review of related risk factors and risk-reduction strategies. *Journal of Clinical Lipidology* 1:575-82

Aronson AL. 1980. Pharmacotherapeutics of the newer tetracyclines. *J Am Vet Med Assoc* 176:1061-8

Arundine M, Tymianski M. 2003. Molecular mechanisms of calcium-dependent neurodegeneration in excitotoxicity. *Cell Calcium* 34:325-37

Asami T, Ito T, Fukumitsu H, Nomoto H, Furukawa Y, Furukawa S. 2006. Autocrine activation of cultured macrophages by brain-derived neurotrophic factor. *Biochem Biophys Res Commun* 344:941-7

Ashwell K. 1991. The distribution of microglia and cell death in the fetal rat forebrain. *Brain Res Dev Brain Res* 58:1-12

B.B. Boycott, J.M. Hopkins, Microglia in the retina of monkey and other mammals; Its distinction from other types of glia and horizontal cells, *Neuroscience,* Volume 6(4), 1981, 679-688,

Badoer E. 1998. Neurons in the hypothalamic paraventricular nucleus that project to the rostral ventrolateral medulla are not activated by hypotension. *Brain Res* 801:224-7

Badoer E. 2001. Hypothalamic paraventricular nucleus and cardiovascular regulation. *Clin Exp Pharmacol Physiol* 28:95-9

Badoer E. 2010a. Microglia: activation in acute and chronic inflammatory states and in response to cardiovascular dysfunction. *Int J Biochem Cell Biol* 42:1580-5

Badoer E. 2010b. Role of the hypothalamic PVN in the regulation of renal sympathetic nerve activity and blood flow during hyperthermia and in heart failure. *Am J Physiol Renal Physiol* 298:F839-46

Badoer E, Merolli J. 1998. Neurons in the hypothalamic paraventricular nucleus that project to the rostral ventrolateral medulla are activated by haemorrhage. *Brain Res* 791:317-20

Badoer E, Ng CW, De Matteo R. 2002. Tonic sympathoinhibition arising from the hypothalamic PVN in the conscious rabbit. *Brain Res* 947:17-24

Badoer E, Ng CW, De Matteo R. 2003. Glutamatergic input in the PVN is important in renal nerve response to elevations in osmolality. *Am J Physiol Renal Physiol* 285:F640-50

Baker RA, Herkenham M. 1995. Arcuate nucleus neurons that project to the hypothalamic paraventricular nucleus: neuropeptidergic identity and consequences of adrenalectomy on mRNA levels in the rat. *J Comp Neurol* 358:518-30

Baliga BS, Weinberger J. 2006. Diabetes and stroke: part one--risk factors and pathophysiology. *Current cardiology reports* 8:23-8

Barger SW, Goodwin ME, Porter MM, Beggs ML. 2007. Glutamate release from activated microglia requires the oxidative burst and lipid peroxidation. *J Neurochem* 101:1205-13

Barger SW, Horster D, Furukawa K, Goodman Y, Krieglstein J, Mattson MP. 1995. Tumor necrosis factors alpha and beta protect neurons against amyloid beta-peptide toxicity: evidence for involvement of a kappa B-binding factor and attenuation of peroxide and Ca2+ accumulation. *Proc Natl Acad Sci U S A* 92:9328-32

Barnes MJ, Lapanowski K, Conley A, Rafols JA, Jen KL, Dunbar JC. 2003. High fat feeding is associated with increased blood pressure, sympathetic nerve activity and hypothalamic mu opioid receptors. *Brain Res Bull* 61:511-9

Beckman JS. 1999. Parsing the effects of nitric oxide, S-nitrosothiols, and peroxynitrite on inducible nitric oxide synthase-dependent cardiac myocyte apoptosis. *Circ Res* 85:870-1

Bennett MR. 2001. Reactive oxygen species and death: oxidative DNA damage in atherosclerosis. *Circ Res* 88:648-50

Bernier L. AA, Boue-Grabot E., Seguela P. . 2010. Functional characterization of P2X4 receptor-mediated pore dilation in microglia. *FENS Abstr* 5

Bianco F, Fumagalli M, Pravettoni E, D'Ambrosi N, Volonte C, et al. 2005. Pathophysiological roles of extracellular nucleotides in glial cells: differential expression of purinergic receptors in resting and activated microglia. *Brain Res Brain Res Rev* 48:144-56

Biggs JE, Lu VB, Stebbing MJ, Balasubramanyan S, Smith PA. 2010. Is BDNF sufficient for information transfer between microglia and dorsal horn neurons during the onset of central sensitization? *Mol Pain* 6:44

Black JA, Liu S, Waxman SG. 2009. Sodium channel activity modulates multiple functions in microglia. *Glia* 57:1072-81

Brancho D, Tanaka N, Jaeschke A, Ventura JJ, Kelkar N, et al. 2003. Mechanism of p38 MAP kinase activation in vivo. *Genes Dev* 17:1969-78

Brooks DP, Nutting DF, Crofton JT, Share L. 1989. Vasopressin in rats with genetic and streptozocin-induced diabetes. *Diabetes* 38:54-7

Brosnan CF, Selmaj K, Raine CS. 1988. Hypothesis: a role for tumor necrosis factor in immune-mediated demyelination and its relevance to multiple sclerosis. *J Neuroimmunol* 18:87-94

Brown H, Kozlowski R, Perry H. 1998. The importance of ion channels for macrophage and microglial activation in vitro. *Glia* 22:94-7

Bruce AJ, Boling W, Kindy MS, Peschon J, Kraemer PJ, et al. 1996. Altered neuronal and microglial responses to excitotoxic and ischemic brain injury in mice lacking TNF receptors. *Nat Med* 2:788-94

Brunner-La Rocca HP, Esler MD, Jennings GL, Kaye DM. 2001. Effect of cardiac sympathetic nervous activity on mode of death in congestive heart failure. *Eur Heart J* 22:1136-43

Buttini M, Limonta S, Boddeke HW. 1996. Peripheral administration of lipopolysaccharide induces activation of microglial cells in rat brain. *Neurochem Int* 29:25-35

Campfield LA, Smith FJ, Guisez Y, Devos R, Burn P. 1995. Recombinant mouse OB protein: evidence for a peripheral signal linking adiposity and central neural networks. *Science* 269:546-9

Cao L, Sun X, Shen E. 1996. Nitric oxide stimulates both the basal and reflex release of vasopressin in anesthetized rats. *Neurosci Lett* 221:49-52

Chabot S, Williams G, Hamilton M, Sutherland G, Yong VW. 1999. Mechanisms of IL-10 production in human microglia-T cell interaction. *J Immunol* 162:6819-28

Cham JL, Badoer E. 2008a. Exposure to a hot environment can activate rostral ventrolateral medulla-projecting neurones in the hypothalamic paraventricular nucleus in conscious rats. *Exp Physiol* 93:64-74

Cham JL, Badoer E. 2008b. Hypothalamic paraventricular nucleus is critical for renal vasoconstriction elicited by elevations in body temperature. *Am J Physiol Renal Physiol* 294:F309-15

Cham JL, Owens NC, Barden JA, Lawrence AJ, Badoer E. 2006. P2X purinoceptor subtypes on paraventricular nucleus neurones projecting to the rostral ventrolateral medulla in the rat. *Exp Physiol* 91:403-11

Chan SH, Wang LL, Wang SH, Chan JY. 2001. Differential cardiovascular responses to blockade of nNOS or iNOS in rostral ventrolateral medulla of the rat. *Br J Pharmacol* 133:606-14

Chapman MJ, Sposito AC. 2008. Hypertension and dyslipidaemia in obesity and insulin resistance: Pathophysiology, impact on atherosclerotic disease and pharmacotherapy. *Pharmacology & Therapeutics* 117:354-73

Charlton JA, Thompson CJ, Baylis PH. 1988. Possible mechanisms responsible for the rise in plasma vasopressin associated with diabetic ketoacidosis in the rat. *J Endocrinol* 116:343-8

Chen A, Kumar SM, Sahley CL, Muller KJ. 2000. Nitric oxide influences injury-induced microglial migration and accumulation in the leech CNS. *J Neurosci* 20:1036-43

Chen F, Cham JL, Badoer E. 2010. High-fat feeding alters the cardiovascular role of the hypothalamic paraventricular nucleus. *Am J Physiol Regul Integr Comp Physiol* 298:R799-807

Chen F, Dworak M, Wang Y, Cham JL, Badoer E. 2008a. Role of the hypothalamic PVN in the reflex reduction in mesenteric blood flow elicited by hyperthermia. *Am J Physiol Regul Integr Comp Physiol* 295:R1874-81

Chen HY, Wu JS, Chen JJ, Cheng JT. 2008b. Impaired regulation function in cardiovascular neurons of nucleus tractus solitarii in streptozotocin-induced diabetic rats. *Neurosci Lett* 431:161-6

Cheng B, Christakos S, Mattson MP. 1994. Tumor necrosis factors protect neurons against metabolic-excitotoxic insults and promote maintenance of calcium homeostasis. *Neuron* 12:139-53

Chessell IP, Hatcher JP, Bountra C, Michel AD, Hughes JP, et al. 2005. Disruption of the P2X7 purinoceptor gene abolishes chronic inflammatory and neuropathic pain. *Pain* 114:386-96

Chessell IP, Michel AD, Humphrey PP. 1997. Properties of the pore-forming P2X7 purinoceptor in mouse NTW8 microglial cells. *Br J Pharmacol* 121:1429-37

Chiodera P, Volpi R, Coiro V. 1994. Inhibitory control of nitric oxide on the arginine-vasopressin and oxytocin response to hypoglycaemia in normal men. *Neuroreport* 5:1822-4

Cho HJ, Kim JK, Park HC, Kim DS, Ha SO, Hong HS. 1998. Changes in brain-derived neurotrophic factor immunoreactivity in rat dorsal root ganglia, spinal cord, and gracile nuclei following cut or crush injuries. *Exp Neurol* 154:224-30

Choi SH, Joe EH, Kim SU, Jin BK. 2003. Thrombin-induced microglial activation produces degeneration of nigral dopaminergic neurons in vivo. *J Neurosci* 23:5877-86

Chugani DC, Kedersha NL, Rome LH. 1991. Vault immunofluorescence in the brain: new insights regarding the origin of microglia. *J Neurosci* 11:256-68

Cohen P, Zhao C, Cai X, Montez JM, Rohani SC, et al. 2001. Selective deletion of leptin receptor in neurons leads to obesity. *J Clin Invest* 108:1113-21

Colton CA, Gilbert DL. 1987. Production of superoxide anions by a CNS macrophage, the microglia. *FEBS Lett* 223:284-8

Cone RD. 1999. The Central Melanocortin System and Energy Homeostasis. *Trends in endocrinology and metabolism: TEM* 10:211-6

Coote JH. 2005. A role for the paraventricular nucleus of the hypothalamus in the autonomic control of heart and kidney. *Exp Physiol* 90:169-73

Coppari R, Ichinose M, Lee CE, Pullen AE, Kenny CD, et al. 2005. The hypothalamic arcuate nucleus: a key site for mediating leptin's effects on glucose homeostasis and locomotor activity. *Cell Metab* 1:63-72

Correa F, Hernangomez M, Mestre L, Loria F, Spagnolo A, et al. 2010. Anandamide enhances IL-10 production in activated microglia by targeting CB(2) receptors: roles of ERK1/2, JNK, and NF-kappaB. *Glia* 58:135-47

Coull JA, Beggs S, Boudreau D, Boivin D, Tsuda M, et al. 2005. BDNF from microglia causes the shift in neuronal anion gradient underlying neuropathic pain. *Nature* 438:1017-21

Cowley MA, Smart JL, Rubinstein M, Cerdan MG, Diano S, et al. 2001. Leptin activates anorexigenic POMC neurons through a neural network in the arcuate nucleus. *Nature* 411:480-4

Craner MJ, Damarjian TG, Liu S, Hains BC, Lo AC, et al. 2005. Sodium channels contribute to microglia/macrophage activation and function in EAE and MS. *Glia* 49:220-9

Cuadros MA, Martin C, Coltey P, Almendros A, Navascues J. 1993. First appearance, distribution, and origin of macrophages in the early development of the avian central nervous system. *The Journal of comparative neurology* 330:113-29

Cuadros MA, Navascues J. 1998. The origin and differentiation of microglial cells during development. *Prog Neurobiol* 56:173-89

Dampney RA, Horiuchi J, Killinger S, Sheriff MJ, Tan PS, McDowall LM. 2005. Long-term regulation of arterial blood pressure by hypothalamic nuclei: some critical questions. *Clin Exp Pharmacol Physiol* 32:419-25

Davalos D, Grutzendler J, Yang G, Kim JV, Zuo Y, et al. 2005. ATP mediates rapid microglial response to local brain injury in vivo. *Nat Neurosci* 8:752-8

Davern PJ, Head GA. 2007. Fos-related antigen immunoreactivity after acute and chronic angiotensin II-induced hypertension in the rabbit brain. *Hypertension* 49:1170-7

De Simone R, Niturad CE, De Nuccio C, Ajmone-Cat MA, Visentin S, Minghetti L. 2010. TGF-beta and LPS modulate ADP-induced migration of microglial cells through P2Y1 and P2Y12 receptor expression. *J Neurochem* 115:450-9

del Rio-Hortega PW. 1927. Cerebral cicatrix. The reaction of neuroglia and microglia to brain wounds. *Bull Johns Hopkins Hosp* 41:278–82

del Rio Hortega PW. 1927. Cerebral cicatrix. The reaction of neuroglia and microglia to brain wounds. *Bull Johns Hopkins Hosp* 41:278–82

Di Bello V, Talarico L, Picano E, Di Muro C, Landini L, et al. 1995. Increased echodensity of myocardial wall in the diabetic heart: an ultrasound tissue characterization study. *Journal of the American College of Cardiology* 25:1408-15

Doba N, Reis DJ. 1973. Acute fulminating neurogenic hypertension produced by brainstem lesions in the rat. *Circ Res* 32:584-93

Doba N, Reis DJ. 1974. Role of central and peripheral adrenergic mechanisms in neurogenic hypertension produced by brainstem lesions in rat. *Circulation research* 34:293-301

Doi N, Dutia MB, Russell JA. 1998. Inhibition of rat oxytocin and vasopressin supraoptic nucleus neurons by nociceptin in vitro. *Neuroscience* 84:913-21

Eder C. 1998. Ion channels in microglia (brain macrophages). *Am J Physiol* 275:C327-42

Eder C. 2005. Regulation of microglial behavior by ion channel activity. *J Neurosci Res* 81:314-21

Elkabes S, DiCicco-Bloom EM, Black IB. 1996. Brain microglia/macrophages express neurotrophins that selectively regulate microglial proliferation and function. *J Neurosci* 16:2508-21

Elmquist JK, Flier JS. 2004. Neuroscience. The fat-brain axis enters a new dimension. *Science* 304:63-4

Esler M, Straznicky N, Eikelis N, Masuo K, Lambert G, Lambert E. 2006. Mechanisms of sympathetic activation in obesity-related hypertension. *Hypertension* 48:787-96

Estevez AG, Radi R, Barbeito L, Shin JT, Thompson JA, Beckman JS. 1995. Peroxynitrite-induced cytotoxicity in PC12 cells: evidence for an apoptotic mechanism differentially modulated by neurotrophic factors. *J Neurochem* 65:1543-50

Eun SY, Hong YH, Kim EH, Jeon H, Suh YH, et al. 2004. Glutamate receptor-mediated regulation of c-fos expression in cultured microglia. *Biochem Biophys Res Commun* 325:320-7

Fabricio AS, Tringali G, Pozzoli G, Melo MC, Vercesi JA, et al. 2006. Interleukin-1 mediates endothelin-1-induced fever and prostaglandin production in the preoptic area of rats. *Am J Physiol Regul Integr Comp Physiol* 290:R1515-23

Fagan SC, Edwards DJ, Borlongan CV, Xu L, Arora A, et al. 2004. Optimal delivery of minocycline to the brain: implication for human studies of acute neuroprotection. *Experimental Neurology* 186:248-51

Fan LW, Pang Y, Lin S, Rhodes PG, Cai Z. 2005a. Minocycline attenuates lipopolysaccharide-induced white matter injury in the neonatal rat brain. *Neuroscience* 133:159-68

Fan LW, Pang Y, Lin S, Tien LT, Ma T, et al. 2005b. Minocycline reduces lipopolysaccharide-induced neurological dysfunction and brain injury in the neonatal rat. *J Neurosci Res* 82:71-82

Farber K, Kettenmann H. 2006. Functional role of calcium signals for microglial function. *Glia* 54:656-65

Felder RB, Francis J, Zhang ZH, Wei SG, Weiss RM, Johnson AK. 2003. Heart failure and the brain: new perspectives. *Am J Physiol Regul Integr Comp Physiol* 284:R259-76

Ferrari D, Chiozzi P, Falzoni S, Dal Susino M, Collo G, et al. 1997a. ATP-mediated cytotoxicity in microglial cells. *Neuropharmacology* 36:1295-301

Ferrari D, Chiozzi P, Falzoni S, Hanau S, Di Virgilio F. 1997b. Purinergic modulation of interleukin-1 beta release from microglial cells stimulated with bacterial endotoxin. *J Exp Med* 185:579-82

Ferraro S, Fazio S, Santomauro M, Cianfrani M, Mossetti G, et al. 1990. Cardiac function and sympathetic activity in young diabetics. *Diabetes research and clinical practice* 8:91-9

Fillit H, Ding WH, Buee L, Kalman J, Altstiel L, et al. 1991. Elevated circulating tumor necrosis factor levels in Alzheimer's disease. *Neurosci Lett* 129:318-20

Fischer HG, Eder C, Hadding U, Heinemann U. 1995. Cytokine-dependent K+ channel profile of microglia at immunologically defined functional states. *Neuroscience* 64:183-91

Fischer W, Krugel U. 2007. P2Y receptors: focus on structural, pharmacological and functional aspects in the brain. *Curr Med Chem* 14:2429-55

Flak JN, Ostrander MM, Tasker JG, Herman JP. 2009. Chronic stress-induced neurotransmitter plasticity in the PVN. *J Comp Neurol* 517:156-65

Flaris NA, Densmore TL, Molleston MC, Hickey WF. 1993. Characterization of microglia and macrophages in the central nervous system of rats: definition of the differential expression of molecules using standard and novel monoclonal antibodies in normal CNS and in four models of parenchymal reaction. *Glia* 7:34-40

Flugel A, Bradl M, Kreutzberg GW, Graeber MB. 2001. Transformation of donor-derived bone marrow precursors into host microglia during autoimmune CNS inflammation and during the retrograde response to axotomy. *J Neurosci Res* 66:74-82

Fordyce CB, Jagasia R, Zhu X, Schlichter LC. 2005. Microglia Kv1.3 channels contribute to their ability to kill neurons. *J Neurosci* 25:7139-49

Francis J, Chu Y, Johnson AK, Weiss RM, Felder RB. 2004a. Acute myocardial infarction induces hypothalamic cytokine synthesis. *Am J Physiol Heart Circ Physiol* 286:H2264-71

Francis J, Zhang ZH, Weiss RM, Felder RB. 2004b. Neural regulation of the proinflammatory cytokine response to acute myocardial infarction. *Am J Physiol Heart Circ Physiol* 287:H791-7

Fraser GE, Luke R, Thompson S, Smith H, Carter S, Sharpe N. 1995. Comparison of echocardiographic variables between type I diabetics and normal controls. *The American journal of cardiology* 75:141-5

Frenkel D, Huang Z, Maron R, Koldzic DN, Moskowitz MA, Weiner HL. 2005. Neuroprotection by IL-10-producing MOG CD4+ T cells following ischemic stroke. *Journal of the neurological sciences* 233:125-32

Friedman JM, Halaas JL. 1998. Leptin and the regulation of body weight in mammals. *Nature* 395:763-70

Frucht DM, Fukao T, Bogdan C, Schindler H, O'Shea JJ, Koyasu S. 2001. IFN-gamma production by antigen-presenting cells: mechanisms emerge. *Trends Immunol* 22:556-60

Garcia MC, Wernstedt I, Berndtsson A, Enge M, Bell M, et al. 2006. Mature-onset obesity in interleukin-1 receptor I knockout mice. *Diabetes* 55:1205-13

Gary DS, Bruce-Keller AJ, Kindy MS, Mattson MP. 1998. Ischemic and excitotoxic brain injury is enhanced in mice lacking the p55 tumor necrosis factor receptor. *J Cereb Blood Flow Metab* 18:1283-7

Gehrmann J. 1996. Microglia: a sensor to threats in the nervous system? *Research in virology* 147:79-88

Gehrmann J, Matsumoto Y, Kreutzberg GW. 1995. Microglia: intrinsic immuneffector cell of the brain. *Brain research* 20:269-87

Geiss LS HW, Smith PJ. 1995. Mortality in non-insulin-dependent diabetes. *In: National Diabetes Data Group, eds. Diabetes in America. 2nd ed.Bethesda, Md: National Institutes of Health, National Institute of Diabetes and Digestive and Kidney Diseases*

Giordana MT, Attanasio A, Cavalla P, Migheli A, Vigliani MC, Schiffer D. 1994. Reactive cell proliferation and microglia following injury to the rat brain. *Neuropathol Appl Neurobiol* 20:163-74

Giuliani F, Hader W, Yong VW. 2005. Minocycline attenuates T cell and microglia activity to impair cytokine production in T cell-microglia interaction. *J Leukoc Biol* 78:135-43

Gonzalez JC, Egea J, Del Carmen Godino M, Fernandez-Gomez FJ, Sanchez-Prieto J, et al. 2007. Neuroprotectant minocycline depresses glutamatergic neurotransmission and Ca(2+) signalling in hippocampal neurons. *Eur J Neurosci* 26:2481-95

Gorba T, Klostermann O, Wahle P. 1999. Development of neuronal activity and activity-dependent expression of brain-derived neurotrophic factor mRNA in organotypic cultures of rat visual cortex. *Cereb Cortex* 9:864-77

Gouty S, Regalia J, Helke CJ. 2001. Attenuation of the afferent limb of the baroreceptor reflex in streptozotocin-induced diabetic rats. *Auton Neurosci* 89:86-95

Graeber MB. 2010. Changing face of microglia. *Science* 330:783-8

Griffin WS, Mrak RE. 2002. Interleukin-1 in the genesis and progression of and risk for development of neuronal degeneration in Alzheimer's disease. *J Leukoc Biol* 72:233-8

Grundy SM, Benjamin IJ, Burke GL, Chait A, Eckel RH, et al. 1999. Diabetes and cardiovascular disease: a statement for healthcare professionals from the American Heart Association. *Circulation* 100:1134-46

Guasti L, Richardson D, Jhaveri M, Eldeeb K, Barrett D, et al. 2009. Minocycline treatment inhibits microglial activation and alters spinal levels of endocannabinoids in a rat model of neuropathic pain. *Mol Pain* 5:35

Guggilam A, Haque M, Kerut EK, McIlwain E, Lucchesi P, et al. 2007. TNF-alpha blockade decreases oxidative stress in the paraventricular nucleus and attenuates sympathoexcitation in heart failure rats. *Am J Physiol Heart Circ Physiol* 293:H599-609

Guo W, Sun J, Xu X, Bunstock G, He C, Xiang Z. 2009. P2X receptors are differentially expressed on vasopressin- and oxytocin-containing neurons in the supraoptic and paraventricular nuclei of rat hypothalamus. *Histochem Cell Biol* 131:29-41

Hagino Y, Kariura Y, Manago Y, Amano T, Wang B, et al. 2004. Heterogeneity and potentiation of AMPA type of glutamate receptors in rat cultured microglia. *Glia* 47:68-77

Hakansson ML, Brown H, Ghilardi N, Skoda RC, Meister B. 1998. Leptin receptor immunoreactivity in chemically defined target neurons of the hypothalamus. *J Neurosci* 18:559-72

Halaas JL, Boozer C, Blair-West J, Fidahusein N, Denton DA, Friedman JM. 1997. Physiological response to long-term peripheral and central leptin infusion in lean and obese mice. *Proceedings of the National Academy of Sciences of the United States of America* 94:8878-83

Halaas JL, Gajiwala KS, Maffei M, Cohen SL, Chait BT, et al. 1995. Weight-reducing effects of the plasma protein encoded by the obese gene. *Science* 269:543-6

Halliwell B. 2001. Role of free radicals in the neurodegenerative diseases: therapeutic implications for antioxidant treatment. *Drugs & aging* 18:685-716

Hasking GJ, Esler MD, Jennings GL, Burton D, Johns JA, Korner PI. 1986. Norepinephrine spillover to plasma in patients with congestive heart failure: evidence of increased overall and cardiorenal sympathetic nervous activity. *Circulation* 73:615-21

Hathway GJ, Vega-Avelaira D, Moss A, Ingram R, Fitzgerald M. 2009. Brief, low frequency stimulation of rat peripheral C-fibres evokes prolonged microglial-induced central sensitization in adults but not in neonates. *Pain* 144:110-8

Havel PJ, Uriu-Hare JY, Liu T, Stanhope KL, Stern JS, et al. 1998. Marked and rapid decreases of circulating leptin in streptozotocin diabetic rats: reversal by insulin. *Am J Physiol* 274:R1482-91

Haynes SE, Hollopeter G, Yang G, Kurpius D, Dailey ME, et al. 2006. The P2Y12 receptor regulates microglial activation by extracellular nucleotides. *Nat Neurosci* 9:1512-9

Hebden RA, Bennett T, Gardiner SM. 1987. Abnormal blood pressure recovery during ganglion blockade in diabetic rats. *Am J Physiol* 252:R102-8

Helwig B, Musch T, Craig R, Kenney M. 2007. Increased interleukin-6 receptor expression in the paraventricular nucleus of
rats with heart failure. *American Journal of Physiology Regulatory Integrative Comparative Physiology* 292:R1165-R73

Henderson LM, Chappell JB, Jones OT. 1988. Internal pH changes associated with the activity of NADPH oxidase of human neutrophils. Further evidence for the presence of an H+ conducting channel. *Biochem J* 251:563-7

Henry CJ, Huang Y, Wynne A, Hanke M, Himler J, et al. 2008. Minocycline attenuates lipopolysaccharide (LPS)-induced neuroinflammation, sickness behavior, and anhedonia. *J Neuroinflammation* 5:15

Hickey WF, Kimura H. 1988. Perivascular microglial cells of the CNS are bone marrow-derived and present antigen in vivo. *Science* 239:290-2

Hide I. 2003. [Mechanism of production and release of tumor necrosis factor implicated in inflammatory diseases]. *Nippon Yakurigaku Zasshi* 121:163-73

Hide I, Tanaka M, Inoue A, Nakajima K, Kohsaka S, et al. 2000. Extracellular ATP triggers tumor necrosis factor-alpha release from rat microglia. *J Neurochem* 75:965-72

Hintz KK, Aberle NS, Ren J. 2003. Insulin resistance induces hyperleptinemia, cardiac contractile dysfunction but not cardiac leptin resistance in ventricular myocytes. *Int J Obes Relat Metab Disord* 27:1196-203

Hoffmann A, Kann O, Ohlemeyer C, Hanisch UK, Kettenmann H. 2003. Elevation of basal intracellular calcium as a central element in the activation of brain macrophages (microglia): suppression of receptor-evoked calcium signaling and control of release function. *J Neurosci* 23:4410-9

Honda S, Kohsaka S. 2001. [Regulation of microglial cell function by ATP]. *Nihon Shinkei Seishin Yakurigaku Zasshi* 21:89-93

Honda S, Sasaki Y, Ohsawa K, Imai Y, Nakamura Y, et al. 2001. Extracellular ATP or ADP induce chemotaxis of cultured microglia through Gi/o-coupled P2Y receptors. *J Neurosci* 21:1975-82

Hopkins PN, Hunt SC, Wu LL, Williams GH, Williams RR. 1996. Hypertension, dyslipidemia, and insulin resistance: links in a chain or spokes on a wheel? *Current opinion in lipidology* 7:241-53

Huggett RJ, Burns J, Mackintosh AF, Mary DA. 2004. Sympathetic neural activation in nondiabetic metabolic syndrome and its further augmentation by hypertension. *Hypertension* 44:847-52

Hunt SA, Abraham WT, Chin MH, Feldman AM, Francis GS, et al. 2005. ACC/AHA 2005 Guideline Update for the Diagnosis and Management of Chronic Heart Failure in the Adult: A Report of the American College of Cardiology/American Heart Association Task Force on Practice Guidelines (Writing Committee to Update the 2001 Guidelines for the Evaluation and Management of Heart Failure): Developed in Collaboration With the American College of Chest Physicians and the International Society for Heart and Lung Transplantation: Endorsed by the Heart Rhythm Society. *Circulation* 112:e154-235

Hynd MR, Scott HL, Dodd PR. 2004. Glutamate-mediated excitotoxicity and neurodegeneration in Alzheimer's disease. *Neurochem Int* 45:583-95

Ibrahim N, Bosch MA, Smart JL, Qiu J, Rubinstein M, et al. 2003. Hypothalamic proopiomelanocortin neurons are glucose responsive and express K(ATP) channels. *Endocrinology* 144:1331-40

Ifuku M, Farber K, Okuno Y, Yamakawa Y, Miyamoto T, et al. 2007. Bradykinin-induced microglial migration mediated by B1-bradykinin receptors depends on Ca2+ influx via reverse-mode activity of the Na+/Ca2+ exchanger. *J Neurosci* 27:13065-73

Illes P, Nieber K, Frohlich R, Norenberg W. 1996. P2 purinoceptors and pyrimidinoceptors of catecholamine-producing cells and immunocytes. *Ciba Found Symp* 198:110-25; discussion 25-9

Imamura K, Ito M, Suzumura A, Asai J, Takahashi A. 1990. Generation and characterization of monoclonal antibodies against rat microglia and ontogenic distribution of positive cells. *Lab Invest* 63:853-61

Infanger DW, Cao X, Butler SD, Burmeister MA, Zhou Y, et al. 2010. Silencing nox4 in the paraventricular nucleus improves myocardial infarction-induced cardiac dysfunction by attenuating sympathoexcitation and periinfarct apoptosis. *Circ Res* 106:1763-74

Inoue K. 2006a. ATP receptors of microglia involved in pain. *Novartis Found Symp* 276:263-72; discussion 73-81

Inoue K. 2006b. The function of microglia through purinergic receptors: neuropathic pain and cytokine release. *Pharmacol Ther* 109:210-26

Inoue K. 2006c. The function of microglia through purinergic receptors: Neuropathic pain and cytokine release. *Pharmacology & Therapeutics* 109:210-26

Inoue K. 2008. Purinergic systems in microglia. *Cell Mol Life Sci* 65:3074-80

Inoue K, Koizumi S, Kataoka A, Tozaki-Saitoh H, Tsuda M. 2009. P2Y(6)-Evoked Microglial Phagocytosis. *Int Rev Neurobiol* 85:159-63

Inoue K, Tsuda M. 2009. Microglia and neuropathic pain. *Glia* 57:1469-79

Irikura VM, Lagraoui M, Hirsh D. 2002. The epistatic interrelationships of IL-1, IL-1 receptor antagonist, and the type I IL-1 receptor. *J Immunol* 169:393-8

James G, Butt AM. 2002. P2Y and P2X purinoceptor mediated Ca2+ signalling in glial cell pathology in the central nervous system. *Eur J Pharmacol* 447:247-60

Jantaratnotai N, Choi HB, McLarnon JG. 2009. ATP stimulates chemokine production via a store-operated calcium entry pathway in C6 glioma cells. *BMC Cancer* 9:442

Ji RR. 2010. Targeting microglial purinergic signaling to improve morphine analgesia. *Pain* 150:377-8

Ji RR, Gereau RWt, Malcangio M, Strichartz GR. 2009. MAP kinase and pain. *Brain Res Rev* 60:135-48

Ji RR, Suter MR. 2007. p38 MAPK, microglial signaling, and neuropathic pain. *Mol Pain* 3:33

Jiang XH, Yu GD, Yin QZ. 1991. [Involvement of solitary tract nucleus in analgesic effect produced by paraventricular nucleus stimulation]. *Sheng Li Xue Bao* 43:120-7

Jouven X, Lemaitre RN, Rea TD, Sotoodehnia N, Empana JP, Siscovick DS. 2005. Diabetes, glucose level, and risk of sudden cardiac death. *Eur Heart J* 26:2142-7

Kadowaki K, Kishimoto J, Leng G, Emson PC. 1994. Up-regulation of nitric oxide synthase (NOS) gene expression together with NOS activity in the rat hypothalamo-hypophysial system after chronic salt loading: evidence of a neuromodulatory role of nitric oxide in arginine vasopressin and oxytocin secretion. *Endocrinology* 134:1011-7

Kalra SP, Dube MG, Pu S, Xu B, Horvath TL, Kalra PS. 1999. Interacting appetite-regulating pathways in the hypothalamic regulation of body weight. *Endocrine reviews* 20:68-100

Kanbar R, Stornetta RL, Cash DR, Lewis SJ, Guyenet PG. 2010. Photostimulation of Phox2b medullary neurons activates cardiorespiratory function in conscious rats. *Am J Respir Crit Care Med* 182:1184-94

Kang YM, Zhang ZH, Xue B, Weiss RM, Felder RB. 2008. Inhibition of brain proinflammatory cytokine synthesis reduces hypothalamic excitation in rats with ischemia-induced heart failure. *Am J Physiol Heart Circ Physiol* 295:H227-36

Kannan H, Hayashida Y, Yamashita H. 1989. Increase in sympathetic outflow by paraventricular nucleus stimulation in awake rats. *Am J Physiol* 256:R1325-30

Kaur C, Hao AJ, Wu CH, Ling EA. 2001. Origin of microglia. *Microsc Res Tech* 54:2-9

Kawabe T, Chitravanshi VC, Kawabe K, Sapru HN. 2008. Cardiovascular function of a glutamatergic projection from the hypothalamic paraventricular nucleus to the nucleus tractus solitarius in the rat. *Neuroscience* 153:605-17

Kawashima H, Saito T, Yoshizato H, Fujikawa T, Sato Y, et al. 2004. Endurance treadmill training in rats alters CRH activity in the hypothalamic paraventricular nucleus at rest and during acute running according to its period. *Life Sci* 76:763-74

Kaye DM, Lefkovits J, Jennings GL, Bergin P, Broughton A, Esler MD. 1995. Adverse consequences of high sympathetic nervous activity in the failing heart. *J.Am.Coll.Cardiol.* 26:1257-63

Kettenmann H, Hoppe D, Gottmann K, Banati R, Kreutzberg G. 1990. Cultured microglial cells have a distinct pattern of membrane channels different from peritoneal macrophages. *J Neurosci Res* 26:278-87

Khanna R, Roy L, Zhu X, Schlichter LC. 2001. K+ channels and the microglial respiratory burst. *American journal of physiology* 280:C796-806

Kim B, Jeong HK, Kim JH, Lee SY, Jou I, Joe EH. 2011. Uridine 5'-Diphosphate Induces Chemokine Expression in Microglia and Astrocytes through Activation of the P2Y6 Receptor. *J Immunol* 186:3701-9

Kim KY, Kim MY, Choi HS, Jin BK, Kim SU, Lee YB. 2002. Thrombin induces IL-10 production in microglia as a negative feedback regulator of TNF-alpha release. *Neuroreport* 13:849-52

Kim SY, Moon JH, Lee HG, Kim SU, Lee YB. 2007. ATP released from beta-amyloid-stimulated microglia induces reactive oxygen species production in an autocrine fashion. *Exp Mol Med* 39:820-7

Kim WG, Mohney RP, Wilson B, Jeohn GH, Liu B, Hong JS. 2000. Regional difference in susceptibility to lipopolysaccharide-induced neurotoxicity in the rat brain: role of microglia. *J Neurosci* 20:6309-16

King KA, Mackie G, Pang CC, Wall RA. 1985. Central vasopressin in the modulation of catecholamine release in conscious rats. *Can J Physiol Pharmacol* 63:1501-5

Kishi T, Hirooka Y, Sakai K, Shigematsu H, Shimokawa H, Takeshita A. 2001. Overexpression of eNOS in the RVLM causes hypotension and bradycardia via GABA release. *Hypertension* 38:896-901

Klein JP, Hains BC, Craner MJ, Black JA, Waxman SG. 2004. Apoptosis of vasopressinergic hypothalamic neurons in chronic diabetes mellitus. *Neurobiol Dis* 15:221-8

Kobayashi K, Yamanaka H, Fukuoka T, Dai Y, Obata K, Noguchi K. 2008. P2Y12 receptor upregulation in activated microglia is a gateway of p38 signaling and neuropathic pain. *J Neurosci* 28:2892-902

Koch LG, Britton SL. 2001. Artificial selection for intrinsic aerobic endurance running capacity in rats. *Physiol Genomics* 5:45-52

Koizumi S, Shigemoto-Mogami Y, Nasu-Tada K, Shinozaki Y, Ohsawa K, et al. 2007. UDP acting at P2Y6 receptors is a mediator of microglial phagocytosis. *Nature* 446:1091-5

Koles L, Furst S, Illes P. 2005. P2X and P2Y receptors as possible targets of therapeutic manipulations in CNS illnesses. *Drug News Perspect* 18:85-101

Kompa AR, See F, Lewis DA, Adrahtas A, Cantwell DM, et al. 2008. Long-term but not short-term p38 MAPK inhibition improves cardiac function and reduces cardiac remodeling post-MI. *Journal of Pharmacology and Experimental Therapeutics* 325:741-50

Kotecha SA, Schlichter LC. 1999. A Kv1.5 to Kv1.3 switch in endogenous hippocampal microglia and a role in proliferation. *J Neurosci* 19:10680-93

Kowalski TJ, Liu SM, Leibel RL, Chua SC, Jr. 2001. Transgenic complementation of leptin-receptor deficiency. I. Rescue of the obesity/diabetes phenotype of LEPR-null mice expressing a LEPR-B transgene. *Diabetes* 50:425-35

Krady JK, Basu A, Allen CM, Xu Y, LaNoue KF, et al. 2005. Minocycline reduces proinflammatory cytokine expression, microglial activation, and caspase-3 activation in a rodent model of diabetic retinopathy. *Diabetes* 54:1559-65

Krall WJ, Challita PM, Perlmutter LS, Skelton DC, Kohn DB. 1994. Cells expressing human glucocerebrosidase from a retroviral vector repopulate macrophages and central nervous system microglia after murine bone marrow transplantation. *Blood* 83:2737-48

Kreutzberg GW. 1995. Microglia, the first line of defence in brain pathologies. *Arzneimittel-Forschung* 45:357-60

Krukoff TL, Mactavish D, Jhamandas JH. 1997. Activation by hypotension of neurons in the hypothalamic paraventricular nucleus that project to the brainstem. *J Comp Neurol* 385:285-96

Krukoff TL, Patel KP. 1990. Alterations in brain hexokinase activity associated with streptozotocin-induced diabetes mellitus in the rat. *Brain Res* 522:157-60

Kubo T, Kihara M. 1986. Contribution of vasopressin to hypertension caused by baroreceptor denervation and nucleus tractus solitarius lesions in rats. *J Pharmacobiodyn* 9:626-9

Kurtz TW, Morris RC, Pershadsingh HA. 1989. The Zucker fatty rat as a genetic model of obesity and hypertension. *Hypertension* 13:896-901

Lamounier-Zepter V, Ehrhart-Bornstein M, Bornstein SR. 2006. Insulin resistance in hypertension and cardiovascular disease. *Best Practice & Research Clinical Endocrinology & Metabolism* 20:355-67

Langosch JM, Gebicke-Haerter PJ, Norenberg W, Illes P. 1994. Characterization and transduction mechanisms of purinoceptors in activated rat microglia. *Br J Pharmacol* 113:29-34

Lee GH, Proenca R, Montez JM, Carroll KM, Darvishzadeh JG, et al. 1996. Abnormal splicing of the leptin receptor in diabetic mice. *Nature* 379:632-5

Lee SM, Yune TY, Kim SJ, Kim YC, Oh YJ, et al. 2004. Minocycline inhibits apoptotic cell death via attenuation of TNF-alpha expression following iNOS/NO induction by lipopolysaccharide in neuron/glia co-cultures. *J Neurochem* 91:568-78

Leo CH, Joshi A, Woodman OL. 2010. Short-term type 1 diabetes alters the mechanism of endothelium-dependent relaxation in the rat carotid artery. *Am J Physiol Heart Circ Physiol* 299:H502-11

Lessard SJ, Rivas DA, Chen ZP, van Denderen BJ, Watt MJ, et al. 2009. Impaired skeletal muscle beta-adrenergic activation and lipolysis are associated with whole-body insulin resistance in rats bred for low intrinsic exercise capacity. *Endocrinology* 150:4883-91

Lessard SJ, Rivas DA, Stephenson EJ, Yaspelkis BB, 3rd, Koch LG, et al. 2011. Exercise training reverses impaired skeletal muscle metabolism induced by artificial selection for low aerobic capacity. *Am J Physiol Regul Integr Comp Physiol* 300:R175-82

Levin BE, Dunn-Meynell AA. 2002. Reduced central leptin sensitivity in rats with diet-induced obesity. *Am J Physiol Regul Integr Comp Physiol* 283:R941-8

Levin SG, Godukhin OV. 2007. Protective effects of interleukin-10 on the development of epileptiform activity evoked by transient episodes of hypoxia in rat hippocampal slices. *Neuroscience and behavioral physiology* 37:467-70

Levine B, Kalman J, Mayer L, Fillit HM, Packer M. 1990. Elevated circulating levels of tumor necrosis factor in severe chronic heart failure. *N Engl J Med* 323:236-41

Li F, Lu J, Wu CY, Kaur C, Sivakumar V, et al. 2008. Expression of Kv1.2 in microglia and its putative roles in modulating production of proinflammatory cytokines and reactive oxygen species. *J Neurochem* 106:2093-105

Li J, Baud O, Vartanian T, Volpe JJ, Rosenberg PA. 2005. Peroxynitrite generated by inducible nitric oxide synthase and NADPH oxidase mediates microglial toxicity to oligodendrocytes. *Proc Natl Acad Sci U S A* 102:9936-41

Li Y, Liu L, Kang J, Sheng JG, Barger SW, et al. 2000. Neuronal-glial interactions mediated by interleukin-1 enhance neuronal acetylcholinesterase activity and mRNA expression. *J Neurosci* 20:149-55

Light AR, Wu Y, Hughen RW, Guthrie PB. 2006. Purinergic receptors activating rapid intracellular Ca increases in microglia. *Neuron Glia Biol* 2:125-38

Lincoln J, Loesch A, Burnstock G. 1989. The hypothalamo-neurohypophysial system in streptozotocin-diabetic rats. Ultrastructural evidence for neuronal alterations in the supraoptic and paraventricular nuclei and in the neurohypophysis. *Journal fur Hirnforschung* 30:425-35

Lindley TE, Doobay MF, Sharma RV, Davisson RL. 2004. Superoxide is involved in the central nervous system activation and sympathoexcitation of myocardial infarction-induced heart failure. *Circ Res* 94:402-9

Liposits Z, Paull WK. 1989. Association of dopaminergic fibers with corticotropin releasing hormone (CRH)-synthesizing neurons in the paraventricular nucleus of the rat hypothalamus. *Histochemistry* 93:119-27

Liu B. 2006. Modulation of microglial pro-inflammatory and neurotoxic activity for the treatment of Parkinson's disease. *The AAPS journal* 8:E606-21

Liu GJ, Kalous A, Werry EL, Bennett MR. 2006. Purine release from spinal cord microglia after elevation of calcium by glutamate. *Mol Pharmacol* 70:851-9

Lloyd-Jones D, Adams RJ, Brown TM, Carnethon M, Dai S, et al. 2010. Heart Disease and Stroke Statistics--2010 Update: A Report From the American Heart Association. *Circulation* 121:e46-215

Lu B, Chow A. 1999. Neurotrophins and hippocampal synaptic transmission and plasticity. *J Neurosci Res* 58:76-87

Lu B, Figurov A. 1997. Role of neurotrophins in synapse development and plasticity. *Rev Neurosci* 8:1-12

Lu B, Martinowich K. 2008. Cell biology of BDNF and its relevance to schizophrenia. *Novartis Found Symp* 289:119-29; discussion 29-35, 93-5

Lu VB, Biggs JE, Stebbing MJ, Balasubramanyan S, Todd KG, et al. 2009a. Brain-derived neurotrophic factor drives the changes in excitatory synaptic transmission in the rat superficial dorsal horn that follow sciatic nerve injury. *J Physiol* 587:1013-32

Lu VB, Biggs JE, Stebbing MJ, Balasubramanyan S, Todd KG, et al. 2009b. Brain-derived neurotrophic factor drives the changes in excitatory synaptic transmission in the rat superficial dorsal horn that follow sciatic nerve injury. *J Physiol* 587:1013-32

Luchsinger JA, Tang MX, Stern Y, Shea S, Mayeux R. 2001. Diabetes mellitus and risk of Alzheimer's disease and dementia with stroke in a multiethnic cohort. *American journal of epidemiology* 154:635-41

Luheshi GN, Gardner JD, Rushforth DA, Loudon AS, Rothwell NJ. 1999. Leptin actions on food intake and body temperature are mediated by IL-1. *Proc Natl Acad Sci U S A* 96:7047-52

Luo J, Quan J, Tsai J, Hobensack CK, Sullivan C, et al. 1998. Nongenetic mouse models of non-insulin-dependent diabetes mellitus. *Metabolism* 47:663-8

Machado BH, Mauad H, Chianca Junior DA, Haibara AS, Colombari E. 1997. Autonomic processing of the cardiovascular reflexes in the nucleus tractus solitarii. *Braz J Med Biol Res* 30:533-43

Maeda K, Tsutamoto T, Wada A, Mabuchi N, Hayashi M, et al. 2000. High levels of plasma brain natriuretic peptide and interleukin-6 after optimized treatment for heart failure are independent risk factors for morbidity and mortality in patients with congestive heart failure. *J Am Coll Cardiol* 36:1587-93

Maffei M, Fei H, Lee GH, Dani C, Leroy P, et al. 1995. Increased expression in adipocytes of ob RNA in mice with lesions of the hypothalamus and with mutations at the db locus. *Proc Natl Acad Sci U S A* 92:6957-60

Makimattila S, Schlenzka A, Mantysaari M, Bergholm R, Summanen P, et al. 2000. Predictors of abnormal cardiovascular autonomic function measured by frequence domain analysis of heart rate variability and conventional tests in patients with type 1 diabetes. *Diabetes care* 23:1686-93

Mander PK, Jekabsone A, Brown GC. 2006. Microglia proliferation is regulated by hydrogen peroxide from NADPH oxidase. *J Immunol* 176:1046-52

Mann DL. 1999a. Mechanisms and models in heart failure: A combinatorial approach. *Circulation* 100:999-1008

Mann DL. 1999b. Mechanisms and models in heart failure: A combinatorial approach. . *Circulation* 100:999-1008

Marco P, Sola RG, Ramon y Cajal S, DeFelipe J. 1997. Loss of inhibitory synapses on the soma and axon initial segment of pyramidal cells in human epileptic peritumoural neocortex: implications for epilepsy. *Brain Res Bull* 44:47-66

Marsh SA, Powell PC, Agarwal A, Dell'Italia LJ, Chatham JC. 2007. Cardiovascular dysfunction in Zucker obese and Zucker diabetic fatty rats: role of hydronephrosis. *Am J Physiol Heart Circ Physiol* 293:H292-8

Martin DS, Haywood JR. 1992. Sympathetic nervous system activation by glutamate injections into the paraventricular nucleus. *Brain Res* 577:261-7

Maslinska D, Laure-Kamionowska M, Kaliszek A. 1998. Morphological forms and localization of microglial cells in the developing human cerebellum. *Folia Neuropathol* 36:145-51

Matsuki T, Horai R, Sudo K, Iwakura Y. 2003. IL-1 plays an important role in lipid metabolism by regulating insulin levels under physiological conditions. *J Exp Med* 198:877-88

Matsumoto Y, Fujiwara M. 1987. Absence of donor-type major histocompatibility complex class I antigen-bearing microglia in the rat central nervous system of radiation bone marrow chimeras. *Journal of neuroimmunology* 17:71-82

Myers MG Jr**. 2004,** Leptin receptor signaling **and the** regulation **of** mammalian physiology**.** *Recent Prog Horm Res.* **59:287-304.**

McGaraughty S, Chu KL, Namovic MT, Donnelly-Roberts DL, Harris RR, et al. 2007. P2X7-related modulation of pathological nociception in rats. *Neuroscience* 146:1817-28

McNamara CA, Sarembock IJ, Gimple LW, Fenton JW, 2nd, Coughlin SR, Owens GK. 1993. Thrombin stimulates proliferation of cultured rat aortic smooth muscle cells by a proteolytically activated receptor. *J Clin Invest* 91:94-8

Mihm MJ, Seifert JL, Coyle CM, Bauer JA. 2001. Diabetes related cardiomyopathy time dependent echocardiographic evaluation in an experimental rat model. *Life Sci* 69:527-42

Millan MH, Millan MJ, Herz A. 1984. The hypothalamic paraventricular nucleus: relationship to brain and pituitary pools of vasopressin and oxytocin as compared to dynorphin, beta-endorphin and related opioid peptides in the rat. *Neuroendocrinology* 38:108-16

Miller AM, Stella N. 2009. Microglial cell migration stimulated by ATP and C5a involve distinct molecular mechanisms: quantification of migration by a novel near-infrared method. *Glia* 57:875-83

Milligan CE, Cunningham TJ, Levitt P. 1991. Differential immunochemical markers reveal the normal distribution of brain macrophages and microglia in the developing rat brain. *J Comp Neurol* 314:125-35

Miskowiak B. 1976. [Histochemical studies of the 3rd ventricle tanocytes in the region of the nucleus arcuatus in rat hypothalamus]. *Endokrynol Pol* 27:319-25

Mizoguchi Y, Ishibashi H, Nabekura J. 2003a. The action of BDNF on GABA(A) currents changes from potentiating to suppressing during maturation of rat hippocampal CA1 pyramidal neurons. *J Physiol* 548:703-9

Mizoguchi Y, Kanematsu T, Hirata M, Nabekura J. 2003b. A rapid increase in the total number of cell surface functional GABAA receptors induced by brain-derived neurotrophic factor in rat visual cortex. *J Biol Chem* 278:44097-102

Mizoguchi Y, Kitamura A, Wake H, Ishibashi H, Watanabe M, et al. 2006. BDNF occludes GABA receptor-mediated inhibition of GABA release in rat hippocampal CA1 pyramidal neurons. *Eur J Neurosci* 24:2135-44

Mizoguchi Y, Monji A, Kato T, Seki Y, Gotoh L, et al. 2009. Brain-derived neurotrophic factor induces sustained elevation of intracellular Ca2+ in rodent microglia. *J Immunol* 183:7778-86

Mizuno T, Kawanokuchi J, Numata K, Suzumura A. 2003. Production and neuroprotective functions of fractalkine in the central nervous system. *Brain Res* 979:65-70

Mizuno T, Sawada M, Suzumura A, Marunouchi T. 1994. Expression of cytokines during glial differentiation. *Brain Res* 656:141-46

MohanKumar SM, MohanKumar PS. 2005. Systemic Interleukin-1beta stimulates the simultaneous release of norepinephrine in the paraventricular nucleus and the median eminence. *Brain Res Bull* 65:451-6

Moller T, Kann O, Verkhratsky A, Kettenmann H. 2000. Activation of mouse microglial cells affects P2 receptor signaling. *Brain research* 853:49-59

Montero-Menei CN, Sindji L, Garcion E, Mege M, Couez D, et al. 1996. Early events of the inflammatory reaction induced in rat brain by lipopolysaccharide intracerebral injection: relative contribution of peripheral monocytes and activated microglia. *Brain Res* 724:55-66

Moore KW, O'Garra A, de Waal Malefyt R, Vieira P, Mosmann TR. 1993. Interleukin-10. *Annual review of immunology* 11:165-90

Moos F, Freund-Mercier MJ, Guerne Y, Guerne JM, Stoeckel ME, Richard P. 1984. Release of oxytocin and vasopressin by magnocellular nuclei in vitro: specific facilitatory effect of oxytocin on its own release. *J Endocrinol* 102:63-72

Morgan DA, Anderson EA, Mark AL. 1995. Renal sympathetic nerve activity is increased in obese Zucker rats. *Hypertension* 25:834-8

Morigiwa K, Fukuda Y, Yamashita M. 2000. [Neurotransmitter ATP and cytokine release]. *Nippon Yakurigaku Zasshi* 115:185-92

Mrak RE, Sheng JG, Griffin WS. 1995. Glial cytokines in Alzheimer's disease: review and pathogenic implications. *Human pathology* 26:816-23

Nagamori K, Ishibashi M, Shiraishi T, Oomura Y, Sasaki K. 2003. Effects of leptin on hypothalamic arcuate neurons in Wistar and Zucker rats: an in vitro study. *Experimental biology and medicine (Maywood, N.J* 228:1162-7

Naito M, Umeda S, Yamamoto T, Moriyama H, Umezu H, et al. 1996. Development, differentiation, and phenotypic heterogeneity of murine tissue macrophages. *J Leukoc Biol* 59:133-8

Nakai M, Tanimukai S, Yagi K, Saito N, Taniguchi T, et al. 2001. Amyloid beta protein activates PKC-delta and induces translocation of myristoylated alanine-rich C kinase substrate (MARCKS) in microglia. *Neurochem Int* 38:593-600

Nakajima K, Hamanoue,M, Shimojo, M, Takei, N, Kohsaka, S. 1989. Characterization of microglia isolated from a primary culture of embryonic rat brain by a simplified method. *Biomedical Research* 10

Nakajima K, Kikuchi Y, Ikoma E, Honda S, Ishikawa M, et al. 1998. Neurotrophins regulate the function of cultured microglia. *Glia* 24:272-89

Nakajima K, Kohsaka S. 1993. Functional roles of microglia in the brain. *Neurosci Res* 17:187-203

Nakajima K, Kohsaka S. 2001. Microglia: activation and their significance in the central nervous system. *Journal of biochemistry* 130:169-75

Nakajima K, Tohyama Y, Kohsaka S, Kurihara T. 2004. Protein kinase C alpha requirement in the activation of p38 mitogen-activated protein kinase, which is linked to the induction of tumor necrosis factor alpha in lipopolysaccharide-stimulated microglia. *Neurochem Int* 44:205-14

Natah SS, Mouihate A, Pittman QJ, Sharkey K. 2005. Disruption of the blood brain barrier during TNBS colitis. *Neurogastroenterology and Motility* 17:433-46

Nikodemova M, Watters JJ, Jackson SJ, Yang SK, Duncan ID. 2007. Minocycline down-regulates MHC II expression in microglia and macrophages through inhibition of IRF-1 and protein kinase C (PKC)alpha/betaII. *J Biol Chem* 282:15208-16

Nimmerjahn A, Kirchhoff F, Helmchen F. 2005. Resting microglial cells are highly dynamic surveillants of brain parenchyma in vivo. *Science (New York, N.Y* 308:1314-8

Niu G, Liao Z, Cai L, Wei R, Sun L. 2008. The combined effects of celecoxib and minocycline hydrochloride on inhibiting the osseous metastasis of breast cancer in nude mice. *Cancer Biother Radiopharm* 23:469-76

Noda M, Nakanishi H, Nabekura J, Akaike N. 2000. AMPA-kainate subtypes of glutamate receptor in rat cerebral microglia. *J Neurosci* 20:251-8

Noland RC, Thyfault JP, Henes ST, Whitfield BR, Woodlief TL, et al. 2007. Artificial selection for high-capacity endurance running is protective against high-fat diet-induced insulin resistance. *Am J Physiol Endocrinol Metab* 293:E31-41

Norenberg W, Appel K, Bauer J, Gebicke-Haerter PJ, Illes P. 1993. Expression of an outwardly rectifying K+ channel in rat microglia cultivated on teflon. *Neurosci Lett* 160:69-72

Norenberg W, Gebicke-Haerter PJ, Illes P. 1992. Inflammatory stimuli induce a new K+ outward current in cultured rat microglia. *Neurosci Lett* 147:171-4

Norenberg W, Langosch JM, Gebicke-Haerter PJ, Illes P. 1994. Characterization and possible function of adenosine 5'-triphosphate receptors in activated rat microglia. *Br J Pharmacol* 111:942-50

North RA, Surprenant A. 2000. Pharmacology of cloned P2X receptors. *Annu Rev Pharmacol Toxicol* 40:563-80

Nutile-McMenemy N, Elfenbein A, Deleo JA. 2007. Minocycline decreases in vitro microglial motility, beta1-integrin, and Kv1.3 channel expression. *J Neurochem* 103:2035-46

Oakes ND, Cooney GJ, Camilleri S, Chisholm DJ, Kraegen EW. 1997. Mechanisms of liver and muscle insulin resistance induced by chronic high-fat feeding. *Diabetes* 46:1768-74

Oehmichen M, Wietholter H, Greaves MF. 1979. Immunological analysis of human microglia: lack of monocytic and lymphoid membrane differentiation antigens. *J Neuropathol Exp Neurol* 38:99-103

Ogata T, Chuai M, Morino T, Yamamoto H, Nakamura Y, Schubert P. 2003. Adenosine triphosphate inhibits cytokine release from lipopolysaccharide-activated microglia via P2y receptors. *Brain Res* 981:174-83

Ohana L, Newell EW, Stanley EF, Schlichter LC. 2009. The Ca2+ release-activated Ca2+ current (I(CRAC)) mediates store-operated Ca2+ entry in rat microglia. *Channels (Austin)* 3:129-39

Ohsawa K, Irino Y, Nakamura Y, Akazawa C, Inoue K, Kohsaka S. 2007. Involvement of P2X4 and P2Y12 receptors in ATP-induced microglial chemotaxis. *Glia* 55:604-16

Ohsawa K, Irino Y, Sanagi T, Nakamura Y, Suzuki E, et al. 2010. P2Y12 receptor-mediated integrin-beta1 activation regulates microglial process extension induced by ATP. *Glia* 58:790-801

Oltman CL, Richou LL, Davidson EP, Coppey LJ, Lund DD, Yorek MA. 2006. Progression of coronary and mesenteric vascular dysfunction in Zucker obese and Zucker diabetic fatty rats. *Am J Physiol Heart Circ Physiol* 291:H1780-7

Opal SM, Wherry JC, Grint P. 1998. Interleukin-10: potential benefits and possible risks in clinical infectious diseases. *Clin Infect Dis* 27:1497-507

Orr AG, Orr AL, Li XJ, Gross RE, Traynelis SF. 2009. Adenosine A(2A) receptor mediates microglial process retraction. *Nat Neurosci* 12:872-8

Orus J, Roig E, Perez-Villa F, Pare C, Azqueta M, et al. 2000. Prognostic value of serum cytokines in patients with congestive heart failure. *J Heart Lung Transplant* 19:419-25

Ota M, Crofton JT, Festavan G, Share L. 1992. Central carbachol stimulates vasopressin release into interstitial fluid adjacent to the paraventricular nucleus. *Brain Res* 592:249-54

Ozolins M, Eady EA, Avery A, Cunliffe WJ, O'Neill C, et al. 2005. Randomised controlled multiple treatment comparison to provide a cost-effectiveness rationale for the selection of antimicrobial therapy in acne. *Health Technol Assess* 9:iii-212

Packer M. 1988. Neurohormonal interactions and adaptations in congestive heart failure. *Circulation* 77:721-30

Padi SS, Kulkarni SK. 2008. Minocycline prevents the development of neuropathic pain, but not acute pain: possible anti-inflammatory and antioxidant mechanisms. *Eur J Pharmacol* 601:79-87

Pajkrt D, Camoglio L, Tiel-van Buul MC, de Bruin K, Cutler DL, et al. 1997. Attenuation of proinflammatory response by recombinant human IL-10 in human endotoxemia: effect of timing of recombinant human IL-10 administration. *J Immunol* 158:3971-7

Panksepp J, Jalowiec JE, Morgane PJ, Zolovick AJ, Stern WC. 1973. Noradrenergic pathways and sleep-waking states in cats. *Exp Neurol* 41:233-45

Pannasch U, Farber K, Nolte C, Blonski M, Yan Chiu S, et al. 2006. The potassium channels Kv1.5 and Kv1.3 modulate distinct functions of microglia. *Mol Cell Neurosci* 33:401-11

Paris MM, Hickey SM, Trujillo M, Ahmed A, Olsen K, McCracken GH, Jr. 1997. The effect of interleukin-10 on meningeal inflammation in experimental bacterial meningitis. *The Journal of infectious diseases* 176:1239-46

Parkhurst CN, Gan WB. 2010. Microglia dynamics and function in the CNS. *Curr Opin Neurobiol* 20:595-600

Parton LE, Ye CP, Coppari R, Enriori PJ, Choi B, et al. 2007. Glucose sensing by POMC neurons regulates glucose homeostasis and is impaired in obesity. *Nature* 449:228-32

Patel KP. 2000. Role of paraventricular nucleus in mediating sympathetic outflow in heart failure. *Heart Failure Review* 5:73-86

Patel KP, Mayhan WG, Bidasee KR, Zheng H. 2010. Enhanced Angiotensin II-mediated Central Sympatho-excitation in Streptozotocin-induced Diabetes: Role of Superoxide Anion. *Am J Physiol Regul Integr Comp Physiol*

Patel KP, Mayhan WG, Bidasee KR, Zheng H. 2011. Enhanced angiotensin II-mediated central sympathoexcitation in streptozotocin-induced diabetes: role of superoxide anion. *Am J Physiol Regul Integr Comp Physiol* 300:R311-20

Patel KP, Zhang K, Kenney MJ, Weiss M, Mayhan WG. 2000. Neuronal expression of Fos protein in the hypothalamus of rats with heart failure. *Brain Res* 865:27-34

Patel KP, Zhang PL, Krukoff TL. 1993. Alterations in brain hexokinase activity associated with heart failure in rats. *Am J Physiol* 265:R923-8

Paxinos G. 2008. *The Chemoarchitectonic Atlas of the Rat Brain, Second Edition*

Pedersen O, Kahn CR, Flier JS, Kahn BB. 1991. High fat feeding causes insulin resistance and a marked decrease in the expression of glucose transporters (Glut 4) in fat cells of rats. *Endocrinology* 129:771-7

Peinado JM, Myers RD. 1987. Norepinephrine release from PVN and lateral hypothalamus during perfusion with 2-DG or insulin in the sated and fasted rat. *Pharmacol Biochem Behav* 27:715-21

Pelleymounter MA, Cullen MJ, Baker MB, Hecht R, Winters D, et al. 1995. Effects of the obese gene product on body weight regulation in ob/ob mice. *Science* 269:540-3

Perregaux D, Gabel CA. 1994. Interleukin-1 beta maturation and release in response to ATP and nigericin. Evidence that potassium depletion mediated by these agents is a necessary and common feature of their activity. *J Biol Chem* 269:15195-203

Perry VH, Crocker PR, Gordon S. 1992. The blood-brain barrier regulates the expression of a macrophage sialic acid-binding receptor on microglia. *J Cell Sci* 101 ( Pt 1):201-7

Perry VH, Gordon S. 1987. Modulation of CD4 antigen on macrophages and microglia in rat brain. *J Exp Med* 166:1138-43

Pfeffer MA, Pfeffer JM, Steinberg C, Finn P. 1985. Survival after an experimental myocardial infarction: beneficial effects of long-term therapy with captopril. *Circulation* 72:406-12

Phillips HS, Hains JM, Armanini M, Laramee GR, Johnson SA, Winslow JW. 1991. BDNF mRNA is decreased in the hippocampus of individuals with Alzheimer's disease. *Neuron* 7:695-702

Phrommintikul A, Tran L, Kompa A, Wang B, Adrahtas A, et al. 2008. Effects of a Rho kinase inhibitor on pressure overload induced cardiac hypertrophy and associated diastolic dysfunction. *Am J Physiol Heart Circ Physiol* 294:H1804-14

Pi R, Li W, Lee NT, Chan HH, Pu Y, et al. 2004. Minocycline prevents glutamate-induced apoptosis of cerebellar granule neurons by differential regulation of p38 and Akt pathways. *J Neurochem* 91:1219-30

Pinteaux E, Inoue W, Schmidt L, Molina-Holgado F, Rothwell NJ, Luheshi GN. 2007. Leptin induces interleukin-1beta release from rat microglial cells through a caspase 1 independent mechanism. *J Neurochem* 102:826-33

Poo MM. 2001. Neurotrophins as synaptic modulators. *Nat Rev Neurosci* 2:24-32

Pooler AM, Arjona AA, Lee RK, Wurtman RJ. 2004. Prostaglandin E2 regulates amyloid precursor protein expression via the EP2 receptor in cultured rat microglia. *Neurosci Lett* 362:127-30

Prabhu SD. 2005. Post-infarction ventricular remodeling: an array of molecular events. *J Mol Cell Cardiol* 38:547-50

Prescott SA, Sejnowski TJ, De Koninck Y. 2006. Reduction of anion reversal potential subverts the inhibitory control of firing rate in spinal lamina I neurons: towards a biophysical basis for neuropathic pain. *Mol Pain* 2:32

Raghavendra V, Tanga F, DeLeo JA. 2003a. Inhibition of microglial activation attenuates the development but not existing hypersensitivity in a rat model of neuropathy. *J Pharmacol Exp Ther* 306:624-30

Raghavendra V, Tanga T, DeLeo JA. 2003b. Inhibition of microglial activation attenuates the development but not existing hypersensitivity in a rat model of neuropathy. *The Journal of Pharmacology and Experimental Therapeutics* 306:624-30

Rana I, Shivanandappa T. 2010. Mechanism of potentiation of endosulfan cytotoxicity by thiram in Ehrlich ascites tumor cells. *Toxicol In Vitro* 24:40-4

Rauchhaus M, Doehner W, Francis DP, Davos C, Kemp M, et al. 2000. Plasma cytokine parameters and mortality in patients with chronic heart failure. *Circulation* 102:3060-7

Remme WJ. 2003. Pharmacological modulation of cardiovascular remodeling: a guide to heart failure therapy. *Cardiovasc Drugs Ther* 17:349-60

Reynolds AY, Zhang K, Patel KP. 1996. Renal sympathetic nerve discharge mediated by the paraventricular nucleus is altered in STZ induced diabetic rats. *Nebr Med J* 81:419-23

Riazi K, MGalic MA, Kuzmiski JB, Ho W, Sharkey K, Pittman QJ. 2008. Microglial activation and TNFalpha production mediate altered CNS excitability following peripheral inflammation. *Proceedings of the National Academy of Sciences* 105:17151-6

Rio-Hortega d. 1932. Microglia. In: Penfield W, editor. Cytology and cellular pathology of the nervous system. *New York: Hoeber.*:481–584

Ritter MR, Banin E, Moreno SK, Aguilar E, Dorrell MI, Friedlander M. 2006. Myeloid progenitors differentiate into microglia and promote vascular repair in a model of ischemic retinopathy. *J Clin Invest* 116:3266-76

Rivest S, Torres G, Rivier C. 1992. Differential effects of central and peripheral injection of interleukin-1 beta on brain c-fos expression and neuroendocrine functions. *Brain Res* 587:13-23

Ross R. 1993. The pathogenesis of atherosclerosis: a perspective for the 1990s. *Nature* 362:801-9

Rothwell N. 2003. Interleukin-1 and neuronal injury: mechanisms, modification, and therapeutic potential. *Brain Behav Immun* 17:152-7

Ryu J, Pyo H, Jou I, Joe E. 2000. Thrombin induces NO release from cultured rat microglia via protein kinase C, mitogen-activated protein kinase, and NF-kappa B. *J Biol Chem* 275:29955-9

Sanz JM, Di Virgilio F. 2000. Kinetics and mechanism of ATP-dependent IL-1 beta release from microglial cells. *J Immunol* 164:4893-8

Sas A, Jones R, Tyor W. 2008. Intra-peritoneal injection of polyclonal anti-interferon alpha antibodies cross the blood brain barrier and neutralize interferon alpha. *Neurochemical research* 33:2281-7

Satoh N, Ogawa Y, Katsuura G, Hayase M, Tsuji T, et al. 1997. The arcuate nucleus as a primary site of satiety effect of leptin in rats. *Neuroscience letters* 224:149-52

Satoh N, Ogawa Y, Katsuura G, Numata Y, Tsuji T, et al. 1999. Sympathetic activation of leptin via the ventromedial hypothalamus: leptin-induced increase in catecholamine secretion. *Diabetes* 48:1787-93

Sattler R, Tymianski M. 2000. Molecular mechanisms of calcium-dependent excitotoxicity. *J Mol Med* 78:3-13

Sattler R, Tymianski M. 2001. Molecular mechanisms of glutamate receptor-mediated excitotoxic neuronal cell death. *Mol Neurobiol* 24:107-29

Savchenko VL, McKanna JA, Nikonenko IR, Skibo GG. 2000. Microglia and astrocytes in the adult rat brain: comparative immunocytochemical analysis demonstrates the efficacy of lipocortin 1 immunoreactivity. *Neuroscience* 96:195-203

Sawada M, Imamura K, Nagatsu T. 2006. Role of cytokines in inflammatory process in Parkinson's disease. *Journal of neural transmission*:373-81

Sawada M, Kondo N, Suzumura A, Marunouchi T. 1989. Production of tumor necrosis factor-alpha by microglia and astrocytes in culture. *Brain Res* 491:394-7

Sawada M, Suzumura A, Hosoya H, Marunouchi T, Nagatsu T. 1999. Interleukin-10 inhibits both production of cytokines and expression of cytokine receptors in microglia. *J Neurochem* 72:1466-71

Sawchenko PE, Swanson LW. 1983. The organization of forebrain afferents to the paraventricular and supraoptic nuclei of the rat. *J Comp Neurol* 218:121-44

Scarlett JM, Jobst EE, Enriori PJ, Bowe DD, Batra AK, et al. 2007. Regulation of central melanocortin signaling by interleukin-1 beta. *Endocrinology* 148:4217-25

Schiefer J, Kampe K, Dodt HU, Zieglgansberger W, Kreutzberg GW. 1999. Microglial motility in the rat facial nucleus following peripheral axotomy. *J Neurocytol* 28:439-53

Schiller N, Shah P, Crawford M, DeMaria A, Devereux R, et al. 1989. Recommendations for quantitation of the left ventricle by two-dimensional echocardiography - American Society of Echocardiography Committee on Standards, Subcommittee on Quantitation of Two- Dimensional Echocardiograms. *Journal of American Society of Echocardiography* 2:358-67

Schwartz MW, Baskin DG, Kaiyala KJ, Woods SC. 1999. Model for the regulation of energy balance and adiposity by the central nervous system. *The American journal of clinical nutrition* 69:584-96

Seo DR, Kim SY, Kim KY, Lee HG, Moon JH, et al. 2008. Cross talk between P2 purinergic receptors modulates extracellular ATP-mediated interleukin-10 production in rat microglial cells. *Experimental & molecular medicine* 40:19-26

Shafton AD, Ryan A, Badoer E. 1998. Neurons in the hypothalamic paraventricular nucleus send collaterals to the spinal cord and to the rostral ventrolateral medulla in the rat. *Brain Res* 801:239-43

Shi P, Diez-Freire C, Jun JY, Qi Y, Katovich MJ, et al. 2010a. Brain Microglial Cytokines in Neurogenic Hypertension. *Hypertension*

Shi P, Diez-Freire C, Jun JY, Qi Y, Katovich MJ, et al. 2010b. Brain microglial cytokines in neurogenic hypertension. *Hypertension* 56:297-303

Simpson JE, Newcombe J, Cuzner ML, Woodroofe MN. 1998. Expression of monocyte chemoattractant protein-1 and other beta-chemokines by resident glia and inflammatory cells in multiple sclerosis lesions. *J Neuroimmunol* 84:238-49

Solle M, Labasi J, Perregaux DG, Stam E, Petrushova N, et al. 2001. Altered cytokine production in mice lacking P2X(7) receptors. *J Biol Chem* 276:125-32

Somm E, Henrichot E, Pernin A, Juge-Aubry CE, Muzzin P, et al. 2005. Decreased fat mass in interleukin-1 receptor antagonist-deficient mice: impact on adipogenesis, food intake, and energy expenditure. *Diabetes* 54:3503-9

Sorokin SP, Hoyt RF, Jr., Blunt DG, McNelly NA. 1992. Macrophage development: II. Early ontogeny of macrophage populations in brain, liver, and lungs of rat embryos as revealed by a lectin marker. *Anat Rec* 232:527-50

Sowers JR. 2003. Obesity as a cardiovascular risk factor. *The American Journal of Medicine* 115:37-41

Spallone V, Gambardella S, Maiello MR, Barini A, Frontoni S, Menzinger G. 1994. Relationship between autonomic neuropathy, 24-h blood pressure profile, and nephropathy in normotensive IDDM patients. *Diabetes care* 17:578-84

Srinivasan K, Patole PS, Kaul CL, Ramarao P. 2004. Reversal of glucose intolerance by by pioglitazone in high fat diet-fed rats. *Methods Find Exp Clin Pharmacol* 26:327-33

Srinivasan K, Viswanad B, Asrat L, Kaul CL, Ramarao P. 2005. Combination of high-fat diet-fed and low-dose streptozotocin-treated rat: a model for type 2 diabetes and pharmacological screening. *Pharmacol Res* 52:313-20

Srivastava A, Shivanandappa T. 2006. Causal relationship between hexachlorocyclohexane cytotoxicity, oxidative stress and Na+, K +-ATPase in Ehrlich Ascites tumor cells. *Mol Cell Biochem* 286:87-93

Stanley BG, Magdalin W, Seirafi A, Nguyen MM, Leibowitz SF. 1992. Evidence for neuropeptide Y mediation of eating produced by food deprivation and for a variant of the Y1 receptor mediating this peptide's effect. *Peptides* 13:581-7

Stence N, Waite M, Dailey M. 2001a. Dynamics of Microglial Activation: A Confocal Time-Lapse Analysis in Hippocampal Slices. *Glia* 33:256-66

Stence N, Waite M, Dailey ME. 2001b. Dynamics of microglial activation: a confocal time-lapse analysis in hippocampal slices. *Glia* 33:256-66

Stevens RJ, Coleman RL, Adler AI, Stratton IM, Matthews DR, Holman RR. 2004. Risk factors for myocardial infarction case fatality and stroke case fatality in type 2 diabetes: UKPDS 66. *Diabetes care* 27:201-7

Storlien LH, James DE, Burleigh KM, Chisholm DJ, Kraegen EW. 1986. Fat feeding causes widespread in vivo insulin resistance, decreased energy expenditure, and obesity in rats. *Am J Physiol* 251:E576-83

Streit WJ, Graeber MB, Kreutzberg GW. 1988. Functional plasticity of microglia: a review. *Glia* 1:301-7

Streit WJ, Kreutzberg GW. 1988. Response of endogenous glial cells to motor neuron degeneration induced by toxic ricin. *J Comp Neurol* 268:248-63

Strle K, Zhou JH, Shen WH, Broussard SR, Johnson RW, et al. 2001. Interleukin-10 in the brain. *Critical reviews in immunology* 21:427-49

Suk K. 2004. Minocycline suppresses hypoxic activation of rodent microglia in culture. *Neurosci Lett* 366:167-71

Suzuki T, Takayama K, Miura M. 1997. Distribution and projection of the medullary cardiovascular control neurons containing glutamate, glutamic acid decarboxylase, tyrosine hydroxylase and phenylethanolamine N-methyltransferase in rats. *Neurosci Res* 27:9-19

Suzumura A, Sawada M, Marunouchi T. 1996. Selective induction of interleukin-6 in mouse microglia by granulocyte-macrophage colony-stimulating factor. *Brain Res* 713:192-8

Sved AF. 1986. Peripheral pressor systems in hypertension caused by nucleus tractus solitarius lesions. *Hypertension* 8:742-7

Sved AF, Imaizumi T, Talman WT, Reis DJ. 1985. Vasopressin contributes to hypertension caused by nucleus tractus solitarius lesions. *Hypertension* 7:262-7

Swynghedauw B. 1999. Molecular mechanisms of myocardial remodeling 79(1): 215-62. *Physiol Rev* 79:215-62

Takenouchi T, Ogihara K, Sato M, Kitani H. 2005. Inhibitory effects of U73122 and U73343 on Ca2+ influx and pore formation induced by the activation of P2X7 nucleotide receptors in mouse microglial cell line. *Biochim Biophys Acta* 1726:177-86

Takenouchi T, Sekiyama K, Sekigawa A, Fujita M, Waragai M, et al. 2010. P2X7 receptor signaling pathway as a therapeutic target for neurodegenerative diseases. *Arch Immunol Ther Exp (Warsz)* 58:91-6

Takeuchi H, Jin S, Wang J, Zhang G, Kawanokuchi J, et al. 2006. Tumor necrosis factor-alpha induces neurotoxicity via glutamate release from hemichannels of activated microglia in an autocrine manner. *J Biol Chem* 281:21362-8

Talman WT, Granata AR, Reis DJ. 1984. Glutamatergic mechanisms in the nucleus tractus solitarius in blood pressure control. *Fed Proc* 43:39-44

Targos B, Baranska J, Pomorski P. 2005. Store-operated calcium entry in physiology and pathology of mammalian cells. *Acta Biochim Pol* 52:397-409

Taylor DL, Diemel LT, Cuzner ML, Pocock JM. 2002. Activation of group II metabotropic glutamate receptors underlies microglial reactivity and neurotoxicity following stimulation with chromogranin A, a peptide up-regulated in Alzheimer's disease. *J Neurochem* 82:1179-91

Taylor DL, Jones F, Kubota ES, Pocock JM. 2005. Stimulation of microglial metabotropic glutamate receptor mGlu2 triggers tumor necrosis factor alpha-induced neurotoxicity in concert with microglial-derived Fas ligand. *J Neurosci* 25:2952-64

Tikka T, Fiebich BL, Goldsteins G, Keinanen R, Koistinaho J. 2001. Minocycline, a tetracycline derivative, is neuroprotective against excitotoxicity by inhibiting activation and proliferation of microglia. *J Neurosci* 21:2580-8

Tikka TM, Koistinaho JE. 2001. Minocycline provides neuroprotection against N-methyl-D-aspartate neurotoxicity by inhibiting microglia. *J Immunol* 166:7527-33

Tokuhara N, Namiki K, Uesugi M, Miyamoto C, Ohgoh M, et al. 2010. N-type calcium channel in the pathogenesis of experimental autoimmune encephalomyelitis. *J Biol Chem* 285:33294-306

Torre-Amione G, Kapadia S, Benedict C, Oral H, Young JB, Mann DL. 1996a. Proinflammatory cytokine levels in patients with depressed left ventricular ejection fraction: a report from the Studies of Left Ventricular Dysfunction (SOLVD). *J Am Coll Cardiol* 27:1201-6

Torre-Amione G, Kapadia S, Lee J, Durand JB, Bies RD, et al. 1996b. Tumor necrosis factor-alpha and tumor necrosis factor receptors in the failing human heart. *Circulation* 93:704-11

Tozaki-Saitoh H, Tsuda M, Miyata H, Ueda K, Kohsaka S, Inoue K. 2008. P2Y12 receptors in spinal microglia are required for neuropathic pain after peripheral nerve injury. *J Neurosci* 28:4949-56

Trang T, Beggs S, Wan X, Salter MW. 2009. P2X4-receptor-mediated synthesis and release of brain-derived neurotrophic factor in microglia is dependent on calcium and p38-mitogen-activated protein kinase activation. *J Neurosci* 29:3518-28

Triarhou LC, Ghetti B. 1991. Serotonin-immunoreactivity in the cerebellum of two neurological mutant mice and the corresponding wild-type genetic stocks. *J Chem Neuroanat* 4:421-8

Tseng CJ, Liu HY, Lin HC, Ger LP, Tung CS, Yen MH. 1996. Cardiovascular effects of nitric oxide in the brain stem nuclei of rats. *Hypertension* 27:36-42

Tsuda M, Mizokoshi A, Shigemoto-Mogami Y, Koizumi S, Inoue K. 2004. Activation of p38 mitogen-activated protein kinase in spinal hyperactive microglia contributes to pain hypersensitivity following peripheral nerve injury. *Glia* 45:89-95

Tsuda M, Shigemoto-Mogami Y, Koizumi S, Mizokoshi A, Kohsaka S, et al. 2003. P2X4 receptors induced in spinal microglia gate tactile allodynia after nerve injury. *Nature* 424:778-83

Tsuda M, Tozaki-Saitoh H, Inoue K. 2010. Pain and purinergic signaling. *Brain Res Rev* 63:222-32

Tsuda M, Ueno H, Kataoka A, Tozaki-Saitoh H, Inoue K. 2008. Activation of dorsal horn microglia contributes to diabetes-induced tactile allodynia via extracellular signal-regulated protein kinase signaling. *Glia* 56:378-86

Tsutamoto T, Hisanaga T, Wada A, Maeda K, Ohnishi M, et al. 1998. Interleukin-6 spillover in the peripheral circulation increases with the severity of heart failure, and the high plasma level of interleukin-6 is an important prognostic predictor in patients with congestive heart failure. *J Am Coll Cardiol* 31:391-8

Tuomilehto J, Rastenyte D, Jousilahti P, Sarti C, Vartiainen E. 1996. Diabetes mellitus as a risk factor for death from stroke. Prospective study of the middle-aged Finnish population. *Stroke; a journal of cerebral circulation* 27:210-5

Turgeon VL, Lloyd ED, Wang S, Festoff BW, Houenou LJ. 1998. Thrombin perturbs neurite outgrowth and induces apoptotic cell death in enriched chick spinal motoneuron cultures through caspase activation. *J Neurosci* 18:6882-91

Uesugi M, Nakajima K, Tohyama Y, Kohsaka S, Kurihara T. 2006. Nonparticipation of nuclear factor kappa B (NFkappaB) in the signaling cascade of c-Jun N-terminal kinase (JNK)- and p38 mitogen-activated protein kinase (p38MAPK)-dependent tumor necrosis factor alpha (TNFalpha) induction in lipopolysaccharide (LPS)-stimulated microglia. *Brain Res* 1073-1074:48-59

Ulmann L, Hatcher JP, Hughes JP, Chaumont S, Green PJ, et al. 2008. Up-regulation of P2X4 receptors in spinal microglia after peripheral nerve injury mediates BDNF release and neuropathic pain. *J Neurosci* 28:11263-8

Vaisse C, Halaas JL, Horvath CM, Darnell JE, Jr., Stoffel M, Friedman JM. 1996. Leptin activation of Stat3 in the hypothalamus of wild-type and ob/ob mice but not db/db mice. *Nat Genet* 14:95-7

van den Brom CE, Bosmans JW, Vlasblom R, Handoko LM, Huisman MC, et al. 2010. Diabetic cardiomyopathy in Zucker diabetic fatty rats: the forgotten right ventricle. *Cardiovasc Diabetol* 9:25

van den Pol AN. 1982. The magnocellular and parvocellular paraventricular nucleus of rat: intrinsic organization. *J Comp Neurol* 206:317-45

van Exel E, Gussekloo J, de Craen AJ, Frolich M, Bootsma-Van Der Wiel A, Westendorp RG. 2002. Low production capacity of interleukin-10 associates with the metabolic syndrome and type 2 diabetes : the Leiden 85-Plus Study. *Diabetes* 51:1088-92

van Giersbergen PL, Palkovits M, De Jong W. 1992. Involvement of neurotransmitters in the nucleus tractus solitarii in cardiovascular regulation. *Physiol Rev* 72:789-824

Vandesande F, DeMey J, Dierickx K. 1974. Identification of neurophysin producing cells. I. The origin of the neurophysin-like substance-containing nerve fibres of the external region of the median eminence of the rat. *Cell Tissue Res* 151:187-200

Vandesande F, Dierickx K. 1975. Identification of the vasopressin producing and of the oxytocin producing neurons in the hypothalamic magnocellular neurosecretroy system of the rat. *Cell Tissue Res* 164:153-62

Vandesande F, Dierickx K, DeMey J. 1975. Identification of the vasopressin-neurophysin II and the oxytocin-neurophysin I producing neurons in the bovine hypothalamus. *Cell Tissue Res* 156:189-200

Vaz M, Jennings G, Turner A, Cox H, Lambert G, Esler M. 1997. Regional sympathetic nervous activity and oxygen consumption in obese normotensive human subjects. *Circulation* 96:3423-9

Veening JG, van der Meer MJ, Joosten H, Hermus AR, Rijnnkels CE, et al. 1993. Intravenous administration of interleukin-1 beta induces Fos-like immunoreactivity in corticotropin-releasing hormone neurons in the paraventricular hypothalamic nucleus of the rat. *J Chem Neuroanat* 6:391-7

Vela JM, Dalmau I, Gonzalez B, Castellano B. 1995. Morphology and distribution of microglial cells in the young and adult mouse cerebellum. *J Comp Neurol* 361:602-16

Verrotti A, Loiacono G, Mohn A, Chiarelli F. 2009. New insights in diabetic autonomic neuropathy in children and adolescents. *Eur J Endocrinol* 161:811-8

Visentin S, Renzi M, Frank C, Greco A, Levi G. 1999. Two different ionotropic receptors are activated by ATP in rat microglia. *J Physiol* 519 Pt 3:723-36

Vita JA, Treasure CB, Nabel EG, McLenachan JM, Fish RD.1990. Coronary vasomotor response to acetylcholine relates to risk factors for coronary artery disease. *Circulation* 81:491-7

Volonte C, Amadio S, D'Ambrosi N, Colpi M, Burnstock G. 2006. P2 receptor web: complexity and fine-tuning. *Pharmacol Ther* 112:264-80

Wajchenberg BL, Feitosa AC, Rassi N, Lerario AC, Betti RT. 2008. Glycemia and cardiovascular disease in type 1 diabetes mellitus. *Endocr Pract* 14:912-23

Wang AL, Yu AC, Lau LT, Lee C, Wu le M, et al. 2005a. Minocycline inhibits LPS-induced retinal microglia activation. *Neurochem Int* 47:152-8

Wang AL, Yu ACH, Lau LT, Lee C, Wu LM, et al. 2005b. Minocycline inhibits LPS-induced retinal microglia activation. *Neurochemistry International* 47:152-8

Watanobe H, Takebe K. 1994. Effects of intravenous administration of interleukin-1-beta on the release of prostaglandin E2, corticotropin-releasing factor, and arginine vasopressin in several hypothalamic areas of freely moving rats: estimation by push-pull perfusion. *Neuroendocrinology* 60:8-15

Wei SG, Yu Y, Zhang ZH, Weiss RM, Felder RB. 2008. Mitogen-activated protein kinases mediate upregulation of hypothalamic angiotensin II type 1 receptors in heart failure rats. *Hypertension* 52:679-86

Wen YR, Suter MR, Ji RR, Yeh GC, Wu YS, et al. 2009. Activation of p38 mitogen-activated protein kinase in spinal microglia contributes to incision-induced mechanical allodynia. *Anesthesiology* 110:155-65

Wilson MA, Molliver ME. 1994. Microglial response to degeneration of serotonergic axon terminals. *Glia* 11:18-34

Wood GW, Gollahon KA, Tilzer SA, Vats T, Morantz RA. 1979. The failure of microglia in normal brain to exhibit mononuclear phagocyte markers. *J Neuropathol Exp Neurol* 38:369-76

Wotjak CT, Naruo T, Muraoka S, Simchen R, Landgraf R, Engelmann M. 2001. Forced swimming stimulates the expression of vasopressin and oxytocin in magnocellular neurons of the rat hypothalamic paraventricular nucleus. *Eur J Neurosci* 13:2273-81

Wu CY, Kaur C, Sivakumar V, Lu J, Ling EA. 2009. Kv1.1 expression in microglia regulates production and release of proinflammatory cytokines, endothelins and nitric oxide. *Neuroscience* 158:1500-8

Wu LJ, Vadakkan KI, Zhuo M. 2007. ATP-induced chemotaxis of microglial processes requires P2Y receptor-activated initiation of outward potassium currents. *Glia* 55:810-21

Wu X, Zhu D, Jiang X, Okagaki P, Mearow K, et al. 2004a. AMPA protects cultured neurons against glutamate excitotoxicity through a phosphatidylinositol 3-kinase-dependent activation in extracellular signal-regulated kinase to upregulate BDNF gene expression. *J Neurochem* 90:807-18

Wu Y, Willcockson HH, Maixner W, Light AR. 2004b. Suramin inhibits spinal cord microglia activation and long-term hyperalgesia induced by formalin injection. *J Pain* 5:48-55

Yamamoto T, Kimura T, Ota K, Shoji M, Inoue M, et al. 1994. Effects of interleukin-1 beta on blood pressure, thermoregulation, and the release of vasopressin, ACTH and atrial natriuretic hormone. *Tohoku J Exp Med* 173:231-45

Yang J, Yang Y, Chu J, Wang G, Xu H, et al. 2009a. Endogenous opiate peptides in the spinal cord are involved in the analgesia of hypothalamic paraventricular nucleus in the rat. *Peptides* 30:740-4

Yang J, Yuan HF, Liu WY, Zhang XX, Feng JP, et al. 2009b. Norepinephrine regulates arginine vasopressin secretion in hypothalamic paraventricular nucleus relating with pain modulation. *Neuropeptides* 43:259-65

Yang Q, Chen SR, Li DP, Pan HL. 2007. Kv1.1/1.2 channels are downstream effectors of nitric oxide on synaptic GABA release to preautonomic neurons in the paraventricular nucleus. *Neuroscience* 149:315-27

Yang W, Oskin O, Krukoff TL. 1999. Immune stress activates putative nitric oxide-producing neurons in rat brain: cumulative effects with restraint. *J Comp Neurol* 405:380-7

Yrjanheikki J, Keinanen R, Pellikka M, Hokfelt T, Koistinaho J. 1998. Tetracyclines inhibit microglial activation and are neuroprotective in global brain ischemia. *Proc Natl Acad Sci U S A* 95:15769-74

Yrjanheikki J, Tikka T, Keinanen R, Goldsteins G, Chan PH, Koistinaho J. 1999. A tetracycline derivative, minocycline, reduces inflammation and protects against focal cerebral ischemia with a wide therapeutic window. *Proc Natl Acad Sci U S A* 96:13496-500

Yu-Ming Kang D-NQ, Carrie Elks and Joseph Francis. 2009. Pro-inflammatory cytokines increase neuronal activity in the hypothalamic paraventricular nucleus and contribute to the pathogenesis of streptozotocin-induced diabetes. *The FESEB Journal 23 (Meeting Abstract Supplement)* (990.8)

Yu Y, Wei S, Zhang Z, Gomez-Sanchez E, Weiss R, Felder R. 2008. Does Aldosterone Upregulate the Brain Renin-Angiotensin
System in Rats With Heart Failure?
. *Hypertension*
51:727-33

Yu Y, Zhang ZH, Wei SG, Serrats J, Weiss RM, Felder RB. 2010. Brain perivascular macrophages and the sympathetic response to inflammation in rats after myocardial infarction. *Hypertension* 55:652-9

Zerbe RL, Feuerstein G. 1985. Cardiovascular effects of centrally administered vasopressin in conscious and anesthetized rats. *Neuropeptides* 6:471-84

Zetterstrom RH, Simon A, Giacobini MM, Eriksson U, Olson L. 1994. Localization of cellular retinoid-binding proteins suggests specific roles for retinoids in the adult central nervous system. *Neuroscience* 62:899-918

Zhang J, De Koninck Y. 2006. Spatial and temporal relationship between monocyte chemoattractant protein-1 expression and spinal glial activation following peripheral nerve injury. *Journal of neurochemistry* 97:772-83

Zhang K, Patel KP. 1998. Effect of nitric oxide within the paraventricular nucleus on renal sympathetic nerve discharge: role of GABA. *Am J Physiol* 275:R728-34

Zhang K, Zucker IH, Patel KP. 1998. Altered number of diaphorase (NOS) positive neurons in the hypothalamus of rats with heart failure. *Brain Res* 786:219-25

Zhang XM, Jin T, Quezada HC, Mix E, Winblad B, Zhu J. Kainic acid-induced microglial activation is attenuated in aged interleukin-18 deficient mice. *J Neuroinflammation* 7:26

Zhang Y, Proenca R, Maffei M, Barone M, Leopold L, Friedman JM. 1994. Positional cloning of the mouse obese gene and its human homologue. *Nature* 372:425-32

Zhang ZH, Wei SG, Francis J, Felder RB. 2003. Cardiovascular and renal sympathetic activation by blood-borne TNF-alpha in rat: the role of central prostaglandins. *Am J Physiol Regul Integr Comp Physiol* 284:R916-27

Zheng H, Li YF, Weiss M, Mayhan WG, Patel KP. 2002. Neuronal expression of fos protein in the forebrain of diabetic rats. *Brain Res* 956:268-75

Zheng H, Mayhan WG, Bidasee KR, Patel KP. 2006. Blunted nitric oxide-mediated inhibition of sympathetic nerve activity within the paraventricular nucleus in diabetic rats. *American journal of physiology* 290:R992-R1002

Zheng JL, Stewart RR, Gao WQ. 1995. Neurotrophin-4/5 enhances survival of cultured spiral ganglion neurons and protects them from cisplatin neurotoxicity. *J Neurosci* 15:5079-87

Zheng LT, Ock J, Kwon BM, Suk K. 2008. Suppressive effects of flavonoid fisetin on lipopolysaccharide-induced microglial activation and neurotoxicity. *Int Immunopharmacol* 8:484-94

Zhu S, Stavrovskaya IG, Drozda M, Kim BY, Ona V, et al. 2002. Minocycline inhibits cytochrome c release and delays progression of amyotrophic lateral sclerosis in mice. *Nature* 417:74-8

Zhuang ZY, Gerner P, Woolf CJ, Ji RR. 2005. ERK is sequentially activated in neurons, microglia, and astrocytes by spinal nerve ligation and contributes to mechanical allodynia in this neuropathic pain model. *Pain* 114:149-59

# Appendix

## *Fig1*

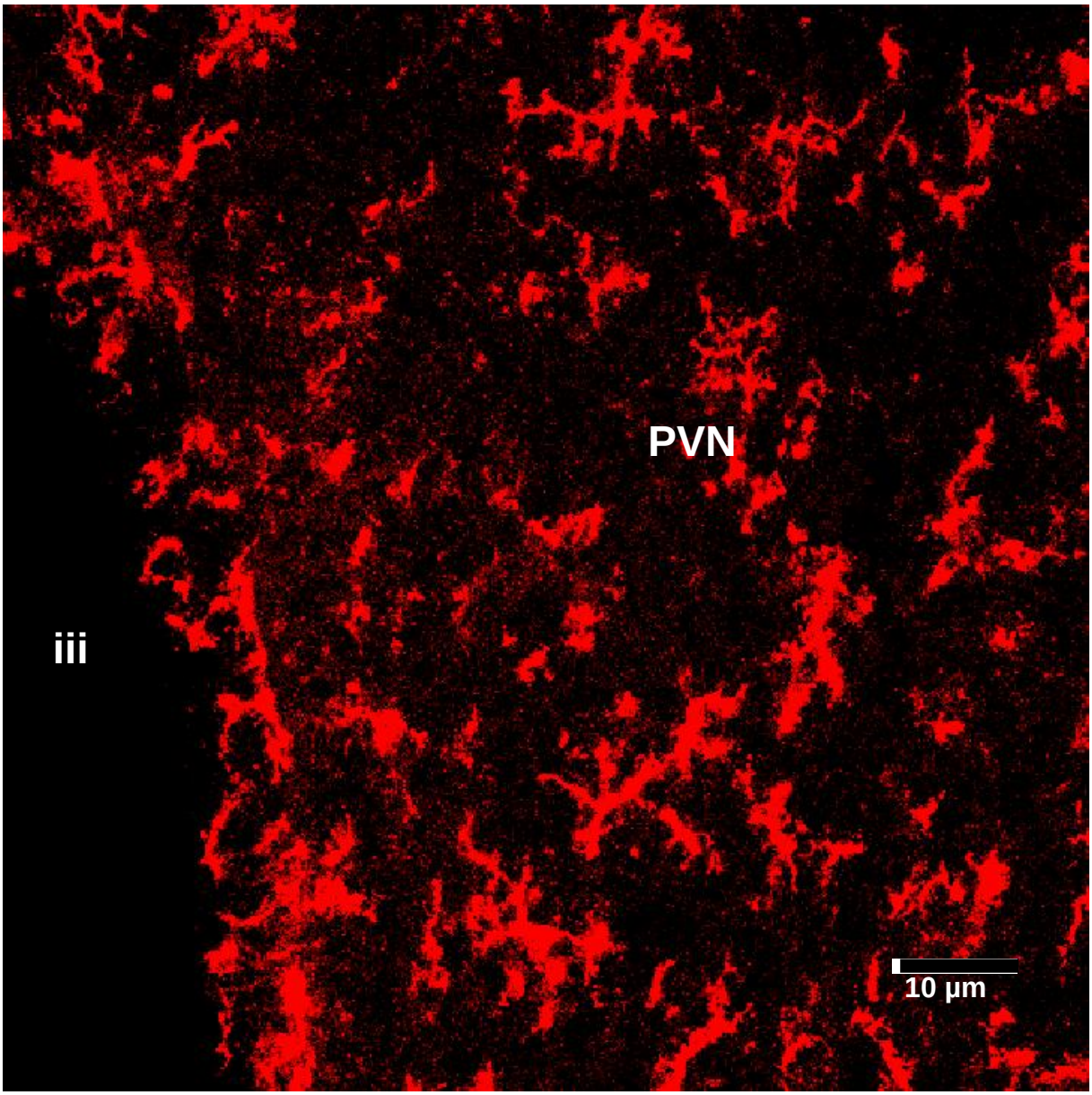

Fig 1: Figure shows OX-42 stained microglia in the PVN of a control rat. It is evident from this figure that microglia are evenly distributed throughout the PVN. The microglia also appeared to have a branched structure with long processes. The distribution and morphology of these microglia clearly suggests that they are not in blood vessels hence they are parenchymal. The image is a projection of a confocal Z-stack.

*Fig 2*

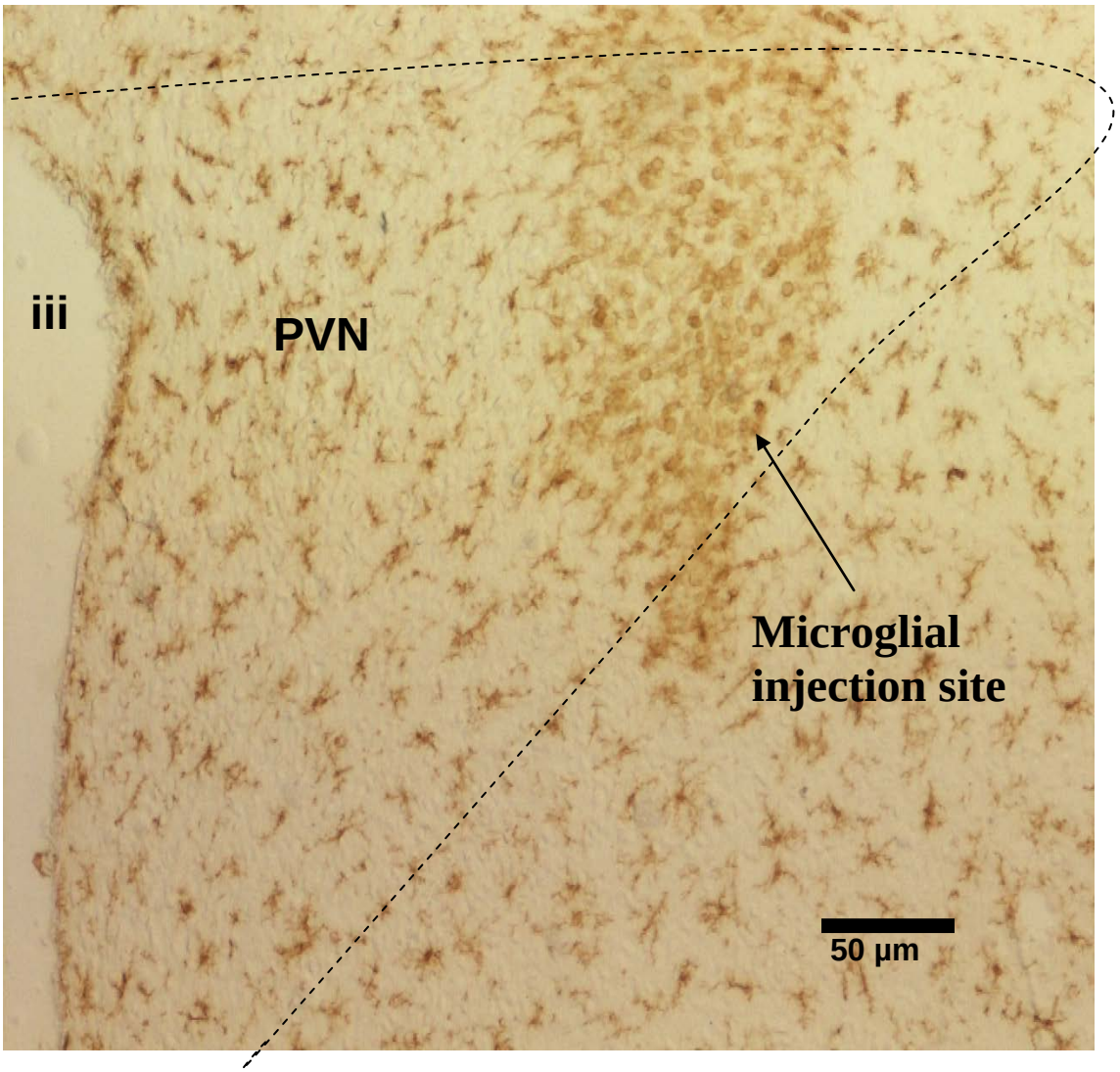

Fig 2: Figure shows OX-42 stained microglia in a brain section from a rat in which ATP-activated microglia were injected into the hypothalamus. Note the change in microglial morphology in the PVN region.